Development of Procedures for Casework Specimen Collection and Processing for Organic Gunshot Residue Analysis

---

A Thesis submitted in fulfilment of the requirements for the award

of the degree

Doctor of Philosophy

from

University of Technology Sydney

by

Regina Verena Taudte

M.Sc., B.Sc.

Centre for Forensic Science

University of Technology Sydney

CERTIFICATE OF AUTHORSHIP AND ORIGINALITY

I, Regina Verena Taudte, certify that the work in this thesis has not previously been submitted for a degree nor has it been submitted as part of the requirements for a degree except as fully acknowledged within the text.

I also certify that the thesis has been written by me. Any help that I have received in my research work and the preparation of the thesis itself has been acknowledged. In addition, I certify that all the information sources and literature used are indicated in the thesis.

Regina Verena Taudte

01.03.2016

LIST OF PUBLICATIONS

The chapters presented in this thesis have been published, accepted for publication or prepared for submission to journals as follows:

Chapter 1 - This chapter includes some parts of the literature review:
R.V. Taudte, A. Beavis, L. Blanes, N. Cole, P. Doble, C. Roux, Detection of Gunshot Residues Using Mass Spectrometry, ***BioMed Research International***, 2014, Article ID 965403, http://dx.doi.org/10.1155/2014/965403

Chapter 2 – R.V. Taudte, A. Beavis, L. Wilson-Wilde, C. Roux, P. Doble, L. Blanes**,** A portable explosive detector based on fluorescence quenching of pyrene deposited on coloured wax-printed μPADs**,** ***Lab Chip*****,** 2013**, 13,** 4164-4172, DOI: 10.1039/C3LC50609F

Chapter 3 – This chapter has been submitted to the ***Journal of Mass Spectrometry***:
R. V. Taudte, C. Roux, D. Bishop, C. Fouracre, A. Beavis, High-throughput screening for smokeless powders and gunshot residues using RapidFire® with tandem mass spectrometry

Chapter 4 – R.V. Taudte, C. Roux, D. Bishop, L. Blanes, P. Doble, A. Beavis, Development of a UHPLC method for the detection of organic gunshot residues using artificial neural networks, ***Analytical Methods***, 2015, **7**, 7447-7454, DOI: 10.1039/C5AY00306G

Chapter 5 – R.V. Taudte, C. Roux, L. Blanes, M. Horder, K.P. Kirkbride, A. Beavis, The Development and Comparison of Collection Techniques for Inorganic and Organic Gunshot Residues, ***Analytical and Bioanalytical Chemistry,*** 2016, **408**, 2567-2576, DOI: 10.1007/s00216-016-9357-7

Chapter 6 - This chapter has been prepared for submission to ***Forensic Science International:***

R.V. Taudte, C. Roux, A. Beavis, Stability of smokeless powder compounds on collection devices

LIST OF CONFERENCES

The research conducted during this project was presented at several international conferences listed below.

Year	Conference	Presentation
2015	7th European Academy of Forensic Science Conference, Prague (Czech Republic)	The Development and Comparison of Procedures for the Combined Collection of Organic and Inorganic Gunshot Residues
2014	22st International Symposium on the Forensic Sciences, Adelaide (Australia)	The Development and Comparison of Procedures for the Combined Collection of Organic and Inorganic Gunshot Residues
2012	21st International Symposium on the Forensic Sciences, Hobart (Australia)	Development of Procedures for Casework Sample Collection and Processing for Organic Gunshot Residue Analysis

ACKNOWLEDGEMENT

Once upon a time, a girl moved to Australia and started a PhD at the University of Technology Sydney. A few years later…she was finally about to finish. The end of an exciting, mind broadening, fulfilling and sometimes exhausting journey is coming close and I would have never made it to this stage without the help and support of many wonderful people.

First and foremost, I would like to express my deepest appreciation to my supervisors, Associate Professor Alison Beavis and Professor Claude Roux. Thank you for giving me the opportunity to undertake this project, supporting me throughout this incredible journey, encouraging me when encouragement was needed, giving me the freedom to try and follow my ideas and the opportunity to grow as a researcher. Thank you so so much Alison, for spending weekends with me on the shooting range, being incredibly supportive and positive throughout this project and making me always feel accomplished after all our meetings. Thank you Claude! I am indebted to you for your support and trust that made it possible for me to come to UTS and the many opportunities you gave me along the way. Both of you have given invaluable contributions to the preparation of the research output from my doctoral work and I cannot put in words how grateful I am for everything you have done for me.

I would like to thank Dr Lucas Blanes, Dr David Bishop and Professor Philip Doble for their constant help and support especially in regards to micropads and analytical chemistry. Thank you Lucas for the many Brazilian barbecues I enjoyed very much and inspiring me to finally learn the guitar.

I am truly grateful to Sergeant Mark Horder. Without you, this research would not have been possible!

In addition, I would like to thank Elizabeth Chan from NSW Health and Joanna Pryke who initialised this project and provided me with valuable feedback specifically in regards to case work applicability.

I would also like to thank Katie McBean from the Microstructural Analysis Unit (UTS), Dr Richard Wuhrer at the University of Western Sydney and Ken Mason for the support with the SEM and the automated gunshot residue software. My apologies for the many desperate emails I sent you when my computer skills repeatedly abandoned me and I experienced issues with the software.

I would like to show my gratitude to everyone involved in the preparation and review process of manuscripts resulting from this research and in the preparation of this thesis. Your constructive feedback greatly improved the written work related to this PhD and I am extremely grateful for your time and efforts.

I would like to thank Microsoft for developing such an amazing program as office. I am in awe of everyone who had to write a PhD thesis without the possibility to automatically update List of Figure and Tables, as well as references using endnote.

I would like to thank my fellow PhD candidates and colleagues at the university: Ali, Fiona, Nadine, Matt, Dan, Anna, Scott, Marie, Joyce, and many more. Our communal lunches, coffee breaks, Friday bar evenings and other social activities made the last four years more than enjoyable and I am so grateful to have found wonderful friends in many of you.

A big thank you to Ronald and the whole Shimoninski family! Every morning I go to work with a big smile on my face – and this is because of you!

Thank you Claire and everyone involved in the UTS Volleyball Club! You managed to distract my mind from PhD work for at least a few hours per week and reminded me that there is a life outside university.

I would like to thank Maiken, who showed me that every obstacle in life is conquerable and who found surprisingly fun in counting particles.

I want to thank my partner Gabriele for his support throughout the whole time. I know the last few years have not been easy for you and I greatly appreciate all the sacrifices you made to make my life easier even though they made your life harder. You have been there for me, always provided constructive feedback and advices. You have been my motivation and inspiration for undertaking a PhD and I greatly appreciate everything you have done for me! I love you so so much, ti amo, LoYuMuMo! You mean the world to me! Always remember how beautiful you are.

Words cannot express how grateful I am and how much I love my family and friends back home in Germany. Despite the 14,000 kilometres including an ocean separating us, you have been there for me every step of the way. You have given me the strength and endurance to not give up when it became difficult and always focus on the positives. You have always believed in me, even when I doubted myself. You have been my rock, my hope and my strength! I could not think of any better support system and cannot thank you enough for your love and friendship.

To all PhD candidates out there:

As my mum would say:”Bleib übrig!”.

TABLE OF CONTENTS

LIST OF FIGURES

LIST OF TABLES

ABBREVIATIONS

1,2-DNG	1,2-Dintiroglycerine
1,3-DNG	1,3-Dinitroglycerine
2,3-DNT	2,3-Dinitrotoluene
2,4-DNDPA	2,4-Dinitrodiphenylamine
2,4-DNT	2,4-Dinitrotoluene
2,6-DNT	2,6-Dinitrotoluene
2-NDPA	2-Nitrodiphenylamine
3,4-DNT	3,4-Dinitrotoluene
3-NT	3-Nitrotoluene
4-A-2,6-DNT	4-Amino-2,6-dinitrotoluene
4-nDPA	4-Nitrosodiphenylamine
4-NT	4-Nitrotoluene
AAS	Atomic absorption spectroscopy
ACN	Acetonitrile
ANN	Artificial Neural Network
APCI	Atmospheric chemical ionisation
AUS	Australia
Ba	Barium
CE	Collision energy
DBP	Dibutyl phthalate
DCM	Dichloromethane
DDNP	Diazodinitrophenol

DEP	Diethyl phthalate
DMP	Dimethyl phthalate
DNB	2,3-Dinitrobenzene
DNT	Dinitrotoluene
DPA	Diphenylamine
EC	Ethyl centralite
EGDN	Ethylene glycol dinitrate
EtOH	Ethanol
FID	Flame ionisation detector
GC	Gas chromatography
GC-TEA	Gas chromatography coupled to thermal energy analyser
GSR	Gunshot residue/s
h	Hour/s
HMF	Heavy-metal free
HMX	Octahydro-1,3,5,7-tetranitro-1,3,5,7-tatrazocine
HPLC	High performance liquid chromatography
IED	Improvised explosive device
IGSR	Inorganic gunshot residues
IMS	Ion mobility spectroscopy
IPA	Isopropanol
ISTD	Internal standard
ISDN	Isosorbide dinitrate
kΩ	Kiloohm

LA-ICP-MS	Laser ablation inductively coupled plasma mass spectrometry
LC	Liquid chromatography
LC-QTOF-MS	Liquid chromatography coupled to quadrupole time of flight mass spectrometry
LED	Light-emitting diode
LF	Lead free
LOD	Limit of detection
LOQ	Limit of quantification
MC	Methyl centralite
MECE	Micellar electrokinetic capillary electrophoresis
MeOH	Methanol
mg	Milligram
min	Minute/s
mL	Millilitre
MLP	Multilayer perceptron
mm	Millimetre
mm^2	Square millimetre
MPP	Minimum peak pair
MRM	Multiple reaction monitoring
ms	Milliseconds
MS	Mass spectrometry/ mass spectrometer
MS/MS	Tandem mass spectrometry
MTBE	Methyl tert-butyl ether
NAA	Neutron activation analysis

NB	Nitrobenzene
NC	Nitrocellulose
ng	Nanogram
NG	Nitroglycerine
NGU	Nitroguanidine
nm	Nanometre
N-nDPA	N-Nitrosodiphenylamine
N,N'-DPU	N,N'-Diphenylurea
NO	Nitrogen monoxide
NO_2	Nitrogen dioxide
NPD	Nitrogen phosphorus detector
NSW	New South Wales
NSWPF	New South Wales Police Force
OGSR	Organic gunshot residues
Pb	Lead
PDMS/DVB	Polydimethylsiloxane/divinylbenzene
PETN	Pentaerythitol tetranitrate
pg	Picogram
PMDE	Pendant mercury drop electrode
ppm	Parts per million
PTFE	Polytetrafluoroethylene
QQQ-MS	Triple quadrupole mass spectrometer
R^2	Coefficient of determination
RDX	Hexahydro-1,3,5-trinitro-1,3,5-triazine
resorcinol	1,3-Benzenediol

rpm	Revolutions per minute
RSD	Relative standard deviation
RT	Room temperature
Sb	Antimony
SDS	Sodium dodecyl sulfate
sec	Seconds
SEM-EDX	Scanning electron microscopy with energy dispersive x-ray spectroscopy
SOP	Standard operating procedure
SPE	Solid phase extraction
SPME	Solid phase microextraction
Sr	Strontium
SD	Standard deviation
TEA	Thermal energy analyser
tetryl	2,4,6-Trinitrophenylmethylnitramine
TNB	1,3,5-Trinitrobenzene
TNT	2,4,6-Trinitrotoluene
UHPLC	Ultra-high performance liquid chromatography
UP	Ultrapure
USA	United States of America
UV	Ultraviolet
TOF-SIMS	Time of flight secondary ion mass spectrometry
W_H	Width after heating
W_N	Nominal width
W_P	Width after printing

µg	Microgram
µL	Microlitre

ABSTRACT

The detection and interpretation of gunshot residues (GSR) plays a crucial role in the investigation of firearm related events. Specimens are commonly collected using GSR stubs with double sided adhesive carbon tape. After collection, the stubs can directly be analysed using scanning electron microscopy with energy dispersive x-ray spectroscopy (SEM-EDX), which is widely used for the detection of inorganic gunshot residues (IGSR) as it provides simultaneous elemental and morphological information of discrete particles. Since SEM-EDX analysis focuses on the detection of characteristic GSR particles incorporating the elements lead, antimony and barium, the relatively recent introduction of lead free (LF) and heavy-metal free (HMF) ammunition challenges the current standard operating procedure (SOP) for GSR analysis. Other problems arise from the recent findings of GSR-like particles from environmental and occupational sources. The incorporation of organic gunshot residues (OGSR) into the current SOP can provide additional and complementary information that is alleged to overcome these limitations. This project focused on the detection and incorporation of OGSR to current GSR SOPs on different levels.

A screening technique was developed for the in-field detection of compounds potentially present in smokeless powders and GSR. The technique was based on microfluidic paper-based analytical devices (μPAD) and fluorescence quenching of pyrene and showed promising results for detecting energetic compounds in OGSR. A portable μPAD reader was built and showed potential for in-field detection of GSR (and explosives).

A second screening technique was developed based on solid phase extraction (SPE). This technique can allow pre-concentration and clean-up of samples before

OGSR analysis, which might be necessary considering the low amounts of OGSR that are commonly detected on specimens directly collected after discharge. A proof-of-concept study using a completely automated on-line SPE robot, the RapidFire®, connected to a triple quadrupole mass spectrometer (QQQ-MS) was conducted showing promising results for the pre-concentration and/or screening of OGSR.

To allow the detection of a broad range of OGSR, an ultra-high performance liquid chromatography (UHPLC) method with ultraviolet (UV) detection and mass spectrometric confirmation using a QQQ-MS was developed using a statistical approach (Artificial Neural Networks (ANN)). This approach was applied for the first time to GSR analysis. The network was trained and used for the prediction of retention times of the target compounds in relation to different gradients. The final UHPLC-UV method was fully validated and tested using simulated case specimens collected at an indoor firing range. It proved sufficiently sensitive and selective for the detection of OGSR from hands and the establishment of smokeless powder profiles.

Three different collection protocols for the recovery of OGSR and IGSR from hands were conceptualised to enable both subsequent OGSR analysis by UHPLC-UV and IGSR analysis by SEM-EDX. Comparing the two superior protocols, the extraction efficiencies of OGSR from alcohol swabs and GSR stubs were found to be comparable, while GSR stubs proved to be more efficient in collecting OGSR. Testing the protocols using simulated case specimens taken at the shooting range confirmed that GSR stubs followed by liquid extraction are more suitable than wipes for a combined collection of OGSR and IGSR.

Finally, the stability of OGSR on collection devices, i.e. alcohol swabs and GSR stubs, was investigated for a time period of 63 days. Interestingly, energetic compounds were found to be relatively stable, while stabilisers, often the target compounds for OGSR, degraded mostly following a negative logarithmic curve. This could be problematic for the developed SOP for the collection and analysis of both OGSR and IGSR, since SEM-EDX analysis is preceding OGSR analysis causing the degradation of compounds of interest.

In summary, an SOP for GSR collection and analysis was developed that could potentially overcome problems arising from LF and HMF ammunitions. Further research studies into persistence and background are necessary to test the value of the developed SOP in a forensic framework.

Chapter 1: INTRODUCTION

Chapter 1: INTRODUCTION

1.1 Project Rationale

From January to September 2012, over 100 firearm-related events have been reported in the Sydney area [1], with a total number of firearm-related crimes across Australia reaching 1217 in 2012 [2]. Moreover, in 2014-2015 there were 3463 firearm charges in New South Wales (NSW), representing an 83 % increase from 2005-2006 [3]. The large number and the gravity of the nature of these crimes demonstrate the significant impact of firearm-related events within Sydney, NSW. The investigation of such incidents generally requires the examination and analysis of different aspects related to firearms. One of these aspects is the examination of gunshot residues (GSR). The detection and analysis of GSR can provide helpful information regarding different facets of firearm-related events. However, recent changes in the ammunition and interpretation issues challenge the current existing protocol for GSR analysis and call for an adjustment to these problems.

1.1 Gunshot Residue Background

When the trigger of a weapon is pulled the firing pin strikes the sensitive primer, which subsequently detonates and produces an intense flame. Hot gases and particles are expelled in the propellant powder, which consequently ignites [4, 5]. High pressure produced by the heated gases forces small particles and vapour to be released from the muzzle together with the projectile as well as other weapon openings [6]. The released particles are referred to as GSR and can be found on the

shooter, the target and the surrounding exhibits as far as 10 m from the discharged firearm [7, 8]. GSR contain burnt and unburnt particles from the primer, the propellant powder, and any other particle source in the weapon [4, 9] and can be separated into two different categories of GSR: organic GSR (OGSR) and inorganic GSR (IGSR).

Most of the organic compounds originate from the propellant powder [10]. Commonly used propellant powders are smokeless powders, which consist mainly of nitrocellulose (NC). Smokeless powders are grouped in three different types: single-base, double-base and triple-base powders. Single-base powders contain NC, double-base powders contain NC and nitroglycerine (NG), and triple-base powders consist of NC, NG, and nitroguanidine (NGU) as main explosive reagents. Additives are also used in the production of ammunition to increase the stability and the longevity of the powder, improve workability and affect burn rate [11, 12]. They work as stabilisers, plasticisers, coolants, gelatinizers, flash inhibitors, moderants, surface lubricants, and anti-wear additives [4]. Diphenylamine (DPA), the centralites and resorcinol are commonly used stabilisers, of which DPA is the most common one and used mainly in single-base powders [13]. Ethyl centralite (EC) is encountered in double-base powder and often replaced by methyl centralite (MC) in Chinese ammunition [6]. The function of stabilisers is to prolong the safe storage time of smokeless powders [14-16]. Nitrogen monoxide (NO) and nitrogen dioxide (NO_2) are released by nitro esters, such as NG or NC, in a spontaneous decomposition process during the aging of propellant powders and work as oxidisers. Stabilisers such as DPA bind these gaseous products and prevent their reaction with NC or NG, which would result in an autocatalytic cycle and further degrade the gunpowder [6, 10, 16, 17]. As a result, DPA becomes nitrated or

nitrosated itself over time, with nitrated derivatives, such as 4-Nitrosodiphenylamine (4-nDPA) or 2-Nitrodiphenylamine (2-NDPA) formed. Plasticisers are mixed with the powder components in order to strengthen the flexibility of the grains. Common plasticisers are glyceryl triacetate (triacetin), and the phthalates, such as dimethyl phthalate (DMP), diethyl phthalate (DEP), and dibutyl phthalate (DBP) [4]. Flash suppressors, such as dinitrotoluene (DNT) or NGU, produce nitrogen gas, which dilutes the muzzle gases [10, 18, 19].

The concentration of additives can vary from around 1 % up to 50 % of the powder mixture [20]. Table 1-1 lists some of the most commonly found organic compounds in GSR.

Table 1-1: List containing some of the most common organic compounds present in gunshot residues [4, 6, 10, 11, 14, 21-24].

Compound	Function
2,4,6-Trinitrotoluene (TNT)	Propellant
2,3-Dinitrotoluene (2,3-DNT)	Flash suppressor
2,4-Dinitrodiphenylamine (2,4-DNDPA)	Stabiliser (derivative of DPA)
2,4-Dinitrotoluene (2,4-DNT)	Flash suppressor
2,6-Dinitrotoluene (2,6-DNT)	Flash suppressor
2-Nitrodiphenylamine (2-NDPA)	Stabiliser (derivative of DPA)
2-Nitrotoluene (2-NT)	Flash suppressor
3,4-Dinitrotoluene (3,4-DNT)	Flash suppressor
4-Nitrosodiphenylamine (4-nDPA)	Stabiliser (derivative of DPA)
4-Nitrotoluene (4-NT)	Flash suppressor
6-Nitrotoluene (6-NT)	Flash suppressor
Akardite I	Stabiliser
Akardite II	Stabiliser, Gelatiniser
Akardite III	Stabiliser, Gelatiniser

Table 1-1 continued: List containing some of the most common organic compounds present in gunshot residues [4, 6, 10, 11, 14, 21-24].

Compound	Function
Butyl centralite (N,N-Dibutylcarbanilide)	Stabiliser, Plasticiser
Camphor	Plasticiser
Cresol	Stabiliser
Diamyl phthalate	Plasticiser
Diazodinitrophenol (DDNP)	Explosive
Dibutyl phthalate (DBP)	Plasticiser
Diethyl phthalate (DEP)	Plasticiser
Dimethyl phthalate (DMP)	Plasticiser
Dimethyl sebacate	Plasticiser
Dinitrocresol	Stabiliser
Diphenylamine (DPA)	Stabiliser
Ethyl centralite (N,N-Diethylcarbanilide)	Stabiliser, Plasticiser
Ethylene glycol dinitrate (EGDN)	Propellant
Ethyl phthalate	Plasticiser
Graphite	Surface moderator
Methyl centralite (N,N-Dimethylcarbanilide)	Stabiliser, Plasticiser
Methyl phthalate	Plasticiser
Nitrocellulose (NC)	Propellant
Nitroglycerine (NG)	Propellant
Nitroguanidine (NGU)	Flash suppressor
N-nitrosodiphenylamine (N-nDPA)	Stabiliser (derivative of DPA)
RDX (Cyclonite)	Propellant
Resorcinol	Stabiliser, Plasticiser
Tetryl	Propellant
Triacetin	Flash suppressor, Plasticiser

Inorganic GSR particles can derive from the ammunition primer, the propellant powder, the cartridge case, the projectile jacket or its core, or from the barrel itself [25]. These particles are formed during the discharge of the weapon. As the temperature and pressure rise, the primer mixture and other sources of IGSR melt and form liquid droplets which subsequently solidify when exposed to lower temperature [26]. Due to this process, IGSR particles commonly develop a spherical shape [27]. However, it shall be noted that the spherical structure can be deformed by strong impact of the particles on a surface [28]. Ammunition primers contain initiating explosives, oxidising agents, fuel, and sensitiser. Lead styphnate is commonly present in the primer [4], largely replacing mercury fulminate which was previously used as an explosive [29]. Inorganic particles that incorporate the elements lead (Pb), barium (Ba) and antimony (Sb) are classified as "characteristic" for GSR [30, 31]. Thus, current GSR analysis is based on the detection of these characteristic inorganic particles. Recently however, numerous different types of lead free (LF) and heavy-metal free (HMF) primers have been commercialised and can increasingly be found in casework [32-34]. This reform is a result of increased concerns over airborne pollution and health problems related to the exposure to highly toxic levels of Pb and other toxic metals present in primers [35]. The replacement of Pb and/or heavy-metals has been accomplished by various manufacturing procedures: for instance enclosing the base of the projectile or the entire projectile with brass, copper or gilding metal; using a non-lead containing sintered metal for the fabrication of the projectile [33]; and replacing Pb, Ba and Sb from the primer mixture with other ingredients such as strontium, potassium-based oxidizers, calcium silicide or diazodinitrophenol (DDNP) [36]. Since these ammunitions do not produce characteristic GSR particles, i.e. particles incorporating

Pb, Ba and Sb, the detection of GSR based on the presence of these particles alone can lead to false-negative results [11, 32, 33]. To date, different elemental profiles of spherical particles produced by LF and/or HMF ammunitions have been elucidated. While LF Sintox ammunition formed particulates mostly containing Ti and Zn [32], the only metal detected in GSR particles from CCI Blazer® Lead Free ammunition was Sr [34]. Other studies found combinations of Al, Si, Cu, and Zn [33] or K, Al, Si, and Ca [35]. These studies indicate that elemental profiles of LF GSR particulates are in agreement with the composition of the respective primers. However, identification of GSR particles formed by these "green" ammunition is susceptible to higher rates of misclassification as the composition is not exclusive to firearm handling [37].

1.2 Screening Tests for GSR

Rapid tests to detect the presence of a substance are referred to as screening tests. These tests can be extremely useful when a large number of items or large surfaces have to be examined. Negative results for the presence of a substance can reduce the number of items to be analysed and therefore result in time and cost savings. Screening tests for GSR are colour/spot tests and have been applied since 1933 [4, 27]. Two famous examples are the "dermal nitrate test" and the "Griess test", which has been altered to become the "Modified Griess test". It is important to note, that these colour tests are not specific for GSR and other oxidising agents can produce a positive colour reaction. Few other colour tests have been invented for screening GSR. Some of them are targeting the metals present in the ammunition primer such as lead or copper [38, 39]. However, the questionable origin of these metals and the

introduction of LF and HMF ammunition primers challenge the application of these colour tests for GSR. The mentioned disadvantages of existing screening techniques for GSR demonstrate the requirements for additional chemical screening tests [4]. In current standard operating procedure (SOPs) for GSR investigations, screening tests for OGSR on hands are practically non-existing. Screening tests targeting IGSR are mostly applied to shooting distance estimation and bullet hole identification [40, 41].

1.3 GSR Collection

The analytical procedure for GSR starts with the collection of the particles. When planning the procedure, several factors have to be considered to determine the correct collection technique. These include the surface to be collected from, e.g. skin, clothing or hair, the nature of the compounds searched for and the technique that will be used for subsequent analysis [42]. The objective of a collection technique is to have maximum collection efficiency [9] and to ensure that the specimens can be prepared for the analysis quickly, easily and efficiently [43]. Traditionally used collection methods for GSR are tape-lifting, swabbing, and vacuum lifting.

The process of tape-lifting involves dabbing the surface of the pertinent object with an adhesive tape for a certain number of times or until the stickiness of the tape is lost. Inorganic particles, the focus of GSR investigations, are commonly collected by double-sided adhesive tape mounted on aluminium stubs [27], which is the most widely accepted collection technique for GSR [9, 27]. An example of a GSR collection kit can be seen in Figure 1-1. A great advantage of the use of so

called GSR stubs is that the stubs can directly be analysed by scanning electron microscopy with energy dispersive x-ray spectroscopy (SEM-EDX).

Figure 1-1: Gunshot residue collection kit with double-sided adhesive on aluminium stubs

Swabbing is the most common collection method of OGSR from hands in casework [4, 44], and can also be applied to clothing and smooth surfaces [45]. The collection process involves moistening a swab of a certain material with an appropriate solvent, wiping it repeatedly over the area of interest followed by extraction and if necessary, a clean-up procedure. Different materials, solvents and extraction techniques have reportedly been applied [20, 46-53]. The choice of the swab material and the solvent should be made considering the compounds of interest and the analytical technique to be used. Requirements of a swabbing system are efficient removal of the residue compounds from the area of interest, extraction of minimal interferences and high stability of the explosives in the solution for the time between the collection and laboratory analysis [54].

In vacuum lifting, an applied vacuum lifts GSR particles from the investigated surface. The particles can then be trapped in a tube and stopped by an incorporated filter [42]. GSR can then be extracted from the filter for subsequent analysis. Vacuum lifting is mostly applied to the collection from clothing, but has also been applied to collection from hands [55]. It is easy in operation and able to collect from a large area in a short time [4]. Advantages of GSR collection from

clothing is the long persistence of OGSR on the garment, e.g. NG has been detected on clothes five days after test firing [50].

The GSR collection techniques listed have been tested and optimised for either IGSR or OGSR and only limited research exists targeting the combined collection [56-59]. The combined collection and sequential analysis of IGSR and OGSR can address the limitations arising from the increased use of LF and HF ammunition and therefore increase the evidential value of GSR investigation.

1.4 GSR Analysis

1.4.1 *IGSR Analysis*

Analytical methods for the investigation of IGSR include neutron activation analysis (NAA) [60-62], atomic absorption spectroscopy (AAS) [63-66], and SEM-EDX [67-71]. Unlike NAA and AAS, which can only determine the concentration of several compounds in a specimen, SEM-EDX is able to provide elemental and morphological information of a single GSR particle [9]. This means SEM-EDX can identify if a particle is characteristic of GSR, with the added feature of being non-destructive making it the internationally accepted method for IGSR analysis [27]. The introduction of LF and HMF ammunition however, challenges SEM-EDX analysis for IGSR as this ammunition produces no characteristic GSR particles.

1.4.2 *OGSR Analysis*

Several methods using different analytical techniques have been developed for OGSR analysis. Requirements for the methods are good separation, high specificity, and sensitive detection [72]. Sensitivity plays a key role for the detection of

propellant powder components since in some propellant powders target compounds such as stabilisers are present at or around 1 % [73, 74]. Sensitivity demands are also tested when specimens are collected several hours (h) after the incident, with only small amounts of OGSR particles remaining on the shooter, e.g. in the nanogram (ng) range [50, 75].

Generally, the applied analytical methods include the separation of the organic compounds followed by their detection. Gas chromatography (GC) has been extensively applied to the analysis of OGSR [12, 13, 44, 58, 76-79]. In GC, the compounds are separated based on their interaction with the stationary phase in a column. The mobile phase is a carrier gas which is usually inert. After separation the compounds can be detected by a variety of different detectors including thermal energy analyser (TEA) [44], flame ionisation detector (FID) [76], nitrogen-phosphorus detector (NPD) [77], and mass spectrometric detector (MS) [13, 78]. GC-TEA has been reported to detect OSGR in the picogram (pg) range and is therefore mostly applied in casework [44, 58, 79]. One limitation of GC to OGSR analysis is the high temperatures applied. Some compounds present in OGSR, such as derivatives of DPA, are thermally unstable and decompose when exposed to these high temperature [4].

High performance liquid chromatography (HPLC) is a good separation technique for both volatile and non-volatile compounds. It therefore presents a more suitable method for the investigation of DPA and its derivatives. In HPLC, separation is based on the interaction of the compounds with the stationary phase in the column and the mobile phase. Mobile phases are solvent systems, which are selected based on the type of compounds being separated. HPLC has been applied to the analysis of OGSR with many different detection methods, such as ultraviolet

(UV) [80], MS [6], or in conjunction with a pendant mercury drop electrode (PMDE) as detector [81]. HPLC-PMDE was able to detect OGSR in the pg range and is therefore often encountered in casework [81].

Micellar electrokinetic capillary electrophoresis (MECE) has also been applied to OGSR detection. In MECE, the compounds are dissolved in an aqueous buffer solution containing charged micelles. A high electric field is applied to the solution resulting in the separation of the compounds due to different migration times in the capillary [11]. Though MECE achieves high resolution and short separation times [82], the sensitivity is unsatisfactory for casework applications [20].

More sophisticated methods including time of flight secondary ion mass spectrometry (TOF-SIMS) [83], tandem mass spectrometry (MS/MS) [15] or desorption electrospray ionisation coupled to mass spectrometry (DESI-MS) [59, 84] have also been applied to OGSR analysis. However, these methods might not always be available to the police.

Mass spectrometric techniques have been applied for both, IGSR and OGSR. An extensive review detailing the technical attributes of various currently available MS methods and their application to GSR analysis has recently been published as part of this project [85].

1.5 GSR Interpretation

Forensic practitioners often assist the judicial system by providing intelligence, investigative, technical, or evaluative reports in their area of expertise. The establishment of an evaluative report usually involves the determination of probability measures based on the forensic findings, data, expert knowledge and

case specific conditions [86]. This can involve the reconstruction and interpretation of events.

For event reconstruction, GSR can provide valuable information regarding various aspects such as the shooting distance estimation or identification of a bullet hole. For the interpretation, all available and relevant information, e.g. the suspect's occupation, activity, time since the discharge, possible contamination sources and other case circumstances should be considered to allow the formation of a robust, logic and informative report that can help the judicial system in reaching a decision about a case. Two different approaches to GSR interpretation exist, namely a "formal" approach and a "case-by-case" approach [27]. A "formal" approach focuses on the chemical composition and shape of GSR particles analysed by SEM-EDX. This approach can be challenged by the introduction of LF and HF ammunitions and thus the possible lack of characteristic GSR particles. A "case-by-case" approach on the other hand, can be applied to OGSR and IGSR and considers factors present at a crime scene by comparing residues found on a specimen to residues from a known source. Though analytical methods can detect the presence of GSR particles, they are not able to provide information about the source of given particles. In order to consider other possible sources of GSR particles, e.g. environmental sources as well as contamination, probability models, i.e. Bayesian networks, have been increasingly constructed and implemented in GSR interpretation [27, 87-89]. It should be noted, that Bayesian networks have only been applied to the interpretation of IGSR and are a relatively new approach to GSR interpretation.

Various aspects of GSR interpretation are based on the detection of characteristic GSR particles, e.g. the identification of a bullet hole or shooting

distance estimation, and are challenged by the introduction of LF and HMF ammunitions. The incorporation of OGSR into current GSR investigation protocols is desirable as it can provide additional information and assist when IGSR analysis is inconclusive.

1.5.1 *Discharge of a Firearm*

A common question asked in court is whether a suspect fired a firearm. Forensic analysts cannot provide the answer to this question easily. It is important to consider, that the simple detection of GSR on a suspect does not confirm that the suspect fired a gun [17]. Traditionally, the association of a person to a firearm-related event is based on the detection of characteristic GSR particles by SEM-EDX. However, as mentioned above, the presence of GSR can be a result of contamination with GSR components through occupational or environmental sources or simply being in the vicinity of the crime scene. The possibility of linking a person to a firearm-related event based on the quantity of particles found on the person has been examined using Bayesian networks [88, 90]. It has been shown, that in some cases the quantity of particles on shooters and bystanders is so similar, that it is impossible to distinguish shooters and bystanders [90].

1.5.2 *Time since Discharge*

The analysis of OGSR has been successfully applied to determine the time since discharge. In a series of studies, organic residues were collected from the inside of barrels of shotguns [76], rifles [91], pistols and revolvers [92], and of spent cartridges [93] with solid phase microextraction (SPME) and analysed by GC-TEA and GC-FID (confirmation of identification by GC-MS), since the combination of these methods can detect a broad range of combustion products. In this method, the

estimation of time since discharge was based on the escape rate of gaseous and other volatile organic residues as a function of time. This approach generated a sound estimate for the time since discharge for shotguns, e.g. whether it was fired within two to three days, one to two weeks ago or more than three weeks ago [76]. Poor results were obtained for rifles since these firearms produce less volatile compounds [91]. For pistols and revolvers the amount of volatile compounds was so low, that the escape rate could only be measured for a couple of days up to two weeks after discharge [92]. It is important to consider, that different factors, such as storage conditions, temperature, cleaning of the barrel after shooting, and number of shots fired can influence the results. These conceptual drawbacks prevent the assessment of the evidential value of a given measurement in terms of determining the time since discharge. Therefore, a novel method based on the assessment of likelihood ratios has been recently developed [94]. Parameters were estimated from shootings carried out with seized reference material and data received through SPME coupled with GC-MS. The time since discharged was questioned by inserting these parameters in a probabilistic model to a hypothetical scenario.

For IGSR the time since discharge cannot be determined in the same way as for OSGR. However, another approach can be applied. In GSR interpretation the persistence of particles plays an important role. It has been showed, that IGSR stay longer on garments than on skin [4, 9, 95, 96] and that larger particles are lost more quickly than smaller ones. Information about the activity of the suspect combined with available knowledge on the persistence of given particles can be used to approximate the time since discharge (within h) [4, 62].

1.5.3 *Linkage of Firearms and/or Ammunitions*

Inorganic GSR are formed when vaporised bullet and primer materials condensate after being released from the firearm [28]. Since different types of ammunitions contain primers with specific compositions, they are assumed to generate different IGSR compositions. Various studies have investigated the influence of the weapon and ammunition type on the production of IGSR and their elemental composition [97, 98]. It was confirmed that ammunition types strongly influence the composition of the formed particles and that mixed compositions particle can assist in the linkage of ammunitions to IGSR. The nickel content, for instance, can vary greatly and it was found that Sellier & Bellot, Prague, ammunitions result in a larger proportion of GSR particles containing nickel than Geco ammunition [97]. Furthermore, the caliber was found to strongly influence the formation of IGSR particles found in cartridge cases [98] as can be seen in Figure 1-2.

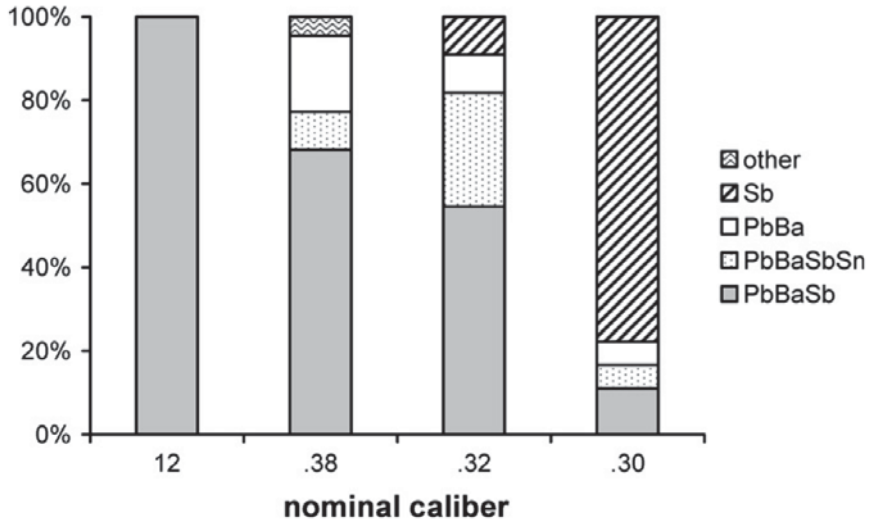

Figure 1-2: Prevalence of inorganic composition found in cartridge cases collected during 2008-2010. Overall, 201 cartridge cases from 69 different ammunitions were submitted for analysis corresponding to 49 criminal cases [98].

Furthermore, the distribution of IGSR particles can give an indication about the weapon type [99, 100]. As the construction of firearms greatly influence the plume formation, the particle distribution can also differ. This is especially the case

for the deposition of GSR on the shooter since the possible sources for this deposition are mainly the ejection mechanism of the spent cartridge of pistols and the notch for the trigger and/or gap between drum and barrel in revolvers (Figure 1-3) [100].

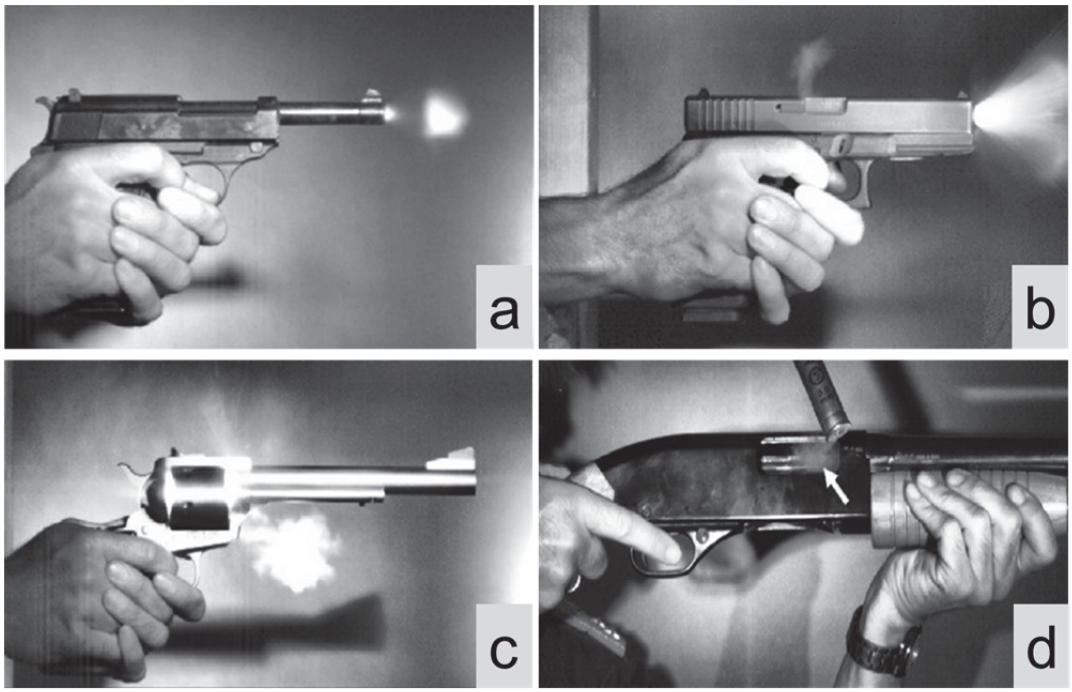

Figure 1-3: Plume formation influenced by the weapon construction. a: pistol-Walther P38 Series (gases and particles at the muzzle begin forming a cone-shape); b: pistol-Glock 17 pistol (vertical jet from the ejection port); c: revolver-Casull 454 (strong emission from the drum/barrel gap); d: shotgun-Pumpgun Winchester Defender 1300 (cloud from the ejection port) [100].

For cabine-type rifles and pump-action shotguns, the probability of finding IGSR on the hands of the shooter greatly depends on whether the chamber/breech is opened for reloading especially since the muzzle is rather distant from the shooter [100]. However, various factors such as different ways of holding a handgun [101] can influence the particle distribution and have to be taken into account when interpreting the findings. In summary, features of IGSR such as their composition and dispersion depend on the type of ammunition and caliber as well as the firearm construction and can therefore – under careful consideration of all circumstances – provide an indication about ammunition and/or firearm used [68].

The composition of smokeless powders is very diverse. Identifying and quantifying organic compounds present in smokeless powders can potentially enable forensic scientists to distinguish the different powders [102]. Since the composition of smokeless powders after burning is similar pre and post discharge, linkage of smokeless powder to OGSR can be achieved by comparing the composition of additives present in smokeless powder and OGSR [13, 103, 104].

In comparison to OGSR, the interpretation of IGSR analysis for linking residues to ammunition is challenging [25, 100]. One reason for this is the so-called memory effect. Ammunition used in previous shootings can leave traces and therefore distort the identification of ammunition used in the actual shooting. This effect is much stronger for ammunition primers than for propellant powder. For OGSR, remaining traces are very small, e.g. 1.5-7.5 % [105] and can only be found after the first discharge. It has been reported that even when present, OGSR traces from previous shootings are not in sufficient high concentrations to result in misidentification of stabilisers or the composition of the powder [106]. Changing the primer type does not result in any consequences for OGSR [105, 107]. For IGSR however, the memory effect is very strong and can lead to misidentification of the ammunition primer. Hereby, the construction of a firearm is generally assumed to have a great influence on the memory effect. The gap between the cylinder and the barrel of a revolver, for instance, can have a strong influence on whether the memory effect is more or less pronounced [98]. Even when a weapon has been cleaned in order to eliminate this effect, it has been relatively difficult to match IGSR and the ammunition used [25, 98, 108].

1.5.4 *Occupational and Environmental Sources*

As previously mentioned, IGSR particles incorporating the elements Pb, Ba and Sb are considered characteristic for GSR. However, recent research has questioned the origin of these particles. Environmental sources as well as occupational ones, such as brake linings [109, 110], fireworks [111-113], paints and cartridge-operation occupations [114, 115] have been encountered as possible sources of IGSR-like particles. As SEM-EDX analysis depends on the detection of Pb, Sb and Ba in discrete inorganic particles, these sources can result in false positive results [11, 32, 33].

For OGSR, NC could be assumed as being the most significant compound as it can be found in single-, double- and triple-base powders. However, its widespread presence in many consumer products, such as lacquers, varnishes, celluloid films, printing, and pharmaceutical products [53] reduce its evidential value drastically.

The most commonly detected and analysed compounds of OGSR are the propellant NG and the stabilisers EC and DPA and its derivatives [116]. However, NG is only present in double- and triple-base smokeless powder and its detection does exclude single-base powders [17]. Therefore, most of the analytical methods are based on the detection of DPA, its derivatives, EC and MC [4]. DPA can be found in rubbers, dyes, explosives, plastics, and pharmaceuticals due to its function as an antioxidant [16, 50]. It is also used as control medium of superficial scald in apples and pears [117]. Therefore, its presence is only significant when detected in combination with its derivatives [6]. EC and MC are reported to be two of the most characteristic OGSR compounds [12]. Grapefruit, orange and pear skins however, have been reported to give a peak at the same retention time as EC when swabbed by a cotton swab and analysed by HPLC in conjunction with electrochemical

detection [117]. This issue might be overcome by the use of analytical methods with the ability to identify compounds such as MS or through the use of two orthogonal methods.

In summary, it is desirable to apply a thorough analytical method capable of detecting a wide range of OGSR compounds as this can potentially increase the evidential value of OGSR in court.

1.6 Contamination

Contamination is a limiting factor for the interpretation of GSR analysis. For IGSR, pollution, defined as the introduction of traces not related to the case by personnel involved in crime scene investigation [118], has been documented to occur through secondary transfer from police vehicles or police officers [119-121]. A study in California demonstrated that 7 % of non-shooting police officers had PbBaSb particles on their hand surfaces, however no officer had more than one particle [122]. On the other hand, police officers from special units actively handling multiple types of weapons showed higher amounts (12 %) of PbBaSb particles with the main source of contamination being the gloves of the officers [119]. Higher amounts of PbBaSb particles were found in Swedish police cars and on crime scene investigators (25 % positive) [123]. Background contamination, which covers all non-pertinent traces present at the crime scene prior to the arrival of first responders, has been recorded on bystanders transferred during a shooting or through tertiary transfer such as hand shaking [124]. For OGSR secondary transfer is less common, however a study in Pittsburgh reported quantifiable amounts of EC on two out of 70 specimens collected from various surfaces of a jail cell and police station and

volunteers undergoing a simulated arrest scenario [125]. The relatively low occurrence of OGSR has been explained by their lipophilic character, which can result in the adhesion of the residues to skin. This adhesion makes OGSR less prone to secondary transfer [126]. Modern collection processes applied to casework are developed with a focus on minimising the possibility of contamination and demonstrating the absence of GSR compounds and particles, e.g. with taking blank specimens from the police vehicle the suspect has been transported in.

1.7 Persistence

The persistence of GSR on a person is of high value for the interpretation of analytical results. While a long persistence of GSR may allow for detection even after a longer time since firearm discharge, the linkage to a specific shooting may be difficult. Residues could originate from a previous shooting and not from the crime in question. A short persistence of GSR on the other side can provide forensic scientists with the possibility to connect the residues to a specific event. However, it can also result in no detection at all [4, 127].

The amount of IGSR retained on a person continuously decreases with time. This is caused by activities of the person and not by chemical degradation [55, 126]. It is assumed that OGSR persist longer on the skin than IGSR due to their lipophilic character and therefore adhesion to skin via intermolecular forces [126].

Studies of OGSR persistence give variable results and have reported persistence times from 1 h (NG) [13] to 4 h (DPA) [126], 8 h (MC) [15], 12 h (MC) [84] and 20 h (NG) [128] after shooting. This might be a consequence of different laboratory conditions, collection processes or analytical methods. Another possible

explanation is the various evaporation times for the different compounds of interest and their skin permeation [127]. This would also justify the longer persistence of OGSR on clothes than on skin [50, 55, 129].

The variability of results suggests that the persistence depends on the surface of the pertinent object and the collection and analytical method applied. It is obvious, that methods with higher recovery efficiency and sensitivity are able to detect OGSR longer after a shooting than methods with lower recovery and sensitivity. However, these methods can also result in a more complex interpretation of the analytical results as the risk of collecting and detecting GSR-like material is increased when method sensitivity improves.

1.8 Conclusion

Gunshot residue analysis is commonly achieved by collecting specimens using GSR stubs which are directly analysed using SEM-EDX. The application of this technique to GSR is based on the detection of Pb, Sb and Ba in discrete IGSR particles. However, this method is challenged by the recent introduction of LF and HMF ammunitions as these ammunitions do not produce characteristic particles and can result in false negative results. Another limitation of GSR analysis involves the non-specific origin of IGSR particles. Environmental and occupational sources, such as brake linings, fireworks, paints and cartridge-operated occupations have been encountered as possible sources of IGSR-like particles. Moreover, the interpretation of IGSR analysis is difficult due to the possibility of contamination by secondary transfer and a strong memory effect. These limitations might be overcome by the combination of IGSR and OGSR analysis since analysis of OGSR can provide

additional information complementary to the one obtained by SEM-EDX. Furthermore, OGSR analysis may be helpful when IGSR analysis is challenged, and could be used as an additional source of information. In order to achieve the collection and analysis of both, OGSR and IGSR, research incorporating both processes into a single procedure is needed.

1.9 Previous Research Focusing on Combined IGSR and OGSR Analysis

Few studies have been published focusing on a collection and detection protocol for both, IGSR and OGSR. Generally, this can be achieved through two different routes.

One possible approach is the sequential analysis of OGSR and IGSR directly from the collection device. In this case, the analytical technique used for OGSR must involve direct surface analysis from the device, e.g. DESI [59, 84]. This ionisation technique enables the in-situ analysis of various surfaces under ambient conditions. DESI-MS/MS has been applied to the analysis of MC and EC from hands, hair, glass, rubber gloves, leather gloves, towel, medical gauze, and adsorbent cotton [84] and DESI-MS to the analysis of DPA, EC, and MC from smokeless powders and stubs after shootings [59]. A drawback of DESI for OGSR analysis is the relatively low sensitivity assumedly due to the adhesive surface of the GSR stub which limits its case applicability.

A recently published study describes the development of a modified collection device enabling the collection and analysis of both, OGSR and IGSR [37]. One half of the modified stub was analysed for IGSR by laser ablation inductively coupled plasma mass spectrometry (LA-ICP-MS), while the other half underwent

Raman spectroscopic analysis for OGSR analysis. It should be noted, that LA-ICP-MS analysis with laser spot size diameters exceeding the GSR particle sizes (in this study 160 µm) fails to resolve adjacent small particles, e.g. 5 µm diameter. Careful data interpretation is required to avoid incorrect conclusions. For example, adjacent particles containing individual heavy metal species may appear to be a single entity with the characteristics of GSR.

Another study also used a modified stub, whereby half of it was covered with paraffin film and polytetrafluoroethylene (PTFE). This half was removed after collection, extracted and analysed using liquid chromatography coupled to time of flight mass spectrometry (LC-QTOF-MS) [56]. However, when applying this approach it is possible to lose valuable OGSR information from the other half of the stub that is analysed by SEM-EDX.

An extraction protocol for OGSR from double-sided adhesive tapes on aluminium stubs has been developed [57]. This extraction was intended to be applied to the stub after SEM-EDX analysis of IGSR. Compounds of interest were NG, 2,4-DNT and 2,6-DNT. Extraction with organic solvents resulted in co-extraction of the adhesive and compounds present in the epidermis, which interfered in the analysis of the compounds of interest. Therefore, an aqueous solution was used, which required high temperature and relatively long sonication. Extraction efficiencies for the compounds varied between 30-90 %. This procedure was broadened to the extraction of 2,4,6-trinitrotoluene (TNT), hexahydro-1,3,5-trinitro-1,3,5-triazine (RDX) and pentaerythritol tetranitrate (PETN) [58], which generated very low recovery rates due to its poor water solubility. Commonly used adhesive tapes on aluminium stubs require carbon coating prior to SEM-EDX. When this extraction protocol was applied to the tape

after carbon-coating and IGSR analysis by SEM-EDX, the extraction efficiency was highly limited, e.g. no NG could be detected by GC-TEA. Hence, optimisation of the proposed extraction protocol is required for casework application and suitability of conductive tapes to the extraction protocol require further exploration.

Recently swabbing and tape-lifting have been compared in their suitability for the collection of IGSR [130]. Though stubbing was found to more efficient for the collection and subsequent analysis of IGSR, it was noted that swabbing could be a good alternative if propellant analysis is required. In this study, however, only one swabbing kit was investigated. It is therefore suggested to enlarge the study of the suitability to IGSR collection to a broader range of different swabbing kits used for OGSR collection.

A vacuum technique for the collection of organic and inorganic GSR from clothing has been developed [131]. After an automated clean-up system and pre-concentration of the OGSR, the residues could be detected by GC-MS or HPLC-PMDE after a single shot. The IGSR particles could be collected and extracted from the same vacuum system and were successfully analysed by SEM-EDX [131]. However, when applied to casework specimens, only five positive results for OGSR and only one positive for characteristic IGSR out of 186 exhibits could be obtained. Extensive clean-up procedures were required, which are time and money consuming and decrease the recovery of GSR with every step involved. This presents an additional challenge to the casework application of vacuum lifting.

As can be seen, only very few research studies have been conducted focusing on collection and detection of both, IGSR and OGSR, that are truly feasible to be applied in casework. The small number and the unsatisfactory results demonstrate

the necessity for further research to overcome the limitations of current GSR analysis.

1.10 Research Aims

As outlined above, current SOPs for GSR investigation typically only target IGSR. However, analysis of organic compounds in GSR can provide additional information, complementary to results obtained by IGSR analysis.

This project focused on the development of SOPs for collection and detection of both OGSR and IGSR to overcome these limitations.

During this project several objectives were addressed:

- **To develop a screening technique targeting the organic explosives potentially present in OGSR (Chapter 2).**

  Previously developed screening techniques targeting OGSR suffer from different drawbacks including the lack of specificity and/or lengthy development procedures. A new portable screening device was developed based on the detection of energetic compounds potentially present in GSR by fluorescence quenching of pyrene on μPADs.

- **To develop a fast and sensitive preparation, screening and analysis method for dirty specimens (Chapter 3).**

  Complex matrices complicate the analysis of OGSR since compounds present in the matrices might coelute with target analytes or interfere with the baseline. In order to address these challenges, clean-up steps are conducted prior analysis. One of the commonly applied clean-up procedures is solid phase extraction (SPE) [6, 131].

An automated on-line SPE method for the detection of OGSR in dirty specimens was developed and optimised using the RapidFire®.

- **To develop and validate an analytical method for a broad range of organic compounds of OGSR (Chapter 4).**

Different methods have been developed for OGSR analysis. While MECE does not offer the required sensitivity and reliability for casework applications, GC is limited by the thermal decomposition of some compounds of interest. Ultra-high performance liquid chromatography (UHPLC) coupled with UV detection was selected because it is sensitive, suitable for the detection of volatile and non-volatile compounds and available in many operational laboratories such as the NSW Police Force. The development of an UHPLC-UV method is assumed to provide the police with a readily available detection method for a broad range of different organic compounds in OGSR.

The low concentration of OGSR observed in casework challenges the applicability of many analytical methods. To prove that the developed UHPLC-UV method is suitable for casework, it was necessary to validate the method determining its limit of detection and quantification, and test specimens collected from the firing range to prove the method's casework applicability.

- **To develop and compare collection and extraction protocols for both inorganic and organic residues (Chapter 5).**

Different collection techniques are applied for OGSR and IGSR. While IGSR are mostly collected by tape-lifting, OGSR, on the other hand, are commonly collected by swabbing. Few studies have been conducted to

develop a Combined Collection Procedure, which would result in one collection device applied to the simultaneous collection of IGSR and OGSR. To obtain optimum performance, different operational protocols were developed, optimised, and compared.

As OGSR concentrations in casework are relatively low, the developed procedure was validated with specimens taken at a firing range to prove their casework applicability.

- **To investigate the influence of storage durations on the degradation of OGSR (Chapter 6).**

The timely analysis of specimens after their collection is not always possible due to large number of specimens or limited instrument availability. Therefore, information about how long specimens can be stored without any loss of the compounds of interest is of great importance.

Gunshot residue stubs and swabs were tested over 63 days for the presence and amount of spiked OGSR in order to determine the stability of the target compounds over this time frame.

Chapter 2: DEVELOPMENT OF A PORTABLE SCREENING TECHNIQUE FOR OGSR USING μPADS

Chapter 2: DEVELOPMENT OF A PORTABLE SCREENING METHOD FOR OGSR USING μPADS

2.1 Background

During the investigation of firearm-related events, screening tests can be applied as a first step to rapidly indicate the likely presence of GSR, to estimate shooting distance [132-135], or to identify a bullet hole [5]. This has become increasingly important in view of the recent increase in international and domestic crimes related to firearms and explosives [4, 136].

The first chemical tests for GSR detection were colour tests targeting nitrates and nitrites in the residues [4], whereby the earliest (1933) is the so called “dermal nitrate test”, “paraffin test”, “Paraffin Gauntlet or Glove”, or “Gonzales test”. Liquid paraffin is sprayed or poured over the fingers, hands and wrists of the suspect with layers of cotton or other fabric in between. After cooling, the paraffin glove is lifted from the hand and treated with DPA in sulfuric acid [137]. The colour formation to a dark violet or dark blue is based on the reaction between DPA in sulfuric acid and nitrates and nitrites present in GSR. However, since this reaction is based on the oxidation of DPA, other non-GSR oxidising agents such as chlorates, dichromates, iodates, bromates, permanganates, or higher metal oxides may also produce a positive reaction and might therefore result in false-positives [4]. A study conducted by Aleksandar showed that out of 250 people who had not handled a weapon, 117 tested positive for the paraffin test [138]. As a result, the paraffin test is commonly not applied anymore. Another famous example is the Griess test which involves

nitrites in GSR being targeted by a primary aromatic amine in an acid solution. When nitrites are present, a diazonium salt is formed which then couples with α-naphthylamine to give a red azo dye [4]. Since α-naphthylamine is a carcinogenic compound, it has been replaced by a less harmful agent that is N-(1-naphthyl)ethylenediamine. This alteration is called the "Modified Griess Test" [139, 140].

Other colour tests target the metals potentially present in GSR. An examples is the sodium rhodizonate test for Pb residues [141], which is the most common and sensitive screening test and applied for the estimation of the shooting distance [40]. Another examples is the dithiooxamide test [142] resulting in a dark-green to black colour when copper is present and blue-violet for nickel.

A drawback of the aforementioned colour tests is their non-specificity for GSR, which can potentially lead to false-positive results for test targeting OGSR. Furthermore, LF and HMF ammunition can produce false-negative results for screening tests targeting metals. Therefore, new screening techniques for the organic GSR compounds are required that allow for fast and sensitive detection and do not affect subsequent OGSR and ISGR analysis. This means that the collection device and the screening substance are not permanently reacting with IGSR particles or OGSR and allow their analysis by SEM-EDX and for example HPLC.

Recently, the use of luminescent markers specific to the detection of GSR has been proposed [143-145]. These markers were added directly to the gun powder, whereby weight ratios were optimised to avoid a decrease in ammunition performance [144]. Promising results were obtained with luminescent GSR observed on shooters' hands, firearms, and along the firing range up to 9 h after shooting and after 16 hand washes [144]. However, increased costs are associated with the

introduction of these markers to ammunition and it is questionable whether manufacturers will adopt the proposed method.

Fluorescence methods have been applied to in-field detection of explosives potentially present in GSR due to their sensitivity, selectivity, simplicity and low cost instrumentation [10, 146-150]. Polymer films have been used as fluorophore sensors to increase the sensitivity of the detection. However, these films are difficult to synthesise and are somewhat limited to the detection of explosives in an aqueous solution [149, 150]. This can be problematic as some explosive compounds are not soluble in aqueous solutions.

Additionally, various "Lab-on-a-chip" devices, particularly capillary electrophoresis-based electrochemical microsystems, have been used in the field of explosive detection [151]. These microsystems are advantageous due to their portability, compact size, relatively easy integration with other systems, low cost and low sample/reagent consumption, and have rapid analysis times [151].

Microfluidic paper-based analytical devices (µPADs) present a new generation of microfluidic devices. Filter paper is used as a fabrication substrate on which hydrophobic microfluidic patterns are imparted to control fluid movement and compartmentalise chemical reactions. Various methods may be employed to construct µPADs including photolithography [152], plotting [153], paper cutting [154], plasma oxidation [155], inkjet printing [156], inkjet etching [157, 158] and wax printing [159-161]. In comparison to other microanalytical devices, µPADs have particular benefits such as no requirement for pumps, adsorption of aqueous fluids, availability in a range of thickness, easy disposal, flexibility and suitability for colorimetric tests [162]. This study focused on the development of a screening

method based on fluorescence quenching on μPADs for the explosive compounds potentially present in GSR.

2.2 Materials and Methods

2.2.1 *Chemicals and Reagents*

Terasil Blue, Orange G and Acid Green were obtained from Sigma Aldrich (St. Louis, MO, USA) in analytical grade. Pyrene (Tokyo Chemical Industries, Tokyo, Japan) and sodium dodecyl sulphate (SDS) (BDH Laboratory Supplies, Poole, England) were also used in analytical grade. Explosives, i.e. trinitrobenzene (TNB), TNT, 2,4-dinitrotoluene (2,4-DNT), 4-amino-2,6-dinitrotoluene (4-A-2,6-DNT), dinitrobenzene (DNB), RDX, PETN, and 2,4,6-trinitrophenylmethylnitramine (tetryl), at a certified concentration of 1000 microgram/millilitre (μg/mL) in acetonitrile (ACN), were obtained from ChemService (West Chester, PA, USA).

Ultrapure (UP) water (18.2 $M\Omega cm^{-1}$) was used throughout all experiments and obtained from a Sartorius 611 water purification system. Methanol (MeOH), ethanol (EtOH), propanol, hexane and ACN were analytical grade (Sigma-Aldrich, Australia). Coffee, tea, Coca Cola™, beer, wine, milk and Mylanta Antacid Dual Action, a stomach antacid, were purchased at Australian supermarkets.

Colour solutions were obtained by dissolving 1 milligram (mg) of Terasil Blue, Orange G and Acid Green each in 1 mL water.

All explosives were stored in an explosion proof fridge (4 °C) securely sealed in appropriate glass containers.

2.2.2 *µPAD Fabrication*

The µPAD fabrication consisted of three steps: (i) Designing the pattern using commercial graphics software; (ii) Wax printing of the designed pattern on filter paper which could be directly inserted in the paper tray of the printer and; (iii) Heating the paper to generate hydrophobic barriers by melting the wax.

CorelDraw 5 software (Corel Corporation, Ontario, Canada) was used to design the microstructures of the µPAD prior to printing the designs on Whatman® 185 millimetre (mm) diameter filter paper grade 40:8 µm (Ashless Grade, Ash 0.007 %). The µPADs were printed with a FujiXerox ColorQube 8870 colour printer (Xerox, Australia). The printed wax channels were melted into the filter paper with a swing-away heat press (GEO Knight & Co, Inc) with pressure and temperature control. An EZ4D microscope (Leica) was used to measure the width of the wax lines. The channel width selected in the software was referred as W_N, the width after printing as W_P, and the width after heating W_H [39].

2.2.2.1 Fabrication Process Optimisation

Different heating temperatures and durations were tested and the process optimised. The tested temperatures included 50, 60, 100, 140, 150, 175, 200 and 250 °C whereby the duration was kept constant at 2 minutes (min).

Furthermore, different heating times were tested ranging from 30 seconds (sec) to 7 min whereby the temperature was kept constant at 150 °C.

2.2.2.2 Wax Barrier Optimisation

Lines of varying widths and colours were printed to evaluate the extent of spreading when heated at 150 ºC for 5 min. The lines' W_N ranged from 0.100 mm to 1.000 mm

with increments of 0.100 mm. All lines were designed and printed in all colours available on the printer; cyan, magenta, yellow and black (colours present the CMYK colour model) and green as a mixed colour. The spreading of the different colours was examined by measuring W_P and W_H of the lines under the microscope. Hydrophobic barriers were tested by generating circles of different colours with 5.000 mm diameter and WN ranging from 0.050 to 0.450 mm. Five microlitre (µL) of a solution of the Terasil Blue, Orange G and Acid Green solutions were deposited inside the wax barriers. Circles with larger diameters and widths (1.100 mm diameter and 0.600 mm W_N) were placed around the inner circle in order to stop liquid from spreading over the filter paper (see Figure 2-8).

2.2.2.3 Influence of Solvents on Wax Barriers

The possible influence of organic solvents on the wax barriers was tested by depositing 5 µL of hexane and MeOH separately in magenta wax circles of 5.000 mm diameter and 0.200 mm W_N, letting the organic solvents dry and applying organic solvent:water mixtures as in the previous experiment.

2.2.2.4 Optimised µPAD Design

After optimisation all µPADs were designed with magenta circles of 5.000 mm diameter and 0.200 mm W_N.

2.2.3 *Pyrene Application*

Since the wax barriers on µPADs are hydrophobic, pyrene had to be applied in an aqueous solution. The relatively low solubility of pyrene complicated this process and different parameters were tested and optimised to overcome this limitation.

2.2.3.1 Increasing the Temperature

A saturated solution of pyrene in water was heated for 30 min to 80 ºC. This solution was filtered using a glass funnel and filter paper and 5 µL of the clear solution were deposited on a magenta circle of 5.000 mm diameter and 0.200 mm W_N and tested for its fluorescence using the VSC 6000.

2.2.3.2 Surfactant Additive

500 mg SDS were added to 100 mL of a saturated solution of pyrene in water. The solution was stirred until every SDS was dissolved and then filtered. Five µL of this solution were deposited on a magenta circle of 5.000 mm diameter and 0.200 mm W_N. Fluorescence of the solution was tested using the VSC 6000.

2.2.3.3 Solvent Ratios

Organic solvents (MeOH, EtOH, propanol, and ACN) were mixed with water in ratios from 10:90 (organic solvent: water) to 100 % organic solvents in increments of 10 %. The mixture was coloured with Terasil Blue (1 mg/mL) and 5 µL applied to magenta circles of 5.000 mm diameter and 0.200 mm W_N.

2.2.3.4 Concentration of Pyrene

Different solutions of pyrene in MeOH:water (80:20) were prepared with concentrations of 0.05 mg/mL, 0.1 mg/mL, 0.25 mg/mL, 0.5 mg/mL, 0.75 mg/mL, and 1 mg/mL. Two µL of these solutions were deposited on magenta circles of 5.000 mm diameter and 0.200 mm W_N. The fluorescence of the different solutions was tested using the VSC 6000. The final process of the µPAD fabrication and fluorophore application is shown in Figure 2-1.

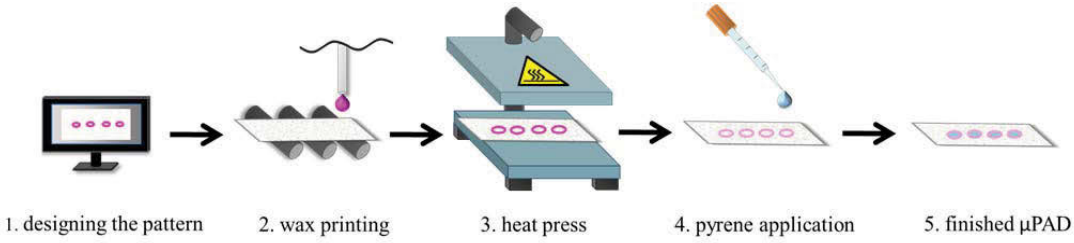

Figure 2-1: Fabrication process of the microfluidic paper-based analytical device (µPAD) and the application of pyrene (fluorophore) on it. The process consists of: 1. designing a µPAD pattern on the computer; 2. printing the pattern on filter paper; 3. heating the printed wax on the paper using a heat press in order to create fully functioning hydrophobic barriers; 4. pipetting pyrene (in 80:20 MeOH:water) to finally create the finished µPAD (5.).

2.2.4 *Detection*

A Video Spectral Comparator VSC 6000 (Foster+Freeman Ltd, England) was employed for fluorescence detection. The instrument contains a high-resolution colour camera, zoom lens, a range of viewing filters, and multiple illumination sources from UV to visible to infrared wavelengths. Fluorescence and fluorescence quenching were visually detected on-screen by exposing the µPAD to an excitation wavelength of 365 nanometre (nm).

2.2.5 *Fluorescence Quenching*

A pyrene solution was prepared by dissolving 2.5 mg of pyrene in 4 mL MeOH. This solution was sonicated for 5 min followed by the addition of 1 mL deionised water producing a 0.5 mg/mL pyrene solution.

2.2.5.1 Preliminary Test

On the wax printed circles, 2 µL of the nine different explosives in concentration of 1000 ppm were pipetted and the fluorescence detected using the VSC 6000.

2.2.5.2 Sensitivity Test

Explosives (2 µL) were applied to the pyrene treated circles in concentrations of 100-1000 parts per million (ppm) with increments of 100 ppm. The limit of detection (LOD) was tested by examining the fluorescence quenching of the different concentrations.

2.2.5.3 Selectivity Test

Eight commonly available consumer products, i.e. coffee, tea, coke, beer, wine, milk and Mylanta Antacid dual action , an anti-acid medication product, were deposited (2 µL) on the pyrene treated circles and the fluorescence tested.

2.2.6 *Portable Explosive Detector Prototype*

An in-house prototype µPAD reader device was built based on the electronic circuits shown in Figure 2-2. All electronic components were procured from Element 14 (au.elemtn14.com). The UV light-emitting diode (LED) (365 nm) was a surface mount device type with 3 W power. The sensor was a 5.000 mm ambient light photodiode (Vishay, TEPT5700).

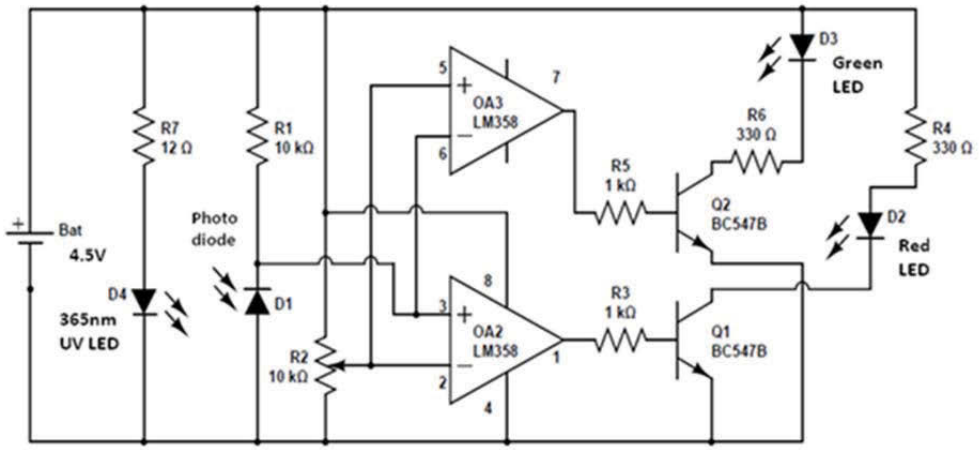

Figure 2-2: Electronic diagram of the microfluidic paper-based analytical device reader (Bat = battery; D1-D4 = photo (D1), red (D2), green (D3) and ultraviolet light-emitting (D4) diodes; OA2 LM358 and OA3 LM358 = dual operational amplifiers (8 pin integrated circuit); Q1 BC547B and Q2 BC547B = bipolar transistors; R1-R7 = resistors with 10 (R1 and R2), 1 (R3 and R5), 330 (R4 and R6) and 12 (R7) kiloohms (kΩ)).

2.3 Results and Discussion

2.3.1 *µPAD Fabrication*

Wax printing was used to generate hydrophobic barriers as it is easy and cost effective [159, 160], requires just very small sample volume [159], is time efficient, with the whole process taking 5-10 min, [160]. It allows for the generation of patterns in different colours to tune channel widths and hydrophobic properties. Figure 2-3 illustrates the product of wax printing in which the wax lines are spread laterally and vertically after controlled heating and pressure application [159]. Vertical spreading creates the hydrophobic barriers, whilst lateral spreading decreases the sharpness of the channel defined by the barrier and also broadens the width of the barrier [159]. During the fabrication process fibres in the paper tend to be more horizontally aligned rather than vertically and spreading is quicker along the fibres, the process of lateral spreading is usually more extensive [159].

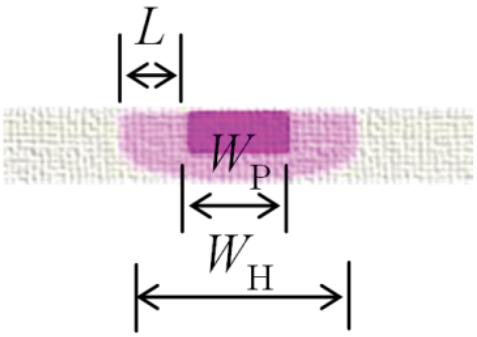

Figure 2-3: Schematic illustration of the spreading process of the wax, where $W_H = W_P + 2L$ with W_H representing the width after heating, W_P the printed width and L the distance between the spreaded wax and the edge of the printed line, adapted from [159].

The resulting channel width W_H after heating is the sum of the original printed channel width, W_P, and twice the distance which the wax spreads from the edge of a printed line, L. The spreading characteristics of the wax are likely to be governed by the wax matrix as well as the components which imparts colour. The heating procedure was initially optimised. Heat press temperatures ranging from 50-250 °C were tested, whereby the time was kept constant for 2 min. With temperatures over 200 °C, the paper discoloured slightly yellow, which was a sign that the paper started to char (Figure 2-4).

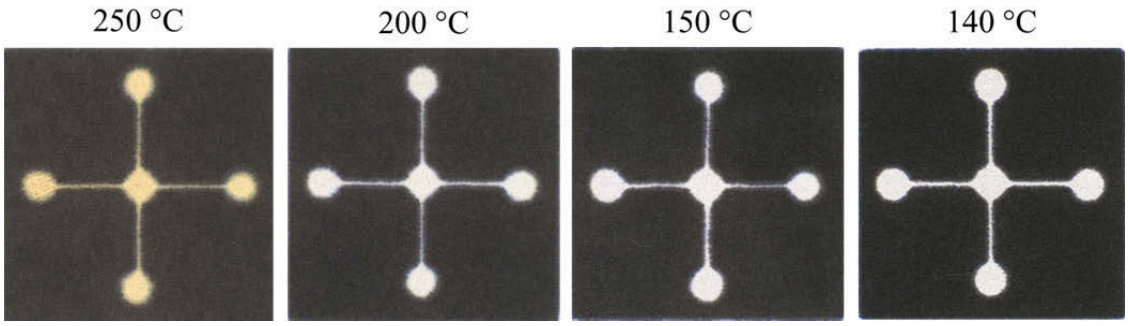

Figure 2-4: Same microfluidic paper-based analytical device design heated at four different temperatures for 5 min. Heating temperature starting from the left side: 250, 200, 150, and 140 °C.

Temperatures below 150 °C produced inconsistent melting of the wax leading to the selection of 150 °C as optimum temperature as the wax melted completely, however no burning of the paper was observed.

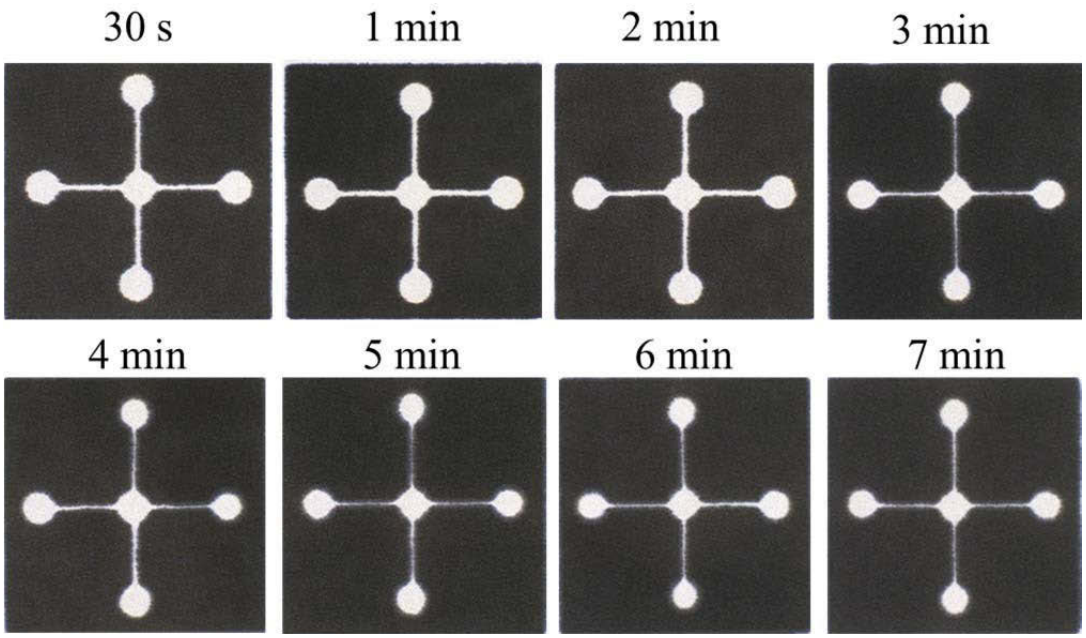

Figure 2-5: Identical microfluidic paper-based analytical device design heated at the same temperature (150 °C) for different times (top line from left: 30s, 1 min, 2 min, 4 min; bottom line from left: 4 min, 5min, 6 min, 7 min).

Of the different times tested (30 sec to 7 min), 5 min provided sufficient time for the melting of the wax and the most repeatable results since the wax channel width did not change when heated for 5 min or longer (Figure 2-5). Therefore, the heating process was kept constant for the entire study at 150 °C for 5 min, which is consistent with a previous study from Lu et al. [160]. As there was no change in the width of the wax channels when heated to temperatures below 60 °C (Appendix I), this temperature was set as maximum storage temperature. Consequently, the fabricated µPADs could easily be kept at ambient temperature even in warmer climates. For every colour, horizontal and vertical lines from 0.100-1.000 mm W_N were measured after printing and after heating (the design can be found in Appendix II) at three different positions as indicated in Figure 2-6. The corresponding data is presented in Appendix III. Figure 2-6 illustrates the differences in the lateral spreading for vertical lines with 0.300 mm W_N measured

after printing (upper line) and after heating (lower line). The corresponding data is presented in Table 2-1.

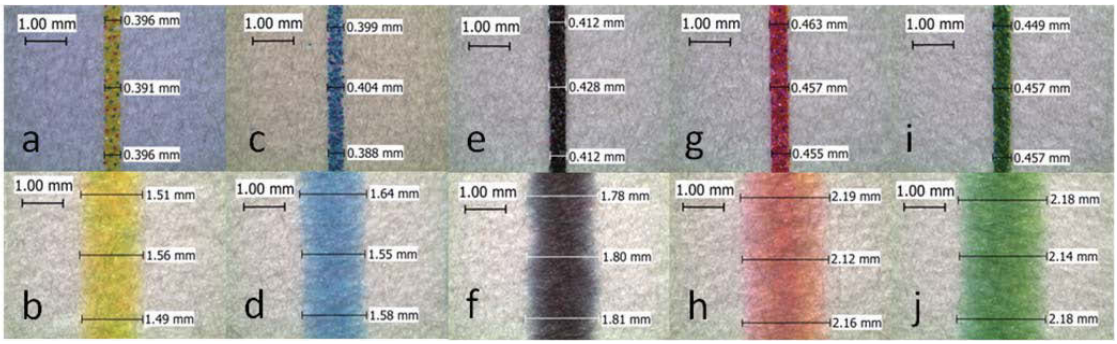

Figure 2-6: Upper line: Printed lines with 0.300 mm W_N using a FujiXerox ColorQube 8870 colour printer, whereby W_N represents the nominal width. Lower line: Printed lines after heating for 5 min at 150ºC using a swing-away heat press (GEO Knight & Co, Inc). Colours tested were yellow (a, b), cyan (c, d), black (e, f), magenta (g, h) and green (i, j). The lines were measured and the pictures taken with an EZ4D microscope (Leica).

Table 2-1: List of the width before (W_p) and after heating (W_H) of vertical lines with 0.300 mm W_N (nominal width) at 150ºC for 5 min using a swing-away heat press.

Colour	W_p [mm]	W_H [mm]
Yellow	0.394 ± 0.003	1.520 ± 0.040
Cyan	0.397 ± 0.009	1.590 ± 0.050
Black	0.417 ± 0.011	1.800 ± 0.020
Magenta	0.458 ± 0.005	2.160 ± 0.040
Green	0.454 ± 0.005	2.170 ± 0.030

Yellow displayed the smallest spread, followed by cyan, black, magenta and green. This trend was consistent for every colour from 0.100 to 1.000 mm W_N with increments of 0.100 mm (Appendix II). A linear relationship between heated and nominal width was observed for all wax colours; however with different slopes (Figure 2-7). It can be seen, that though cyan displayed increased spreading compared to yellow at nominal widths between 0.100 and 0.700 mm, yellow spread more than cyan starting from 0.800 mm W_N. The linear relationship indicates that the printing and heating process is predictable across these widths.

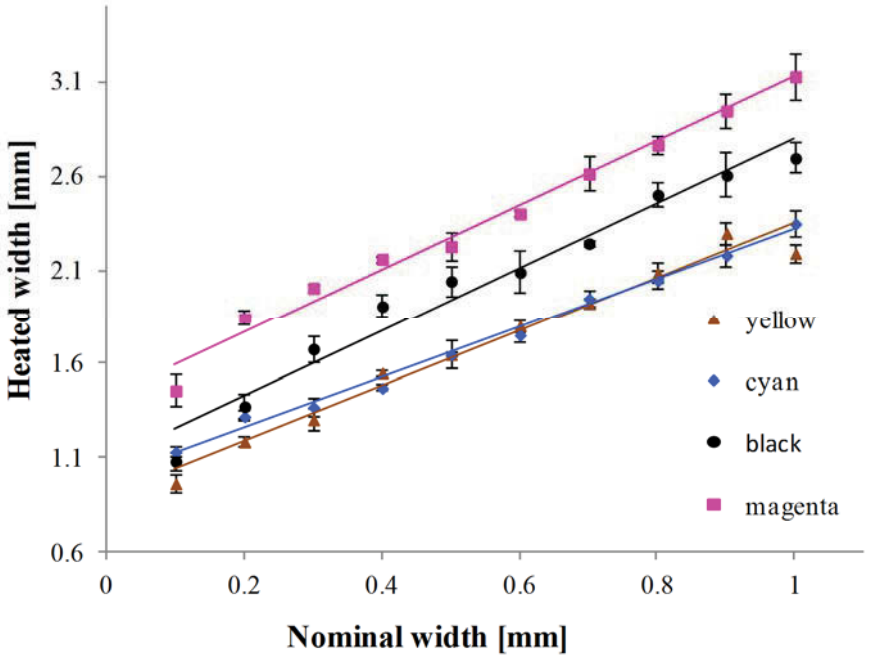

Figure 2-7: Nominal widths against widths after heating for the CMYK colours present in the four different solid inks used in the ColorQube 8870 colour printer.

The quality of hydrophobic barriers was optimised by determining the smallest W_N required for producing fully functioning hydrophobic barriers for every colour present in the four solid inks used in the printer (CMYK colours) plus the colour green representing a mixed colour. Terasil Blue solution (Figure 2-8), Orange G solution and Acid Green solution (Appendix IV) were deposited in circles of varying W_N (from 0.050-0.450 mm) and colour (Figure 2-8, Appendix IV) [159]. The "high" volume of 5 µL (forming a convex meniscus on the paper surface) was chosen as it could fully fill the inner and outer circle.

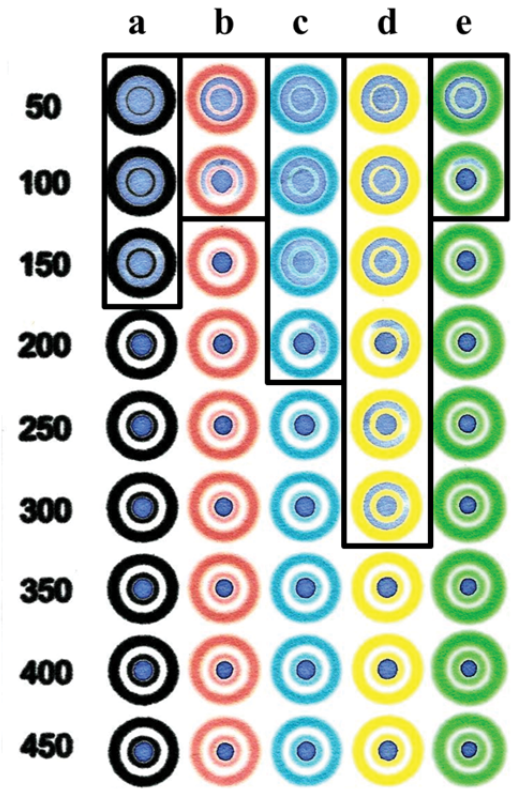

Figure 2-8: Coloured hydrophobic circles in black (a), magenta (b), cyan (c), yellow (d) and green (e) with minimal widths of the inner circle from 0.050 to 0.450 mm with increments of 0.050 mm (see left column). All circles are filled with 5 µL of a 1 mg/mL Terasil Blue aqueous solution. The marked areas highlight inner circles which are not reliable hydrophobic barriers as the solution does not stay within them. Image taken under visible light [159].

Full functioning barriers were apparent at different widths for the various colours. After heating magenta and green created full hydrophobic barriers with a W_N of 0.120 mm, black with 0.175 mm for Terasil Blue and Orange G (0.230 mm for Acid Green), cyan with 0.250 mm for Terasil Blue and Orange G (0.260 mm for Acid Green), and yellow with 0.325 mm. These results are consistent with the trend seen in Figures 2-6 and Figure 2-7 and may be explained by the larger spread of magenta and green in comparison to the other colours upon heating.

A similar procedure was performed with circles of 0.050-0.300 mm W_N with increments of 0.050 mm for five mixed colours; orange, dark green, light green, blue and dark purple; and a reference standard, magenta (Appendix V).

All mixed colours (except light green) produced reliable hydrophobic barriers at a W_N of 0.130 mm. This observation was consistent with results for magenta. Light green did not exhibit fully functioning hydrophobic barriers even at 0.300 mm W_N, most likely due to the high ratio of yellow which showed relatively small spreading. Similar results were obtained for the three test solutions (Figure 2-8 (Terasil Blue), Appendix IV (Acid Green and Orange G)), indicating that the dyes had no significant influence on the experiment.

For further experiments, all μPAD patterns were designed in magenta with W_N of 0.200 mm. Magenta was the most suitable colour for the generation of reliable hydrophobic barriers for two reasons. Firstly, it showed the largest spreading when compared to cyan, yellow and black. Secondly, it is a single colour and possible inconsistencies caused by colour mixing could therefore be excluded. The four ColorQube 8870 solid inks are made of polyethylene and fatty amine waxes (50-60 %), resin (10-20 %) and dye (≤ than 5 %), although the exact composition of each one of the four solid inks is proprietary information. Two different batches of inks were tested and the results were similar implying that at least for this printer magenta produces better hydrophobic barriers than the other standard colours.

2.3.2 *Application: Explosive Detection by Fluorescence Quenching*

Once the μPADs were fabricated, a fluorescent reagent was deposited within the hydrophobic barrier. Under UV light, the reagent fluoresced, while in contact with explosives the fluorescence was quenched. A schematic of explosive detection by fluorescence quenching can be seen in Figure 2-9.

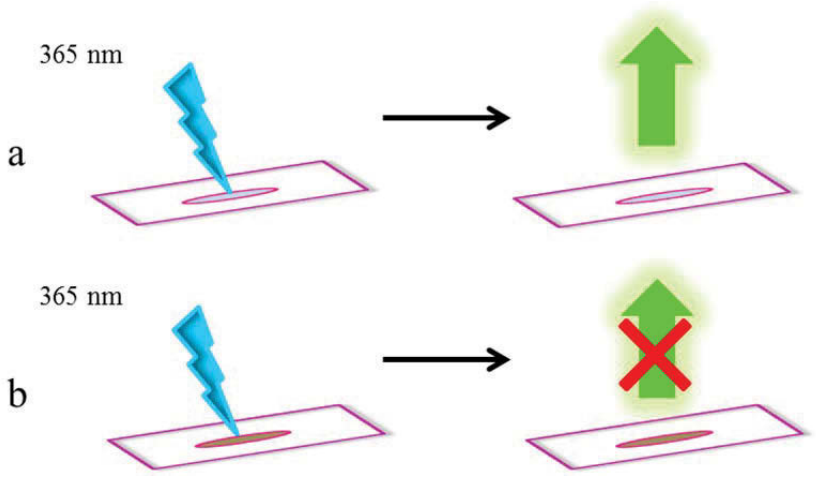

Figure 2-9: Schematic of explosive detection based on fluorescence quenching. a) Pyrene is deposited in the circled area on the microfluidic paper-based analytical device (µPAD) and emits light upon excitation by a light source with 365 nm. b) When explosives are present on top of pyrene on the circled area on the µPAD, no light is emitted upon excitation.

Pyrene is a flat polycyclic aromatic hydrocarbon soluble in several different organic solvents, however just sparingly soluble in water (0.135 mg/L) [163]. Pyrene was selected as the fluorophore based on its excellent relative fluorescence power of 0.345 [163] and its known quenching in the presence of explosive material [164]. The interaction mechanism between the electron-rich polycyclic aromatic structure of pyrene and the electron-withdrawing explosives relies on the formation of charge transfer complexes (Figure 2-10). Hereby electrons are withdrawn from the excited-state fluorophore to the ground-state quencher [165, 166].

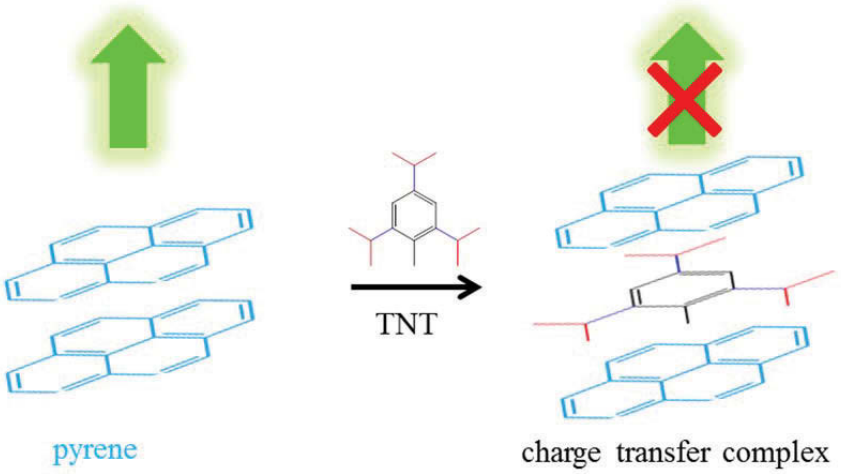

Figure 2-10: Interaction mechanism between pyrene and trinitrotoluene (TNT; representing the quencher). Left side: Pyrene alone exhibits fluorescence upon excitation. Right side: No fluorescence is detection due to the formation of a charge transfer complex between the electron-rich pyrene and electron-withdrawing explosive (here TNT) [167].

However, the pyrene application to the µPADs was found to be problematic. The water solubility and therefore pyrene concentration in water was too low for fluorescence detection. On the other hand, the hydrophobicity of the wax channels restricted the application of pyrene in organic solvents to the µPADs. It was assumed that less polar solvent molecules than water, e.g. MeOH, EtOH, propanol and ACN (solvents usually used to dissolve explosives), would interact with the fatty acids in the solid ink allowing the passage of the solvents. Two reported approaches to increase the water solubility of pyrene, i.e. increasing the temperature [168] and adding surfactants [169], were both tested without success. Increasing the temperature (80 °C) did not result in a satisfactory pyrene concentration and the surfactant property of SDS lowered the surface tension of water so that the pyrene-SDS solution did not stay compartmentalised in the barrier (Figure 2-12 b and c).

The possibility of first dissolving the pyrene in an organic solvent and then mixing the organic solution with water and applying the dispersion to the hydrophobic channels was investigated. To find the required ratio of water:organic solvent for µPAD application, coloured (Terasil Blue) dispersions with different

ratios (from 10:90 to 100:0) were deposited on circles printed in magenta ink. The results can be seen in Figure 2-11.

For MeOH:water (column A), a ratio of 80:20 respectively displayed satisfactory hydrophilic properties for the application on µPADs. An EtOH:water mixture required a 50 % water ratio, whilst a propanol:water mixture required a 90 % water ratio. Therefore each incorporation of a methylene group in the alcohol molecule reduced the capacity of retention of the solution on the µPAD by 30-40 %. This sequence of alcohols (MeOH, EtOH, propanol) was expected and can be explained by the different solubility of alcohols in water caused by the different sizes of the nonpolar carbon chain. ACN showed satisfactory hydrophilic properties when mixed with water in a 50:50 ratio similar to EtOH.

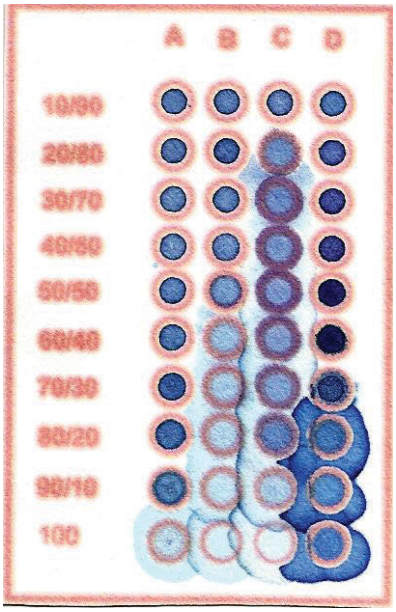

Figure 2-11: Column A-MeOH:water mixture, B-EtOH:water mixture, C-propanol:water mixture and D-ACN:water mixture. Ratios of organic solvents:water are given in the left column starting from 10 % organic solvent at the top to 100 % at the bottom. Picture is taken with visible light. All solutions are coloured with 1 mg/mL Terasil Blue.

As organic solvents were able to penetrate the wax barriers, experiments were conducted to test whether this process resulted in any change of the barrier quality. Hexane (hydrophobic solvent) and MeOH (hydrophilic solvent) were separately pipetted (5 µL) in the µPAD circles and allowed to dry. Afterwards,

coloured solvent:water mixtures were deposited on the µPAD (Appendix VI, same design as in Figure 2-11). Treated (Appendix VI) and untreated (previous experiment, Figure 2-11) barriers showed similar hydrophilic character. It was therefore concluded, that organic solvents do not have noticeable influence on the quality of the wax barriers. MeOH:water (80:20) was chosen as the solvent system for all experiments as the water percentage was the smallest in comparison to the other organic solvents and the pyrene concentration and thus fluorescence relatively high (Figure 2-12 d).

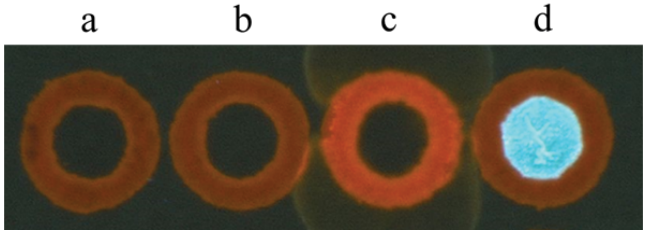

Figure 2-12: Comparison of various techniques to increase the pyrene solubility in aqueous solution: blank (a), saturated pyrene solution after heating (30 min, 80 °C), saturated pyrene solution with sodium dodecyl sulfate (c), 0.5 mg/mL pyrene solution (80:20 methanol:water) (d).

Different pyrene concentrations were tested from 0.1 to 1 mg/mL for their fluorescence under the VSC 6000 instrument (Figure 2-13). A concentration of 0.5 mg/mL pyrene in MeOH:water (80:20) was determined as optimal concentration for further experiments. While lower concentrations (0.1 and 0.25 mg/mL) did not show satisfactory fluorescence, higher concentrations (up to 1 mg/mL) were extremely fluorescent.

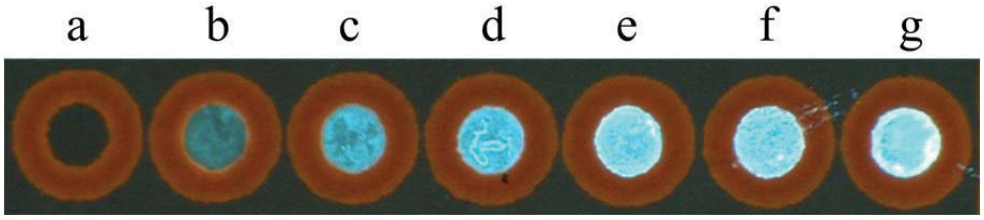

Figure 2-13: Fluorescence of pyrene in various concentrations: blank (a), 0.05 mg/mL (b), 0.1 mg/mL (c), 0.25 mg/mL (d), 0.5 mg/mL (e), 0.75 mg/mL (f), and 0.1 mg/mL (d).

It was observed that high fluorescence could interfere with the detection of explosives in low concentrations as no change in the fluorescence was noticed. One µL of the optimised pyrene solution (0.5 mg/mL in 80:20 MeOH:water) was deposited in the hydrophobic barrier of the µPAD. Under UV light, the µPAD fluoresced, while in contact with explosives the fluorescence was quenched.

Ten different explosives were tested for fluorescence quenching of pyrene with the VSC 6000 instrument. The choice of explosives was based on covering a range of classes of explosives such as nitrate esters (PETN), nitro aromatics (TNT, 2,4-DNT, 4-A-2,6-DNT, 4-NT, DNB, NB) and nitro amines (RDX, tetryl) that are potentially present in GSR. One µL of the explosive solution (1000 ppm) was deposited within the hydrophobic barriers of the µPAD. All of the explosives gave positive results as shown in Figure 2-14.

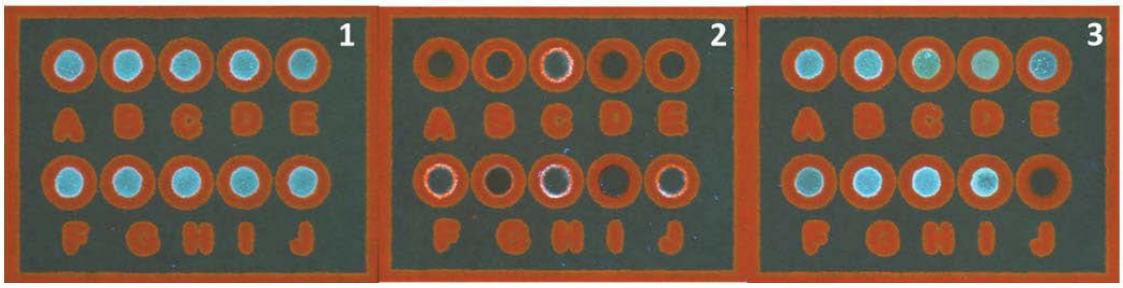

Figure 2-14: Microfluidic paper-based analytical device (µPAD) with 1 µL of 0.5 mg/mL pyrene solution in methanol : water (80:20) on circles with 5.000 mm diameter generated under the same conditions as in Figure 2-3. 2- Same µPAD after the deposition of 1 µL of 10 different explosives (A: TNB, B: 1,3-DNB, C: NB, D: TNT, E: 2,4-DNT, F: 4-NT, G: 4-A-2,6-DNT, H: RDX, I:tetryl, J:PETN) demonstrating fluorescence quenching. 3- µPAD generated under the same conditions with nine different non-explosive substances and one explosive (A: negative control, B: water, C: milk, D: coffee, E: tea, F: coke, G: beer, H: wine, I: Mylanta Antacid Dual Action and J: TNT (positive control)).

As can be seen in Figure 2-14.2 the affinity between explosive and pyrene depends of the chemical composition of the explosive. TNT (D) for example displayed higher fluorescence quenching in comparison with 2,4-DNT (E), which is notable by the presence of a faint white ring between the wax and sample area of the circle (E) in comparison to a fully black sample area in (D). This was also observed

for TNB (A) and 1,3-DNB (B) and can be explained by the higher amount of electron withdrawing groups. TNT and TNB have both three electron withdrawing groups (NO_2) on the aromatic ring, whereby 2,4-DNT and 1,3-DNB have only two.

The LODs of the seven explosives tested using the VSC 6000 instrument were determined by visually examining pyrene quenching when explosives were deposited on top with concentration ranging between 100 ppm to 600 ppm (2 μL). It was found to be between 100 (TNT, TNB) and 600 ppm (NB).

It was observed that solvents such as ACN and MeOH, can decrease the fluorescence of pyrene when used to prepare standard solutions. However, this decrease was extremely limited and could be easily distinguished from fluorescence quenching caused by the deposition of explosives.

The selectivity of the method was investigated by examining eight commonly available selected substances (water, milk, coffee, tea, coke, beer, wine, Mylanta Antacid Dual Action) for their ability to quench the fluorescence of the μPAD device compared to a negative and positive control. All tests for the eight randomly selected substances were negative (Figure 2-14.3). Preliminary data indicated that the selectivity of the technique was good, with no false positives detected.

2.3.3 *Portable Explosive Detector Prototype*

A small, portable instrument was built for the field detection of explosives. This instrument incorporated a 365 nm UV LED as a light source and a photodiode as a light sensor. The use of a high power LED was necessary to ensure sufficient excitation of pyrene. The detection cell, where the μPAD was inserted, had a gap of 0.5 mm between the light source and sensor. When the UV LED was turned on, the UV light (365 nm) excited the pyrene on the μPAD which emitted visible light. This

light was captured by the photodiode sensor at 500 nm on the other side of the µPAD (Figure 2-15). The sensitivity of the photosensor was relatively low at 365 nm, which was important in order to avoid interferences with the UV light that passes through the paper. When a new µPAD device was inserted in the instrument, calibration was achieved by presenting a circle with only pyrene to the sensor and adjusting the potentiometer R2 (see Figure 2-2) until the green LED was turned on. The green light signalled that no explosives were present on the µPAD. If explosives were on the µPAD, fluorescence quenching shifted the wavelength which was usually emitted by the pyrene and a red light flashed to alert the analyst (see D2 – Figure 2-2).

The instrument was tested by sampling a 10 centimetre x 10 centimetre bench surface which had been thoroughly cleaned and was free from any explosive material. A cotton swab moistened with MeOH:water (80:20) was used as collection device. After collection, the swab was gently pressed on top of a circle on the µPAD. The µPAD was then inserted into the instrument which displayed a green light, indicating no detection of explosives. After re-sampling the bench surface homogeneously spiked with TNT (3 µL of 1000 ppm solution) and exposing the respective µPAD, the instrument displayed a red flashing light indicating the detection of explosives.

A preliminary test of all 10 explosives which had previously given positive results using the VSC 6000 instrument also resulted in a positive response with the portable prototype and no false-positives were detected. These results demonstrate the suitability of the prototype µPAD reader to explosive screening. Figure 2-15 illustrates the portable explosive detector prototype.

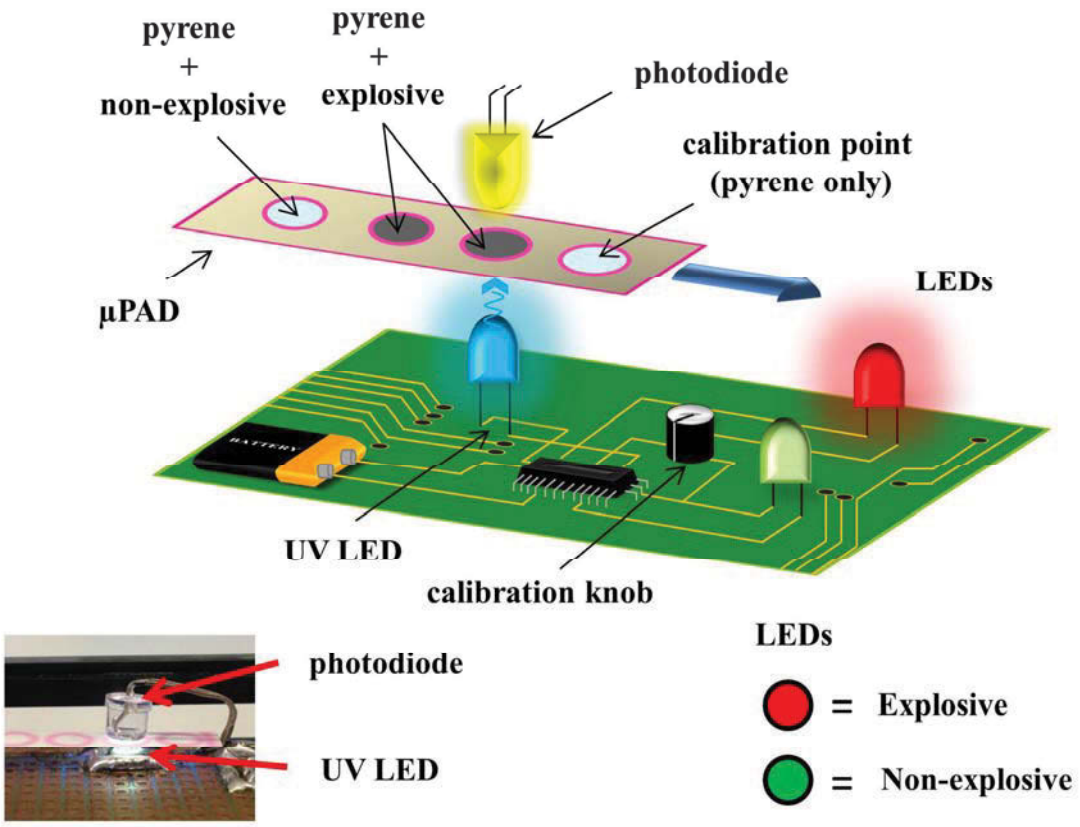

Figure 2-15: Illustration of the portable explosive detector prototype. The first step (not shown) includes inserting the calibration point between the ultraviolet light-emitting diode (LED) and the photodiode and turning the calibration knob until the green LED flashes. The second step (displayed in the Figure) shows the detection of explosives on the microfluidic paper-based analytical device.

2.3.4 *Optimisation*

As the sensor has a 5 mm diameter, this diameter was chosen as an ideal size for the circle printed on the µPAD. Three different pyrene concentrations, i.e. 0.10 mg/mL, 0.25 mg/mL and 0.50 mg/mL were tested. Optimal performance was found when 1 µL of 0.25 mg/mL pyrene solution was deposited on the µPAD. Minimum detectable masses for the target compounds using the optimised conditions are shown in Table 2-2.

Table 2-2: Minimum detectable masses of 10 explosives using the prototype explosive detector and the optimised microfluidic paper-based analytical device (1µL 0.25 mg/mL pyrene, 5 mm diameter circle).

TNT	2,4-DNT	4-A-2,6-DNT	TNB	1,3-DNB	RDX	PETN	tetryl
0.2 µg	0.5 µg	0.3 µg	0.1 µg	0.7 µg	0.8 µg	0.8 µg	0.4 µg

The developed method was tested using a specimen taken from the hands of a shooter after discharge of a firearm (one shot using a pistol (Sport King) with 22 LR High Velocity (Remington, USA) ammunition). No explosive were detected on the specimen. This result could be attributed to explosives not being present in the residue for this firearm-ammunition combination. Further, this could be a results of having no explosives collected using the moistened (MeOH:water 80:20) µPAD or the LODs of the target explosives could be not sensitive enough for OGSR detection.

It is worth noting that the proposed specimen collection using the optimised µPADs results in the loss of information about GSR deposition patterns. These patterns can provide helpful information in regards to shooting distance and can assist in the differentiation of GSR and GSR-like particles. Future research should therefore investigate non-destructive screening techniques without actually removing the GSR or changing the GSR deposition pattern.

2.4 Conclusion

An innovative, rapid, cost-effective, portable and simple screening method for the detection of explosives possibly present in GSR based on µPADs has been developed. µPADs were created by printing magenta ink on a filter paper using a FujiXerox ColorQube 8870 wax printer and heating the paper at 150 ^{o}C for 5 min with a heat press. The µPADS were stable at temperatures up to 60 ºC suggesting the field use in high temperature climates is possible.

Pyrene was successfully deposited on the µPADs by dissolving it MeOH and adding water to the solution to create a 80:20 ratio dispersion. Ten different

explosives representing nitrate esters, nitro aromatics and nitro amines gave positive results with the VSC 6000 and the portable in-house built instrument with detection limits in the ng range. The method is able to detect explosives in aqueous or organic solutions, which is beneficial when specimens have to be taken from skin. No false positives were detected indicating a good selectivity of the developed method that can potentially be applied to skin or other surfaces. As fluorescence quenching using pyrene is based on the formation of a charge-transfer complex, the substrate-OGSR reaction is non-destructive and present OGSR can be extracted and confirmed by more sophisticated analytical techniques. Moreover, the collection circle can be hole punched, mounted on a GSR stubs and analysed for IGSR by SEM-EDX.

However, hand swabs taken after one discharge using a pistol (Sport King) with 22 LR High Velocity (Remington, USA) ammunition could not be tested positive. This could be either due to no explosives being present on the hand after the discharge, failure of the collection procedure to remove any OGSR present or the level of any residues being below the LOD of the analytical method.

Therefore, this study needs to be expanded to further examine the selectivity of the method and identify any potential false positives to therefore increase the value of the technique in a forensic perspective. Furthermore, future research should focus on improving the sensitivity and robustness of the developed method and the portable prototype, which can potentially result in its casework applicability. This can be achieved in two ways: (1) Optimising the instrument by using different LEDs and developing a more sensitive detection mechanism or (2) Optimising the µPAD by testing various different fluorophores or colour reagents that are able to react with additives, particularly stabilisers, in smokeless powders.

Chapter 3: High-throughput Screening for Smokeless Powders and Gunshot Residues using RapidFire® with Tandem Mass Spectrometry

Chapter 3: HIGH-THROUGHPUT SCREENING FOR SMOKELESS POWDERS AND GUNSHOT RESIDUES USING RAPIDFIRE® WITH TANDEM MASS SPECTROMETRY

3.1 Introduction

Considering the relatively low amounts of OGSR that are commonly encountered in case specimens, pre-concentration techniques might offer the necessary solution to enable detection of OGSR. SPE is often performed during sample preparation to isolate and concentrate analytes which are present in low abundance or to clean up complex matrices [131]. The sample extract is loaded on a sorbent, which has previously been conditioned. A washing step is applied in order to remove interferences before the analyte is eluted from the sorbent. Commonly, this procedure is performed manually, which is time consuming and labour intensive. Semi-automated and automated offline SPE procedures have been developed as a rapid and simple alternative to completely manual SPE processes. However, these still suffer from limitations such as the requirement for some manual sample handling during the loading, washing and elution steps, which are still time consuming.

For GSR specimens, SPE has been applied when swabs [6, 170] or vacuum devices [131] were used as collection device from skin (hands) or clothing. Even though the SPE procedure was automated using a manifold or Millilab 1A™ workstation, the procedures reported in the literature were not rapid, e.g. 33 min

[170]. Shorter sample preparation times are required especially when high-throughput is required.

A recent development in the SPE area is the introduction of a fully automated system called RapidFire®. This system couples to a high resolution mass spectrometer such as a triple quadrupole mass spectrometer (QQQ-MS), which offers the necessary sensitivity and higher degree of specificity when operated in multiple reaction monitoring (MRM) mode.

This chapter describes a proof-of-concept study focusing on the application of the SPE RapidFire® system coupled to a QQQ-MS to the analysis of smokeless powders/GSR.

The method has the potential to be applied to GSR specimens collected from a suspected shooter, unfired smokeless powders in ammunition and potentially from specimens originating from improvised explosive devices (IEDs) comprising relevant compounds.

3.2 Materials and Methods

3.2.1 *Reagents and Standards*

All solvents including ACN, MeOH, isopropanol (IPA), acetone, n-hexane, methyl tert-butyl ether (MTBE) and dichloromethane (DCM) were obtained in HPLC grade from ChemSupply Pty Ltd, Gillman, SA, Australia. UP grade water (18.2 MΩcm-1) was obtained from a Sartorius 611 water purification system. The targeted OGSR compounds included 2,4 DNT, EC, DPA, 2-NDPA, NG and were purchased from AccuStandard (New Haven, CT, USA) in a certified concentration of 1000 µg/mL in

ACN. These compounds were chosen to represent the expected compounds groups potentially present in smokeless powders or GSR, i.e. explosive (NG), flash suppressor (2,4 DNT), and stabilisers (EC, DPA, 2-NDPA, MC). Ten ppm mixed standard solutions were prepared (100 ng injected; 10 µL) to optimise the SPE method. Calibration curves were prepared using concentrations ranging from 0.5-500 ng (10 µL of 0.05-50 ppm) for all tested compounds.

3.2.2 *RapidFire® – Automated On-line Solid Phase Extraction*

3.2.2.1 Instrument

RapidFire® (Agilent Technologies, Santa Clara, US) is a high throughput SPE system designed for the completely automated and efficient analysis of biochemical assays and samples in biological matrices such as serum [171] or plasma [172, 173]. The system operates as fully automated, on-line, microfluidic sample preparation system incorporating an Agilent BenchBot Robot for automated sample plate handling, three Agilent 1260 Quaternary pumps for software-controlled solvent switching between four available solvents. Samples are aspirated (10 µL) directly from well plates and transferred to a microscale cartridge, which is located on a cartridge holder designed for up to 12 cartridges. A washing step can be applied to the cartridge to clean up the samples. Finally, the sample is eluted from the cartridge and directly introduced to the MS, in this case a QQQ-MS. Figure 3-1 illustrates the simplified setup of the RapidFire® instrumentation.

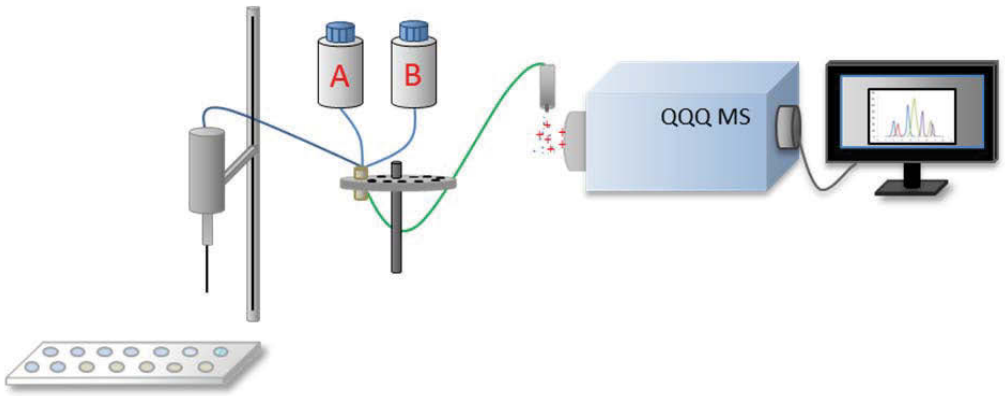

Figure 3-1: Scheme of the RapidFire® connected to an Agilent triple quadrupole mass spectrometer (QQQ-MS).

3.2.2.2 Optimisation

Different parameters were optimised including cartridge type, elution solvent and aspiration and loading times. Each optimisation experiment was conducted in triplicates using a 10 ppm mixed aqueous standard solution of the target compounds.

Nine different cartridges were evaluated during the optimisation process including a Type 0 (Blank packing for testing), Type A and A2 (C4 packing for small molecules, peptides and oligos), Type B (Cyano packing for hydrophobic compounds), Type C (C18 packing for proteins), Type D (Hypercarb packing for hydrophilic compounds and small compounds), Type E (C8 packing for proteins), Type F (Phenyl packing for aromatic compounds), and Type H1 (HILIC packing for hydrophilic compounds and small molecules) cartridge. The 10 ppm mixed standard solution was loaded onto the cartridges and eluted using IPA at a flow rate of 0.75 mL/min. This flow rate was chosen since the elevated pressure using IPA would exceed the recommended maximum pressure on the instrument (13 MPa) using higher flow rates. The efficiency of each cartridge was calculated as % recovery of 10 ppm mix when directly injected into the QQQ-MS (10 µL).

Furthermore, several elution solvents and solvent compositions were evaluated. These included ACN, MeOH, n-hexane:acetone (80:20), MeOH:DCM

(80:20), MeOH:IPA (1:1), acetone, and IPA, which were chosen to represent a range of different solvent polarities. All solvents contained 0.1 % formic acid to facilitate ionisation in the atmospheric pressure chemical ionisation (APCI) source. The 10 ppm mixed standard solution was loaded onto the Type C C18 cartridge and eluted using the different solvents at a flow rate of 0.75 mL/min and the % recovery calculated. For all cartridge and solvent test, the loading and elution times were 3000 milliseconds (ms) each.

Finally, several loading times between 2000 and 8000 ms with 2000 ms increments were tested. The 10 ppm mix solution was loaded onto a Type C C18 cartridge using the various loading times and eluted from the cartridge using IPA at 0.75 mL/min.

The optimised on-line SPE method consisted of sample loading during 3000 ms using UP water at a flowrate of 1.25 mL/min on a Type C C18 cartridge followed by elution of the target compounds for 3000 ms using IPA at 0.75 mL/min. Both solvents contained 0.1 % formic acid to facilitate ionisation in the APCI source.

3.2.2.3 Calibration Curves

Using the optimised method, calibration curves were constructed with concentrations ranging from 0.02-40 ppm (10 µL injected) of the target compounds. Hereby, the LODs were calculated as (3.3*σ)/S, where σ is the standard deviation (SD) of the slope and S the slope of the calibration curve. Limits of quantification (LOQs) were based on 3.3*LOD.

3.2.3 *Triple Quadrupole Mass Spectrometer*

The RapidFire® was connected to an Agilent Technologies 6490 QQQ-MS. The instrument was controlled by MassHunter Acquisition software version B.06.00 (Agilent Technologies) and connected to an APCI ion source (G1947 B) (Agilent Technologies). Using a 0.12 mm ID capillary, the SPE eluate was directly introduced to the MS. The conditions for the MRM were optimised either using the Optimizer Software (Agilent Technologies) or manually and are presented in Chapter 4, Table 4-2. Hereby, the most abundant and specific ions were chosen.

3.2.4 *Simulated Case Specimens*

Two specimens collected from the hand of a shooter after firing a weapon were tested using the developed method. These GSR specimens were obtained from the New South Wales Police Force (NSWPF) firing range in Sydney, Australia. The specimens were prepared using the developed extraction method (Chapter 5, 5.2.4.4) except that the final solvent was UP water instead of ACN:MeOH. In brief, after collection, alcohol swabs (Kendall, Webcol) were extracted using 5 mL MTBE, sonicated for 5 min and the liquid dried under a gentle stream of nitrogen. Finally, the specimens were reconstituted in 200 µL of UP water.

3.3 Results and Discussion

3.3.1 *Optimisation*

Various loading times, cartridge types, elution solvents as well as flow rates and were tested in order to optimise the automated SPE method.

Nine different cartridges were compared for their efficiencies in retaining the target compounds loaded in water, which were then eluted using IPA. The % recovery of the target compounds areas using the different cartridges is displayed in Figure 3-2.

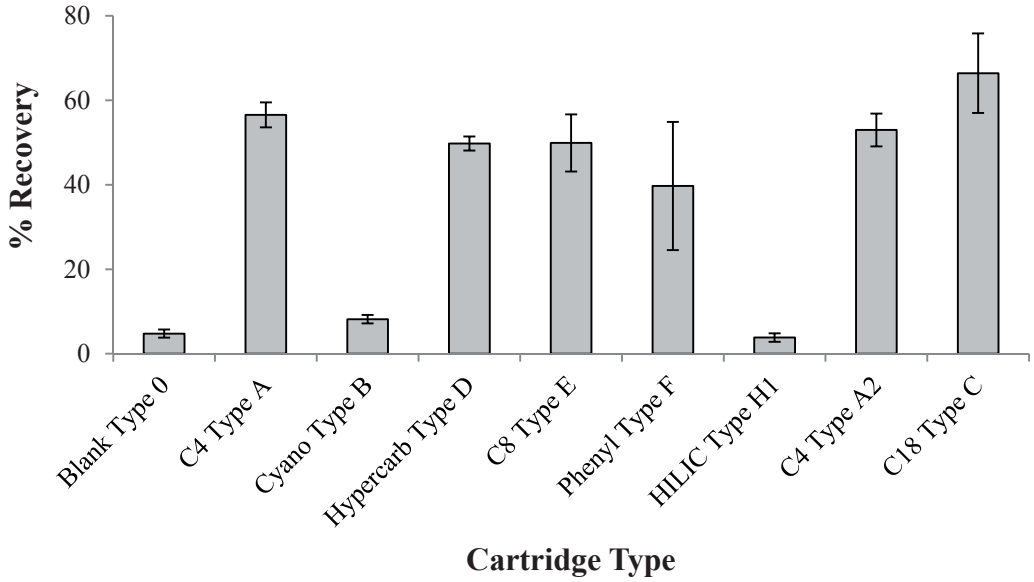

Figure 3-2: Sum of the % recoveries of the target compounds using nine different cartridge types. Different cartridges were loaded with a 10 ppm mixed standard (10 µL) of the target compounds and were eluted using isopropanol (0.75 mL/min). Error bars represent standard deviations (n = 3).

The highest sum of % recoveries was obtained using a C18 cartridge. This cartridge was determined as most suitable for OGSR sample preparation although the SD using this cartridge was relatively high in comparison to most others. It should be noted that C4 Type A and C4 Type A2 cartridges also showed potential and future work should test the following optimisation steps using these two cartridges.

Over 99 % of the sum of the recoveries is the response of the stabilisers (DPA, 2-NDPA, MC and EC). In the context of firearm related events, this is extremely relevant. As previous research [6] and the results in Chapter 4 and 5 have shown, the majority of organic compounds detected after a firearm has been

discharged were found to be stabilisers, e.g. DPA, its derivatives such as 2-NDPA or N-nDPA , EC or MC [6, 174, 175]. Since the recovery of these compounds represented over 99 % of the overall recovery, approximately 65 %, automated SPE using the RapidFire® appears suitable for the analysis of specimens taken from firearm related events. For future research it would be interesting to evaluate Chromosorb 104-Amberlite or XAD-4 SPE cartridges since those have previously reported as suitable to GSR or smokeless powder specimens and showed greater (more than twice) recoveries of the target compounds than a C18 cartridge [131, 176].

Different elution solvents and solvent compositions were also compared for their efficiency to elute the target compounds from the cartridge. A summary of the extraction efficiencies represented as sum of the detected areas of the target compounds is shown in Figure 3-3. The lowest extraction efficiencies were found using acetone, while the highest were found for IPA. Considering both, the extraction efficiencies and SDs (shown as error bars in Figure 3-3; n = 3), the most suitable elution solvent was IPA.

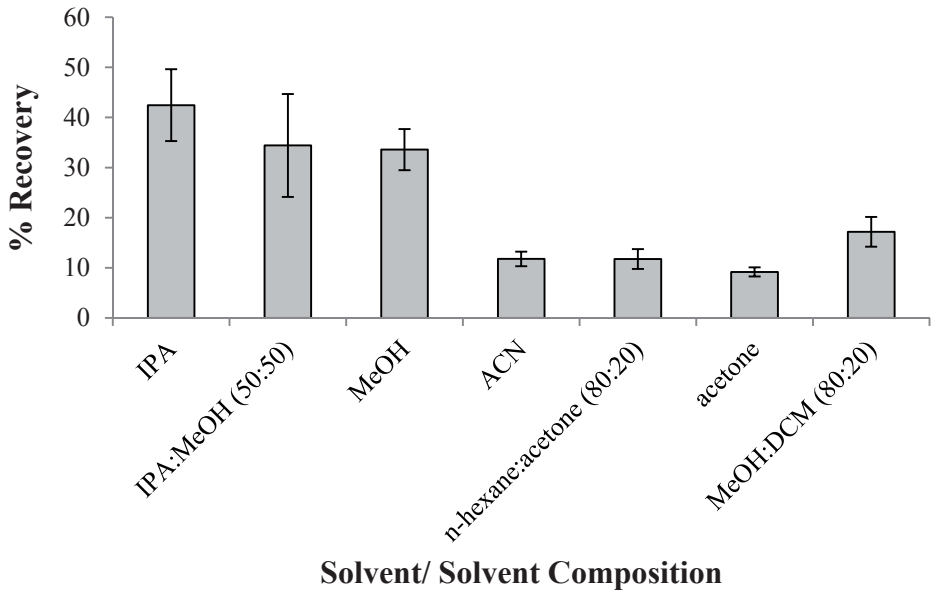

Figure 3-3: Extraction efficiencies of different solvents/solvent compositions presented as sum of the % recoveries of the target compounds. A C18 Type C cartridge was loaded with a 10 ppm mixed standard and eluted using the solvent/solvent system at 0.75 mL/min. Error bars represent standard deviations (n = 3). IPA = isopropanol, MeOH = methanol, ACN = acetonitrile, DCM = dichloromethane.

Different loading times between 2000 and 8000 ms were tested and no significant differences (Student's t-test, paired, two-tailed, p = 0.0985) were found.

Using the optimised method, calibration curves were constructed. An example total ion chromatogram of the calibration standards is provided in Figure 3-4 showing the short analysis time with only 8 sec per sample. The LODs and LOQs of all compounds are shown in Table 3-1.

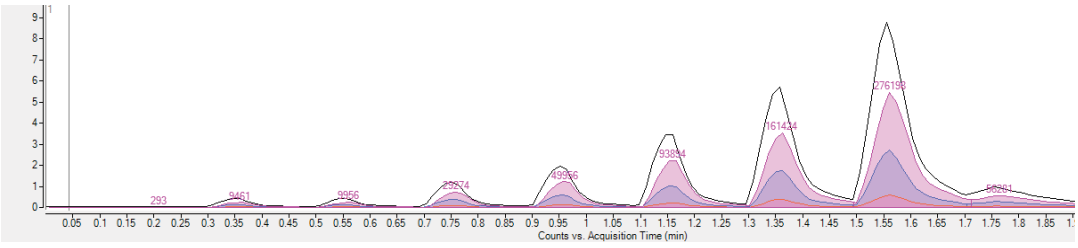

Figure 3-4: Total ion chromatogram demonstrating the very short analysis time per sample.

Table 3-1: Limits of detection (LODs) and limits of quantification (LOQs) of the target compounds in ng when loaded onto a C18 cartridge and eluted using isopropanol (0.75 mL/min).

	DPA	2-NDPA	EC	MC	NG	2,4-DNT
LOD [ng]	2.70	2.87	0.86	1.48	1.87	1.28
LOQ [ng]	14.3	9.48	2.85	4.89	6.16	4.23

The coefficient of determination (R^2) values for the different compounds were 0.9678 (DPA), 0.9740 (2-NDPA), 0.9932 (EC), 0.9803 (MC), 0.9701 (2,4-DNT), 0.9163 (NG) with a linear range from 0.02-40 ppm (10 µL injected).

DPA and NG saturated the cartridge when 25 ppm was loaded, while no saturation was observed for the other compounds in the tested range.

3.3.2 *Simulated Case Specimens*

The optimised method was applied to specimens collected at a firing range. The amount of each target compound [ng] detected in the specimens is shown in Table 3-2. It should be noted that all sample extracts loaded onto the cartridges were in pure water. Considering the insolubility (EC) or low solubility (DPA, NG, 2,4-DNT, 2-NDPA) of the target analytes in water, further experiments should be conducted in which the organic solvent in the extract is not completely dried, but only diluted with water before loading. This is expected to result in a higher detection of the target compounds.

Table 3-2: Recoveries [ng] of the target compounds from simulated gunshot residue specimens collected at a firing range. Shooting A: Three shots using a pistol with 44 Rem Magnum (PMC) (Smith&Wesson); Shooting B: Three shots using shotgun (Remington, USA) with SuperX (12 gauge, Winchester, Australia). ND = not detected.

Compound	Shooting A [ng]	Shooting B [ng]
EC	0.6*	ND
DPA	ND	0.78*
2-NDPA	ND	ND
2,4-DNT	ND	ND
NG	1.37	ND

*below LOD

The proposed automated SPE technique could be incorporated in current SOPS for GSR or post-blast analysis as a preliminary screening test to prioritise analysis of specimens.

3.4 Conclusion

A RapidFire® method was developed for the automated on-line SPE analysis of several compounds present in smokeless powders and GSR, i.e. DPA, 2 NDPA, EC, NG, and 2,4-DNT. The method is fully automated, requires only 8 seconds per sample/specimen and is able to detect the target compounds down to the low ng level.

However, only some of the target analytes were detected in the specimens taken from the hands of a shooter at a firing range. Furthermore, the detected compounds were mainly found in levels below their LODs and LOQs suggesting that the method is not sufficiently sensitive and should undergo further optimisation

in order to meet casework requirement. Additional investigations into the optimum cartridge type, cartridge size and elution solvent could contribute to lower detection limit and increased recoveries and allow the method to be applied to the analysis of smokeless powder samples (ammunition or IEDS) and specimens taken from firearm related incidents (GSR).

Additionally, further testing on real-case specimens should be undertaken in order to investigate the possibility to pre-concentrate samples/specimens on microscale cartridges and explore limitations such as matrix suppression, or enhancement and SPE cartridge saturation. As mentioned previously, the application of more sensitive analytical techniques has the potential to introduce complexity to the interpretation process. Therefore, it is crucial that further optimisation of the SPE method does not result in the detection of material that might lead to misidentification.

Chapter 4: Development of a UHPLC Method for the Detection of Organic Gunshot Residues using Artificial Neural Network

Chapter 4: DEVELOPMENT OF A UHPLC METHOD FOR THE DETECTION OF OGSR USING ARTIFICIAL NEURAL NETWORKS

4.1 Background

After obtaining a screening result, any suspected presence of GSR should be confirmed using an appropriate analytical technique. Requirements for this technique are accurateness and reliability allowing the interpretation of the obtained data which can provide helpful information. [177].

Due to the capability to selectively identify a single GSR particle based on morphology and elemental composition, SEM/EDX spectroscopy continues to be the method of choice for GSR identification in forensic casework and is unequalled by any other bulk analysis method [4, 178]. This method can confirm the presence of Pb, Ba and Sb supporting the detection of characteristic GSR particles. In the 1970s LF and HMF ammunitions were introduced to the market to decrease the exposure of frequent shooters to toxic gases and hazardous particulates released from the primer and the bullet itself [35]. Although these ammunitions have been available for few decades, recent changes in gun laws of some US states (e.g. California) prohibiting lead ammunition for hunting [179] and the shift of other groups, most notable the US military, to LF ammunition [180] accentuate the need for new methods of analysis of LF and HMF ammunition. To date, different elemental profiles of spherical particles produced by LF and/ or HMF ammunitions have been elucidated [32-35]. These studies induce that elemental profiles of LF

GSR particulates are in agreement with the composition of the respective primers. However, identification of GSR particles formed by these "green" ammunitions is problematic. The composition is not exclusive to firearm handling [11, 32-34, 37] and IGSR particles from "green" ammunition can potentially derive from sources other than firearms. As a result, SEM/EDX analysis of IGSR from LF and HMF ammunition can potentially lead to false-negative result. Moreover, interpretation issues correlating to memory effects [98], GSR-like particles from environmental and occupational sources [109, 111, 115], and secondary transfer [119, 121] constitute additional challenges.

It is important to point out, that particle analysis by SEM/EDX spectroscopy continues to be the method of choice for GSR analysis, and LF and HMF only constitutes a small proportion of the ammunition on the market at present. However, the increasing trend towards green ammunition and the associated limitations call for an adjustment of current SOPs for GSR investigation.

The analysis of OGSR originating from the propellant powder provides additional information, complementary to that obtained by SEM-EDX. Thus, incorporation of OGSR analysis to existing SOPs is necessary to address the pitfalls associated with current GSR detection techniques. This incorporation must give consideration to the necessary sequencing of the organic and inorganic analyses, ensuring one does not impact on or preclude the subsequent testing.

When developing an analytical method, it is important to include both, OGSR from propellant powder as well as from primer mixtures to target the majority of the compounds potentially present.

Organic GSRs may be analysed using a variety of analytical methods including liquid chromatography (LC) [6, 181], GC [13, 131], MECE [21],

TOF-SIMS [83], and DESI-MS [59, 85]. LC is a very suitable technique, as it allows the separation and identification of thermally labile compounds potentially present in GSR such as DPA and its derivatives. The analysis of these compounds would be problematic using GC for example due to the high temperatures applied. UHPLC, an adaption of HPLC, provides a new potential for method development and analysis as the decreased particle size column packing (sub-2 μm) allows for efficiency advantages over traditional HPLC and decreased run times [182].

Traditional LC method development consists of changing individual parameters one at a time, while keeping all others constant. This is a time consuming and challenging process given the large number of parameters and their possible interactions. An additional difficulty can be posed when a large number of compounds require separation, as in the case of OGSR analysis. An alternative route for rapid method development is the application of ANNs which are predictive data-processing programs that mimic the way the human brain processes information. The processing units in ANNs consist of neurons, units and nodes arranged in several interconnected layers [183]. Multilayer perceptron (MLP) ANNs are constructed with three layers; the input layer, hidden layer and output layer [184]. Each node of the input layer is associated with an experimental factor. The data is processed in the hidden layer by an activation function, whilst each node in the output layer is associated to a response [183]. An advantage of ANNs against other predictive statistical network approaches is the capacity of an ANN to learn from a set of training examples that contain both the input and output data [183]. A potential deficiency of ANNs is the possibility to over-learn or over-fit the network. In such cases, the ANN functions well with the training data points; however, its predictive capacity for other data points is sub optimal. Overlearning can be

minimised by monitoring the error of predictions with a verification data set. Verification error that is greater than the training indicates over-fitting [185]. ANNs have been applied to the separations of herbicides [186], cosmetic preservatives [187], benzodiazepines [184], and organic explosives [188], peptides [187], fatty acid methyl esters [189].

This is the first time this predictive data-processing program was applied to the development of an analytical method for OGSR by UHPLC.

4.2 Materials and Methods

4.2.1 *Reagents and Standards*

A summary of the target OGSR compounds is provided in Table 4-1.

The internal standard (ISTD) 2-naphthol (99.0 % certified purity) was obtained from Dr. Ehrenstorfer (Augsburg, Bavaria, Germany). It was chosen based on previous literature [11] and also applied in another study by Thomas et al. [181]. A different ISTD, namely isosorbide dinitrate (ISDN), was also tested since it was reported in the PhD thesis by Romolo [42]. However, ISDN coeluted with early eluting energetic compounds and was therefore not used. 1000 ppm stock solutions of DBP, 4-nDPA, 2,4-DNDPA, N,N'-DPU, and 2-naphthol were prepared in HPLC grade ACN:MeOH (1:1) (ChemSupplies Pty Ltd, Gillman, SA, Australia). MTBE and DCM were also supplied by ChemSupplies Pty Ltd (Gillman, SA, Australia). UP grade water (18.2 MΩcm-1) was obtained from a Sartorius 611 water purification system.

Table 4-1: List of target compounds, abbreviations, and functions in propellant powder or primer (indicated in brackets), the standard concentrations, and brand [4, 6, 11, 21, 22].

Compound	Abbreviation	Function	Standard concentration	Source
Nitroglycerin	NG	Propellant	1000 µg/mL in ACN	Cerilliant (Round Rock, TX, USA)
1,2-Dinitroglycerin	1,2-DNG	Explosive	100 µg/mL in ACN	AccuStandard (New Haven, CT, USA)
1,3-Dinitroglycerin	1,3-DNG	Explosive	100 µg/mL in ACN	AccuStandard (New Haven, CT, USA)
Nitroguanidine	NGU	flash suppressor	100 µg/mL in MeOH	AccuStandard (New Haven, CT, USA)
2,4,6-Trinitrotoluene	TNT	explosive, sensitiser	1000 µg/mL in ACN	ChemService (West Chester, PA, USA)
2,3-Dinitrotoluene	2,3-DNT	flash suppressor	99.5 % certified purity	Dr. Ehrenstorfer GmbH (Augsburg, Bavaria, Germany)
2,4-Dinitrotoluene	2,4-DNT	flash suppressor	1000 µg/mL in ACN	ChemService (West Chester, PA, USA)
2,6-Dinitrotoluene	2,6-DNT	flash suppressor	1000 µg/mL in ACN	ChemService (West Chester, PA, USA)
3,4-Dintirotoluene	3,4-DNT	flash suppressor	1000 µg/mL in MeOH	ChemService (West Chester, PA, USA)
4-Amino-2,6-dinitrotoluene	4-A-2,6-DNT	flash suppressor	1000 µg/mL in ACN	ChemService (West Chester, PA, USA)
3-Nitrotoluene	3-NT	explosive, flash suppressor	1000 µg/mL in ACN	ChemService (West Chester, PA, USA)
1,3,5-Trinitrobenzene	TNB	Explosive	1000 µg/mL in ACN	ChemService (West Chester, PA, USA)
1,3-Dinitrobenzene	1,3-DNB	Explosive	1000 µg/mL in ACN	ChemService (West Chester, PA, USA)

Table 4-1 continued: List of target compounds, abbreviations, and functions in propellant powder or primer (indicated in brackets), the standard concentrations, and brand [4, 6, 11, 21, 22].

Compound	Abbreviation	Function	Standard concentration	Source
Nitrobenzene	NB	explosive	1000 µg/mL in ACN	ChemService (West Chester, PA, USA)
N,N'-Diphenylurea	N,N'-DPU	stabiliser, plasticiser	97.5 % certified purity	Dr. Ehrenstorfer GmbH (Augsburg, Bavaria, Germany)
Methyl centralite	MC	stabiliser, plasticiser	100 µg/mL in 50 % ACN	AccuStandard (New Haven, CT, USA)
Ethyl centralite	EC	stabiliser, plasticiser	500 µg/mL in ACN	AccuStandard (New Haven, CT, USA)
1,3-Benzenediol	resorcinol	stabiliser, plasticiser	100 µg/mL in MeOH	AccuStandard (New Haven, CT, USA)
Dimethyl phthalate	DMP	plasticiser	1000 µg/mL in MeOH	AccuStandard (New Haven, CT, USA)
Diethyl phthalate	DEP	plasticiser	100 µg/mL in MeOH	AccuStandard (New Haven, CT, USA)
Dibutyl phthalate	DBP	plasticiser	99% certified purity	ChemService (West Chester, PA, USA)
Diphenylamine	DPA	stabiliser	1000 µg/mL in MeOH	AccuStandard (New Haven, CT, USA)
2-Nitrodiphenylamine	2-NDPA	stabiliser (derivative of DPA)	100 µg/mL in ACN	AccuStandard (New Haven, CT, USA)
4-Nitrosodiphenylamine	4-nDPA	stabiliser (derivative of DPA)	99 % certified purity	ChemService (West Chester, PA, USA)
N-Nitrosodiphenylamine	N-nDPA	stabiliser (derivative of DPA)	1000 µg/mL in MeOH	AccuStandard (New Haven, CT, USA)
2,4-Dinitrodiphenylamine	2,4-DNDPA	stabiliser (derivative of DPA)	97.5 % certified purity	Dr. Ehrenstorfer GmbH (Augsburg, Bavaria, Germany)

Table 4-1 continued: List of target compounds, abbreviations, and functions in propellant powder or primer (indicated in brackets), the standard concentrations, and brand [4, 6, 11, 21, 22].

Compound	Abbreviation	Function	Standard concentration	Source
Ethylene glycol dinitrate	EGDN	explosive	100 µg/mL in ACN	AccuStandard (New Haven, CT, USA)
Pentaerythritol tetranitrate	PETN	explosive, sensitiser	1000 µg/mL in ACN	ChemService (West Chester, PA, USA)
Octahydro-1,3,5,7-tetranitro-1,3,5,7-tetrazocine	HMX	explosive	1000 µg/mL in ACN:MeOH (1:1)	AccuStandard (New Haven, CT, USA)
Hexahydro-1,3,5-trinitro-1,3,5-triazine	RDX	explosive	1000 µg/mL in ACN	ChemService (West Chester, PA, USA)
2,4,6-Trinitrophenylmethylnitramine	tetryl	sensitiser (primer)	1000 µg/mL in ACN	ChemService (West Chester, PA, USA)
Diazodinitrophenol	DDNP	initiating explosive (primer)	100 µg/mL in ACN	AccuStandard (New Haven, CT, USA)

4.2.2 *Instrumentation*

4.2.2.1 *Ultra-high Performance Liquid Chromatography*

A 1290 HPLC (UHPLC) system from Agilent Technologies was used for all analyses. The system incorporated a binary pump, vacuum degasser, standard autosampler, thermostats for the column and sample compartments, and a UV detector. UV was monitored at 214 nm and 254 nm. ChemStation software (version B 04.02, Agilent Technologies) was used for instrument control, data acquisition and analysis. Standards and specimens were analysed on a Zorbax RRHD Eclipse XDB-C18 3x100 mm, 1.8 µm (Agilent Technologies) using a flow rate of 0.8 mL/min and a 1 µL injection volume. A 1290 Infinity in-line filter (0.2 µm, Agilent Technologies) was installed to prolong column lifetime.

4.2.2.2 *Triple Quadrupole Mass Spectrometry*

Confirmation of the compounds detected by UHPLC analysis with UV detection was achieved using mass spectrometric detection using an Agilent Technologies 6490 QQQ-MS controlled by MassHunter software version B.06.00 (Agilent Technologies). The MS was connected to an APCI ion source (G1947 A/B) from Agilent Technologies. MRM mode was used, which provides a high degree of certainty in identifying compounds based on their precursor-to-product transitions. The conditions for the MRM of the compounds were optimised either using the Optimizer Software (Agilent Technologies) or manually and are shown in Table 4-2. The most abundant and specific ions were chosen.

Table 4-2: Triple quadrupole mass spectrometric conditions in multiple reaction monitoring mode for the target organic gunshot residues.

Compound	Ionization Mode	Precursor Ion [m/z]	Product Ion 1 [m/z]	CE (Voltage)	Product Ion 2 (m/z)	CE (Voltage)	Product Ion 3 (m/z)	CE (Voltage)
1,2-DNG	APCI-	181.01	85	9	-	-	-	-
1,2-DNG	APCI+	183.03	77.0	37	51.2	77	-	-
2,4-DNDPA	APCI-	258.0	211.0	45	181.0	45	165.0	45
2,4-DNT	APCI+	183.04	166.0	21	139.3	41	127.9	41
2-naphthol*	APCI+	145.07	104.0	9	62.9	12	60.1	5
2-NDPA	APCI+	215.08	197.0	9	180.9	29	180.0	13
4-A-2,6-DNT	APCI-	196.0	149.0	15	119.0	15	-	-
4-nDPA	APCI+	199.09	182.0	21	128.0	45	126.9	53
DBP	APCI+	279.2	205.0	5	149.0	13	121.0	41
DDNP	APCI-	183.0	137.0	25	123.0	25	109.0	25
DEP	APCI+	223.1	177.0	5	149.0	13	121	33
DMP	APCI+	195.07	167	9	163	9	135	29

Table 4-2 continued: Triple quadrupole mass spectrometric conditions in multiple reaction monitoring mode for the target organic gunshot residues.

Compound	Ionization Mode	Precursor Ion [m/z]	Product Ion 1 [m/z]	CE (Voltage)	Product Ion 2 (m/z)	CE (Voltage)	Product Ion 3 (m/z)	CE (Voltage)
DPA	APCI+	170.1	152.1	33	93.0	29	78.0	57
EC	APCI+	269.16	148.1	13	119.9	25	92.1	37
EGDN	APCI+	154.0	127.0	15	122.0	15	67.0	15
HMX	APCI+	297.1	177.0	21	-	-	-	-
MC	APCI+	241.14	134.1	13	106.0	33	93.1	29
m-DNB	APCI+	169.0	168	21	139.5	61	115.1	49
m-NT	APCI+	138.06	111.0	12	97.0	13	96.0	13
N,N'-DPU	APCI+	213.1	120.0	17	94.0	21	77.0	45
NB	APCI-	122.02	95.1	5	-	-	-	-
NB	APCI+	124.04	107.0	21	97.0	13	81.8	21
NG	APCI-	226.0	195.9	9	133.9	21	75.9	21
NGU	APCI+	105.04	77.0	5	73.1	5	64.1	13

Table 4-2 continued: Triple quadrupole mass spectrometric conditions in multiple reaction monitoring mode for the target organic gunshot residues.

Compound	Ionization Mode	Precursor Ion [m/z]	Product Ion 1 [m/z]	CE (Voltage)	Product Ion 2 (m/z)	CE (Voltage)	Product Ion 3 (m/z)	CE (Voltage)
N-nDPA	APCI+	199.0	181.0	35	128.0	45	77.0	55
PETN	APCI+	317.0	182.4	45	109.1	29	-	-
RDX	APCI+	223.0	206.0	53	76.9	65	51.0	77
resorcinol	APCI+	111.1	83.0	13	70.1	5	65.1	21
tetryl	APCI+	288.0	173.7	37	87.9	17	-	-
TNB	APCI+	214.0	94.1	33	76.9	5	51.1	80
TNT	APCI+	228.0	166.1	41	150.7	41	129.2	45

*internal standard

4.2.3 *Experimental Design*

Preliminary scouting experiments were conducted to determine independent mobile phase parameters and to define the experimental space. A mixture of the compounds was injected and different selectivity variables tested. It was determined that mobile phase strength and temperature had the greatest influence on the resolution of the OGSR mix, which is in agreement with previous studies [190-192]. These two factors were investigated to establish their influence on the resolution of the compounds of interest, whereby mobile phase and temperature were changed and the shift of the retention time and peak width was measured. The mobile phase was the most significant factor affecting resolution, followed by the temperature. MeOH/water was selected as mobile phase as it has been previously applied to GSR analysis and presents a smaller environmental hazard than ACN [193]. No buffer was used. An initial MeOH concentration of 30 % was chosen as the starting concentrations for all gradients as this ensured that all compounds eluted after the void time. Linear gradient slopes of 0.6, 1.2, 1.8, 3.0 and 6.0 % MeOH/min at 23 °C were examined. A schematic diagram of the experimental space is shown in Figure 4-1. All 33 compounds (32 OGSR and one ISTD) were run individually in duplicates at the five different gradients to provide the training data (average retention times) for the ANN. Aliquots of the stock standards were diluted for UHPLC analysis in ACN:MeOH (1:1) to generate solutions at working concentrations of 20 ppm with 20 ng injected. Two gradients at 0.7 %/min and 4.6 %/min, were used to provide verification data in order to examine the suitability of the ANN for the prediction of the average retention times.

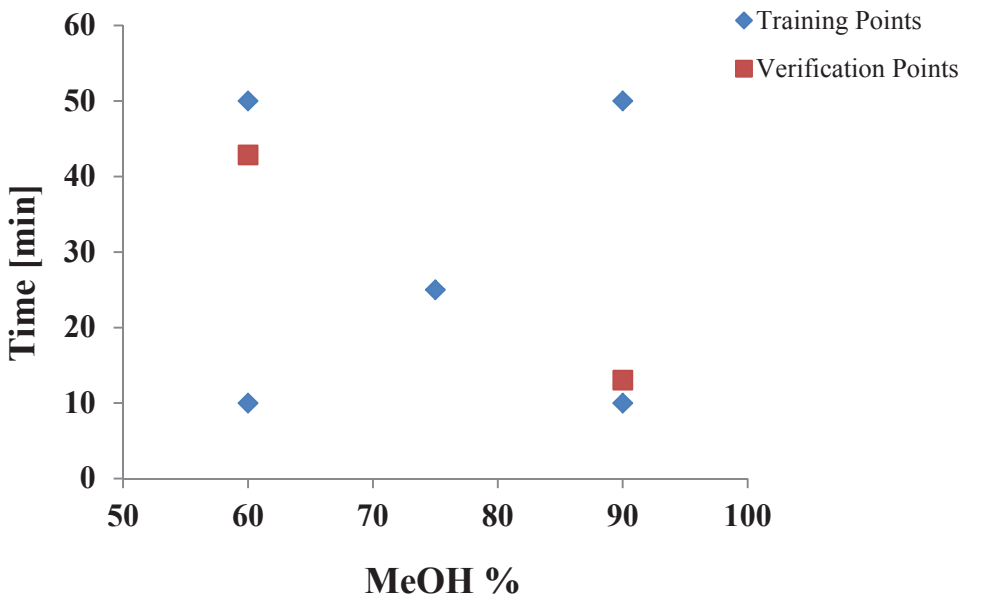

Figure 4-1: Representation of gradients defining the experimental space for input data to the Artificial Neural Network. Five gradients were used as training points to train the network, two gradients were used as verification data to mitigate overlearning.

4.2.4 *Artificial Neural Network*

Trajan Neural Networks, Version 6.0 (Trajan Software Ltd.), was used for simulating the ANNs and predicting optimised experimental conditions. The slopes of the five different gradients were presented to the software as input data and the average retention times of the 33 compounds for each different gradient were used as output values. An automated heuristic approach was applied to determine the optimal architecture of the ANN. During this process, the number of nodes in the hidden layer in the architecture was varied, and the network with the lowest error selected. This network was used to predict gradients between 0.6 %/min and 6 %/min with increments of 0.1 %/min.

4.2.5 *Additional Separation Optimisation*

The best separation by the ANN identified from the shortest time and highest resolution was further optimised by varying the temperature to 23, 35, 37, 39, 41, 43, and 45 °C. The initial MeOH concentration was optimised by monitoring peak shape and number of peaks at 30, 25, 20, 15, and 10 % of MeOH. Isocratic intervals were also introduced to the gradient profile to further separate the structural isomers and improve low resolution areas of the chromatogram.

4.2.6 *Method Validation*

Working standard solutions in the range of 0.1-100 ppm (0.1-100 ng injected) in seven replicates were used to construct calibration curves. LODs were calculated using (3.3*σ)/S, where σ is the SD of the slope and S the slope of the calibration curve. LOQs were based on 3.3*LOD. Intra and inter-day variations were examined by analysing the standards on three randomly chosen days with n = 7 in the morning and n = 7 in the evening.

4.2.7 *Ammunitions, Firearms and Specimen Preparation*

4.2.7.1 OGSR Collection from Hands and Specimen Preparation

Test shootings were conducted at the indoor firing range of the NSWPF in Sydney, Australia, to evaluate the method for its applicability to real case specimens. Twelve different kinds of ammunition and eight different firearms were used. A list of the firearms and ammunitions is presented Table 4-3.

Table 4-3: List of firearms and ammunition combinations used at the indoor shooting range. LF primer = lead free primer.

Comb No	Caliber	Ammunition Manufacturer (Country of origin)	Firearm Model and Mechanism	Firearm Brand(Country of origin)
1	WinClean 45 (LF primer)	Winchester (Australia)	Semi-automatic pistol Model 1911A1	Colt (USA)
2	45 Auto CP	Winchester (Australia)	Semi-automatic pistol Model 1911A1	Colt (USA)
3	44 Rem Magnum	PMC (USA)	Double-action revolver Model 629-4	Smith&Wesson (USA)
4	44 Rem Magnum	Winchester (Australia)	Double-action revolver Model 629-4	Smith&Wesson (USA)
5	9 mm Parabellum	Blazer, CCI (USA)	Semi-automatic pistol Model 92FS-CAL.9	Beretta (Italy)
6	357 Magnum	Winchester (Australia)	Double-action revolver Model 686-3	Smith&Wesson (USA)
7	357 Magnum	PMC (USA)	Double-action revolver Model 686-3	Smith&Wesson (USA)
8	22 LR High Velocity	Remington (USA)	Semi-automatic pistol Sport King	High Standard (USA)
9	22 LR High Velocity Superspeed	Winchester (Australia)	Semi-automatic pistol Sport King	High Standard (USA)
10	22 LR High Velocity	Remington (USA)	Self-loading rifle (bolt action) Model 70	Marlin (USA)
11	22 LR High Velocity Superspeed	Winchester (Australia)	Self-loading rifle (bolt action) Model 70	Marlin (USA)
12	40 Smith&Wesson WinClean (LF primer)	Winchester (Australia)	Semi-automatic pistol Model 22	Glock (Austria)
13	40 Smith&Wesson	Winchester (Australia)	Semi-automatic pistol Model 22	Glock (Austria)
14	12 gauge (SuperX)	Winchester (Australia)	Pump-action shotgun Model 870	Remington (USA)

Before every discharge, the shooter thoroughly cleaned his hands and control specimens were taken. Specimens were collected after one discharge and after three discharges for every ammunition-firearm combination. After firing the weapon, specimens were collected from the hands of the shooter. The specimen collection involved wiping alcohol swabs (Webcol^{TM}, Kendall, USA) over the hands until the wipes was almost dry. Subsequently, the wipes were deposited in scintillation vials and stored in a refrigerator at 4 °C. Five mL MTBE were added to the swab in a scintillation vial. After 5 min sonication, the solvent was removed under a steady stream of nitrogen gas and the specimen reconstituted in 196 µL of mobile phase and 4 µL ISTD was added. The specimen was filtered using a 0.2 µm syringe filter prior to analysis by UHPLC.

4.2.7.2 Unburned Smokeless Powder Collection and Sample Preparation

Unburned smokeless powder samples were collected from the same ammunition boxes used for the firing tests. The cartridge was opened and the powder transferred into scintillation for transport. The smokeless powders were extracted according to literature [80, 102, 181]. 250 µL of DCM was added to 5 mg of powder and left overnight in the dark. The following day, a 20 µL aliquot was taken and dried under nitrogen gas. The sample was reconstituted in 39.2 µL of MeOH and 0.8 µL ISTD was added. One µL of the samples were injected onto the UHPLC.

4.3 Results and Discussion

4.3.1 *Artificial Neural Network Training*

The separation of the large number of explosives possibly present in OGSR is problematic due to the significant number of isomers, such as DNT and/or amino-DNT isomers. The use of an ANN is an efficient means to separate the greatest number of compounds with a linear gradient. Further small refinements may then be made such as increasing temperature, varying initial MeOH concentration, and introduction of isocratic conditions in regions of poor separation, particularly where the structural isomers elute.

Initially, the ANN training data consisted of five linear gradient slopes as the independent input variables, whilst the average of the duplicate retention times for each of the 33 standards was used as the dependent output variables. These 165 experimental points were used to construct a suitable ANN architecture to adequately model the response surface and is shown in Table 4-4.

Table 4-4: Input data for supervised training of the Artificial Neural Network. The data consists of the average retention times (n = 2) [min] of each target compound at five different gradient conditions. MeOH = methanol.

Average Retention Times [min]					
Gradient [% MeOH/min]	**0.6**	**1.2**	**1.8**	**3**	**6**
NGU	0.546	0.546	0.543	0.547	0.544
resorcinol	1.003	1.016	1.010	0.999	1.000
HMX	1.408	1.396	1.387	1.374	1.332
1,3-DNG	1.641	1.641	1.621	1.596	1.560
1,2-DNG	2.004	1.999	1.958	1.946	1.847
EGDN	2.429	2.391	2.354	2.294	2.157
RDX	2.744	2.679	2.616	2.511	2.295
TNB	4.149	3.977	3.794	3.513	3.043
1,3-DNB	5.210	4.921	4.627	4.184	3.498
NB	6.337	5.850	5.437	4.812	3.880
NG	7.548	6.822	6.246	5.424	4.224
DDNP	7.950	7.029	6.373	5.458	4.209
DMP	8.474	7.217	6.382	5.309	3.972
tetryl	8.990	7.768	6.928	5.798	4.344
TNT	9.190	8.047	7.200	6.077	4.579
3,4-DNT	10.035	8.552	7.490	6.189	4.520
4-A-2,6-DNT	10.616	9.005	7.897	6.478	4.740
2,4-DNT	10.878	9.243	8.273	6.749	4.967
2,6-DNT	11.199	9.433	8.261	6.815	4.947
2,3-DNT	11.346	9.444	8.186	6.620	4.779
2-naphthol	14.944	11.712	9.833	7.679	5.317
3-NT	15.037	12.074	10.258	8.146	5.681
PETN	16.843	13.169	11.022	8.552	5.820
N,N'-DPU	19.298	14.148	11.503	8.686	5.778
DEP	23.002	16.014	12.681	9.367	6.050
4-nDPA	23.735	16.547	13.106	9.670	6.218
N-nDPA	30.347	20.138	15.580	11.152	7.009
MC	32.210	20.755	15.850	11.236	6.960
DPA	34.982	22.782	17.423	12.328	7.593
2,4-DNDPA	37.885	24.199	23.356	12.859	7.870
2-NDPA	45.256	27.836	20.752	14.269	8.550
EC	48.607	28.905	21.232	14.392	8.497
DBP	60.256	34.433	24.812	16.443	9.448

An iterative heuristic process resulted in a multi-layer perceptron network with one input node, 19 nodes in the hidden layer, and 33 nodes in the output layer representing the retention times of the 33 compounds (Figure 4-2).

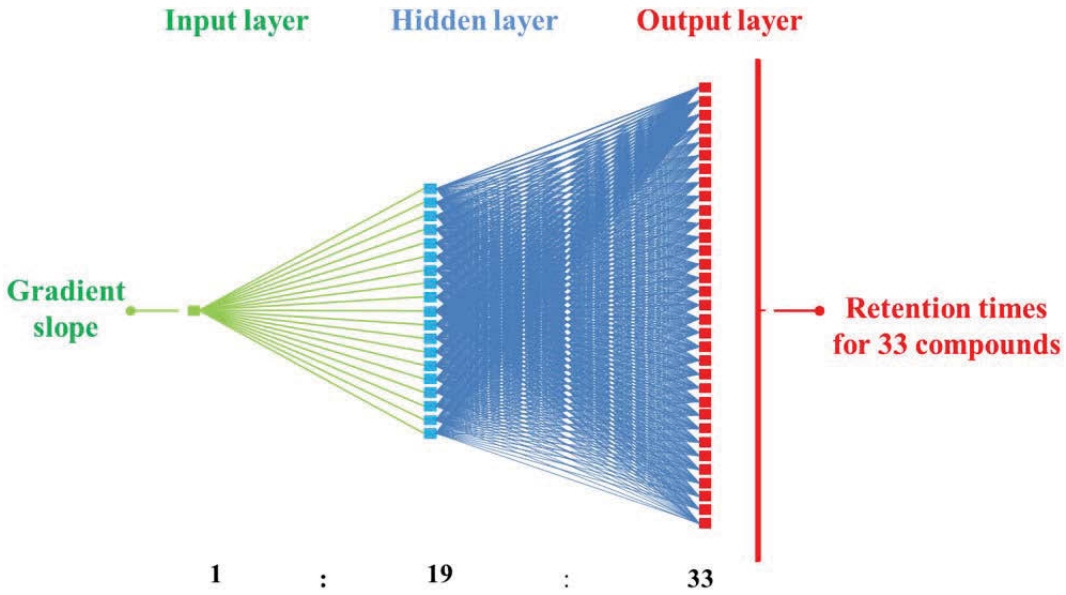

Figure 4-2: Schematic diagram of the 1:1-19-33:33 multilayer perceptron network providing the smallest error for the prediction of the retention times of the 33 compounds of interest. The gradient slope represents the input data, the retention times are given through the output data.

This network was used to predict retention times for all compounds within the experimental space with gradient increments of 0.1 %/min. Using this data the differences between adjacent peaks were calculated. Then the calculated retention time differences were filtered in order to find the minimum peak pair (MPP) difference (the retention time difference between two closest peaks) for each gradient. The MPP differences are presented with the runtimes of the gradients in Table 4-5. Further, using these MMP differences of each gradient a response resolution plot was constructed (Figure 4-3). The difference between the two closest peaks gives an indication of the resolution achieved when using the specific gradient as it shows how well resolved the two closest peaks in a chromatogram are.

Table 4-5: List of predicted minimum peak pair (MPP) and runtimes [min] of gradients ranging from 0.6-6 %/min with increments of 0.1 %/min. MeOH = methanol.

Gradient [% MeOH/min]	MPP [min]	Runtime [min]
0.6	0.0400	60.64
0.7	**0.1200**	**54.04**
0.8	0.0920	48.52
0.9	0.0600	43.92
1	0.0000	40.09
1.1	0.0440	36.90
1.2	0.0410	34.22
1.3	0.0400	31.96
1.4	0.0420	30.03
1.5	0.0100	28.38
1.6	0.0080	26.94
1.7	0.0182	25.68
1.8	0.0035	24.55
1.9	0.0233	23.54
2	0.0414	22.62
2.1	0.0313	21.78
2.2	0.0133	21.00
2.3	0.0028	20.27
2.4	0.0173	19.59
2.5	0.0301	18.95
2.6	0.0300	18.34
2.7	0.0200	17.76
2.8	0.0090	17.22
2.9	0.0020	16.70
3	0.0100	16.20
3.1	0.0056	15.73
3.2	0.0020	15.29
3.3	0.0010	14.87
3.4	0.0000	14.46
3.5	0.0040	14.08
3.6	0.0060	13.72

Figure 4-5 continued: List of predicted minimum peak pair (MPP) and runtimes [min] of gradients ranging from 0.6 – 6 %/min with increments of 0.1 %/min. MeOH = methanol.

Gradient [% MeOH/min]	MPP [min]	runtime [min]
3.7	0.0090	13.39
3.8	0.0110	13.07
3.9	0.0140	12.77
4	0.0150	12.48
4.1	0.0170	12.22
4.2	0.0100	11.98
4.3	0.0020	11.75
4.4	0.0080	11.54
4.5	0.0190	11.34
4.6	**0.0210**	**11.16**
4.7	0.0140	11.00
4.8	0.0060	10.85
4.9	0.0010	10.72
5	0.0020	10.60
5.1	0.0090	10.49
5.2	0.0120	10.40
5.3	0.0143	10.32
5.4	0.0114	10.26
5.5	0.0088	10.20
5.6	0.0030	10.16
5.7	0.0040	10.13
5.8	0.0027	10.11
5.9	0.0012	10.10
6	0.0001	10.10

The highest point on the response resolution plot (0.7 %/min MeOH) represented the best performing gradient in terms of resolution. However, the predicted analysis time was 54.0 min, which is of limited practical use. Therefore a compromise between resolution and runtime was made, with the gradient at

4.6 %/min offering a suitable outcome in terms of run time and resolution. This gradient separated 22 compounds, whilst 11 compounds co-eluted.

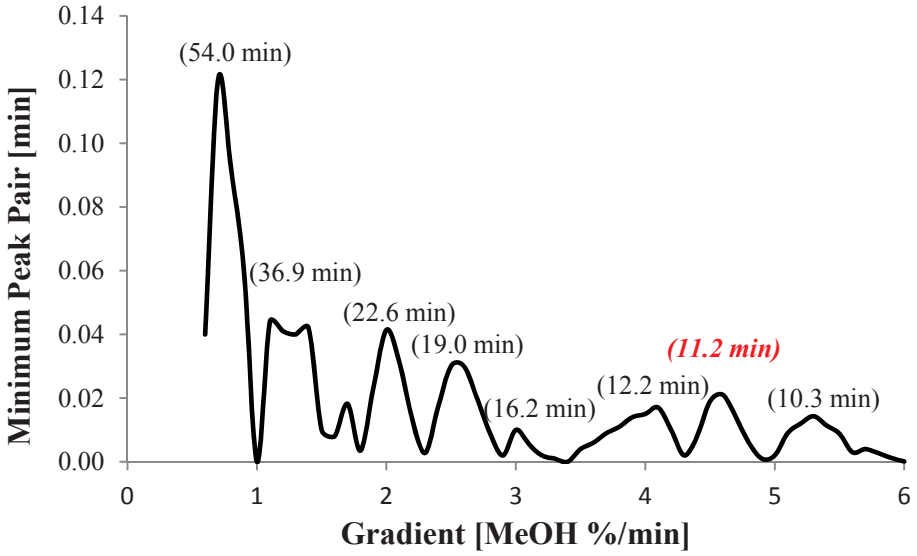

Figure 4-3: Response Resolution Plot. The minimum peak pair is plotted versus the gradient (% MeOH/min), whereby MeOH stands for methanol. The run times of the maxima of the minimum peak pairs (representing the best resolution) are shown in the brackets. The gradient with 4.6 %/min MeOH increase was used as it provided efficient resolution and short analysis time.

The possibility of overfitting was eliminated by running the individual standards at gradients of 0.7 %/min and 4.6 %/min for use as verification data points for retraining of the ANN. Using the same process as described before, the ANN with the smallest error was again determined to be a MLP network with 1:1-19-33:33 architecture.

This together with the high correlation (R^2 = 0.999 and 0.992 for 0.7 %/min and 4.6 %/min respectively) between observed and predicted retention times demonstrated that the ANN adequately described the response surface. Differences between measured and predicted retention times ranged from 0 (DPA at 0.7 %/min, DDNP, tetryl, 4-A-2,6-DNT, 2,3-DNT, 2-naphthol at 4.6 %/min) to 7.437 % (DPA at 4.6 %/min) and are listed in Table 4-6. Two graphs demonstrating the relationship between predicted and observed retention times for the two gradients, i.e. 0.7 %/min and 4.6 % /min are shown in Figure 4-4.

Table 4-6: List of predicted and observed retention times [min] and % relative standard deviation (% RSD) values of the target compounds using the gradients 0.7 % MeOH/min and 4.6 % MeOH/min. rt = retention time, MeOH = methanol.

	0.7 % MeOH/min			4.6 % MeOH/min		
	predicted rt [min]	observed rt [min]	% RSD	predicted rt [min]	observed rt [min]	% RSD
NGU	0.546	0.549	0.437	0.546	0.550	0.551
resorcinol	1.007	1.071	4.363	0.993	1.048	3.778
HMX	1.405	1.436	1.548	1.354	1.368	0.717
1,3-GDN	1.641	1.694	2.252	1.570	1.616	2.033
1,2-DGN	2.003	2.072	2.412	1.892	1.919	0.994
EGDN	2.420	2.449	0.857	2.215	2.237	0.702
RDX	2.733	2.794	1.574	2.384	2.422	1.112
TNB	4.120	4.240	2.028	3.201	3.304	2.246
1,3-TNB	5.152	5.305	2.073	3.725	3.841	2.166
NB	6.234	6.336	1.151	4.214	4.274	1.006
DMP	7.376	7.568	1.820	4.380	4.464	1.337
NG	8.212	8.280	0.582	4.562	4.732	2.587
DDNP	8.726	8.370	2.945	4.601	4.601	**0.000**
tetryl	8.928	8.993	0.514	4.798	4.798	**0.000**
3,4-DNT	9.693	9.760	0.486	4.841	4.895	0.786
TNT	10.070	10.553	3.312	5.026	5.121	1.321
4-A-2,6-DNT	10.200	10.553	2.406	5.268	5.268	**0.000**
2,3-DNT	10.490	10.571	0.544	5.313	5.313	**0.000**
2,6-DNT	10.950	10.972	0.142	5.474	5.439	0.454
2,4-DNT	13.050	12.975	0.408	5.508	5.579	0.906
2-naphthol	13.440	13.620	0.941	6.110	6.110	0.000
3-NT	14.300	14.353	0.262	6.337	6.305	0.358
N,N'-DPU	15.970	16.242	1.194	6.644	6.520	1.332
PETN	18.050	18.170	0.469	6.669	6.618	0.543
DEP	21.220	19.264	6.833	6.891	6.741	1.556
4-nDPA	21.960	21.321	2.088	7.260	7.108	1.496

Table 4-6 continued: List of predicted and observed retention times [min] and % relative standard deviation (% RSD) values of the target compounds using the gradients 0.7 % MeOH/min and 4.6 % MeOH/min. rt = retention time, MeOH = methanol.

	0.7 % MeOH/min			4.6 % MeOH/min		
	predicted rt [min]	**observed rt [min]**	**% RSD**	**predicted rt [min]**	**observed rt [min]**	**% RSD**
N-nDPA	27.940	27.919	0.053	7.940	7.349	5.467
MC	29.170	29.086	0.204	8.176	8.335	1.362
2,4-DNDPA	31.760	31.726	0.076	8.362	9.120	6.132
DPA	34.800	34.800	**0.000**	8.404	9.337	**7.437**
EC	40.770	40.333	0.762	9.830	10.160	2.335
2-NDPA	43.680	43.169	0.832	10.250	10.369	0.816
DBP	54.040	53.321	0.947	11.160	11.658	3.087

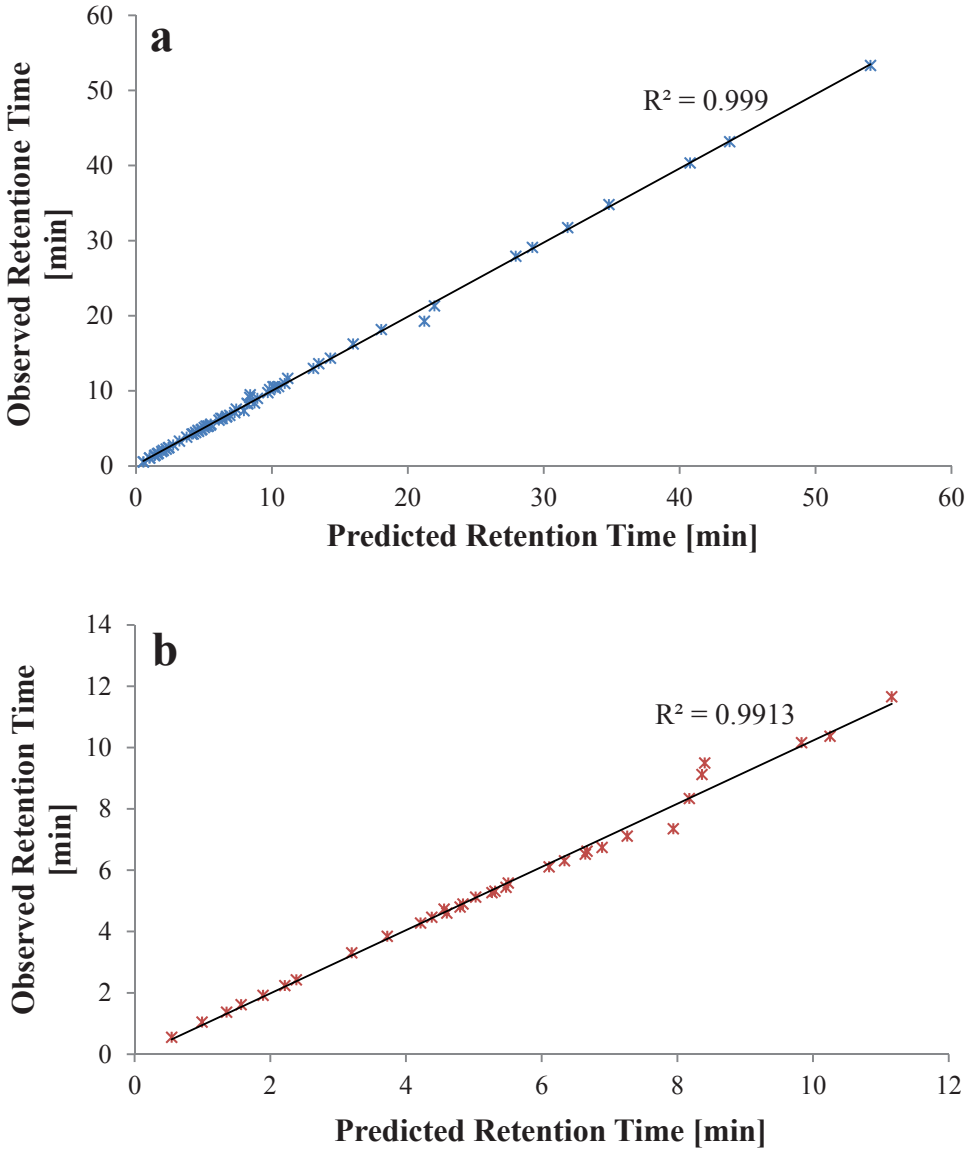

Figure 4-4: Graph showing the correlation between observed retention time [min] and predicted retention time [min] for the gradient 0.7 % MeOH/min (a) and the gradient 4.6 % MeOH/min (b). MeOH = methanol.

4.3.2 *Additional Optimisation*

The slope determined by the ANN was accompanied by an additional optimisation process which consisted of modifications to the initial MeOH concentration, increasing the column temperature and incorporation of isocratics steps.

The initial MeOH concentration of the mobile phase had the strongest influence on the first eight peaks (NGU, resorcinol, DDNP, RDX, 1,3-DNG, 1,2-DNG, EGDN, HMX). It was found that especially RDX and HMX eluted earlier

using a higher initial concentration. While RDX and 1,3-DNG were coeluting with 5 % MeOH, a complete baseline separation was achieved using an initial MeOH concentration of 10 % whereby higher initial concentrations improved the resolution between these two compounds. The peaks of EGDN and HMX were baseline separated using 5 and 10 % MeOH, however started to coelute from 15 % with increasing starting concentration until their sequence of elution changed over 30 % initial MeOH concentration with HMX eluting before EGDN. Using an initial MeOH concentration of 10 % all of the first eight peaks were baseline separated and clearly distinguishable. The retention time change of the first eight compounds depending on the initial MeOH % is shown in Figure 4-5, whereby the blue circled area highlights the peak difference of RDX (a) and 1,3-DNG (b) and the red area the peak difference of EGDN (c) and HMX (d). For visualisation purposes, 10, 20, 30, 40, and 50 mAU were added to the absorbances of the chromatograms with initial MeOH concentrations of 10, 15, 20, 25, and 30 % respectively.

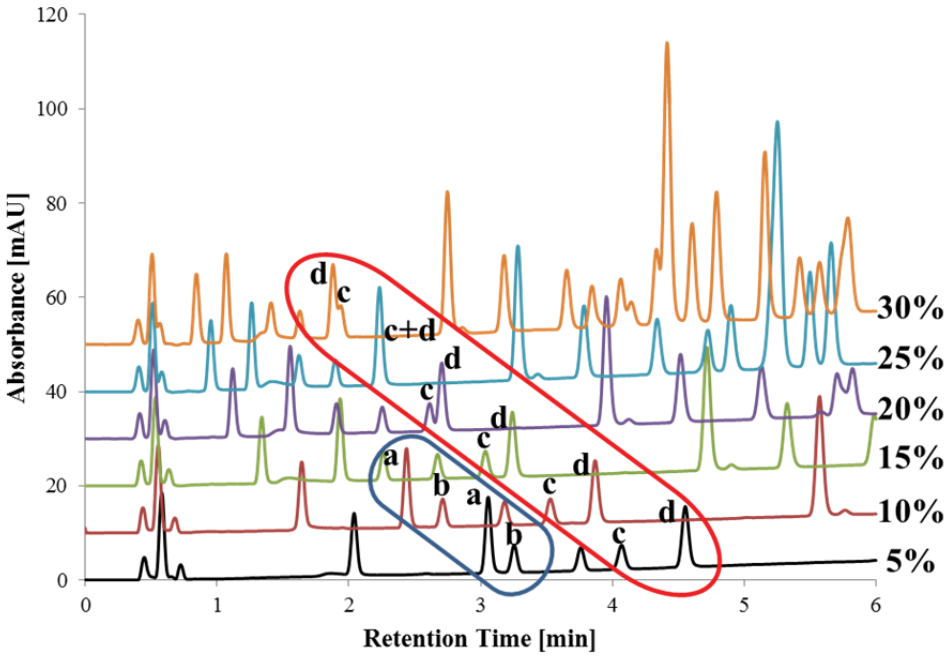

Figure 4-5: Early sections of the chromatograms when using different initial methanol (MeOH) concentrations (5-30 %). The blue circled area highlights the relationship between RDX (a) and 1,3-DNG (b) with different initial MeOH %, while the red area shows the relationship between EGDN (c) and HMX (d).

The influence of temperature had variable effects on the different compounds tested. The relationship between the retention time and temperature for each compound can be expressed through the van't Hoff relationship and used for the prediction of the separation as reported previously [191-193]. Resolution has also been shown to improve with increasing temperature [193]. When comparing the compounds of interest, changing the temperature had the highest effect on the selectivity of ionisable and polar compounds. This phenomenon has previously been explained to occur due to a current change of the pKa [190] and has also been supported by other studies [193]. Increasing the temperature to 43 °C further increased the resolution due to improved mass transfer with 27 peaks separated.

Two isocratic steps were then introduced to separate tetryl, TNT, DMP and the DNT isomers, with the optimal separation of the 33 target analytes shown in Figure 4-6.

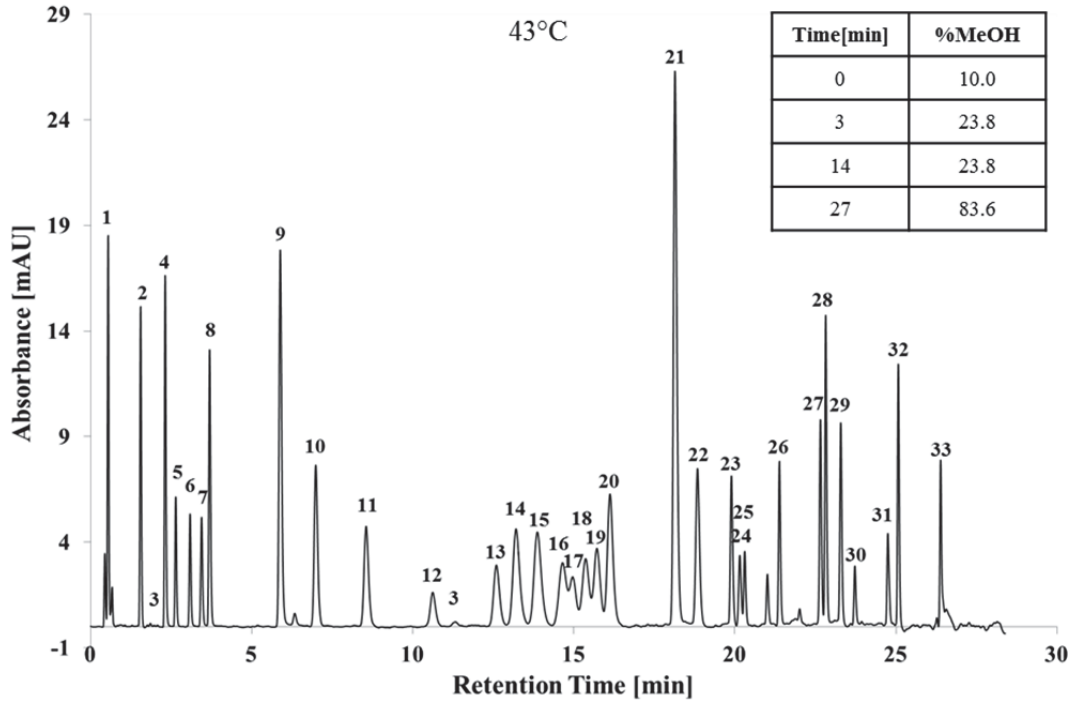

Figure 4-6: Optimised separation of 32 organic gunshot residue compounds under 214 nm. 1 = NGU, 2 = resorcinol, 3 = DDNP, 4 = RDX, 5 = 1,3-DNG, 6 = 1,2-DNG, 7 = EGDN, 8 = HMX, 9 = TNB, 10 = 1,3-DNB, 11 = NB, 12 = NG, 13 = tetryl, 14 = TNT, 15 = 4-A-2,6-DNT, 16 = 3,4-DNT, 17 = DMP, 18 = 2,4-DNT, 19 = 2,6-DNT, 20 = 2,3-DNT, 21 = 2-naphthol (internal standard), 22 = m-NT, 23 = DEP, 24 = N,N'-DPU, 25 = PETN, 26 = 4-nDPA, 27 = MC, 28 = N-nDPA, 29 = DPA, 30 = 2,4-DNDPA, 31 = 2-NDPA, 32 = EC, 33 = DBP. 20 ng of each compound were injected.

4.3.3 *Method Validation*

The analytical figures of merit are shown in Table 4-7. The method showed high linearity with R^2 between 0.988 (DDNP) and 0.999 (2,3-DNT, m-NT, 4-A-2,6-DNT, 2-NDPA, DMP, DBP, N, N'-DPU). Standard errors of the calibration curve ranged between 4.3 $x10^{-3}$ (resorcinol) and 3.4 x 10^{-5} (2,4-DNDPA). The lowest relative standard deviation (RSD) of the capacity factors was DBP at 0.0100 % (DBP), whilst the highest was for NGU at 4.00 %. Peak area % RSDs ranged between 0.201 % (1,3-DNG) and 1.55 % (2,4-DNDPA). The LODs were between 0.03 ng (N, N'-DPU, 2-NDPA) and 0.21 ng (DDNP) at 214 nm, comparable to values previously reported using UHPLC-UV detection [181]. LOQs were between 0.10 ng (N,N'-DPU, 2-NDPA) and 0.71 ng (2,4-DNDPA). These LODs indicated that the

method was suitable for casework application [4, 6, 84, 194]. Intra and interday variations were determined over a three day period by comparing the peak area of the seven replicate analyses. The mean intraday variation across the three day period was between 0.22 % RSD (NGU) and 9.7 % RSD (2-NDPA). The interday variation ranged from 0.017 % RSD (N,N'-DPU) to 12 % RSD (2,4-DNDPA).

Table 4-7: Figures of merit for the detection of gunshot residue compounds by ultraviolet detection at 214 nm with n = 7; % RSD = % relative standard deviation.

Compound	Average Retention Time [min]	Time % RSD	Area % RSD	Capacity Factor, k'	k' % RSD	R^2	y-intercept	Slope	Standard Error of the Slope	Sensitivity	
										LOD [ng]	LOQ [ng]
1,2-DNG	3.134	1.2	0.78	4.91	1.5	0.995	-0.00066	0.0039	$1.0x10^{-4}$	0.085	0.26
1,3-DNG	2.693	0.13	0.20	4.08	0.14	0.996	-0.0018	0.0046	$9.5x10^{-5}$	0.068	0.21
2,3-DNT	16.07	0.047	0.45	29.3	0.044	0.999	-0.014	0.019	$2.3x10^{-4}$	0.041	0.12
2,4-DNT	16.16	0.12	0.30	29.5	0.13	0.993	0.030	0.010	$4.0x10^{-4}$	0.13	0.40
2,4-DNDPA	23.94	0.019	1.6	44.2	0.020	0.990	0.0070	0.00048	$3.4x10^{-5}$	0.23	0.71
2,6-DNT	15.60	0.021	0.23	28.4	0.028	0.997	-0.017	0.012	$2.5x10^{-4}$	0.069	0.21
3,4-DNT	14.51	0.028	0.27	26.34	0.034	0.998	-0.018	0.014	$2.5x10^{-4}$	0.062	0.18
2-NDPA	24.77	0.013	0.47	45.7	0.018	0.999	-0.0023	0.011	$1.2x10^{-4}$	0.035	0.10
4-A-2,6-DNT	13.76	0.075	0.37	25.0	0.069	0.999	-0.015	0.017	$2.3x10^{-4}$	0.044	0.13
4-nDPA	20.99	0.015	0.73	38.6	0.015	0.998	-0.0033	0.0030	$5.4x10^{-5}$	0.059	0.18
DBP	26.38	0.012	0.66	48.8	0.010	0.999	-0.0015	0.0069	$7.4x10^{-5}$	0.034	0.11
DDNP	1.848	0.16	0.40	2.48	0.22	0.988	-0.041	0.0045	$2.9x10^{-4}$	0.21	0.65
DEP	21.51	0.022	1.2	39.6	0.019	0.989	-0.014	0.012	$4.6x10^{-4}$	0.13	0.40
DMP	14.91	0.073	0.47	27.1	0.084	0.999	-0.0065	0.0089	$1.1x10^{-4}$	0.039	0.12
DPA	23.30	0.031	0.46	42.9	0.018	0.995	-0.018	0.013	$3.7x10^{-4}$	0.091	0.28

Table 4-7 continued: Figures of merit for the detection of gunshot residue compounds by ultraviolet detection at 214 nm with n = 7; % RSD = % relative standard deviation.

Compound	Average Retention Time [min]	Time % RSD	Area % RSD	Capacity Factor, k'	k' % RSD	R^2	y-intercept	Slope	Standard Error of the Slope	Sensitivity	
										LOD [ng]	LOQ [ng]
EC	25.05	0.010	0.42	46.3	0.011	0.993	-0.010	0.015	$4.7x10^{-4}$	0.11	0.32
EGDN	3.435	0.074	0.25	5.48	0.13	0.995	-0.0010	0.0046	$1.2x10^{-4}$	0.087	0.26
HMX	3.706	0.17	0.33	5.97	0.13	0.996	-0.012	0.012	$2.6x10^{-4}$	0.075	0.23
m-DNB	7.018	0.20	0.33	12.2	0.13	0.997	-0.013	0.014	$2.8x10^{-4}$	0.065	0.20
m-NT	18.81	0.019	0.39	34.5	0.022	0.999	-0.0059	0.015	$1.8x10^{-4}$	0.041	0.12
MC	22.80	0.010	0.18	42.0	0.013	0.996	-0.010	0.016	$3.7x10^{-4}$	0.079	0.24
NB	8.593	0.21	0.36	15.1	0.13	0.997	-0.012	0.012	$2.4x10^{-4}$	0.068	0.20
NG	10.55	0.033	1.3	18.9	0.029	0.991	-0.00023	0.0039	$1.7x10^{-4}$	0.14	0.43
NGU	0.5430	0.070	0.69	0.0200	4.0	0.991	0.0030	0.011	$3.6x10^{-4}$	0.11	0.33
N,N'-DPU	19.86	0.016	0.72	36.5	0.013	0.999	0.0042	0.0088	$9.0x10^{-5}$	0.034	0.10
N-nDPA	22.67	0.030	0.77	41.7	0.019	0.996	-0.014	0.013	$3.2x10^{-4}$	0.080	0.24
PETN	20.17	0.055	0.56	37.0	0.026	0.995	-0.0073	0.0046	$1.4x10^{-4}$	0.10	0.31
RDX	2.323	0.19	0.37	3.37	0.16	0.996	-0.014	0.014	$3.3x10^{-4}$	0.079	0.24
resorcinol	1.548	0.17	0.59	1.92	0.39	0.992	0.00090	0.013	$4.3x10^{-3}$	0.11	0.32
tetryl	12.51	0.074	0.40	22.6	0.086	0.998	-0.017	0.017	$2.8x10^{-4}$	0.054	0.16

Table 4-7 continued: Figures of merit for the detection of gunshot residue compounds by ultraviolet detection at 214 nm with n = 7; % RSD = % relative standard deviation.

Compound	Average Retention Time [min]	Time % RSD	Area % RSD	Capacity Factor, k'	k' % RSD	R^2	y-intercept	Slope	Standard Error of the Slope	Sensitivity	
										LOD [ng]	LOQ [ng]
TNB	5.913	0.19	0.34	10.1	0.089	0.996	-0.025	0.025	$5.9x10^{-4}$	0.078	0.24
TNT	13.26	0.20	0.55	23.9	0.11	0.996	-0.019	0.017	$3.8x10^{-4}$	0.075	0.23
2-naphthol*	18.16	0.068	0.79	33.2	0.049	N/A	N/A	N/A	N/A	N/A	N/A

*: internal standard

The method was applied to a real case scenario using smokeless powder samples and hand swab specimens taken after shooting a firearm. A total of 78 test fires were conducted in triplicate. The specimen preparation of the hand swabs was previously developed and tested on samples taken from skin spiked with OGSR (Chapter 5). Possible interferences were only found for DBP. Example chromatograms for lead containing 40 S&W before and after shooting using a 22 Glock (Austria) are shown in Figure 4-7.

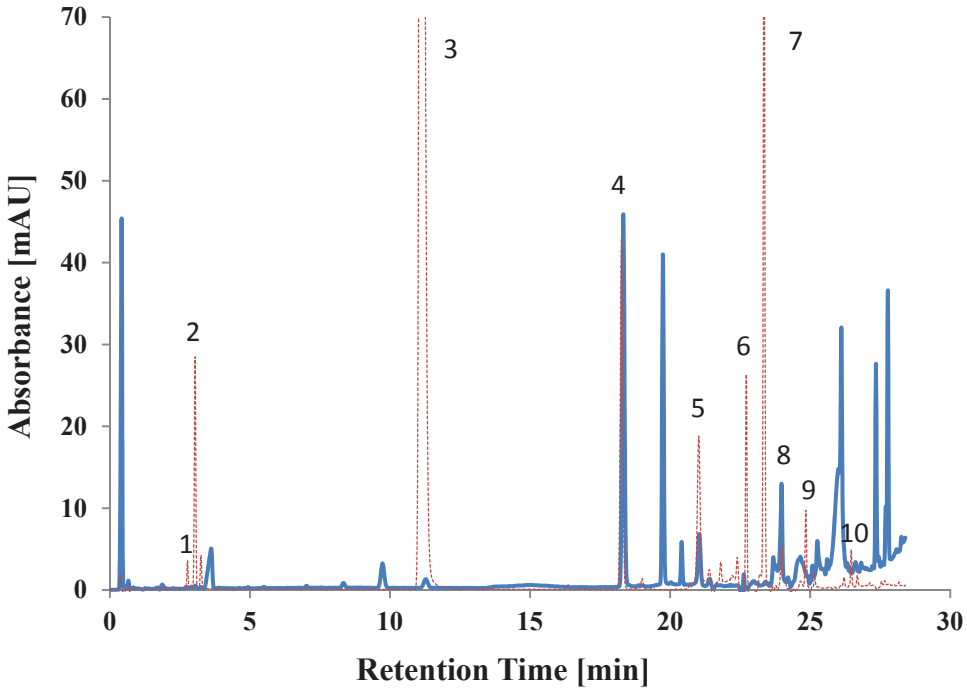

Figure 4-7: Overlayed chromatograms of smokeless powder before shooting (40 S&W, Winchester, Australia; red dashed line) and the gunshot residues collected from the hands of a shooter after discharge using a 22 Glock pistol (blue line). 1 = 1,2-DNG, 2 = 1,3-DNG, 3 = NG, 4 = 2-naphthol (internal standard), 5 = DEP, 6 = MC, 7 = DPA, 8 = 2,4-DNDPA, 9 = EC, 10 = DBP.

Various OGSR were detected in the unburned smokeless powders and hand swab specimens. The presence and identity of all compounds detected by UHPLC analysis with UV detection were confirmed by mass spectrometric detection using an Agilent Technologies 6490 QQQ-MS in MRM mode. A detailed table showing all detected compounds in the unburnt powders and OGSR collected from hands by

swabbing is provided in Appendix VII. Please note, that Appendix VII also provides the results of OGSR collection and extraction from GSR stubs in order to compare the collection efficiencies of alcohol swabs and GSR stubs in Chapter 5. Only the results using alcohol swabs were used in this Chapter (4) to evaluate the applicability of the developed UHPLC to simulated case specimen. Each of the tested powders included NG, indicating they were all double based powders. In the hand swab specimens NG was found in 62.2 % of the specimens, 1,2-DNG in 66.7 %, and 1,3-DNG in 34.6 %. The stabilisers DPA, EC, and MC were detected in 47.4, 73.5, and 72.9 % of the hand swab specimens respectively. The fact that EC and MC were detected in approximately 75 % of the hand swab specimens after firing ammunition is of high importance since MC and EC, are considered to be the most characteristic compounds for OGSR [37, 62]. DPA alone is not characteristic for OGSR. However, when detected in combination with its derivatives, it is considered as indicative for OSGR [63]. DPA derivatives detected included N-nDPA (5.1 %), 4-nDPA (6.4 %), and 2-NDPA (75.6 %). Therefore, the results show that the developed method can provide vital information in the investigation of a firearm related event. Additionally, the combined detection of the various compounds increases the evidential value of the developed method for OSGR investigation.

Moreover, the method was able to quantify the compounds of interest present in smokeless powder samples and hand swab specimens after only a single cartridge was discharged (Appendix VII results for hand swabs). For the different powders tested before and after shooting, differences in the chemical composition could be found. This indicated that it could be possible to establish profiles for each powder. The method therefore has the potential to distinguish between different ammunitions

based on their varying composition and potentially link ammunition to the OGSR found on the hands of a shooter.

The masses of the detected compounds were relatively low (in the low ng range), which is in consistent with previous reported masses [2, 64] and underlines the need for a sensitive method as developed here. It is recommended to use a MS/MS method after the compounds have been separated using the developed technique in order to verify the presence of compounds in the powder and/or hand swabs.

It is important to consider, that swabs were used in order to collect OGSR from the hands of a shooter. Studies comparing swabbing of OGSR to other commonly applied collection techniques can inform on which technique is most suitable for OGSR collection. Applying the most suitable collection technique might ultimately improve the collection efficiency and increase the levels of OGSR detected. Since police commonly uses GSR stubs in order to collect IGSR from hands, it should be investigated whether OGSR extracted from GSR stubs can be detected using the developed method.

In order to implement this method in routine casework additional research is required along with individual laboratory validation studies in order to ensure that quality standards for OGSR investigations are met.

4.4 Conclusion

A gradient UHPLC method was developed for the quantitative analysis of 32 OGSR using an ANN for rapid optimisation. The ANN was trained with average retention times and provided excellent correlation between observed and predicted retention

times with errors between 0 and 7.44 %. The ANN predicted a gradient at 4.6 %/min MeOH providing the best compromise between resolution and run time, with 22 compounds baseline separated. Further optimisations of the initial MeOH concentration, temperature and implementation of two isocratic steps resulted in separation of all 32 OGSR and the ISTD. The final method separated all of the target analytes in under 27 min with LODs between 0.03 and 0.21 ng at 214 nm. The LODs were lower than previously reported methods of OGSR analyses in simulated scenarios [4, 6, 84, 194]. The large number of target compounds and low LODs indicate the method is applicable for forensic investigations of firearm related incidents. OGSR were detected in a real case scenario whereby specimens were taken from a shooter's hands at a shooting range.

Chapter 5: Development and Comparison of Collection Techniques for the Combined Collection of OGSR and IGSR

Chapter 5: Development and Comparison of Collection Techniques for the Combined Collection of OGSR and IGSR

5.1 Background

A collection protocol allowing the efficient removal of IGSR as well as OGSR was needed to enable the analysis of IGSR using SEM-EDX in combination with OGSR analysis using the developed UHPLC method (Chapter 4). Analysis of OGSR can be incorporated into the SOP by either separating OGSR and IGSR from the collection device to enable their subsequent analysis or directly and non-destructively analysing both OGSR and IGSR *in situ* on a single collection device. Important aspects to consider when developing such a protocol are the surface from which GSR are collected, collection and extraction efficiencies, the possibility of extraction of interfering substances and interference with subsequent analytical techniques [127]. The collection efficiency of the collection device plays a central role for both approaches.

Common collection devices used are tape lifts [11], swabs [6, 195] or vacuum devices [44, 131], with tape lifts and swabs being mainly applied to the collection of GSR from skin and vacuum devices applied to clothing [27, 196].

Different techniques and protocols have previously been developed. One of these protocol applied only one specimen container for swab extraction and the clean-up of the extracts in order to minimise any specimen loss and contamination issues. It was proposed that IGSR could be retrieved by filtration using a membrane. The method was tested for RDX, DNT, NG, PETN, and TNT using HPLC with

electrochemical reductive detection [15]. However, no stabilisers were tested and no data of the recovery of IGSR is available.

Two studies focused on the extraction of NG, 2,4-DNT [57], TNT, RDX, and PETN [58] from GSR stubs using liquid extraction. Four solvents (acetone, DCM, water, and water/EtOH mixture) were evaluated. The protocol involved a time consuming double stage extraction using two different solvent systems and analysis using GC-TEA and ion mobility spectroscopy (IMS). Considering the relatively long sample extraction, low number of solvents tested and only relatively few target compounds (not involving any stabilisers), further investigations are required in order to optimise this protocol for a large number of potentially present OGSR and improve its practicality. A recent report further demonstrated the suitability of GSR stubs for the collection and extraction of OGSR, but did not refer to an optimisation of the used parameters or an extraction efficiency [175].

In two relatively recent studies, newly developed collection devices were introduced [37, 56]. Half of a GSR stub was covered with PTFE, allowing the non-covered half to be analysed for IGSR using SEM-EDX [56] and the PTFE half to be liquid extracted for analysis of OGSR using LC-QTOF-MS [56]. Advantages of the modified device were the possibility to simultaneously analyse OGSR and IGSR and that the IGSR half of the stub stayed intact and could be re-analysed if required. The device proved suitable for the collection and extraction of OGSR from simulated case specimens, however no IGSR study was conducted [56]. A similar collection device was used in another study [37]. The PTFE half of the stub was analysed using micro Raman spectroscopy and the carbon coated side subjected to LA-ICP-MS. However, separating one collection device in two areas raises the possibility of

losing important OGSR or IGSR that are collected on the other side of the stub given the heterogeneous distribution on the stub.

Alternative surface analysis techniques directly applicable to the collection device have been studied including DESI-MS [59], Raman spectroscopy [8, 197] or Fourier transform infrared spectroscopy [197]. However, these methods have still limited applicability due to their relatively low sensitivity or selectivity and are only considered as screening tools at this stage.

Most of the previously developed collection protocols were optimised and tested for only one type of GSR – inorganic or organic – and there is a strong need for the development and optimisation of a collection protocol that is sensitive and selective for OGSR detection but does not compromise IGSR analysis by SEM-EDX. The research presented in this chapter focused on the development and comparison of different collection protocols for the combined collection and subsequent analysis of IGSR and OGSR. The optimised protocols were compared in regards to extraction efficiencies of a wide range of target OGSR and collection efficiencies of these compounds from hands. The two superior protocols were then further tested and compared using specimens taken at simulated case scenarios.

5.2 Materials and Methods

5.2.1 *Reagents and Standards*

Most solvents and chemicals used are stated in Chapter 4 (4.2.1). Additionally, EtOH and IPA were obtained from ChemSupply Pty Ltd, Gillman, SA, Australia. Bromobenzene (analytical standard, Supelco) and sodium azide were purchased from Sigma Aldrich, USA. UP grade water was obtained from a Sartorius 611 water

purification system. Out of the 32 OGSR used in Chapter 4, 15 were chosen for developing and optimising different collection and extraction techniques. This choice was made so that all targeted compound classes, i.e. nitroaromatics, nitro esters, nitramines, phthalates, centralites, were represented. The target compounds included resorcinol, RDX, HMX, tetryl, PETN, TNT, 2,4-DNT, 4-A-2,6-DNT, NG, TNB, m-DNB, DPA, N-nDPA, EC, and DBP. As in Chapter 4, 2-naphthol was used as ISTD.

5.2.2 *Instrumentation*

5.2.2.1 Ultra-high Performance Liquid Chromatography

The method developed in Chapter 4 was used for the detection and identification of OGSR. The instrument parameters were identical to those previously optimised and presented in 4.2.2.1. The optimised LC method conditions are listed in Table 5-1. Additionally, a UHPLC guard column (Eclipse XDB-C18, 3.00 mm, 1.8 µm; Agilent Technologies) was installed for the analysis of GSR stub extracts.

Table 5-1: Gradient reversed phase program for the ultra-high performance liquid chromatographic separation of the targeted organic gunshot residues.

Time[min]	% MeOH	% H_2O	Gradient MeOH [%/min]
0	10.0	90.0	4.6
3	23.8	76.2	Isocratic
14	23.8	76.2	4.6
27	83.6	16.4	Isocratic

5.2.2.2 Triple Quadrupole Mass Spectrometry

As in Chapter 4, a 6490 QQQ-MS (Agilent Technologies) was used for the confirmation of compounds previously detected by UV. The instrument parameters are stated in 4.1.2.2 and a list with the MRM conditions for the target compounds potentially present in OGSR is presented in Table 4-2.

5.2.2.3 Gas Chromatography Mass Spectrometry

A 7890 GC coupled to a 5975 MS (Agilent Technologies) equipped with a HP-5MS column (30 m x 0.250 mm x 0.250 μm) was used for the SPME analysis of bromobenzene spiked on GSR stubs. Run conditions were based on previous literature [196]. The SPME fibre was thermally desorbed in a SPME inlet liner (Restek Corporation, Bellefonte, PA, USA) at an injector temperature of 250 °C using splitless injection. The temperature program involved an initial temperature of 50 °C, which was raised to 200 °C at a rate of 6 °C/min. At 27 min the temperature was raised by 20 °C to reach 300 °C at 32 min (total run time). A NIST library (2008) was used for MS identification.

5.2.2.4 Scanning Electron Microscopy with Energy Dispersive X-ray Spectroscopy

Inorganic GSR analysis was achieved using a Zeiss Evo LS15 SEM (Germany) with a SDD XFlash 5030 detector (Bruker, Germany) and a Diode 5 Channel backscatter detector. The analysis was automated using the GSR Professional software (Eastern Analytical Sprl, Belgium). The set-up of an automated run consists of different steps which are as follows: (i) Inserting the sample holder, which can hold eight samples and one stub incorporating the standards for the backscatter detector calibration

(Faradays cup, carbon, silicon, germanium, niobium, and gold); (ii) Calibrating the backscatter detector; (iii) Entering the numbers of samples, sample name and their position on the holder; (iv) Entering analysis time per sample, particle sizes, and element range, and (v) Focusing on each sample. For filter analysis (Protocol 1, 5.2.3), the SEM was used in extended pressure mode (90 Pa) to avoid charging of the specimen. The accelerating voltage was 25 kV in order to allow the detection of Pb. Furthermore 1 nanoampere probe current was used, whereby it was tested that the response for gold on the calibration standard was 50,000 counts per second. For GSR stubs (Protocol 2, 5.2.4), the SEM was operated under high vacuum with otherwise same conditions as for the filters. Due to practical reasons, the maximum collection area on each stub/ filter was 6 square mm (mm^2), whereby the analysis time was limited to 4 h per stub or filter. A homogenous distribution of the particles was adopted for comparison purposes with the data presented as particles/mm^2. It is acknowledged that this is a strong simplification and does not represent the true distribution on the stub surface after collection.

5.2.3 *Protocol 1 (Swabbing followed by Liquid Extraction)*

Kendall™ alcohol swabs were used throughout all experiments. These wipes have previously been reported as suitable for the collection of organic explosives [137, 198]. Figure 5-1 shows a swabbing kit used for the collection of GSR.

Figure 5-1: Swabbing kit used for the collection of gunshot residues by medi wipes. The kit includes a pair of gloves, plastic tweezers, a scintillation vial, Kendall^{TM} alcohol swab, and pen.

Generally, for GSR collection, alcohol wipes are repeatedly wiped over the area of interest (hands) until the wipe solvent (IPA:water, 70:30) is almost completely evaporated. The wipes are stored in a fridge at 4 °C before being prepared for analysis. Solvent (5 mL) is added to the wipes followed by sonication and/or centrifugation. This solvent volume (5 mL) was chosen so that the swab was completely covered. The solution is filtered through 10 µm and 0.8 µm isopore polycarbonate membrane filters (13 mm diameter, Merck Millipore) in Swinnex Filter Holders (Merck Millipore). *The extracts are reduced under a continuous flow of nitrogen until the volume of each extract is ca 1.5 mL. The reduced extracts are transferred to vials and further dried until the solvent is completely evaporated. Finally, the residues are reconstituted in 196 µL ACN:MeOH (1:1), 4 µL of volumetric ISTD (20 ppm final concentration) is added and the solutions filtered through 0.2 µm PTFE syringe filters before analysis by UHPLC with dual wavelength UV detection and confirmed using MS/MS.* This sample pre-concentration and reconstitution procedure with subsequent UHPLC analysis

(shown in italics) will further be referred to as *pre-concentration and analysis procedure*.

The 0.8 µm isopore membrane filters are directly mounted on a GSR stub for analysis using SEM-EDX. A schematic of Protocol 1 can be seen in Figure 5-2.

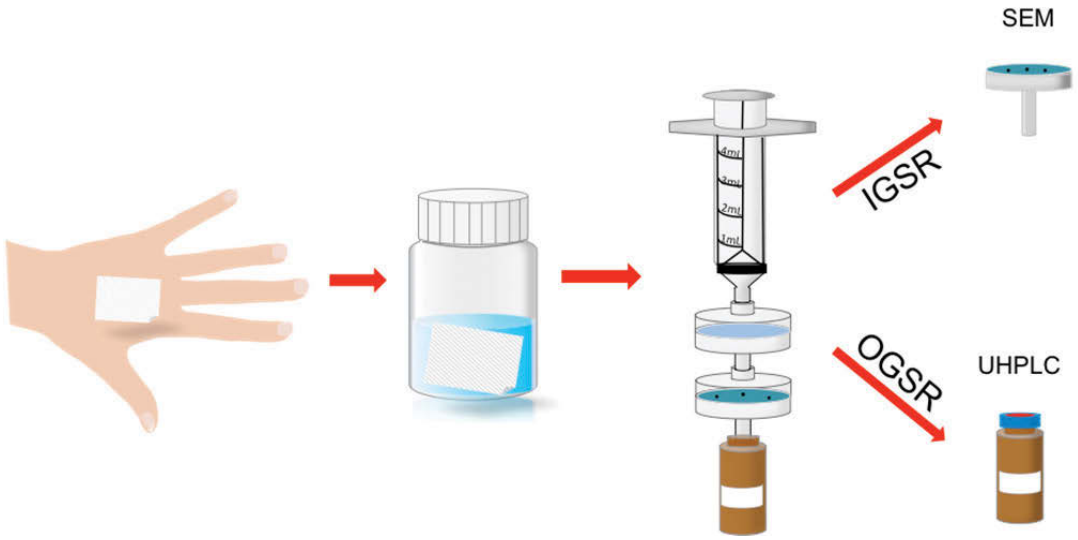

Figure 5-2: Scheme of specimen preparation using alcohol wipes as collection devices. After collection, the swab is liquid extracted in 5 mL solvent and the extract filtered using two syringe filters (10 µm and 0.8µm). The inorganic particulates are hereby collected on the second syringe filter which is directly mounted on a gunshot residue stub for subsequent analysis by scanning electron microscopy with energy dispersive x-ray spectroscopy (SEM-EDX). The extract is dried under a stream of nitrogen and reconstituted in 196 µL solvent and 4 µL volumetric internal standard are added for ultra-high performance liquid chromatography (UHPLC) analysis.

Different parameters of the protocol were optimised, whereby all optimisation experiments were conducted in triplicates and blanks were prepared in between each sample set.

5.2.3.1 Extraction Solvent Comparison

Different solvents were tested for their extraction efficiency for the 15 targeted OGSR. Most of the solvents were chosen based on previous studies reporting their applications to the extraction of explosives or OGSR. The tested solvents included ACN [137, 198], MeOH [199], IPA:water (70:30), ACN:water (1:1), water, acetone [54], DCM, and MTBE [200, 201]. Alcohol wipes were spiked with a known amount of OGSR (25 ng of each compound) and left to dry for 15 min to allow the

compounds to bind to the swabbing material. After that, 5 mL of solvent were added and the swabs with solvent sonicated for 15 min followed by 5 min centrifugation. This was followed by the *pre-concentration and analysis procedure* previously described. The extraction efficiency for each solvent was determined by the % recovery of the originally spiked amount.

5.2.3.2 Extraction Technique Comparison

Two different extraction techniques, sonication and centrifugation, were compared for their efficiency when used alone or in combination. Additionally it was investigated whether heating during sonication would result in a higher extraction of the OGSR. Each scenario was tested using three different spike concentrations of the target compounds, i.e. 12, 20, and 30 ng. After letting the spiked compounds bind to the swabbing material for 15 min, 5 mL of MTBE were added and the wipes extracted using four different extraction scenarios:

a) 15 min sonication
b) 5 min centrifugation at 4 revolutions per minute (rpm)
c) combined techniques (15 min sonication followed by 5 min centrifugation), further referred to as comb techn
d) combined techniques + increased T (15 sonication with increased temperature (45 °C) followed by 5 min centrifugation), further referred to as comb techn + T. No higher temperature was chosen to avoid any loss of thermally instable compounds such as NG.

After following the *pre-concentration and analysis procedure* the extraction efficiency was calculated as % recovery of the originally spiked OGSR amount.

5.2.3.3 Effect of Multiple Extractions

For single extraction, the extraction protocol for the solvent comparison (presented in section 5.2.3.1) excluding the centrifugation step using ACN, MTBE, and acetone was followed. For double extraction, the wipes were extracted twice using the same solvent each time and 15 min sonication. The extracts were combined and then prepared following the *pre-concentration and analysis procedure*.

5.2.3.4 Sonication Times

Different sonication times (5, 10, 15, 20 min) were investigated. Hereby, the same procedure as for the solvent tests excluding the centrifugation step was followed (presented in section 5.2.3.1), however different sonication times were applied. In contrast to the other optimisation tests, 2,4-DNT and m-DNB were not tested during this step due to limited availability.

5.2.3.5 Optimised Condition

The optimised protocol consisted of adding 5 mL of MTBE to the wipes followed by 5 min sonication. The solutions were filtered through 10 µm and 0.2 µm isopore membrane filters, polycarbonate, with 13 mm diameter (Merck Millipore) in Swinnex Filter Holders (Merck Millipore) and further prepared using the *pre-concentration and analysis procedure*. The 0.8 µm isopore membrane filters were directly mounted on a GSR stub for analysis using SEM-EDX.

5.2.3.6 Interference Test

Many different compounds can be found on skin. It was tested whether these compounds could interfere with the targeted OGSR. For this purpose, hands were spiked with 25 ng of the targeted OGSR. Following complete drying of the spiking

solution on hands (30 sec – 1 min), the hands were instantly swabbed with alcohol wipes until almost completely dry and the wipes placed in scintillation vials. The extraction procedure followed the optimised conditions described (section 5.2.3.5) using MTBE.

5.2.4 *Protocol 2 (GSR Stubs followed by Liquid Extraction)*

Stubs for the collection of GSR were purchased from Ted Pella Inc., USA and are presented in Chapter 1, Figure 1-1. The stubs were already assembled consisting of a plastic holder with an aluminium stub with a double sided carbon tape on top (12 mm diameter) and a clear plastic cup to avoid contamination. The proposed procedure for collection using GSR is as follows: The stubs are dabbed over the area of interest (hands) until no longer sticky (30-50 dabbings) and are kept in a refrigerator at 4 °C before SEM-EDX analysis. After analysis for IGSR, the stubs are deposited in a scintillation vial and solvent (5.5 mL) is added followed by sonication. 5.5 mL solvent are required to completely cover the stubs. The stubs are removed from the solution, which is prepared following the *pre-concentration and analysis procedure*. Figure 5-3 displays the specimen collection and reparation involved in Protocol 2.

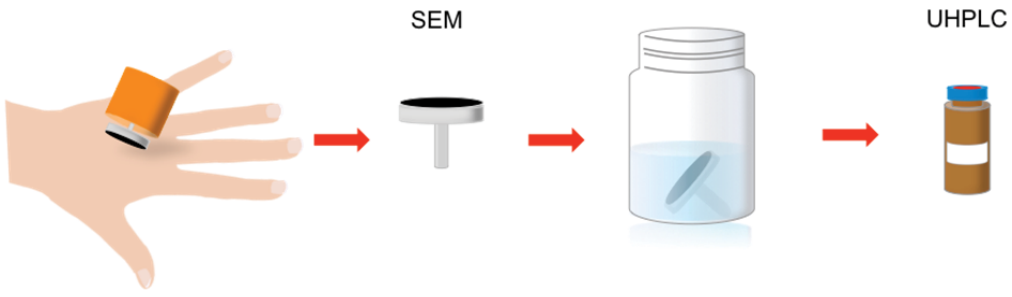

Figure 5-3: Scheme of specimen collection and preparation using gunshot residue (GSR) stubs as collection device and liquid extraction. After collection using the GSR stubs, the stubs are analysed for inorganic GSR using scanning electron microscopy with energy dispersive x-ray spectroscopy (SEM-EDX). This is followed by liquid extraction in 5.5 mL solvent, the extract is dried under a stream of nitrogen and reconstituted in 196 µL solvent and 4 µL volumetric internal standard for organic GSR analysis using ultra-high performance liquid chromatography (UHPLC).

Different parameters were optimised whereby all experiments were performed in triplicates with blanks and the extraction efficiency was calculated as % recovery of the OGSR spike amount.

5.2.4.1 Extraction Solvent Comparison

The solvents tested were chosen based on the ones used in Protocol 1 (Section 5.2.3.1) and since they had previously been reported in literature. The six solvents/solvent systems included ACN, MeOH, ACN:MeOH (1:1), MTBE [200], acetone [175], and 80 % (v/v) of 0.1 % (w/v) aqueous sodium azide and 20 % ethanol [57, 58], which will be referred to as Zeichner solution based on the author. The stubs were spiked with 30 ng of each of the target OGSR and left for drying (20 min). After drying, the stubs were placed in scintillation vials. Then 5.5 mL solvent were added followed by sonication for 15 min. The stubs were removed from the vials, the extracts worked up following the *pre-concentration and analysis procedure*.

5.2.4.2 Effect of Temperatures and Multiple Extractions

GSR stubs were spiked with 15 ng of the standards and dried for 20 min. After depositing the stubs in scintillation vials, 5.5 mL of the three superior solvents from the Extraction Solvent Comparison (5.2.4.1), ACN, MeOH, and acetone, were added. For each solvent, four different scenarios were tested:

a) extracting each stub once by 15 min sonication at room temperature (RT)
b) extracting each stub once using 15 min sonication with applied heat (~45 °C)
c) extracting each stub twice using 15 min sonication at RT and combining the extracts

Based on the results obtained from single extractions with and without heating (a significant difference between heating and non-heating was only found when using MeOH), double extraction was only tested without heating.

After extraction, the stubs were removed and the extracts prepared following the *pre-concentration and analysis procedure*.

5.2.4.3 Sonication Times

GSR stubs were spiked with 13 ng of OGSR standards and dried for 20 min. After depositing the stubs in scintillation vials 5.5 mL acetone were added and the vials sonicated for four different times (5, 10, 15, 20 min) at ambient temperature. After sonication, the GSR stubs were removed and the extracts prepared following the *pre-concentration and analysis procedure*.

5.2.4.4 Optimised Conditions

The final protocol consisted of placing the GSR stubs in a scintillation vial followed by adding 5.5 mL of acetone and sonication for 5 min at ambient temperatures. The stubs were removed from the solutions, which were prepared following the *pre-concentration and analysis procedure*.

5.2.4.5 Interference Test

Hands were spiked with 20 ng of the target OGSR. Instantly after the hands were dry, GSR stubs were dabbed over the skin until the stubs was no longer sticky (30-50 dabbings). The stubs were placed in scintillation vials and extracted as listed in the optimised conditions above (5.2.4.4) using three different solvents, ACN, MeOH, and acetone, and prepared following the *pre-concentration and analysis procedure*.

5.2.5 *Protocol 3 (GSR Stubs followed by Solid Phase Microextraction)*

For SPME collection, scintillation vials had to be used since the openings of the commonly used SPME vials (~10 mm Ø openings) were too small for GSR stubs (12 mm Ø). One hole (2 mm diameter) was screwed in each scintillation lid. After depositing GSR stubs in the scintillation vials and screwing the lids on, the holes were covered with paraffin film in order to avoid loss of the semivolatile OGSR. The SPME fibre was 65 µm polydimethylsiloxane/divinylbenzene (PDMS/DVB), Stableflex, 24 Ga with a manual holder (Supelco, Sigma Aldrich, US). The fibre was chosen based on an optimisation study reported in the literature [196]. The paraffin film over the hole was pinched and the fibre introduced into the vial. After headspace extraction, the fibre was withdrawn from the scintillation vial and directly immersed in a vial containing 196 µL of ACN:MeOH (1:1) and 4 µL of volumetric ISTD (20 ppm final concentration) for 5 min. Between each collection, the fibre was immersed in solvent blanks to ensure that no volatiles remained on the fibre and no carry-over occurred. A schematic of Protocol 3 can be seen in Figure 5-4.

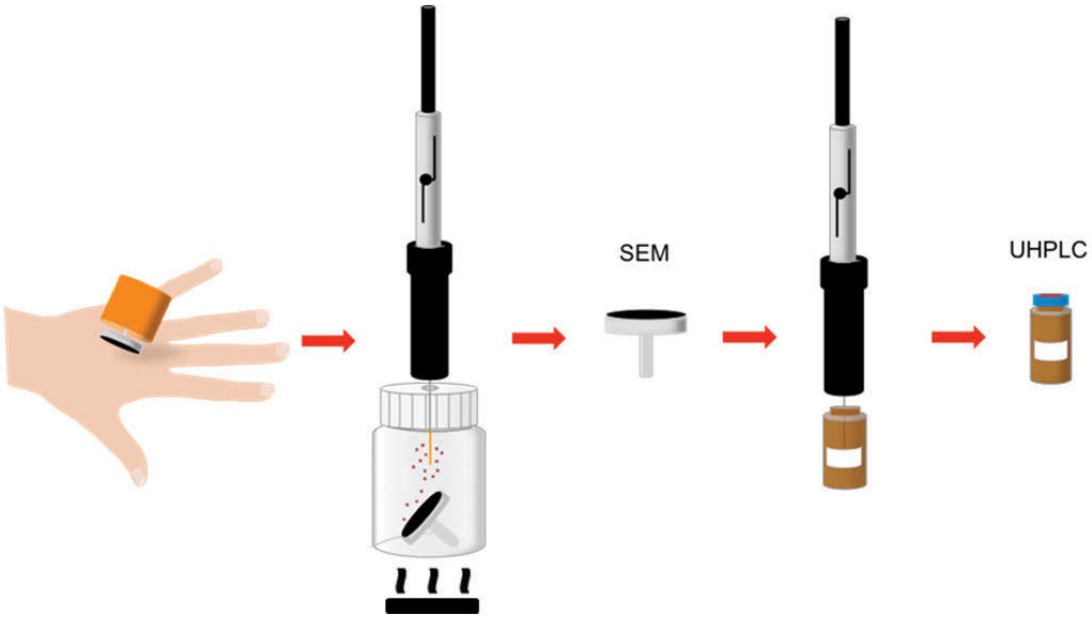

Figure 5-4: Scheme of specimen preparation using gunshot residue (GSR) stubs as collection devices and solid phase microextraction (SPME). After collection, the organic compounds are heated and absorbed by the SPME fibre. The stub is analysed by scanning electron microscopy with energy dispersive x-ray spectroscopy (SEM-EDX) for inorganic GSR. The organic compounds are desorbed from the fibre by direct immersion of the fibre in 196 µL solvent and 4 µL volumetric internal standard (5 min) and analysed using a previously developed ultra-high performance liquid chromatography method.

5.2.5.1 Heating Temperature

To test different extraction temperatures, GSR stubs were spiked with a known amount (20 ng) of the compounds of interest and placed in the modified scintillation vials. The vials were heated in a dry block heater to temperatures ranging from 30-150 ºC with 20 ºC increments. Exposure time of the fibre to the heated stub was chosen to be 1 h, based on the work of Burleson who indicated that 45 min was necessary for reliable detection of OGSR from a single partially burnt gunpowder particle [77].

5.2.5.2 Effect of GSR Stub Adhesive

To investigate whether the limited extraction of OGSR was due to the GSR stub adhesive of liquid immersion, GSR stubs were spiked with a volatile compound (bromobenzene) at three different concentrations (20 ppm, 100 ppm, 2000 ppm). The spiked GSR stubs as well as a blank stub were extracted using SPME (1 h at

100 °C) and the fibre subsequently immersed in 196 µL ACN:MeOH (1:1) and 4 µL ISTD and analysed by UHPLC-UV.

5.2.5.3 Effect of Liquid Immersion

To test whether the liquid immersion step was the inhibiting factor, a GSR stubs was spiked with 1000 ppm bromobenzene. After SPME extraction (1 h at 100 °C), the SPME fibre was analysed using GC-MS.

5.2.6 *Simulated Case Specimens*

In order to compare the two superior OGSR collection protocols in regards to their overall performance (i.e., both OGSR and IGSR recovery), test firings were conducted at the indoor firing range of the NSWPF in Sydney, Australia. The different ammunitions and firearms used are listed in Table 4-3. Control specimens were taken from thoroughly cleaned hands before every discharge. Specimens were collected from the hands of the shooter after one and three discharges for every ammunition-firearm combination in three replicates. When alcohol wipes were used for collection, the wipes were placed in scintillation vials. The specimens, scintillation vials and GSR stubs, were stored in a refrigerator at 4 °C before analysis. To allow comparison the efficiency of both collection protocols for IGSR collection, the numbers of particle classifications per area were calculated for all stubs whereby a homogenous distribution of the particles on the stub was assumed. It is important to note that during Protocol 1 the solution is filtered through two syringe filters (10 and 0.8 µm), with the latter membrane subsequently analysed by SEM-EDX. Therefore, only particles dimensions between 0.8 and 10 µm were in scope for SEM-EDX.

5.3 Results and Discussion

Three protocols were developed for the combined collection of OGSR and IGSR. Protocol 1 was based on alcohol wipes as collection devices, while Protocol 2 and Protocol 3 involved GSR stubs.

Blanks were collected throughout the optimisation of the collection protocols as well as at the shooting range. No target compounds were detected on blanks from the extraction studies using wipes or stubs, as well as the specimens taken from the hands of the shooter.

5.3.1 ***Protocol 1***

5.3.1.1 Extraction Solvent Comparison

Of the different solvents tested, ACN yielded in the highest mean extraction efficiency over all compounds (76 %) followed by MTBE (74 %), DCM (71 %) and acetone (66 %). Additionally, ACN resulted in the lowest % RSD (6.55 %), followed by MeOH (6.63 %), acetone (7.06 %), and MTBE (14.01 %). ACN was identified as the most suitable solvent for the extraction of OGSR, which is in accordance with previously tests focusing on the extraction of explosives by DeTata et al. [137] and Song-im et al. [198]. In a recent study by McCord and Thomas [175] acetone was used as extraction solvent for OGSR, but in this study it was found inferior to ACN, MTBE and DCM. A study by Perret et al. used MeOH as extraction solvent for explosives and stabilizers from hand swabs [199].

The overall most suitable solvent was determined to be MTBE as the evaporation time for MTBE is shorter than for ACN (vapour pressure of MTBE is

27.2 kPa and of ACN is 9.71 kPa (at 20.0 °C)) and it is compatible with the particle filters that were later used for combined OGSR-IGSR analysis, which was a major drawback for ACN.

The % recoveries of each of the target compounds are listed in Table 5-2 and displayed in Figure 5-5. The % RSD values (n = 3) are listed in Table 5-3.

Table 5-2: Percentage recoveries of the compounds of interest liquid extracted (5 mL solvent, 15 min sonication followed by 5 min centrifugation) from spiked swabs (25 ng) using eight extraction solvents (ACN, MeOH, IPA:water (70:30), ACN:water (1:1), water, acetone, DCM, MTBE) measured in triplicates. ACN = acetonitrile, MeOH = methanol, IPA = isopropanol, DCM = dichloromethane, MTBE = methyl tertbutyl ether. After liquid extraction, the extracts were dried under a steady stream of nitrogen and reconstituted in 196 µL ACN:MeOH (1:1) and 4 µL volumetric internal standard.

Compound	ACN	MeOH	IPA:water	ACN:water	water	acetone	DCM	MTBE
resorcinol	78.3	69.8	69.7	72.5	67.4	72.3	59.2	72.2
RDX	87.0	73.8	79.0	85.6	85.3	79.9	85.3	81.4
HMX	81.2	70.6	73.6	80.5	81.2	73.7	80.3	75.9
TNB	84.0	68.7	64.5	55.1	51.9	73.6	82.0	80.2
m-DNB	49.7	28.1	24.3	6.34	5.86	29.1	33.1	57.1
NG	74.7	59.6	37.5	14.1	17.7	58.4	66.4	73.7
tetryl	56.8	15.7	30.3	8.74	11.3	40.0	30.4	63.1
TNT	81.6	53.2	45.6	16.7	14.3	68.0	69.6	77.3
4-A-2,6-DNT	53.4	62.5	62.8	61.1	61.4	60.5	72.3	48.9
2,4-DNT	61.0	40.5	26.3	0.00	0.00	40.5	45.9	61.9
PETN	93.3	74.8	72.2	86.0	78.1	82.5	92.0	83.5
N-nDPA	70.9	57.5	30.4	10.6	0.00	49.9	53.8	64.5
DPA	82.6	54.8	49.3	12.9	0.00	84.6	96.6	86.1
EC	93.7	82.8	66.6	36.9	23.0	82.3	87.8	88.9
DBP	98.3	90.4	85.0	76.7	30.6	92.5	106	88.6
Mean	76.4	60.2	54.5	41.6	35.2	65.9	70.7	73.6

Table 5-3: Percentage relative standard variations (n = 3) for the extraction of the target compounds spiked on alcohol swabs (25 ng) by liquid extraction (5 mL solvent, 15 min sonication followed by 5 min centrifugation) using the eight tested extraction solvents. ACN = acetonitrile, MeOH = methanol, IPA = isopropanol, DCM = dichloromethane, MTBE = methyl tertbutyl ether. After liquid extraction, the extracts were dried under a steady stream of nitrogen and reconstituted in 196 µL ACN:MeOH (1:1) and 4 µL volumetric internal standard.

Compound	ACN	MeOH	IPA:water	ACN:water	water	acetone	DCM	MTBE
resorcinol	3.22	3.43	7.18	1.61	33.5	6.85	52.9	13.5
RDX	3.41	4.26	2.23	1.12	4.28	5.36	12.0	14.5
HMX	3.53	3.92	2.58	1.67	6.19	5.44	11.2	14.5
TNB	2.70	3.84	18.73	11.3	99.9	6.11	11.1	14.6
m-DNB	10.7	9.90	121	29.3	N/A	3.05	71.9	14.3
NG	2.43	1.32	93.2	86.8	N/A	6.29	28.4	14.3
tetryl	11.5	32.3	107	4.76	28.5	29.0	69.9	16.3
TNT	2.95	7.06	59.9	82.3	N/A	8.18	5.78	15.1
4-A-2,6-DNT	24.8	8.11	13.9	5.84	22.4	5.68	20.6	13.5
2,4-DNT	5.95	2.77	110	N/A	N/A	3.55	54.7	14.3
PETN	3.22	4.22	40.3	3.86	15.7	4.95	1.20	14.6
N-nDPA	1.17	1.44	90.7	54.4	N/A	5.38	24.1	14.4
DPA	13.7	2.16	77.0	23.1	94.2	5.72	23.9	7.52
EC	5.13	9.74	32.6	12.3	109	4.02	20.1	14.3
DBP	3.94	5.04	3.79	1.99	N/A	6.37	1.87	14.3
Mean	6.55	6.63	52.0	22.9	46.0	7.06	27.3	14.0

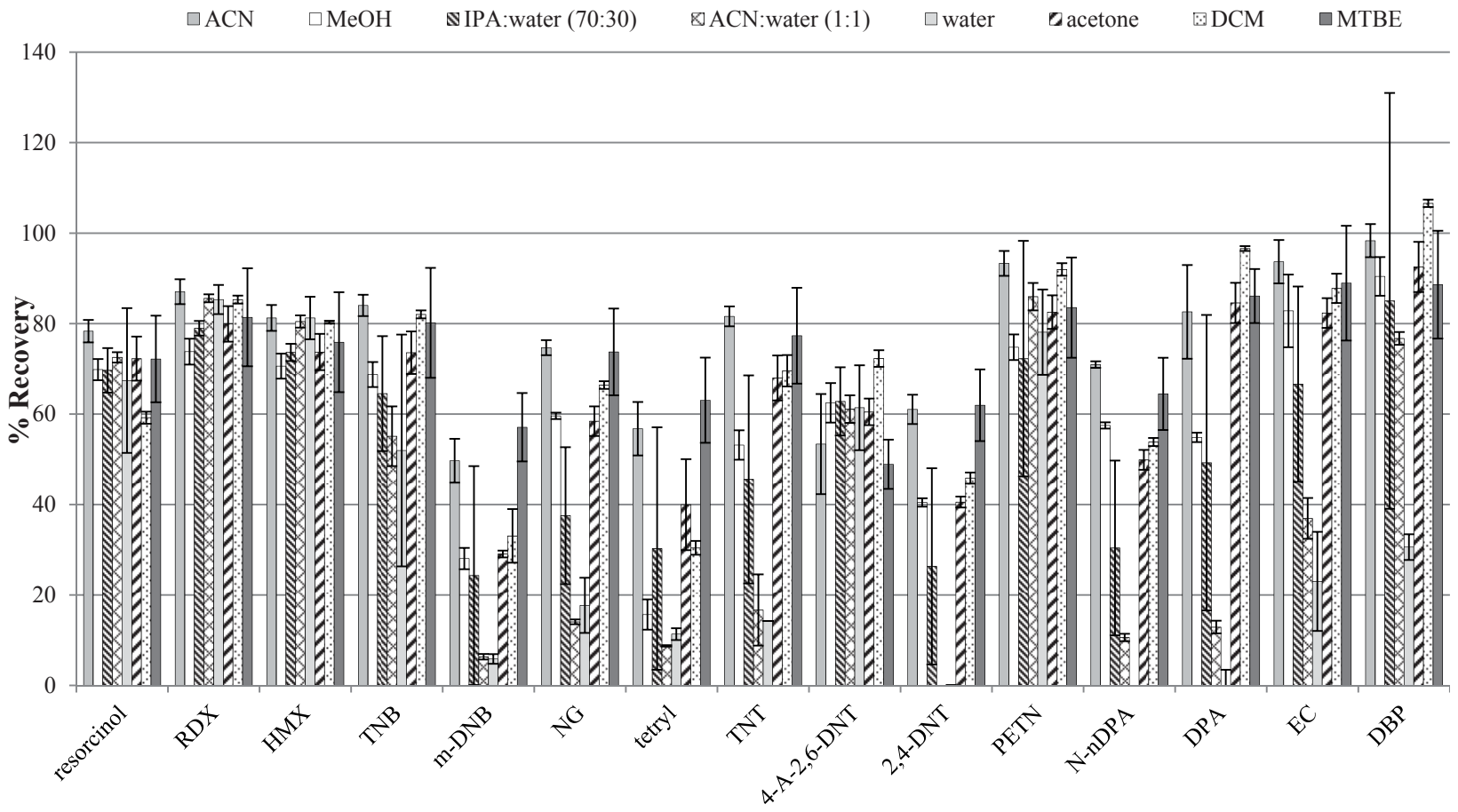

Figure 5-5: Percentage recoveries of the target organic gunshot residues extracted from spiked swabs (25 ng) by liquid extraction (5 mL solvent, 15 min sonication followed by 5 min centriguation) using eight different solvents/solvent systems. Error bars represent standard deviations (n = 3). ACN = acetonitrile, MeOH = methanol, IPA = isopropanol, DCM = dichloromethane, MTBE = methyl tertbutyl ether. After liquid extraction, the extracts were dried under a steady stream of nitrogen and reconstituted in 196 µL ACN:MeOH (1:1) and 4 µL volumetric internal standard.

5.3.1.2 Extraction Technique Comparison

The mean extraction efficiencies of the different scenarios over the three different spike concentrations were 80 % (sonication), 72 % (centrifugation), 72 % (comb techn) and 73 % (comb techn + T) and are shown in Figure 5-6.

The results indicate that centrifugation decreases the extraction efficiency. A possible reason might be that during the centrifugation process, a part of the OGSR settles at the bottom of the swab and is therefore not extracted. The recoveries were compared using a Student's t-test (paired, two-tailed). The p-values are shown in Table 5-6 a (conc 1 = 12 ng spike), b (conc 2 = 20 ng spike), c (conc 3 = 30 ng), and d (overall). No significant differences were found for concentration 2 (20 ng) between centrifugation and comb techn, and between sonication and comb techn + T. For concentration 3 (30 ng) no significant differences were found between centrifugation and comb technique, centriguation and comb techn + T, as well as between comb techn and comb techn + T. Sonication alone resulted in the highest extraction efficiencies for all three tested concentrations and showed the smallest % RSD. Furthermore, it was overall significantly better (Table 5-6 d) from the other scenarios. Overall, extraction recoveries decreased with increasing concentrations. Since OGSR in real case specimens are commonly in low concentrations [56, 84], this is not problematic.

Detailed % recovery values for the target compounds using the different techniques are listed in Table 5-4 and the respective % RSD values in Table 5-5. Individual block diagrams for the three different concentrations tested by each technique can be found in Appendix VIII.

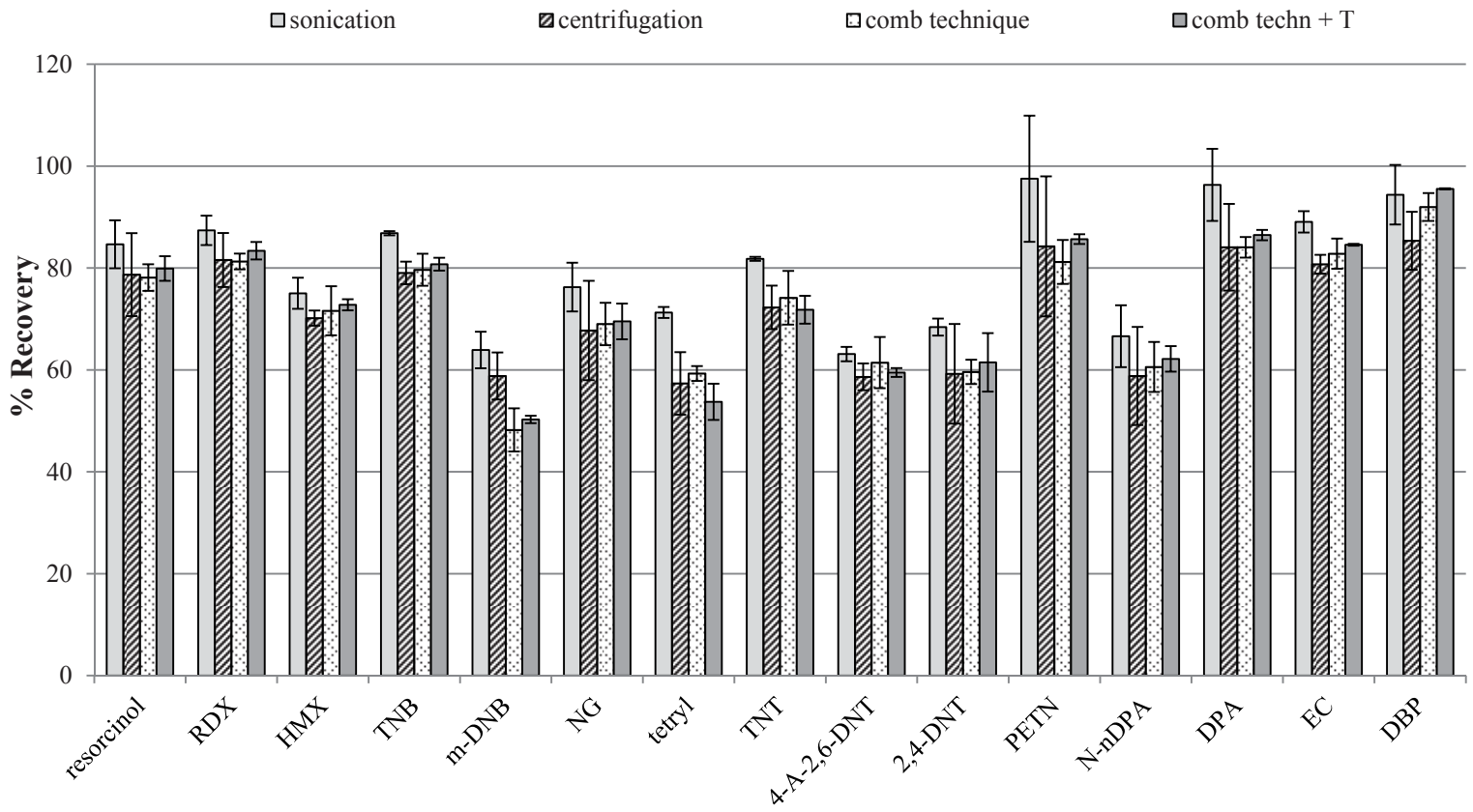

Figure 5-6: Percentage recoveries of the target compounds when liquid extracted (5 mL methyl tertbutyl ether) from spiked alcohol wipes (presented here the overall % recoveries from 12, 20, and 30 ng) using four different techniques, i.e. sonication (15 min at ambient temperatures), centrifugation (5 min), comb technique (sonication (15 min)+centrifugation (5 min)) at room temperature, comb technique + T (15 min heated (45 ºC) sonication followed by centrifugation). Error bars represent standard deviations (n = 3). After liquid extraction, the extracts were dried under a steady stream of nitrogen and reconstituted in 196 µL aceonitrile:methanol (1:1) and 4 µL volumetric internal standard.

Table 5-4: Percentage recoveries of the different target compounds liquid extracted from spiked alcohol wipes (12, 20, and 30 ng) using 5 mL methyl tert-butyl ether using four different extraction techniques (sonication (15 min at ambient temperatures), centrifugation (5 min), comb technique (15 min sonication+5 min centrifugation) at ambient temperatures, comb technique + T (heated (45 ºC) sonication (15 min) followed by centrifugation (5 min)). Spiked amounts were 12 ng, 20 ng, 30 ng. After liquid extraction, the extracts were dried under a steady stream of nitrogen and reconstituted in 196 µL acetonitrile:methanol (1:1) and 4 µL volumetric internal standard.

Compound	sonication			centrifugation			comb techn			comb techn + T		
	12 ng	20 ng	30 ng	12 ng	20 ng	30 ng	12 ng	20 ng	30 ng	12 ng	20 ng	30 ng
resorcinol	86.0	88.6	79.4	83.4	83.4	69.3	78.5	80.6	75.4	81.1	90.3	68.3
RDX	90.6	86.4	85.1	85.9	83.2	75.7	82.8	79.7	81.3	85.4	90.5	74.3
HMX	71.9	75.3	77.9	69.3	71.9	69.3	67.0	71.3	76.6	69.4	79.9	69.1
TNB	86.7	86.5	87.3	81.5	78.5	77.2	77.2	78.5	83.2	79.8	86.9	75.5
m-DNB	67.9	62.7	61.1	61.9	61.0	53.5	45.5	46.1	53.1	50.4	54.6	45.9
NG	81.7	74.2	72.9	78.6	59.7	65.0	73.6	65.4	68.1	73.9	73.9	60.8
tetryl	70.5	72.5	70.8	63.0	50.8	58.3	60.5	57.7	59.7	59.2	48.0	54.1
TNT	82.1	82.0	81.4	77.0	68.6	71.2	69.1	73.8	79.6	71.4	71.9	72.1
4-A-2,6-DNT	63.3	61.6	64.4	60.6	55.7	59.7	56.0	62.5	65.8	59.4	58.5	60.5
2,4-DNT	70.3	67.5	67.4	68.8	49.3	59.6	60.8	56.9	61.2	63.1	67.3	54.0
PETN	106	104	83.3	99.4	80.8	72.5	85.8	77.3	80.5	91.1	92.3	73.6
N-nDPA	70.9	59.7	69.3	65.8	47.8	62.8	56.6	59.2	66.1	57.4	70.5	58.6
DPA	100	92.5	92.0	92.2	75.3	84.7	86.3	82.3	83.6	89.6	93.8	76.0
EC	86.7	89.9	90.6	82.7	79.1	80.4	81.3	81.0	86.2	83.9	91.9	77.9
DBP	100	90.9	91.2	90.3	86.6	79.1	94.3	88.9	92.7	98.0	100	83.8
mean	82.7	79.6	78.3	77.4	68.8	69.2	71.7	70.7	74.2	74.2	78.3	67.0
overall mean		80.2			71.8			72.2			73.2	

Table 5-5: Percentage relative standard variations of the recoveries of target compounds (n = 3) from spiked swabs (12, 20, and 30 ng) using 5 mL methyl tertbutyl ether and the four different extraction techniques, i.e. sonication (15 min at ambient temperatures), centrifugation (5 min), comb technique (15 min sonication+5 min centrifugation) at ambient temperatures, comb technique + T (heated (45 ºC) sonication (15 min) followed by centrifugation (5 min)). After liquid extraction, the extracts were dried under a steady stream of nitrogen and reconstituted in 196 µL acetonitrile:methanol (1:1) and 4 µL volumetric internal standard.

Compound	sonication	centrifugation	comb techn	comb techn + T
resorcinol	5.56	10.3	3.34	13.9
RDX	3.31	6.51	1.90	9.89
HMX	4.05	2.12	6.72	8.49
TNB	0.48	2.78	3.94	7.14
m-DNB	5.60	7.84	8.80	8.57
NG	6.26	14.4	6.04	10.9
tetryl	1.52	10.7	2.48	10.4
TNT	0.48	5.89	7.11	0.51
4-A-2,6-DNT	2.23	4.47	8.17	1.69
2,4-DNT	2.44	16.5	4.00	11.1
PETN	12.7	16.3	5.31	12.2
N-nDPA	9.13	16.4	8.11	11.6
DPA	7.35	10.1	2.40	10.8
EC	2.36	2.28	3.57	8.31
DBP	6.20	6.67	2.98	11.2
mean	4.64	8.88	4.99	9.10

Table 5-6: Student's t-test (paired, two-tailed) results between the recoveries of the spiked (12, 20, and 30 ng) organic gunshot residues on alcohol swabs using 5 mL methyl tertbutyl ether and the different extraction techniques, i.e. sonication (15 min), centrifugation (5 min), comb technique (15 min sonication+5 min centrifugation) at ambient temperatures, comb technique + T (heated (45 ºC) sonication (15 min) followed by centrifugation (5 min)). After liquid extraction, the extracts were dried under a steady stream of nitrogen and reconstituted in 196 µL acetonitrile:methanol (1:1) and 4 µL volumetric internal standard. Table a shows the results for conc 1 (12 ng), b for conc 2 (20 ng), c for conc 3 (30 ng), and d overall. The p-values are listed in the tables, whereby a p-value < 0.05 indicates a significant difference. P-values indicating no significant between the different techniques are shown in bold and italics.

a	**conc 1**		
	sonication	**centrifugation**	**comb techn**
centrifugation	8.4262E-06		
comb techn	1.6860E-06	0.0005	
comb techn + T	1.1774E-05	0.0195	3.9720E-05

b	**conc 2**		
	sonication	**centrifugation**	**comb techn**
centrifugation	3.2261E-05		
comb techn	0.0002	***0.2630***	
comb techn + T	***0.6188***	0.0005	0.0010

c	**conc 2**		
	sonication	**centrifugation**	**comb techn**
centrifugation	1.3460E-10		
comb techn	0.0004	0.0002	
comb techn + T	3.2065E-09	0.02765	2.1274E-14

d	**overall**		
	sonication	**centrifugation**	**comb techn**
centrifugation	3.0381E-08		
comb techn	5.8578E-06	***0.6652***	
comb techn + T	6.0736E-05	***0.1959***	***0.1599***

5.3.1.3 Effect of Multiple Extractions

In a recent study by Thomas and McCord [175] two extractions of the same swab resulted in higher recoveries of OGSR than extracting the swab only once. This scenario was also evaluated in this project. The results demonstrate that when using any of the tested solvents (ACN, MTBE and acetone), RDX, HMX, 4-A-2,6-DNT, and EC had higher recoveries when double extracted. TNB, 2,4-DNT, DPA had also higher recoveries when double extracted using MTBE and acetone as solvents. However, overall no significant differences (Student's t-test, paired, two-tailed; p-values: 0.8817, 0.4079, 0.4066 for ACN, MTBE and acetone, respectively) between single and double extraction were identified for all conditions and compounds tested. It was found for that when extracting a swab twice using MTBE, an interference for DBP was identified using the UV detector. Furthermore, for double extraction involving acetone, interference for EC was found. Due to the detected interferences, the lack of a significant difference and shorter preparation times, single extraction was used for all further experiments.

The results are presented in Figure 5-7 (ACN), 5-8 (MTBE), and 5-9 (acetone). The % recoveries of the spiked amounts are listed in Table 5-7 and the % RSD values in Table 5-8.

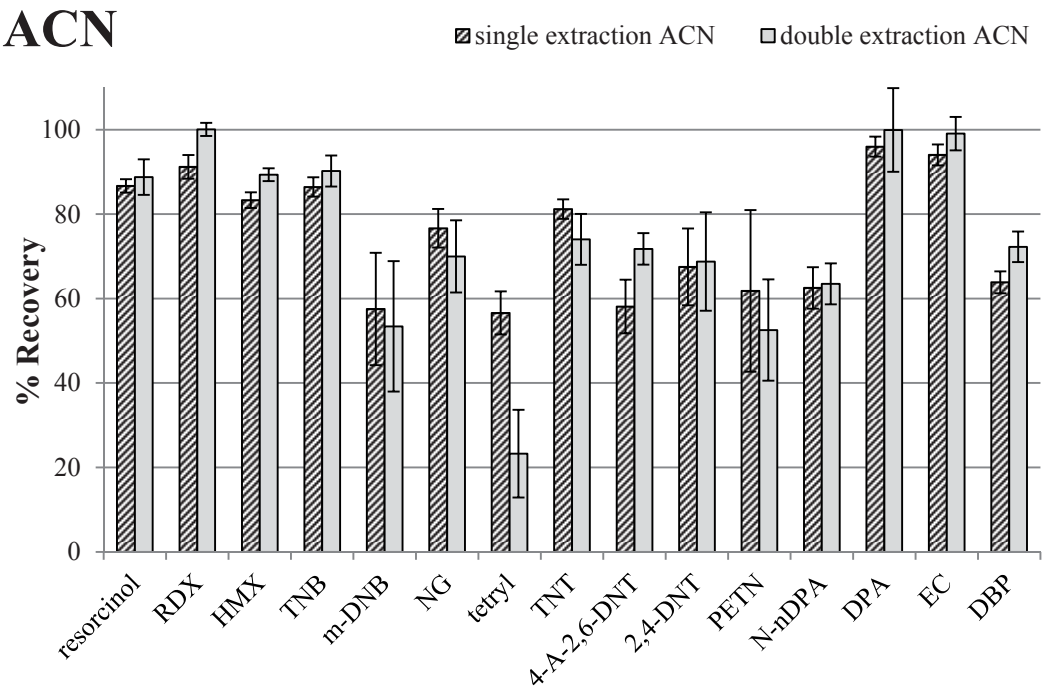

Figure 5-7: Comparison of the % recoveries of the target organic gunshot residue compounds spiked (25 ng) on alcohol swabs when performing single (15 min sonication at ambient temperatures) or double liquid extraction (2 x 15 min sonication at ambient temperatures and combining the extracts) of the alcohol wipes using 5 mL acetonitrile (ACN). After liquid extraction, the extracts were dried under a steady stream of nitrogen and reconstituted in 196 µL ACN:methanol (1:1) and 4 µL volumetric internal standard. Error bars represent standard deviations (n = 3).

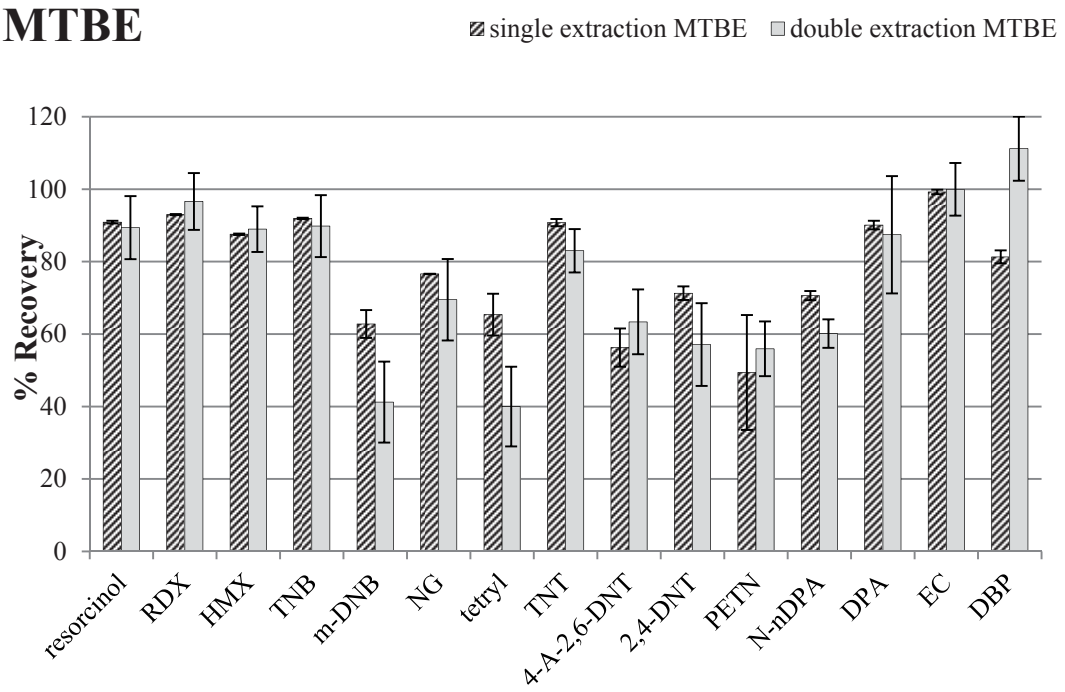

Figure 5-8: Comparison of the % recoveries of the target organic gunshot residue compounds spiked on alcohol wipes (25 ng) when performing single (15 min sonication at ambient temperatures) or double liquid extraction (2 x 15 min sonication at ambient temperatures and combining the extracts) of the alcohol wipes using 5 mL methyl tert-butyl ether (MTBE). After liquid extraction, the extracts were dried under a steady stream of nitrogen and reconstituted in 196 µL acetonitrile:methanol (1:1) and 4 µL volumetric internal standard. Error bars represent standard deviations (n = 3).

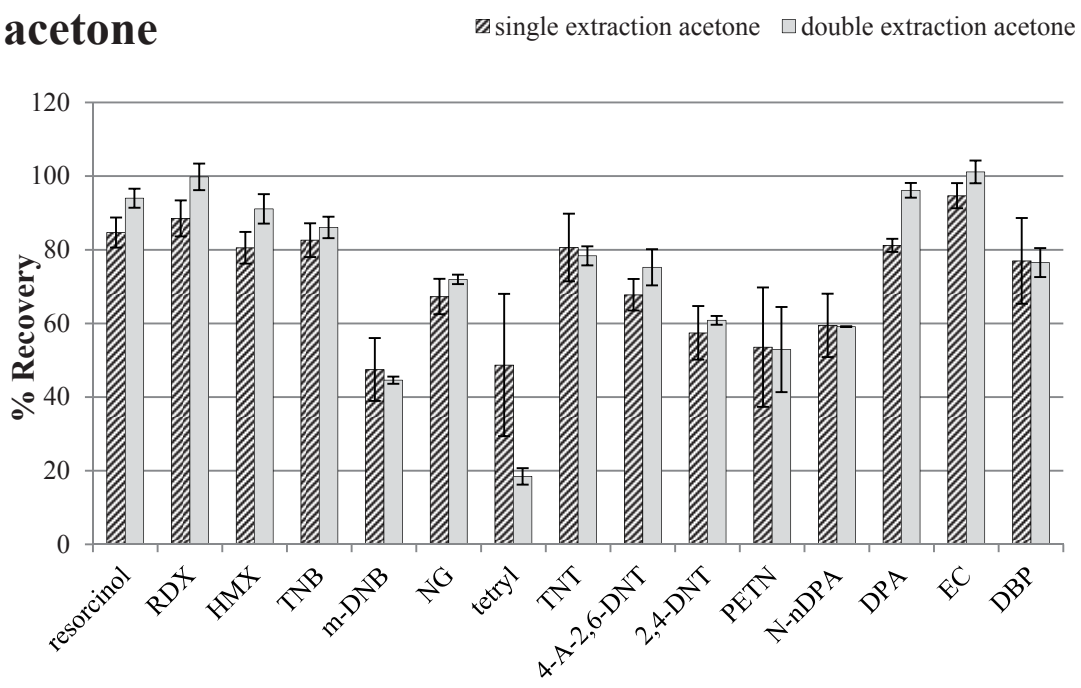

Figure 5-9: Comparison of the recoveries of the target organic gunshot residue compounds spiked on alcohol swabs (25 ng) when performing single (15 min sonication at ambient temperatures) or double extraction (2 x 15 min sonication and combining the extracts) of the alcohol wipes using 5 mL acetone. After liquid extraction, the extracts were dried under a steady stream of nitrogen and reconstituted in 196 µL acetonitrile:methanol (1:1) and 4 µL volumetric internal standard. Error bar represent standard deviations (n = 3).

Table 5-7: Percentage recoveries of the target organic gunshot residue compounds spiked on alcohol swabs (25 ng) when extracting the swabs using 5 mL of different solvents, i.e. acetonitrile (ACN), methyl tert-butyl ether (MTBE), and acetone and sonication (single extraction: 15 min, double extraction: 2 x 15 min and combining the extracts) at ambient temperatures. After liquid extraction, the extracts were dried under a steady stream of nitrogen and reconstituted in 196 µL ACN:methanol (1:1) and 4 µL volumetric internal standard. Interferences (% recoveries > 100 %) are indicated in bold and italics.

Compound	ACN		MTBE		acetone	
	single extr.	double extr.	single extr.	double extr.	single extr.	double extr.
resorcinol	86.7	88.8	90.9	89.4	84.7	94.0
RDX	91.2	100	93.0	96.6	88.5	99.8
HMX	83.3	89.3	87.6	89.0	80.6	91.1
TNB	86.4	90.2	91.9	89.8	82.6	86.1
m-DNB	57.5	53.4	62.8	41.2	47.5	44.6
NG	76.6	67.0	76.6	69.5	67.3	72.0
tetryl	56.6	23.3	65.4	40.0	48.7	18.4
TNT	81.2	74.0	90.8	83.0	80.6	78.4
4-A-2,6-DNT	58.1	71.8	56.3	63.4	67.8	75.3
2,4-DNT	67.5	68.8	71.3	57.1	57.4	60.8

Table 5-7 continued: Percentage recoveries of the target organic gunshot residue compounds spiked on alcohol swabs (25 ng) when liquid extracting the swabs using 5 mL of different solvents, i.e. acetonitrile (ACN), methyl tert-butyl ether (MTBE), and acetone and sonication (single extraction: 15 min, double extraction: 2 x 15 min and combining the extracts) at ambient temperatures. After liquid extraction, the extracts were dried under a steady stream of nitrogen and reconstituted in 196 µL ACN:methanol (1:1) and 4 µL volumetric internal standard. Interferences (% recoveries > 100 %) are indicated in bold and italics.

Compound	ACN		MTBE		acetone	
	single extr.	double extr.	single extr.	double extr.	single extr.	double extr.
PETN	61.8	52.5	49.4	55.9	53.6	52.9
N-nDPA	62.5	63.5	70.6	60.1	59.5	59.1
DPA	96.0	99.9	90.1	87.4	81.2	96.2
EC	94.0	99.1	99.2	100	94.7	100
DBP	63.9	72.3	81.3	***111***	77.0	76.5
mean	74.9	74.5	78.5	75.6	71.4	73.8

Table 5-8: Percentage relative standard varations of the % recoveries (n = 3) of the spiked (25 ng) target organic gunshot residues on alcohol swabs liquid extracted using 5 mL of different solvents (acetonitrile (ACN), methyl tert-butyl ether (MTBE), and acetone) and single (sonication for 15 min) and double extraction (2 x sonication for 15 min and combining the extracts) at ambient temperatures. After liquid extraction, the extracts were dried under a steady stream of nitrogen and reconstituted in 196 µL ACN:methanol (1:1) and 4 µL volumetric internal standard.

Compound	ACN		MTBE		acetone	
	single extr.	double extr.	single extr.	double extr.	single extr.	double extr.
resorcinol	1.91	4.91	0.41	10.1	2.86	2.86
RDX	3.37	1.69	0.18	8.85	3.92	3.92
HMX	4.59	1.81	0.26	7.54	4.67	4.67
TNB	2.80	4.27	0.21	10.0	3.55	3.55
m-DNB	26.6	33.7	6.99	33.3	2.63	2.63
NG	6.68	13.9	0.09	18.4	2.02	2.02
tetryl	10.3	64.2	9.90	33.4	19.6	19.6
TNT	2.97	8.50	1.15	7.49	3.45	3.45
4-A-2,6-DNT	9.09	5.81	10.9	16.0	7.28	7.28
2,4-DNT	15.9	19.1	2.96	23.1	2.22	2.22
PETN	36.1	27.4	38.9	16.0	26.1	26.1
N-nDPA	9.05	8.79	2.05	7.57	0.13	0.13

Table 5-8 continued: Percentage relative standard varations of the % recoveries (n = 3) of the spiked (25 ng) target organic gunshot residues on alcohol swabs liquid extracted using 5 mL of different solvents (acetonitrile (ACN), methyl tert-butyl ether (MTBE), and acetone) and single (sonication for 15 min) and double extraction (2 x sonication for 15 min and combining the extracts) at ambient temperatures. After liquid extraction, the extracts were dried under a steady stream of nitrogen and reconstituted in 196 µL ACN:methanol (1:1) and 4 µL volumetric internal standard.

Compound	ACN		MTBE		acetone	
	single extr.	double extr.	single extr.	double extr.	single extr.	double extr.
DPA	2.70	10.9	1.45	20.6	2.29	2.29
EC	2.80	4.23	0.66	7.70	3.22	3.22
DBP	4.69	5.68	2.46	8.62	5.76	5.76
mean	9.30	14.3	5.24	15.2	5.98	5.98

5.3.1.4 Sonication Time Optimisation

Four different sonication times: 5, 10, 15, and 20 min, were compared. The mean recoveries were relatively similar with the best extraction recoveries for 20 min (60 %) followed by 15 min (56 %), 5 min (54 %) and 10 min (53 %). No significant difference ($p < 0.05$) was found between the different times except for 20 min and 10 min (Table 5-11). The % RSD values were lowest for 15 min (8.48 %), followed by 10 min (15.42 %), 20 min (18.17 %), and finally 5 min (21.67 %). Although 15 min appeared to be the most suitable sonication time in regards to % recovery and % RSD, 5 min was chosen for further experiments, as there was no significant difference between 5 min and 15 min (Table 5-11). In detail, a 5 minute extraction time was superior for resorcinol and tetryl, 15 min for RDX, TNT, N-nDPA, DPA, and DBP, and 20 min for HMX, TNB, NG, 4-A-2,6-DNT, PETN, and EC. Interestingly, longer extraction times (>20 min) resulted in the presence of UV interferences for RDX and DBP using UV detection indicated by their recoveries being over 100 % (values shown in bold and italics in Table 5-9). The % recoveries

of the different compounds when using the four different sonication times are shown in Figure 5-10 and listed in Table 5-9. The % RSD (n = 3) are listed in Table 5-10.

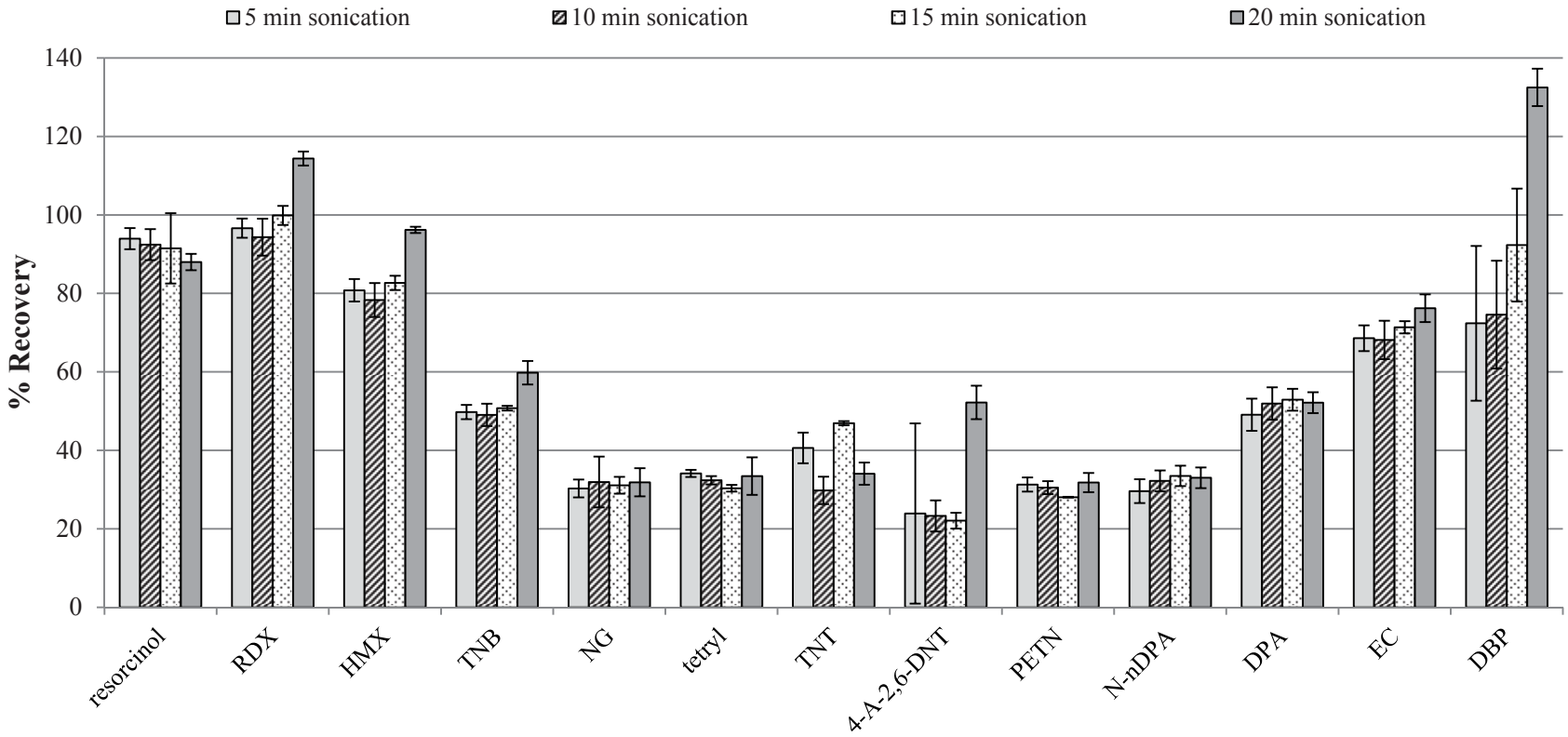

Figure 5-10: Percentage recoveries of the target compounds spiked on alcohol swabs (25 ng) when liquid extracted using 5 mL methyl tert-butyl ether and four different sonication times (5, 10, 15, and 20 min) at ambient temperatures. After liquid extraction, the extracts were dried under a steady stream of nitrogen and reconstituted in 196 µL acetonitrile:methanol (1:1) and 4 µL volumetric internal standard. Error bars represent standard deviations (n=3).

Table 5-9: Percentage recoveries of the spiked (25 ng) target compounds on alcohol swabs liquid extracted using 5 mL methyl tert-butyl ether as extraction solvent and four different sonication times (5, 10, 15, and 20 min) at ambient temperatures. After liquid extraction, the extracts were dried under a steady stream of nitrogen and reconstituted in 196 µL acetonitrile:methanol (1:1) and 4 µL volumetric internal standard. The numbers in italics highlight the presence of interference indicated by % recoveries being higher than 100 %.

Compound	5 min	10 min	15 min	20 min
resorcinol	94.0	92.4	91.5	88.0
RDX	96.6	94.3	99.9	***114***
HMX	80.8	78.3	82.7	96.2
TNB	49.8	49.1	50.8	59.8
NG	30.3	31.9	31.1	31.9
tetryl	34.1	32.4	30.4	33.5
TNT	40.6	29.8	46.9	34.1
4-A-2,6-DNT	23.9	23.3	22.1	52.2
PETN	31.3	30.5	28.1	31.8
N-nDPA	29.6	32.2	33.5	33.0
DPA	49.1	51.9	52.9	52.2
EC	68.6	68.1	71.4	76.2
DBP	72.4	74.6	92.3	***132***
Mean	53.9	53.0	56.4	60.1

Table 5-10: Percentage relative standard variations (n = 3) of the liquid extractions of the on alcohol swabs spiked (25 ng) target organic gunshot residues using 5 mL methyl tertbutyl ether for the different sonication times (methyl tert-butyl ether as extraction solvent). After liquid extraction, the extracts were dried under a steady stream of nitrogen and reconstituted in 196 µL acetonitrile:methanol (1:1) and 4 µL volumetric internal standard.

Compound	5 min	10 min	15 min	20 min
resorcinol	3.55	5.31	12.2	3.01
RDX	3.25	6.41	3.07	1.91
HMX	3.69	5.74	2.29	0.93
TNB	4.52	7.22	1.50	5.97
NG	12.8	33.3	11.6	18.6
tetryl	8.93	12.5	13.0	49.9
TNT	66.1	9.41	1.49	6.66

Table 5-10 continued: Percentage relative standard variations (n = 3) of the liquid extractions of the on alcohol swabs spiked (25 ng) target organic gunshot residues using 5 mL methyl tertbutyl ether for the different sonication times (methyl tert-butyl ether as extraction solvent). After liquid extraction, the extracts were dried under a steady stream of nitrogen and reconstituted in 196 µL acetonitrile:methanol (1:1) and 4 µL volumetric internal standard.

Compound	5 min	10 min	15 min	20 min
4-A-2,6-DNT	52.5	16.5	8.74	13.1
PETN	23.7	24.4	2.11	30.3
N-nDPA	44.2	27.9	24.1	25.6
DPA	28.5	23.9	15.3	15.2
EC	9.38	14.2	4.15	8.29
DBP	20.6	13.8	10.7	56.7
Mean	21.7	15.4	8.48	18.2

Table 5-11: P-values of the Student's t-test (paired, two-tailed) between the % recoveries of the on alcohol swabs spiked (25 ng) target organic gunshot residues when liquid extracted using 5 mL methyl tertbutyl ether and four different sonication times (5, 10, 15, and 20 min). After liquid extraction, the extracts were dried under a steady stream of nitrogen and reconstituted in 196 µL acetonitrile:methanol (1:1) and 4 µL volumetric internal standard.. Significant difference (p-values < 0.05) is indicated in bold and italics.

	5 min	10 min	15 min
10 min	0.3569		
15 min	0.1660	0.0896	
20 min	0.0588	***0.0341***	0.0690

5.3.1.5 Optimised condition

The optimised conditions for the extraction of the targeted OGSR from swabs were as follows: After collection, the alcohol wipes were placed in scintillation vials and 5 mL MTBE added. Following a 5 min sonication, the solutions were transferred to other scintillation vials, whereby they were filtered through two filters, a 10 µm and 0.8 µm isopore membrane filter. The 0.8 µm filters were placed on GSR stubs for subsequent IGSR analysis using SEM-EDX. The extracts were dried down under a steady stream of nitrogen to volumes of 1.5 mL. After transferring the reduced

extracts to GC/HPLC vials they were further reduced until completely dry. The residues were reconstituted in 196 µL ACN:MeOH (1:1) and 4 µL ISTD (20 ppm final concentration) and analysed by UHPLC-UV.

5.3.1.6 Interference test

Samples collected from spiked hands were tested for the presence of interferences and the collection efficiency of alcohol wipes for OGSR. The hand samples were extracted using MTBE as it was determined to be the superior solvent in section 5.3.1.1. Figure 5-11 presents the individual extraction recoveries using MTBE (optimised condition) when alcohol wipes were spiked and the collection efficiencies of the alcohol wipes for OGSR when a mixture standard was spiked directly on hands. For calculating the collection efficiencies, the extraction recoveries of the target OGSR were considered. Using MTBE, the highest collection efficiency was found for NG (26 %), the lowest for TNB (9 %). The differences between the concentrations recovered from spiked swabs and from spiked skin represent losses presumably due to skin permeation [127], and the collection efficiency of the swab. EC and DPA derivatives have been shown to have low evaporative and absorptive loss in contrast to DPA and DMP [127].

Figure 5-11 presents the individual extraction recoveries using MTBE (optimised condition) when alcohol wipes were spiked and the collection efficiencies of the alcohol wipes for OGSR when a mixture standard was spiked directly on hands. The % recoveries and % RSD of the target compounds collected from hands using MTBE are listed in Table 5-12.

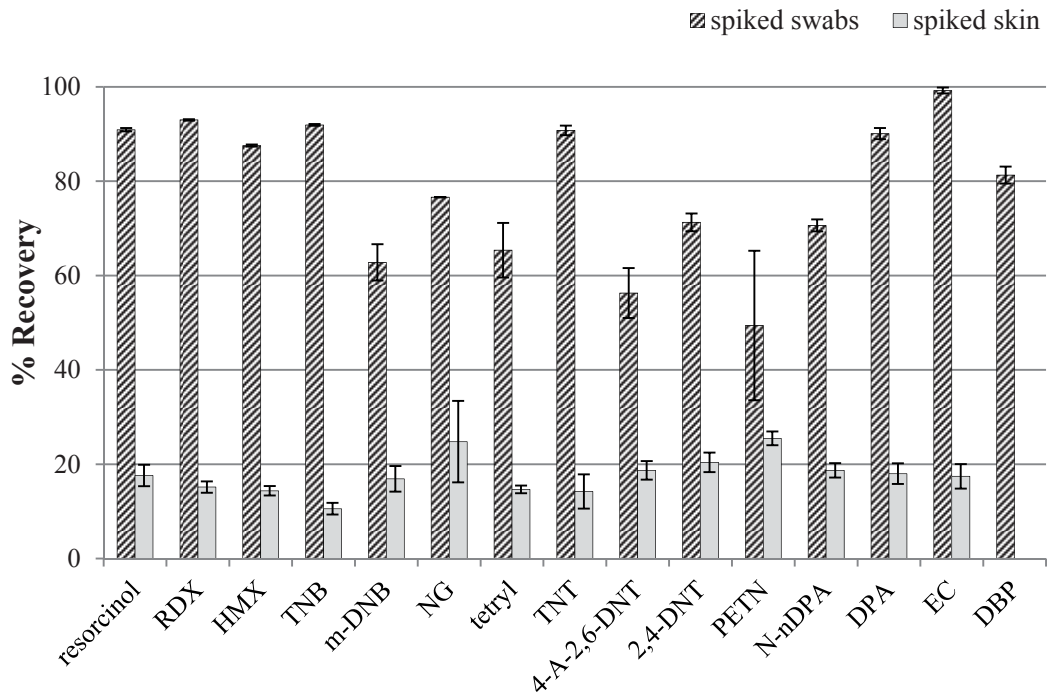

Figure 5-11: Percentage recoveries of 15 tested organic gunshot residue compounds from spiked hands (25 ng) collected using alcohol swabs that were liquid extracted using the optimised extraction conditions (5 min sonication at ambient temperatures using 5 mL methyl tert-butyl ether). After liquid extraction, the extracts were dried under a steady stream of nitrogen and reconstituted in 196 µL acetonitrile:methanol (1:1) and 4 µL volumetric internal standard. The recovery of DBP from hands is excluded in the chart. Interferences to DBP were extracted from hands and prohibited the determination of its recovery. Error bars represent standard deviations (n = 3).

Table 5-12: Percentage recoveries and % relative standard variations (% RSDs) of the targeted compounds from spiked hands (25 ng) collected using alcohol swabs that were liquid extracted using 5 mL methyl tert-butyl ether and 5 min sonication (normalised to the extraction efficiencies of the solvents). After liquid extraction, the extracts were dried under a steady stream of nitrogen and reconstituted in 196 µL acetonitrile:methanol (1:1) and 4 µL volumetric internal standard. Interferences are indicated by % recoveries > 100 % (italics, bold).

Compound	% Recovery	% RSD
resorcinol	17.6	17.7
RDX	15.2	19.4
HMX	14.4	14.0
TNB	10.6	23.8
m-DNB	16.9	89.8
NG	24.8	80.3
tetryl	14.7	32.3
TNT	14.2	53.1

Table 5-12 continued: Percentage recoveries and % relative standard variations (% RSDs) of the targeted compounds from spiked hands (25 ng) collected using alcohol swabs that were liquid extracted using 5 mL methyl tert-butyl ether and 5 min sonication (normalised to the extraction efficiencies of the solvents). After liquid extraction, the extracts were dried under a steady stream of nitrogen and reconstituted in 196 µL acetonitrile:methanol (1:1) and 4 µL volumetric internal standard. Interferences are indicated by % recoveries > 100 % (italics, bold).

Compound	% Recovery	% RSD
4-A-2,6-DNT	18.7	66.1
2,4-DNT	20.4	30.6
PETN	25.5	37.2
N-nDPA	18.7	31.3
DPA	18.0	29.4
EC	17.4	22.2
DBP	***128***	53.7
mean	17.6	40.1

5.3.2 ***Protocol 2***

5.3.2.1 Extraction Solvent comparison

Considering both mean extraction efficiency and % RSD values, MeOH (71 %, 9.13 % RSD) and acetone (68 %, 5.93 % RSD) proved to be the most suitable extraction solvents. ACN and MTBE followed with mean % recoveries of 69 % and 63 % and % RSD values of 13.00 % and 4.93 %, respectively. This result is consistent with a recent study by McCord and Thomas [175] that used acetone for the extraction; however they did not report any extraction % recovery. Furthermore, these authors reported that the solvent system previously developed for the extraction of GSR stubs by Zeichner [57] did not provide satisfactory results [175]. This study supports these results as the solvent system applied by Zeichner et al. only achieved 7 % overall recoveries of the spiked amounts. Interestingly, UV interferences for DBP were detected using ACN and MeOH, resulting in an

unreliable quantification of DBP using these solvents (highlighted in bold and italics in Table 5-13). Acetone was identified as the most suitable solvent as its evaporation characteristics makes it more time efficient and also due to the fact that ACN and MeOH lead to the extraction of UV interferences.

The % recoveries of the individual compounds extracted using the different solvents are shown in Figure 5-12 and listed in Table 5-13. The % RSD values (n = 3) are listed in Table 5-14.

Table 5-13: Percentage recoveries of the individual compounds of the spiked amount (30 ng) from gunshot residue stubs liquid extracted using 5.5 mL of six different solvents/solvent systems including acetonitrile (ACN), methanol (MeOH), ACN:MeOH (1:1), methyl tert-butyl ether (MTBE), acetone, and Zeichner solution and 15 min sonication at ambient temperatures. After liquid extraction, the extracts were dried under a steady stream of nitrogen and reconstituted in 196 µL ACN:MeOH (1:1) and 4 µL volumetric internal standard. ND = not detected.

Compound	ACN	MeOH	ACN:MeOH	MTBE	acetone	Zeichner
resorcinol	80.3	86.0	55.4	65.5	75.0	ND
RDX	71.4	72.3	50.7	49.2	66.6	34.8
HMX	66.2	66.7	43.7	53.6	62.0	24.3
TNB	91.0	92.0	62.1	79.4	81.9	ND
m-DNB	39.7	42.1	37.8	47.2	61.0	ND
NG	61.1	62.4	47.3	56.1	64.0	ND
tetryl	75.5	76.6	55.0	69.0	55.7	ND
TNT	72.5	72.7	51.6	63.4	67.9	ND
4-A-2,6-DNT	71.9	72.9	47.9	62.4	68.6	18.7
2,4-DNT	49.3	50.1	42.0	50.6	60.7	ND
PETN	18.5	16.5	13.0	15.7	18.3	11.0
N-nDPA	75.0	76.2	60.5	69.9	69.1	ND
DPA	79.3	85.3	64.2	95.6	88.7	ND
EC	80.5	82.4	54.7	73.6	80.2	ND
DBP	***106***	***107***	66.8	90.2	98.7	12.6
mean	69.2	70.8	50.2	62.8	67.9	6.76

Table 5-14: Percentage relative standard variations (n = 3) of the recoveries of the target compounds spiked (30 ng) on gunshot residues and liquid extracted from stubs using 5.5 mL of six different solvents/solvent systems (acetonitrile (ACN), methanol (MeOH), ACN:MeOH, methyl tert-butyl ether (MTBE), acetone, Zeichner solution) and 15 min sonication at ambient temperatures. After liquid extraction, the extracts were dried under a steady stream of nitrogen and reconstituted in 196 µL ACN:MeOH (1:1) and 4 µL volumetric internal standard. ND = not detected.

Compound	ACN	MeOH	ACN:MeOH	MTBE	acetone	Zeichner
resorcinol	9.25	2.60	33.2	1.38	2.10	ND
RDX	5.68	2.98	31.9	11.7	0.07	16.7
HMX	5.05	2.91	33.2	7.30	0.46	17.5
TNB	6.28	2.18	32.4	3.17	3.41	ND
m-DNB	39.3	40.4	43.8	2.88	4.82	ND
NG	9.28	3.02	22.0	2.76	2.67	ND
tetryl	5.38	0.75	29.1	4.68	16.5	ND
TNT	5.73	3.23	32.9	2.88	1.16	ND
4-A-2,6-DNT	8.23	3.51	30.0	4.16	4.23	30.3
2,4-DNT	25.5	21.7	40.8	2.12	2.40	ND
PETN	27.6	27.3	34.3	13.6	33.8	87.2
N-nDPA	17.6	9.97	25.2	2.68	1.57	ND
DPA	14.8	5.97	31.4	5.54	9.78	ND
EC	8.08	0.09	33.3	4.73	1.03	ND
DBP	7.23	10.3	30.0	4.34	5.05	21.8
mean	13.0	9.13	32.2	4.93	5.93	34.7

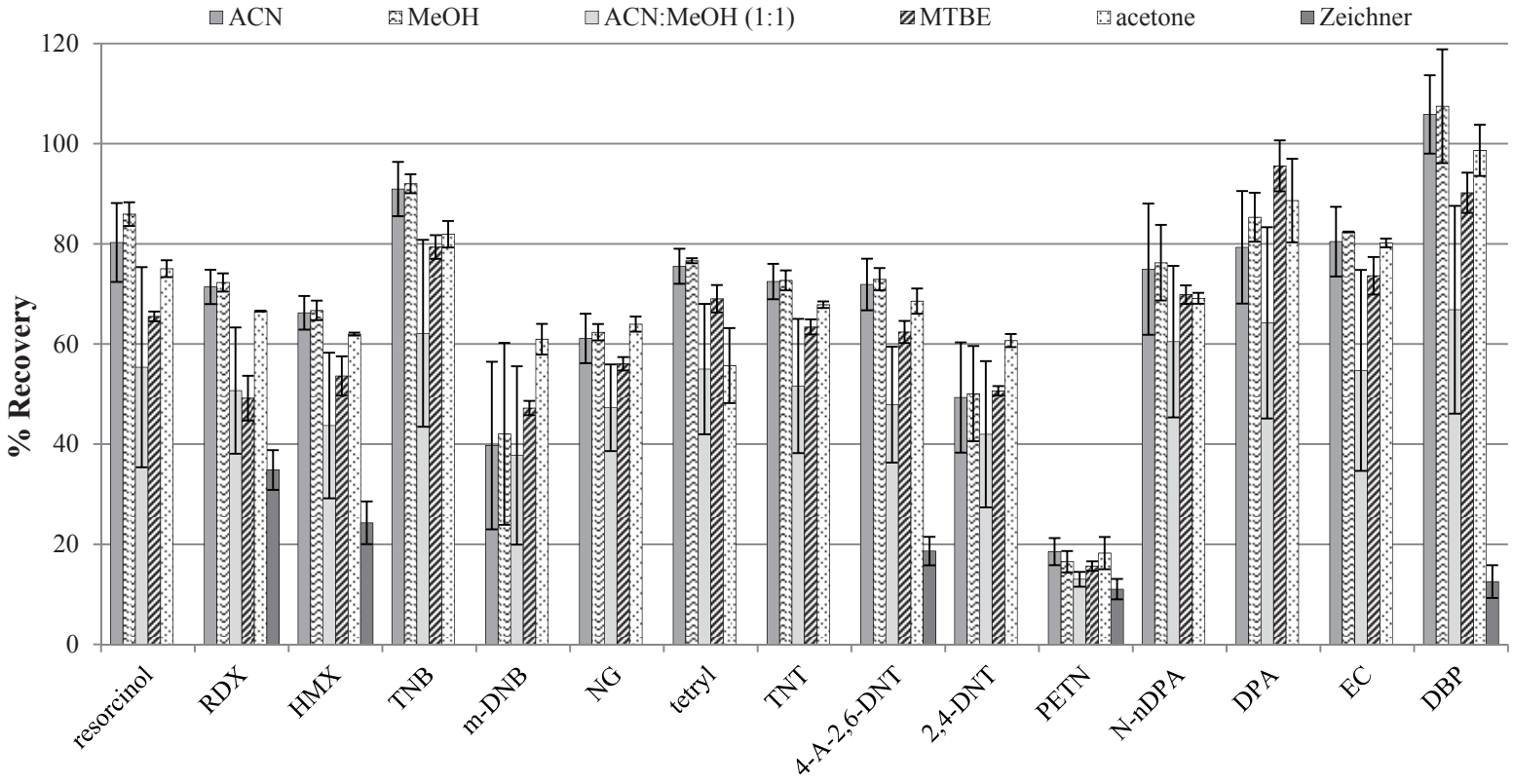

Figure 5-12: Percentage recoveries of the targeted organic gunshot residue compounds from spiked gunshot residue stubs (30 ng) liquid extracted using 5.5 mL of the different solvents tested (ACN = acetonitrile, MeOH = methanol, MTBE = methyl tert-butyl ether) and 15 min sonication. After liquid extraction, the extracts were dried under a steady stream of nitrogen and reconstituted in 196 µL ACN:MeOH (1:1) and 4 µL volumetric internal standard. Error bars represent standard deviations (n = 3).

5.3.2.2 Effect of Temperatures and Multiple Extractions

Protocol 2 was also tested to ascertain whether heating during sonication and extracting a GSR stub twice would increase the extraction efficiency. This test was conducted with the three most suitable solvents, i.e. ACN, MeOH, and acetone (Figure 5-13, Figure 5-14, and Figure 5-15, respectively). Selection of solvent and extraction conditions was based on maximising the recovery and precision. Upon performing the Student's t-test (paired, two-tailed, Table 5-17), a single extraction involving acetone at ambient temperature was selected. It should be noted that for DBP and PETN interferences were found which prohibited the quantification of these compounds (indicated by their % recoveries being higher than 100 %; italics in Table 5-15). The % recoveries are listed in Table 5-15 and % RSD values in Table 5-16.

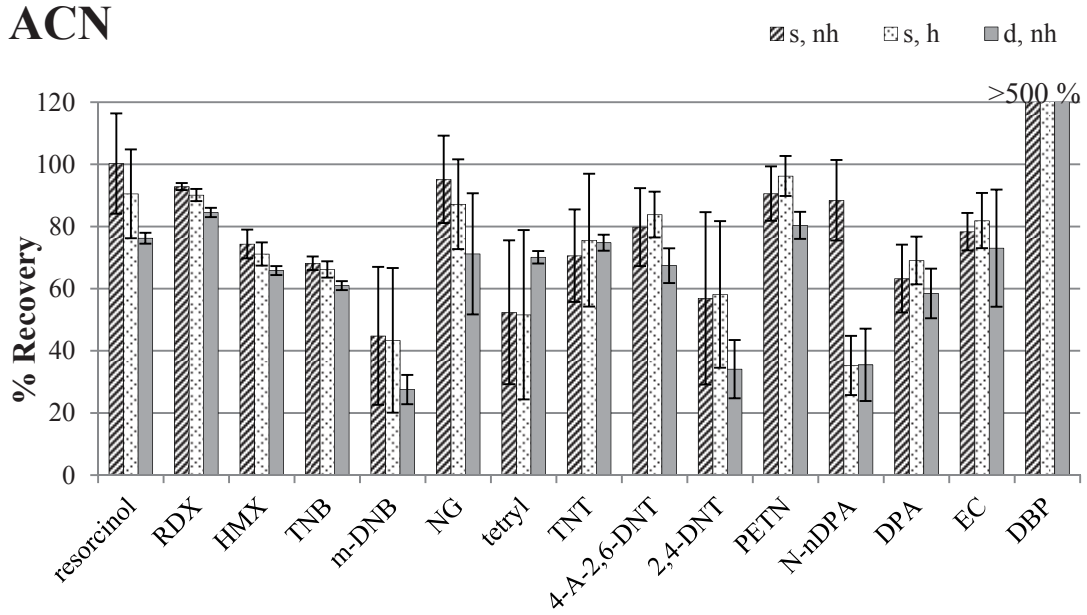

Figure 5-13: Percentage recoveries of the target compounds liquid extracted from spiked (15 ng) gunshot residue stubs using three different conditions and 5.5 mL acetonitrile (ACN). The conditions were: s, nh = single extraction, non-heated (15 min sonication at ambient temperatures); s, h = single extraction, heated (15 min sonication at 45 ºC); d, nh = double extraction, non-heated (2 x 15 min sonication at ambient temperatures and combining the extracts). After liquid extraction, the extracts were dried under a steady stream of nitrogen and reconstituted in 196 µL ACN:methanol (1:1) and 4 µL volumetric internal standard. Error bars represent standard deviations (n = 3).

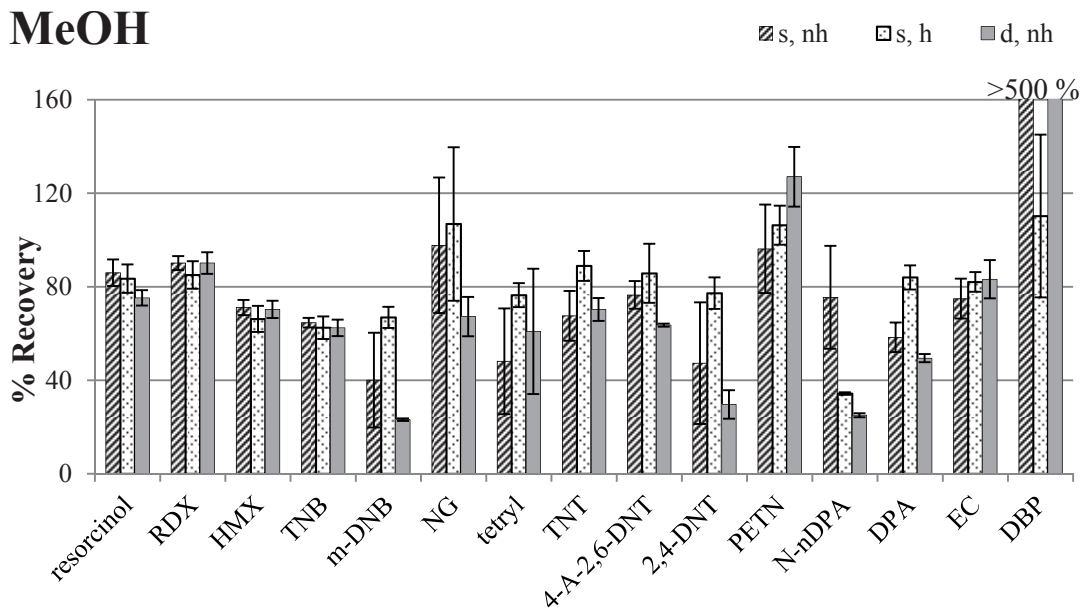

Figure 5-14: Percentage recoveries of the target compounds liquid extracted from spiked (15 ng) gunshot residue stubs using three different conditions and 5.5 mL methanol (MeOH). The conditions were: s, nh = single extraction, non-heated (15 min sonication at ambient temperatures); s, h = single extraction, heated (15 min sonication at 45 ºC); d, nh = double extraction, non-heated (2 x 15 min sonication at ambient temperatures and combining the extracts). After liquid extraction, the extracts were dried under a steady stream of nitrogen and reconstituted in 196 µL acetonitrile:MeOH (1:1) and 4 µL volumetric internal standard. Error bars represent standard deviations (n = 3).

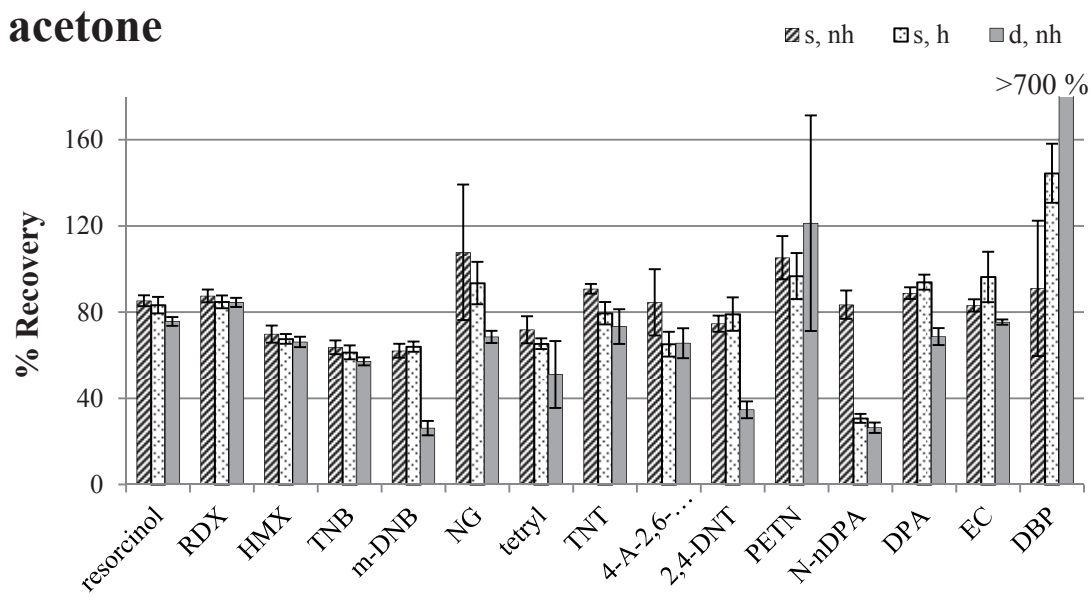

Figure 5-15: Percentage recoveries of the target compounds liquid extracted from spiked (15 ng) gunshot residue stubs using three different conditions and 5.5 mL acetone. The conditions were: s, nh = single extraction, non-heated (15 min sonication at ambient temperatures); s, h = single extraction, heated (15 min sonication at 45 ºC); d, nh = double extraction, non-heated (2 x 15 min sonication at ambient temperatures and combining the extracts). After liquid extraction, the extracts were dried under a steady stream of nitrogen and reconstituted in 196 µL acetonitrile:methanol (1:1) and 4 µL volumetric internal standard. Error bars represent standard deviations (n = 3).

Table 5-15: Percentage recoveries of the target compounds liquid extracted using three different extraction techniques and 5.5 mL of different solvents (acetonitrile (ACN), methanol (MeOH) and acetone) from spiked (15 ng) gunshot residue stubs. The techniques are: s,nh: single extraction without heating (15 min sonication at ambient temperatures); s,h: single extraction with heating (15 min sonication at 45 ºC); d,nh: double extraction without heating (2 x 15 min sonication at ambient temperatures and combining the extracts). After liquid extraction, the extracts were dried under a steady stream of nitrogen and reconstituted in 196 µL ACN:MeOH (1:1) and 4 µL volumetric internal standard. Values in bold and italics are non-conclusive as interferences from stubs were detected.

Compound	ACN			MeOH			acetone		
	s, nh	s, h	d, nh	s, nh	s, h	d, nh	s, nh	s, h	d, nh
resorcinol	100	90.5	76.2	86.0	83.5	75.3	85.3	83.2	75.7
RDX	92.8	90.1	84.5	90.2	85.1	90.2	87.5	84.8	84.5
HMX	78.9	75.7	70.3	75.6	70.7	74.8	74.3	72.1	70.6
TNB	68.2	66.2	61.0	64.6	62.5	62.4	63.7	61.3	57.1
m-DNB	44.8	43.4	27.6	40.1	66.9	23.2	62.1	63.9	26.1
NG	95.2	87.2	71.2	97.7	100	67.2	98.9	93.5	68.5
tetryl	52.4	51.6	70.1	48.1	76.4	60.9	71.8	65.3	51.0
TNT	35.3	37.8	37.4	33.8	44.5	35.2	45.4	39.8	36.7
4-A-2,6-DNT	66.0	77.5	73.8	23.3	90.4	62.9	54.7	60.2	69.4
2,4-DNT	56.9	58.2	34.1	47.3	77.3	29.6	74.7	79.1	34.7
PETN	90.6	96.2	80.4	96.2	***106***	***127.1***	***105***	96.7	***121***
N-nDPA	88.4	88.2	88.7	75.5	85.8	62.6	83.5	76.7	65.9
DPA	63.2	69.1	58.4	58.4	84	49.5	88.8	93.9	68.6
EC	78.3	81.9	73.0	74.9	82.1	83.2	83.09	96.3	75.3
DBP	***576***	***492***	***1020***	***635***	***110***	***1110***	***91.0***	***144***	***745***
mean	72.2	72.4	64.8	65.1	80.2	64.6	77.7	76.2	64.7

Table 5-16: Percentage relative standard deviations (n = 3) of the target compounds liquid extracted from spiked (15 ng) gunshot residue stubs using three different techniques and 5.5 mL of different solvents (acetonitrile (ACN), methanol (MeOH) and acetone). The techniques are: s,nh: single extraction without heating (15 min sonication at ambient temperatures); s,h: single extraction with heating (15 min sonication at 45 ºC); d,nh: double extraction without heating (2 x 15 min sonication at ambient temperatures and combining the extracts). After liquid extraction, the extracts were dried under a steady stream of nitrogen and reconstituted in 196 µL ACN:MeOH (1:1) and 4 µL volumetric internal standard.

Compound	ACN			MeOH			acetone		
	s, nh	s, h	d, nh	s, nh	s, h	d, nh	s, nh	s, h	d, nh
resorcinol	18.5	18.5	2.81	7.84	8.68	5.32	3.49	5.50	3.32
RDX	1.47	2.62	2.16	3.96	8.50	6.21	4.12	4.32	3.08
HMX	6.04	5.08	2.14	4.46	8.15	5.08	5.54	3.25	3.51
TNB	3.60	4.42	2.67	3.58	8.69	6.39	5.61	5.91	3.70
m-DNB	92.2	103	69.1	105	9.76	21.9	7.84	5.51	61.9
NG	16.4	18.6	31.5	32.7	33.6	14.5	31.9	11.7	4.79
tetryl	66.3	79.9	3.85	73.8	8.73	61.8	11.6	5.19	46.3
TNT	28.7	37.6	4.60	21.8	9.15	9.55	3.11	8.58	14.8
4-A-2,6-DNT	18.3	10.2	9.95	9.09	17.0	1.23	21.0	10.7	12.9
2,4-DNT	69.9	57.7	55.8	86.5	11.2	49.2	6.54	12.6	22.4
PETN	12.0	8.18	6.89	24.0	9.39	11.6	11.4	13.5	48.2
N-nDPA	27.7	51.1	61.9	65.1	3.14	10.5	15.8	15.0	24.9
DPA	28.9	17.6	24.2	19.3	8.77	7.23	4.27	5.11	9.11
EC	11.2	15.5	38.9	16.9	7.29	14.0	4.90	16.3	2.42
DBP	62.6	64.8	21.2	64.9	37.3	4.32	42.3	10.7	39.8
mean	28.7	30.7	22.6	33.8	10.9	16.0	9.79	8.79	18.7

Table 5-17: Results (p-values) of the Student's t-tests (paired, two-tailed) between the recoveries when liquid extracting the spiked (15 ng) target compounds from gunshot residue stubs using 5.5 mL of different solvents (acetonitrile (ACN), methanol (MeOH) and acetone) and the three different conditions: s,nh = single extraction without heating (15 min sonication at ambient temperatures); s,h = single extraction with heating (15 min sonication at 45 ºC); d, nh = double extraction without heating (2 x 15 min sonication at ambient temperatures and combing the extracts). After liquid extraction, the extracts were dried under a steady stream of nitrogen and reconstituted in 196 µL ACN:MeOH (1:1) and 4 µL volumetric internal standard. P-values < 0.05 (bold, italics) indicate a significant difference.

	ACN		**MeOH**		**Acetone**	
	s, nh	**d, nh**	**s, nh**	**d, nh**	**s, nh**	**d, nh**
s, h	0.9167	***0.0153***	***0.0126***	***0.0155***	0.4400	***0.0346***
d, nh	***0.0386***		0.9144		***0.0154***	

5.3.2.3 Sonication Times

The highest overall recovery was obtained applying sonication to the samples for 5 min. In detail, RDX, HMX, TNB, m-DNB, NG, tetryl, TNT, 24-DNT, PETN, N-nDPA, DPA and EC were all extracted most successfully using this time. Additionally, sonication for 5 min resulted in the lowest % RSD (n = 3) values. Sonication for 10 min and longer resulted in the extraction of UV interferences for NG and PETN (shown in bold and italics in Table 5-18). However, there was no significant difference (Student's t-test, paired, two-tailed) between any of the tested times (Table 5-20). Due to the high recoveries as well as not extracting UV interferences, sonication for 5 min was chosen for all further experiments.

Percentage recoveries of the compounds are displayed in Figure 5-16, listed in Table 5-18 and % RSD values in Table 5-19.

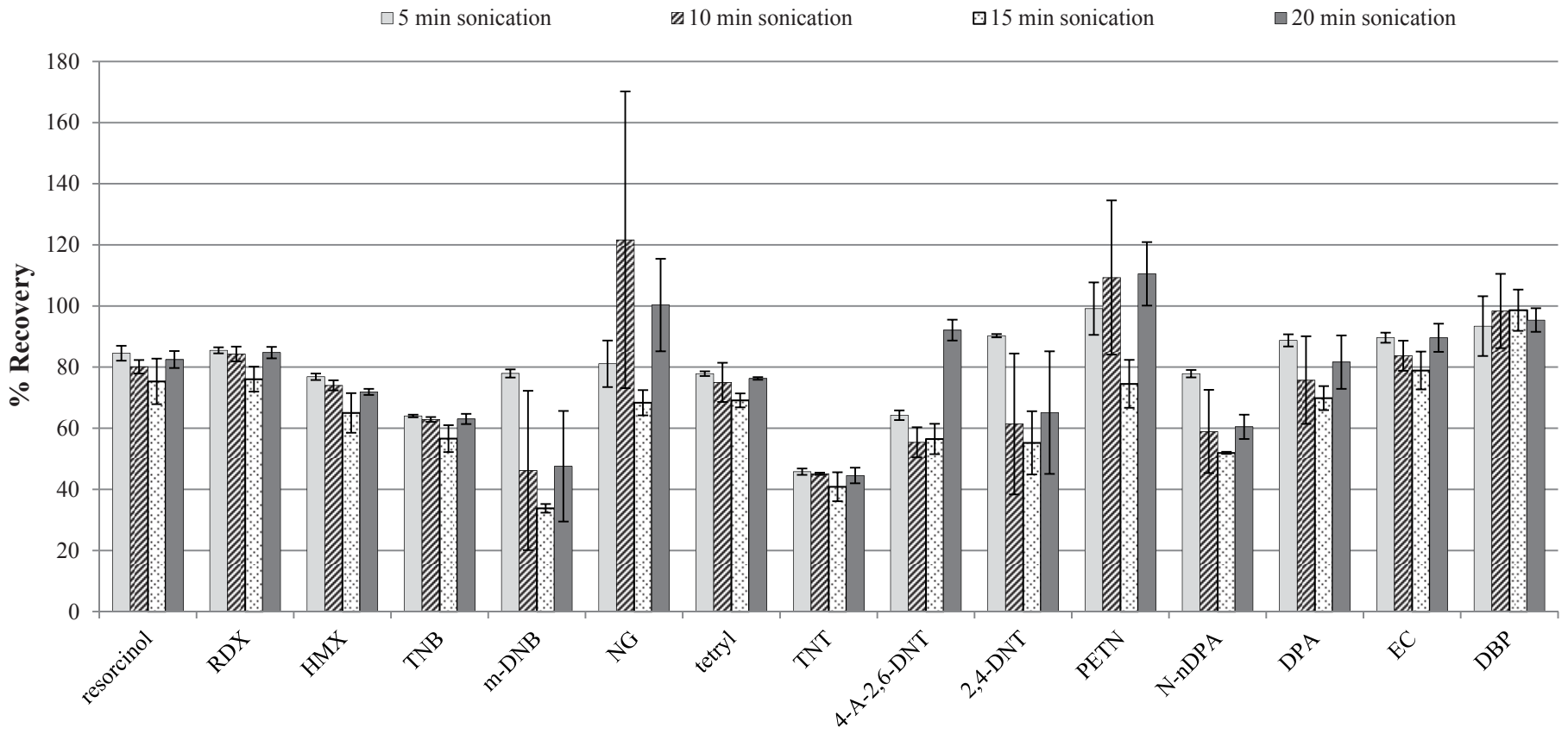

Figure 5-16: Percentage recoveries of the individual compounds liquid extracted from spiked (13 ng) gunshot residue stubs using 5.5 mL acetone and four different sonication times (5, 10, 15, and 20 min) at ambient temperatures. After liquid extraction, the extracts were dried under a steady stream of nitrogen and reconstituted in 196 µL acetonitrile:methanol (1:1) and 4 µL volumetric internal standard. Error bars represent standard deviations (n = 3).

Table 5-18: Percentage recoveries of the targeted organic gunshot residue (GSR) compounds from spiked (13 ng) GSR stubs using 5.5 mL acetone and four different sonication times (5, 10, 15, 20 min) at ambient temperatures. After liquid extraction, the extracts were dried under a steady stream of nitrogen and reconstituted in 196 µL acetonitrile:methanol (1:1) and 4 µL volumetric internal standard. Values in bold and italics indicate the extraction of interferences and are therefore inconclusive.

Compound	5 min	10 min	15 min	20 min
resorcinol	84.5	80.1	75.3	82.5
RDX	85.5	84.3	76.1	84.7
HMX	76.9	74.0	65.0	71.9
TNB	64.0	62.9	56.6	63.0
m-DNB	77.9	46.2	33.8	47.6
NG	81.1	***122***	68.4	***100***
tetryl	77.9	75.0	69.1	76.3
TNT	45.8	45.1	40.9	44.5
4-A-2,6-DNT	64.2	55.4	56.5	92.1
2,4-DNT	90.3	61.4	55.2	65.1
PETN	99.1	***109***	74.5	***111***
N-nDPA	77.9	58.9	51.9	60.5
DPA	88.7	75.8	69.9	81.7
EC	89.6	83.7	78.9	89.6
DBP	93.4	98.4	98.6	95.4
mean	79.8	75.5	64.7	77.7

Table 5-19: Percentage relative standard deviations (n = 3) of the different organic gunshot residue compounds spiked (13 ng) on gunshot residue stubs and liquid extracted using 5.5 mL acetone and four different sonication times (5, 10, 15, 20 min) at ambient temperatures. After liquid extraction, the extracts were dried under a steady stream of nitrogen and reconstituted in 196 µL acetonitrile:methanol (1:1) and 4 µL volumetric internal standard.

Compound	5 min	10 min	15 min	20 min
resorcinol	3.51	3.42	12.4	4.12
RDX	1.48	3.64	6.99	2.82
HMX	1.44	2.31	10.4	1.41
TNB	0.78	1.44	9.09	3.03
m-DNB	2.48	117	14.4	76.6
NG	10.8	43.7	7.17	16.9

Table 5-19 continued: Percentage relative standard deviations (n = 3) of the different organic gunshot residue compounds spiked (13 ng) on gunshot residue stubs and liquid extracted using 5.5 mL acetone and four different sonication times (5, 10, 15, 20 min) at ambient temperatures. After liquid extraction, the extracts were dried under a steady stream of nitrogen and reconstituted in 196 µL acetonitrile:methanol (1:1) and 4 µL volumetric internal standard.

Compound	5 min	10 min	15 min	20 min
tetryl	1.35	11.7	4.68	0.79
TNT	1.48	0.52	7.91	3.81
4-A-2,6-DNT	2.11	6.33	7.41	4.24
2,4-DNT	0.80	55.6	29.3	44.3
PETN	10.9	28.3	14.4	11.5
N-nDPA	2.10	34.3	0.99	9.60
DPA	3.32	30.9	9.67	16.7
EC	2.69	8.89	12.3	7.49
DBP	13.2	15.4	8.55	5.08
mean	3.89	24.23	10.4	13.9

Table 5-20: P-values (Student's t-test, paired, two-tailed) between the mean extraction recoveries of the target compounds spiked (13 ng) on gunshot residues and liquid extracted using 5.5 mL acetone and four different sonication times (5, 10, 15, 20 min) at ambient temperatures. After liquid extraction, the extracts were dried under a steady stream of nitrogen and reconstituted in 196 µL acetonitrile:methanol (1:1) and 4 µL volumetric internal standard.

	5 min	10 min	15 min
10 min	0.8817		
15 min	0.0658	0.2624	
20 min	0.8626	0.7448	0.4079

5.3.2.4 Optimised Condition

The optimised protocol was as follows: Following IGSR analysis by SEM-EDX, the stubs were placed in scintillation vials and 5.5 mL acetone was added followed by sonication for 5 min at RT. The stubs were removed from the vials and the extract dried under a steady stream of nitrogen to approximately 1.5 mL and transferred to GC/HPLC vials and further reduced to complete dryness. The residues were

reconstituted in 196 µL ACN:MeOH (1:1) and 4 µL volumetric ISTD (20 ppm final concentration) and analysed by UHPLC-UV.

5.3.2.5 Interference Test

Finally, the uptake efficiency of GSR stubs to OGSR from hands and presence of interferences were examined. The extraction of these samples followed the optimised parameters (5.3.2.4) using acetone as extraction solvent.

In all skin samples (spiked and blank), peaks at 3.02, 4.00, 14.03, 20.05 min (PETN), 25.46, 25.67, and 26.27 min (DBP) were found. These peaks were found in samples taken from two different persons and are tentatively identified as compounds present on skin that have not been removed despite washing the hands thoroughly, or to source from the stub material. Since the peaks coelute with PETN and DBP, these two compounds cannot be UV detected or quantified using the developed method.

The % recoveries of PETN were above 100 % for two samples which indicates that interferences were collected from hands (highlighted in bold and italics in Table 5-21). For any other targeted OGSR, the system peaks are not problematic.

Overall, the collection efficiencies were higher than could be achieved using swabs, ranging from 24 % (TNB) to 73 % (DPA). Interestingly, TNB had the lowest collection efficiencies for both swabs and stubs. This could be a result of high evaporation or absorption in the skin. Considering the vapour pressure of TNB (20 Pa at 20 °C), the main reason is assumed to be absorption.

The % recoveries from spiked stubs as well as from spiked skin using GSR stubs as collection device and the optimised conditions using acetone as extraction

solvents are shown in Figure 5-17. Percentage recoveries and % RSDs from spiked skin using GSR stubs and acetone as extraction solvents are listed in Table 5-21.

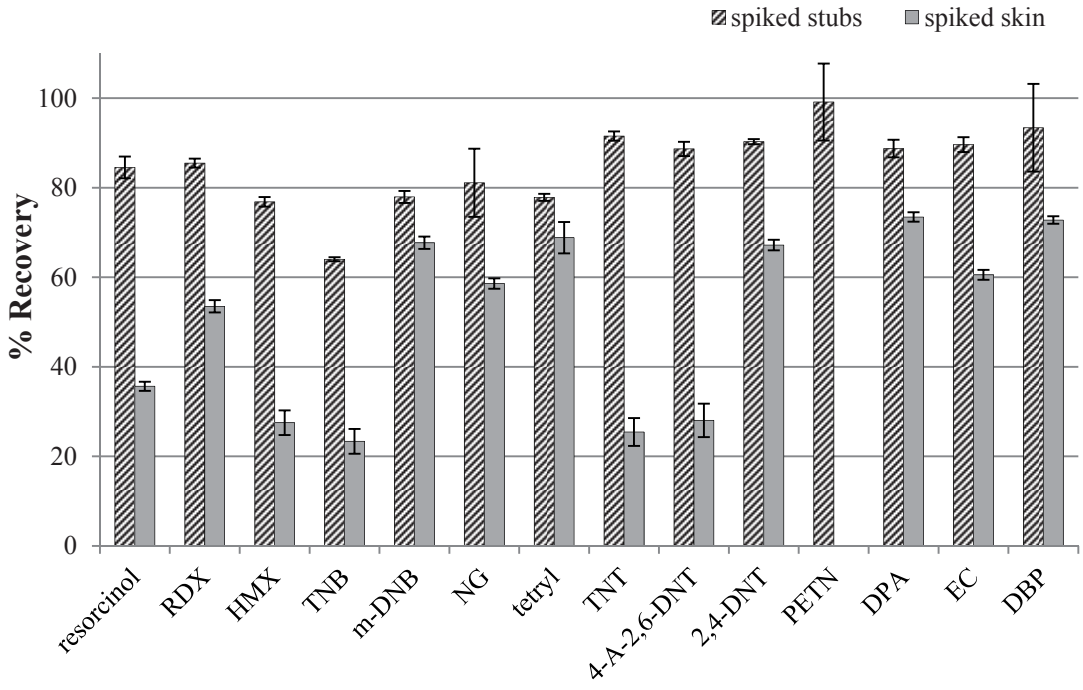

Figure 5-17: Percentage recoveries of 15 tested organic gunshot residue (GSR) compounds from spiked hands.(20 ng) collected using GSR stubs and liquid extracted using the optimised extraction conditions (5 min sonication at ambient temperatures using 5.5 mL acetone). After liquid extraction, the extracts were dried under a steady stream of nitrogen and reconstituted in 196 µL acetone:methanol (1:1) and 4 µL volumetric internal standard. The recovery of PETN from hands is excluded in the chart. Interferences to PETN were extracted from hands and prohibited the determination of its recovery. Error bars represent standard deviations (n = 3).

Table 5-21: Percentage recoveries and % relative standard deviations (% RSDs) of the spiked (20 ng) target compounds on hands collected by gunshot residue stubs which were liquid extracted using 5.5 mL acetone and 5 min sonication. After liquid extraction, the extracts were dried under a steady stream of nitrogen and reconstituted in 196 µL acetonitrile:methanol (1:1) and 4 µL volumetric internal standard. The % recoveries were normalised to the extraction efficiency from stubs using this solvent. The mean was calculated excluding the values for PETN and DBP due to the possibility to extract interferences. % Recoveries >100 % are highlighted in bold and italics.

Compound	% Recovery	% RSD
resorcinol	35.7	27.1
RDX	53.5	49.1
HMX	27.5	47.1
TNB	23.4	53.0
m-DNB	67.7	56.8
NG	58.6	44.0

Table 5-21 continued: Percentage recoveries and % relative standard deviations (% RSDs) of the spiked (20 ng) target compounds on hands collected by gunshot residue stubs which were liquid extracted using 5.5 mL acetone and 5 min sonication. After liquid extraction, the extracts were dried under a steady stream of nitrogen and reconstituted in 196 µL acetonitrile:methanol (1:1) and 4 µL volumetric internal standard. The % recoveries were normalised to the extraction efficiency from stubs using this solvent. The mean was calculated excluding the values for PETN and DBP due to the possibility to extract interferences. % Recoveries >100 % are highlighted in bold and italics.

Compound	% Recovery	% RSD
tetryl	68.8	***134***
TNT	25.4	53.8
4-A-2,6-DNT	28.0	71.9
2,4-DNT	67.2	48.1
PETN	72.8	7.26
DPA	73.5	53.5
EC	60.5	59.5
DBP	72.8	48.6
mean	33.1	58.2

5.3.3 *Protocol 3*

Commonly SPME is a great and easy to use extraction technique used for the headspace extraction of volatile compounds in conjunction with desorption under elevated temperatures in a GC inlet. Since some of the compounds targeted in this study are thermally labile and can degrade under elevated temperatures, UHPLC analysis was utilised. Therefore, after headspace collection, the fibre was directly immersed in solvent which was subsequently analysed by UHPLC.

The first optimisation step was to determine an appropriate immersion time for the fibre in the solution to ensure desorption of all compounds and no carry-over to the next headspace extraction. Exposure of the fibre to the solution for 5 min was sufficient to desorb all compounds of interest. Longer exposure times were avoided as the fibre material can degrade when immersed in the solution.

Two peaks at 5.540 min and 6.757 min were present in all chromatograms, blanks and samples. These peaks are believed to be system peaks sourced from the fibre material when immersed in the solution.

5.3.3.1 Heating Temperature

The % recoveries for any compound at any temperature tested are shown in Figure 5-18 and Table 5-22 and did not exceed 25 %, inferior to that achieved using either achieved in Protocol 1 and 2. Therefore, no further investigations, e.g. into fibre exposure times, were conducted.

The low % recoveries can be explained by SPME being an equilibrium extraction tool and not a quantitative extraction technique. Furthermore, the adhesive nature of the carbon tape and the semivolatile nature of the target compounds could strongly limit the extraction efficiency. This was tested using a volatile compound, bromobenzene, spiking it directly on GSR stubs, and immersing the fibre in liquid, which was subsequently analysed by direct injection into the QQQ-MS. No bromobenzene could be detected in any of the samples. Furthermore, headspace samples of spiked (bromobenzene) GSR stubs were analysed using GC-MS, which is the common technique coupled with SPME. Since no bromobenzene could be detected in the sample, it was assumed that the reason for the relatively low extraction recoveries is the adhesive nature of the GSR stubs, which might be interacting to some degree with the compounds of interest.

It should also be noted, that fibres lasted only a relatively short time due to the direct immersion in a solution (<70 extractions).

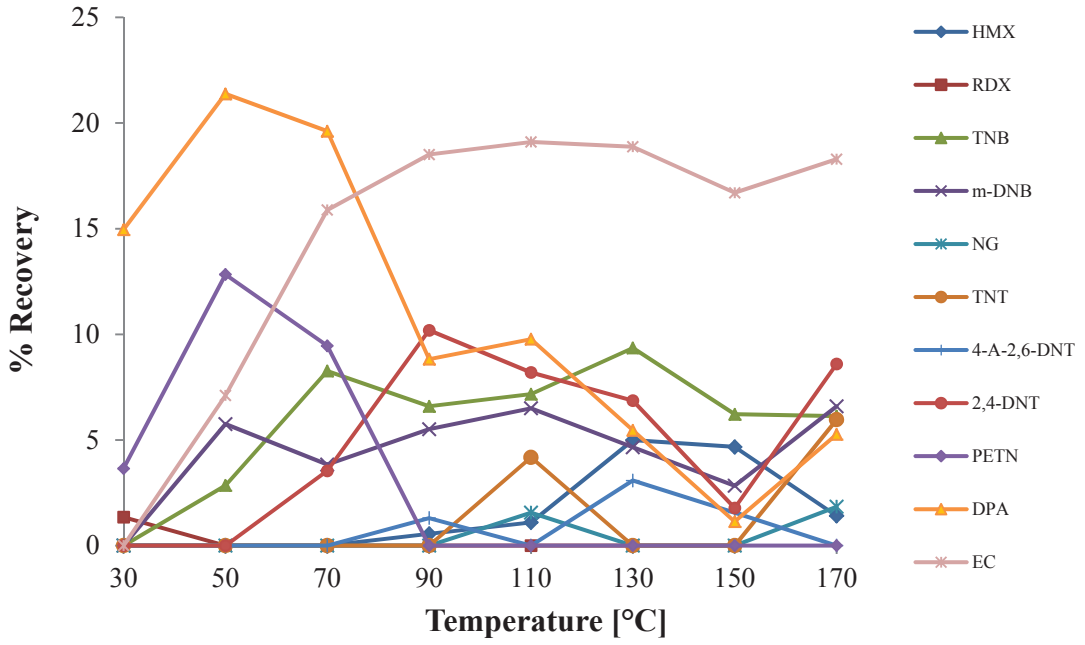

Figure 5-18: Percentage recoveries of the target organic gunshot residue (GSR) compounds spiked on GSR stubs (20 ng) and extracted using solid phase microextraction at different temperature ranging from 30-170 °C with 20 °C increments. The 65 µm polydimethylsiloxane/divinylbenzene fibre (was exposed for 1 hour, followed by 5 min direct immersion in the solvent system (196 µL acetonitrile:methanol (1:1) and 4 µL volumetric internal standard) that was subsequently analysed by ultra-high performance liquid chromatography with ultraviolet detection.

Table 5-22: Percentage recoveries of the spiked (20 ng) organic gunshot residue (GSR) compounds from GSR stubs heated at different temperatures ranging from 30 to 150 °C with 20 °C increments extracted using solid phase microextraction (SPME). The SPME fibre (65 µm polydimethylsiloxane/divinylbenzene) was exposed for 1 hour followed by 5 min direct immersion in the solvent system (196 µL acetonitrile:methanol (1:1) and 4 µL volumetric internal standard) that was subsequently analysed by ultra-high performance liquid chromatography with ultraviolet detection. ND = not detected.

Compound	T [°C]							
	30	**50**	**70**	**90**	**110**	**130**	**150**	**170**
RDX	1.35	ND	ND	ND	ND	ND	ND	ND
HMX	ND	ND	ND	0.56	1.10	4.99	4.67	1.41
TNB	ND	2.85	8.27	6.59	7.17	9.36	6.22	6.13
m-DNB	ND	5.76	3.84	5.51	6.50	4.66	2.83	6.60
NB	ND	ND	ND	ND	ND	ND	ND	ND
NG	ND	ND	ND	ND	1.56	ND	ND	1.84
tetryl	ND	ND	ND	ND	ND	ND	ND	ND
TNT	ND	ND	ND	ND	4.18	ND	ND	5.96
4-A-2,6-DNT	ND	ND	ND	1.31	ND	3.08	1.56	ND
DMP	ND	ND	ND	ND	ND	ND	ND	ND
2,4-DNT	ND	ND	3.54	10.2	8.20	6.86	1.78	8.60
2-naphthol	ND	ND	ND	ND	ND	ND	ND	ND
m-NT	4.01	ND	ND	ND	2.41	2.83	2.22	1.27
PETN	3.65	12.8	9.46	ND	ND	ND	ND	ND
4-nDPA	ND	ND	ND	ND	ND	ND	ND	ND
N-nDPA	71.7	79.1	34.9	ND	ND	ND	ND	ND
DPA	15.0	21.4	19.6	8.83	9.77	5.46	1.14	5.27
2-NDPA	ND	ND	ND	ND	19.5	23.6	25.1	12.9
EC	ND	7.11	15.9	18.5	19.1	18.9	16.7	18.3
DBP	ND	ND	ND	ND	ND	ND	ND	ND

5.3.4 *Comparison of Protocol 1 and Protocol 2*

Table 5-23 compares the two most efficient extraction protocols: alcohol swabs and GSR stubs with liquid extraction. While the extraction efficiency (liquid extraction) from both collection devices are very similar (79 % from swabs and 80 % from stubs) and no significant difference could be found, skin collection efficiencies were significantly higher for stubs (49 %) than for swabs (18 %). A drawback of these two protocols is their destructive nature.

Table 5-23: Overview and comparison of the two optimised and superior collection protocols. The optimised collection protocol involving alcohol swabs consists of liquid extracting the swab using 5 mL methyl tertbutyl ether and 5 min sonication at ambient temperatures. After liquid extraction, the extracts were dried under a steady stream of nitrogen and reconstituted in 196 µL acetonitrile (ACN):methanol (MeOH) (1:1) and 4 µL volumetric internal standard. The optimised collection protocol involving gunshot residue stubs consists of liquid extracting the stub using 5.5 mL acetone and 5 min sonication at ambient temperatures. After liquid extraction, the extracts were dried under a steady stream of nitrogen and reconstituted in 196 µL ACN:MeOH (1:1) and 4 µL volumetric internal standard.

		Swabs	**Stubs**
Extraction Efficiency (swab/stub spike)	Mean	79 %	80 %
	Range	50 % (PETN) – 98 % (EC)	64 % (TNB) – 98 % (PETN)
	Difference	No significant difference (p = 0.24133)	
Skin Collection (skin spike)	Mean	18 %	49 %
	Range	9 % (TNB) – 26 % (NG)	24 % (TNB) – 73 % (DPA)
	Difference	Significant difference (p = 0.00052)	

5.3.5 *Simulated Case Specimens*

5.3.5.1 Efficiency for IGSR Analysis

Finally, Protocol 1 and 2 were compared for both IGSR and OGSR analysis using specimens collected at a firing range. Since the second installed filter in Protocol 1 (see Figure 5-2), which undergoes SEM-EDX, collects particles with sizes between 0.8 and 10 µm, only these particles sizes were considered for comparison. This size range also covers the typical diameters of IGSR particles [26]. Additionally, only spherical particles were considered. An example of an X-ray spectra and picture of the associated GSR particle is presented in Figure 5-19.

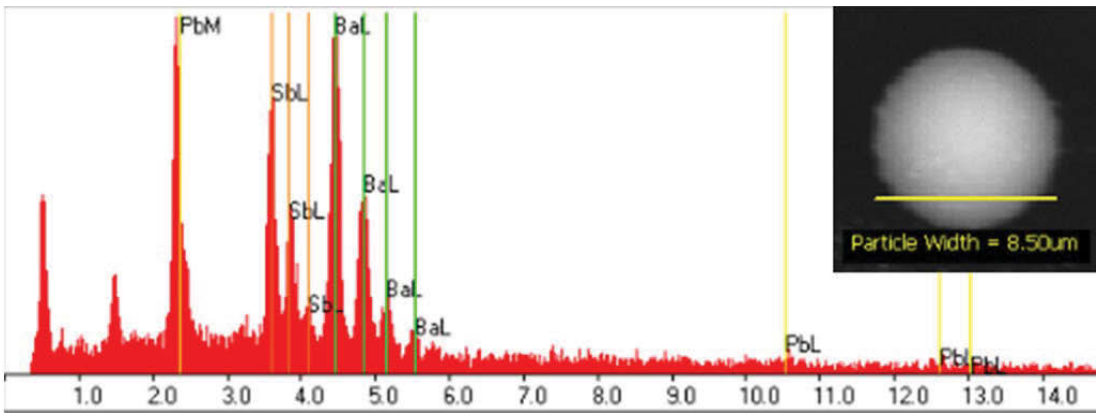

Figure 5-19: X-ray spectra and picture of a spherical 8.50 µm wide gunshot residue particle incorporating the elements lead (Pb), antimony (Sb), and barium (Ba) analysed using scanning electron microscopy coupled with energy dispersive X-ray spectroscopy.

A list of the average number (n = 3) of spherical PbBaSb particles with sizes between 0.8 and 10 µm using stubs and swabs for all ammunition-firearm combinations is provided in Appendix XI. Table 5-24 lists examples for the results obtained from three ammunition-firearm combinations.

Table 5-24: List of average number of characteristic (incorporating Pb, Ba and Sb) gunshot residue (GSR) particles (sizes between 0.8 and 10 µm) using three different ammunition-firearm combinations per mm^2 when collected using medi swabs or GSR stubs (one shot, n = 3). The stubs and swabs were not carbon coated before analysis using scanning electron microscopy coupled with energy dispersive X-ray spectroscopy.

	Swabs [PbBaSb/mm^2]	**Stubs [PbBaSb/mm^2]**
Pistol (USA) 9 mm Parabellum (Luger)	ND	1.268
Pistol (USA) 22 LR High Velocity (Winchester)	0.110	0.604
Glock (Austria) 40 Smith&Wesson (Winchester)	0.060	1.042

The number of characteristic GSR particles/mm^2 detected when using swabs was significantly lower than when detected using stubs (Student's t-test, paired, two-tailed, p = 0.0049 for the three ammunition-firearm combinations in Table 5-24). On some swab filters, no IGSR particulates were collected at all, while on the other hand characteristic IGSR particles could be found on nearly all GSR stubs (Table 5-24 ammunition-firearm combination pistol (USA) with 9 mm Parabellum (Luger) collected using alcohol swabs; further examples see Appendix IX). This could be the result of an interior collection efficiency of swabs for IGSR, which would be in agreement with a previously reported study [130]. Another reason could be that IGSR particles are lost during the specimen treatment and are not collected on the syringe filters. IGSR analysis was found to be strongly affected using Protocol 1, suggesting that swabs are not suitable as collection devices for both OGSR and IGSR. Furthermore, it was noticed that the number of shots, i.e. one or three, generally correlated with the number of IGSR detected in that three shots resulted in a higher number of GSR particles detected using stubs. Interestingly,

firing LF ammunition resulted in the formulation of characteristic GSR particles incorporating Pb, Sb, and Ba. This could be a result of not having the firearms cleaned sufficiently before firing (memory effect), having a different lead source in the ammunition such as the cartridge case or contamination, although this can be excluded due to particle free blanks collected in between each shooting. For more detailed information about the number of characteristic IGSR particles collected from the hands of a shooter using alcohol swabs or GSR stubs after discharge of the various ammunition-firearm combinations, please see Appendix IX.

5.3.5.2 Efficiency for OGSR Analysis

With the exception of NG, no additional energetic compounds were detected in any of the simulated case specimens. This is in accordance with previous studies [56, 174] and supports the hypothesis that protocols for OGSR analysis should target stabilisers namely DPA, its derivatives and the centralites. Additional OGSR were detected in some specimens (Appendix VII; please note that Appendix VII presents the OGSR results obtained when specimen were collected using both, alcohol swabs and GSR stubs. The results using alcohol swabs were previously obtained and used in Chapter 4 in order to evaluate the developed and optimised UHPLC method for its case applicability). These compounds include DNGs, DEP and DBP. The relatively high amount of NG detected could be a result of the firearm-ammunition combinations used or the relatively high collection and extraction efficiencies of NG using either optimised Protocol 1 or 2. Using stubs resulted in generally higher OGSR quantities being detected, and also in the detection of some compounds such as DPA or N-nDPA in specimens, which were not detected using swabs. This is important for future research investigating models to link ammunition and unfired

smokeless powders using UHPLC results, which requires detailed smokeless powder and OGSR profiles.

Table 5-28 list the six most prevalent OGSR detected in the same three ammunition-firearm combinations as listed in Table 5-25. Example chromatograms of hand specimens collected using alcohol swabs (red line), GSR stubs (green line) and the associated unfired smokeless powder (blue line) of the ammunition-firearm combination Pistol (Glock, Austria)-40 Smith&Wesson (Winchester, USA) are shown in Figure 5-20.

Table 5-25: List of the six most prevalent organic gunshot residue (OGSR) compounds detected in the simulated case specimens (one shot, n = 3); ND = not detected. This table presents the results after collecting OGSR from the hands of a shooter after one discharge of three exemplary ammunition-firearm combination (n = 3). Collection was achieved using alcohol swabs and gunshot residue (GSR) stubs, which were liquid extracted using the optimised protocols (swabs: 5 min sonication at ambient temperatures using 5 mL methyl tertbutyl ether; GSR stubs: 5 min sonication at ambient temperatures using 5.5 mL acetone). The results of the remaining ammunition-firearm combinations are presented in Appendix VII.

	Collection device	**NG [ng]**	**DPA [ng]**	**2-NDPA [ng]**	**N-nDPA [ng]**	**MC [ng]**	**EC [ng]**
Pistol (USA) 9 mm Parabellum (Luger)	swabs	2.82 [ND-5.46]	ND	6.00 [4.12-7.40]	ND	ND	2.11 [ND-4.05]
	stubs	8.87 [6.65-14.46]	1.91 [1.47-2.18]	4.20 [ND-5.72]	1.59 [1.45-1.77]	ND	2.68 [2.19-2.66]
Pistol (USA) 22 LR High Velocity (Remington)	swabs	13.91 [ND-43.33]	ND	1.81 [0.74-3.05]	ND	ND	0.83 [0.66-1.45]
	stubs	7.97 [ND-14.26]	3.78 [1.82-7.12]	2.13 [1.84-2.19]	2.86 [2.05-4.03]	ND	3.07 [ND-5.14]
Glock (Austria) 40 Smith&Wesson (Winchester)	swabs	3.25 [ND-9.76]	ND	3.75 [0.91-5.73]	ND	0.87 [0.53-1.08]	2.54 [1.40-4.07]
	stubs	14.39 [ND-16.60]	1.51 [1.48-1.57]	2.16 [1.87-2.64]	2.35 [1.85-2.79]	1.38 [ND-2.12]	2.67 [2.27-2.99]

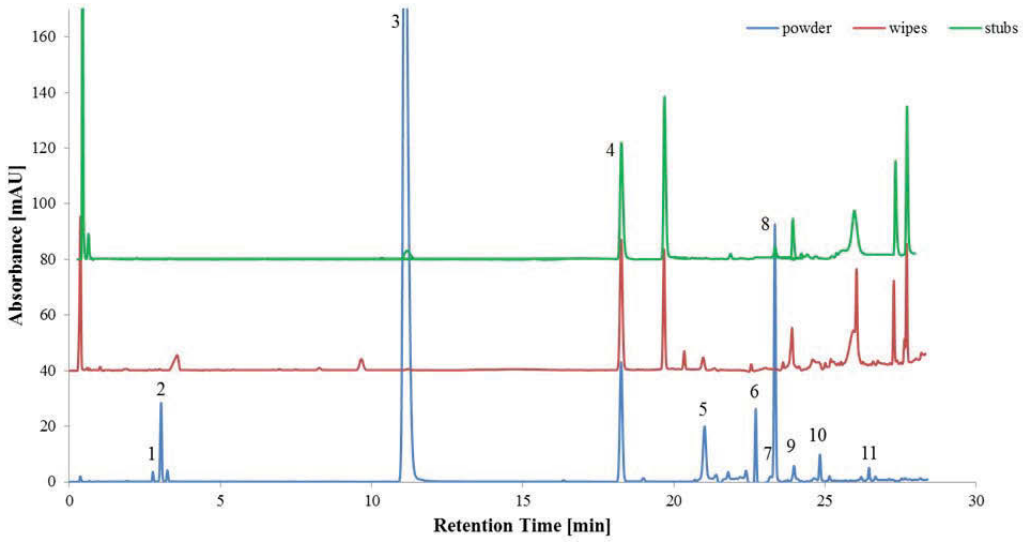

Figure 5-20: Overlayed example chromatograms of smokeless powder before shooting (40 S&W, Winchester, Australia; blue line) and the gunshot residues (GSR) collected from the hands of a shooter after one discharge using a 22 Glock pistol collected using alcohol wipes (red line) and GSR stubs (green line). Alcohol swabs and GSR stubs were liquid extracted following the optimised protocols (swabs: 5 min sonication at ambient temperatures using 5 mL methyl tertbutyl ether); GSR stubs: 5 min sonication at ambient temperatures using 5.5 mL acetone). 1 = 1,2-DNG, 2 = 1,3-DNG, 3 = NG, 4 = 2-naphthol (ISTD), 5 = DEP, 6 = MC, 7 = N-nDPA, 8 = DPA, 9 = 2-NDPA, 10 = EC, 11 = DBP.

Interestingly, the number of shots did not correlate with the amount of OGSR recovered. This has also been found by a previous study, which explained it as a result of the inherent stochastic nature of the deposition and not a result of the extraction protocol [127]. Other reasons could be that OGSR deposited on the hands might be removed with the next shot, or that the difference of OGSR between one and three shots is relatively minor. The concentrations of OGSR detected in this study are generally higher than those detected in a previously reported study [56]. This could be a result of different firearms and ammunition, extracting not half, but the total collection device, or the detailed optimisation of the protocol. Overall, subjecting GSR stubs to SEM-EDX followed by liquid extraction was the best of the tested processes for recovery and analysis OGSR and IGSR and its feasibility for casework application has been demonstrated in a simulated case scenario.

In a forensic framework, further research is required in order to allow valuable and accurate interpretation of the analytical results obtained. This should

include studies about OGSR transfer and background, and the distribution of OGSR on hands. The last point might provide information about the possibility to distinguish between a shooter and bystander. This corresponds to a significant body of work that falls beyond the scope of the present research and is currently being investigated at the University of Technology Sydney through complementary doctoral studies by Matthieu Maitre.

It is important to consider that although specimens were collected directly after discharge and with only one collection device per hands, OGSR amounts were relatively low (low ng range). It is therefore reasonable to assume that in real case specimens OGSR amounts would be in even lower concentrations due to more elapsed time after discharge and other loss mechanisms such as absorption into the skin. Therefore, more research focusing on pre-concentration techniques for OGSR is needed.

5.4 Conclusion

Three collection protocols for the combined collection and analysis of OGSR and IGSR were developed and optimised for the extraction of a wide range of organic target compounds. Liquid extraction was found to be superior to SPME in its extraction efficiency; the latter was found to be ineffective.

The collection efficiency of stubs was significantly superior to swabs for both IGSR and OGSR on skin. The analysis of specimens collected at a shooting range confirmed that collecting OGSR and IGSR on GSR stubs followed by SEM-EDX and liquid extraction was not only a practical method for combined OGSR and IGSR detection but the best of the tested methods.

The recommended protocol consists of collection using GSR stubs, SEM-EDX analysis then liquid extraction using acetone for 5 min at RT and pre-concentration of the extract by drying and reconstituting it in a smaller amount of solvent prior to UHPLC analysis. This protocol has the potential to greatly increase the probative value of GSR in an investigation. For example, if a single stub were to show evidence of primer-derived particles (even double and single element particles) together with evidence of "ammunition-specific" compounds such as N-nDPA or EC then the findings would be much stronger than either evidence in isolation.

Chapter 6: Stability of Smokeless Powder Compounds on Collection Devices

Chapter 6: STABILITY OF SMOKELESS POWDER COMPOUNDS ON COLLECTION DEVICES

6.1 Background

Numerous factors influence the probability of detecting GSR. These include the time since discharge, environmental conditions during discharge, the weapon and ammunition used, collection efficiency and instrument limitations. However, in an operational laboratory it is likely that specimens will require a period of storage which could also influence the detection of OGSR. Very few studies have investigated the influence of storage conditions on the degradation of smokeless powder compounds. A study by Twibell et al. investigated the stability of NG at different concentrations in eight solvents including acetone, which was determined as superior extraction solvent from GSR stubs in Chapter 5 [54]. Mean rates of loss were between 1 %/day (for 8 ng/µL NG) and 3 %/day (for 0.08 ng/µL NG). NG completely disappeared in aqueous solutions, attributed to the presence and growth of microorganisms. Therefore, the addition of preservatives such as sodium azide or sodium metabisulfite was suggested [54].

In order to provide a recommendation for optimal specimen handling and storage, more information is required on the influence of storage conditions and durations on compounds present in smokeless powders degradation. To evaluate the impact of storage duration on collected specimens, a time study on the degradation of spiked OGSR on two collection devices, GSR stubs and swabs, was conducted.

6.2 Materials and Methods

6.2.1 *Reagents and Standards*

The target compounds were identical to those previously listed in 4.2.1 and 5.2.1, namely resorcinol, RDX, HMX, tetryl, TNT, 2,4-DNT, 4-A-2,6-DNT, NG, TNB, m-DNB, DPA, N-nDPA, and EC. PETN and DBP were excluded as interferences for these compounds were previously found. As in Chapter 4 and Chapter 5, 2-naphthol was employed as ISTD. UP grade water was obtained from a Sartorius 611 water purification system. MTBE, acetone and ACN were purchased from ChemSupply Pty Ltd, Gillman, SA, Australia.

6.2.2 *Instruments and Conditions*

The instrument parameters were identical to those previously optimised and validated Chapter 4 and are summarised in section 4.2.2.1 and 5.2.2.1.

6.2.3 *Experimental Design*

Swabs and GSR stubs were spiked with 10 ng (10 µL of a 1 ppm mixed standard solution) of the target compounds and left to dry. Although spiking experiments do not fully represent the conditions in a real case scenario, this simplification was used in order to allow for sample standardisation and improved repeatability [202]. Following drying, spiked swabs and stubs as well as blanks were stored in a refrigerator at 4 ºC until extracted. On various days after the initial spiking, samples (in triplicates) and blanks were extracted following the previously optimised and presented extraction protocols in 5.2.3.5 (swabs) and 5.2.4.4 (stubs). The swabs and stubs were extracted 0, 1, 2, 4, 8, 15, 22, 29, 40, 49, and 63 days after being spiked.

6.2.4 *Data Analysis and Definitions*

The recovery was calculated as percentage of the originally spiked amount. For the overall degradation, the difference was calculated between the averages of the first two and the last two days. This adjustment was used in order to avoid incorrect degradation representation due to an outlier on the first or last day. Compounds were classified as stable when the mean of the degradation on stubs and swabs was less than 15 %.

6.3 Results and Discussion

The results collected in this study indicated that the degradation patters for the target compounds were quite varied, although some general trends can be observed in Figure 6-1.

Firstly, all compounds, with the exception of 2,4-DNT on swabs, undergo the highest degree of degradation during the first week of storage. Most of the recorded degradation occurred during the first four days. For example EC showed degraded 88 % of the overall degradation during the first four days, TNT 77 %.

Considering the proposed specimen collection and analysis procedures in Chapter 5, this trend is more problematic when using GSR stubs than alcohol swabs (Protocol 2, 5.2.4). In the protocol involving stubs, SEM-EDX analysis precedes liquid extraction and OGSR analysis by UHPLC. Depending on the operational demands of the laboratory, a lengthy period of storage may be required if selecting this analytical sequence. It is therefore possible that many of the target OGSR, especially NG, N-nDPA, DPA, and EC, might have degraded to below their respective LOD. During the protocol involving alcohol swabs (Protocol 1, 5.2.3),

wipes can be directly liquid extracted after collection. Therefore, the high degree of degradation during the first few days is less problematic.

Moreover, for most compounds apart from EC (after day 40), and TNT (after day 49), recoveries from stubs were higher than for swabs. This result is attributable to the collection device material and not the extraction process as liquid extraction recoveries were found to be similar using the optimised conditions involving swabs and stubs (Chapter 5, Table 5-28). The cotton fibre of the alcohol swabs might form stronger interactions with the target compounds over time than the carbon adhesive on the stubs. It is also possible that the cotton material reacts with the compounds promoting their degradation. The SDs between swabs and stubs were comparable (Table 6-1).

Compounds commonly present in OGSR such as NG, DPA, or EC showed a high degree of degradation overall with 16, 49 and 70 % for DPA, NG, and EC respectively from GSR stubs and 75, 33 and 52 % for DPA, NG, and EC from swabs respectively from swabs compared to samples directly extracted after spiking. Since these are commonly targeted OGSR, preceding SEM-EDX of the specimens or longer storage durations could cause degradation of the compounds.

In contrast, RDX, HMX, TNB, m-DNB, resorcinol, 4-A-2,6-DNT, N-nDPA, and 2,4-DNT were considered stable with the mean degradation (from stubs and swabs) less than 15 % over the 63 days study. Interestingly, this covers most of the energetic compounds tested and indicates that these compounds are more stable under these storage conditions.

Overall, relatively high % RSD were found in the triplicate measurements taken each sampling day (Table 6-1). In addition to the variations obtained during sample preparation (around 15 % RSD, Chapter 5), differences in storage conditions

such as light influence, opening refrigerator doors, proper closing of the lids, could lead to deviations in % recoveries and could help explain the large variances. Table 6-1 displays the overall degradation [%] of the individual compounds over the 63 days, the SDs and whether a compound was classified as stable or not.

Table 6-1: Degradation [%] and mean standard deviations (SDs) [%] (n = 3) of the target compounds over 63 days extracted using the optimised protocol (Chapter 5) from spiked (10 ng) gunshot residue stubs and swabs. Stable compounds are defined as compounds degrading less than 15 % on GSR stubs and alcohol swabs.

Compound	Stubs			Swabs		
	Stable	Degradation [%]	Mean SD [%]	Stable	Degradation [%]	Mean SD [%]
resorcinol	✓	13	10.3	✓	10	8.92
RDX	✓	8	9.23	✓	0	7.15
HMX	✓	7	11.2	✓	0	7.44
TNB	×	17	10.7	✓	7	6.41
m-DNB	✓	-9	9.70	✓	4	2.72
NG	×	49	10.4	×	33	15.7
tetryl	×	51	5.64	✓	0	5.88
TNT	×	31	8.50	×	16	5.86
4-A-2,6-DNT	✓	4	9.00	✓	13	2.33
2,4-DNT	✓	-3	4.73	×	20	2.86
N-nDPA	✓	13	15.4	×	27	10.3
DPA	×	16	14.9	×	75	11.7
EC	×	70	7.87	×	52	7.71

One of the most relevant compounds in the context of firearm related events is NG and it is worth noting that the compound could not be detected on any swabs

after day 15. This is in agreement with previous studies that reported the relatively rapid degradation of NG due to its instability [54, 203].

Another interesting observation is the increased recovery of compounds including m-DNB (on GSR stubs), 4-A-2,6-DNT (on GSR stubs), and 2,4-DNT (on GSR stubs and swabs). These compounds are all derivatives of possible degradation products formed by other compounds present on the spiked collection devices. The initial decrease followed by an increase of 2,4-DNT could be attributable to the degradation of TNT forming a di-nitrated analogue. Similar scenarios might occur for m-DNB (TNB degradation), 4-A-2,6-DNT (TNT degradation and amination) and N-nDPA (a derivative of DPA). The concentration of N-nDPA decreases during the first few days and stabilises around day 20 (Figure 6-1 k), which could be a result of a nitrosation of DPA involving the degradation products of NG.

As previously stated in Chapter 1 (section 1.1) nitro esters present in smokeless powders (NC in single base powder; NC and NG and double base powder; and NC, NG and NGU in triple base powder) can deteriorate and release NO and NO_2 during the aging process or when exposed to elevated temperatures [16]. As free NO and NO_2 can further cause autocatalytic degradation of the smokeless powders, stabilisers such as DPA and EC are added in order to scavenge this products. The stabilisers become nitrated or nitrosated themselves, which can occur on different positions on the molecules and therefore result in the formation of various products [16]. One classical explanation of the nitration of DPA for instance is based on the rearrangement of N-nitrosoamine to a C-nitroso compound (Fisher-Hepp reaction), which then undergoes oxidation [204]. Another explanation is that the only nitrosation and principal reaction DPA is undergoing is N-nitrosation. This can be followed by denitrosation and direct nitration to form mononitro derivates

[16, 205]. Schemes of the possible nitration and nitrosation mechanism of DPA have previously been published [16, 205].

The formation of derivates can allow for the possibility of detecting compounds that are not present in the associated unfired smokeless powder, which might complicate the possibility to link OGSR to unfired smokeless powders based on their OGSR profile. However, further research investigating the degradation patter of OGSR is needed to either support or reject the proposed theory. Additionally, a better understanding of the degradation of smokeless powder and OGSR could allow the identification of degradation products that are forming in the powder or OGSR specimens over time and are not originally in the unfired smokeless powder. These compounds could be characteristic for smokeless powders/OGSR and be used for their identification.

Since spiking standard solution on the swabs or GSR stubs might only be a simplified approach and not represent real case work conditions, future studies should involve more realistic sample matrices on the collection devices. This could involve the usage of simple custom devices that can be mounted on the muzzle of the firearm and allow for collection of released particles or raw propellant particles that can be deposited on the alcohol swab or GSR stubs.

Individual plots for the % recovery for each compound from swabs and GSR stubs over time are shown in Figures 6-1.

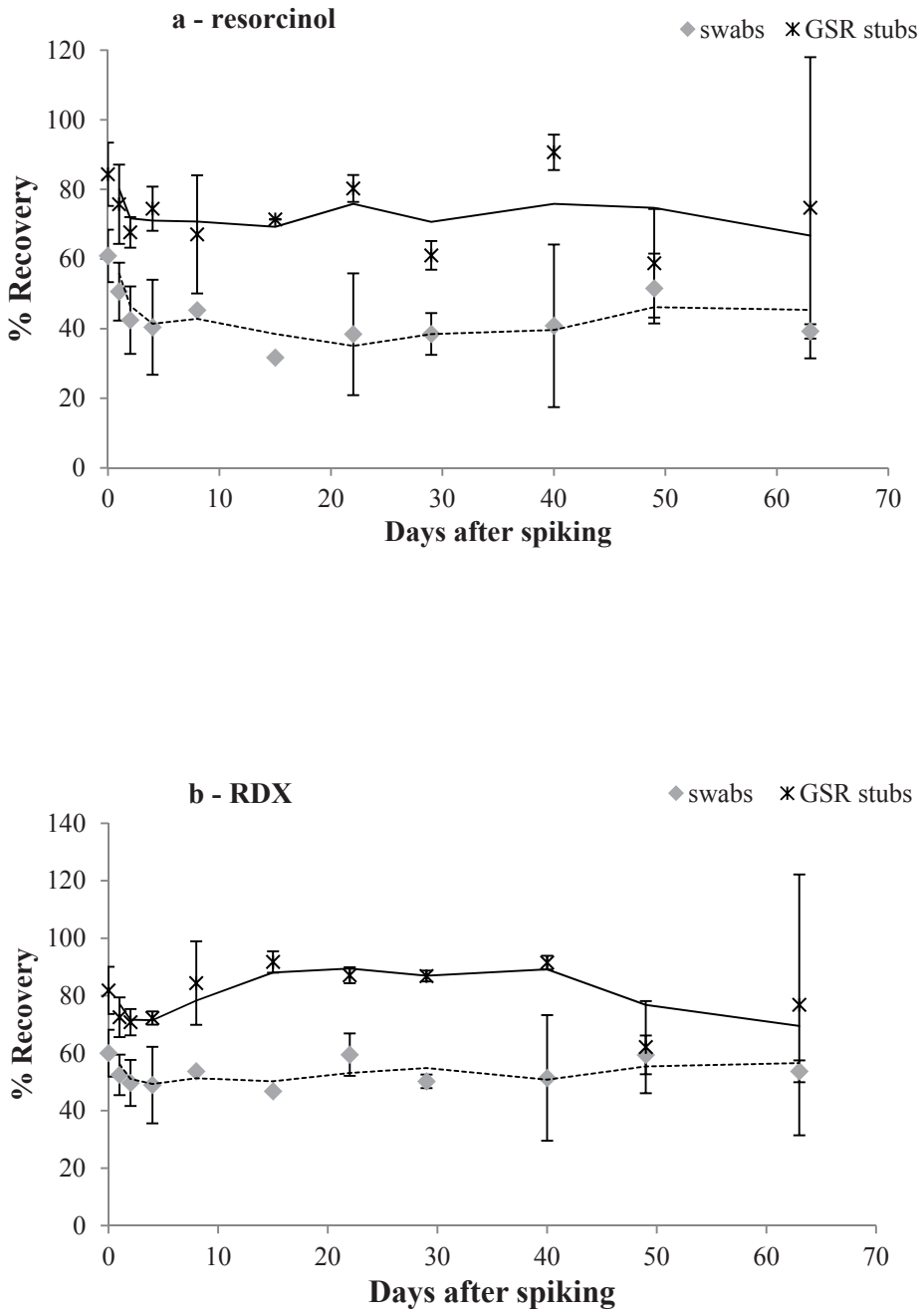

Figure 6-1: Percentage recoveries of the different target compounds, namely resorcinol (a), RDX (b), HMX (c), TNB (d), m-DNB (e), NG (f), tetryl (g), TNT (h), 4-A-2,6-DNT (i), 2,4-DNT (j), N-nDPA (k), DPA (l), and EC (m) extracted using the optimised protocols (Chapter 5) from spiked swabs and stubs on several days after initial spiking. The days involved day 0, 1, 2, 4, 8, 15, 22, 29, 40, 49, 63. The spike amount of each compound was 10 ng. Error bars represent standard deviations (n = 3).

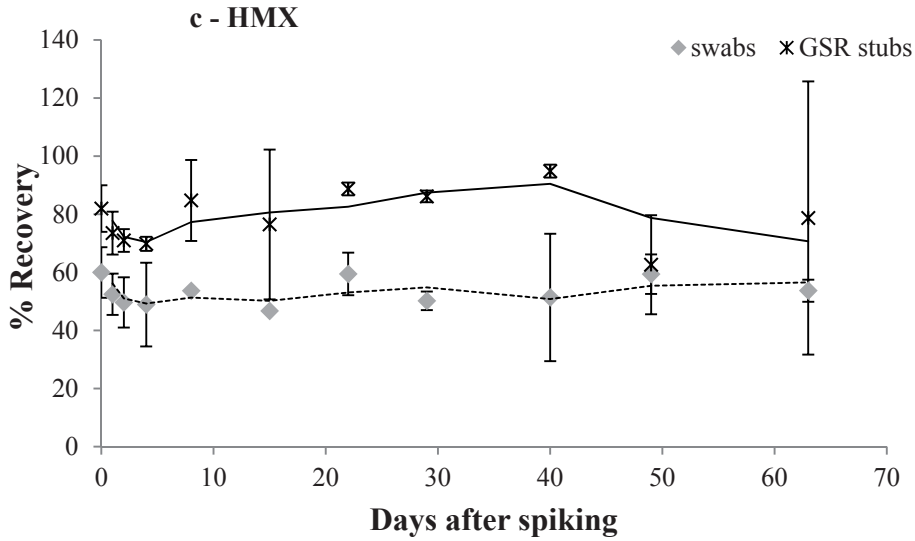

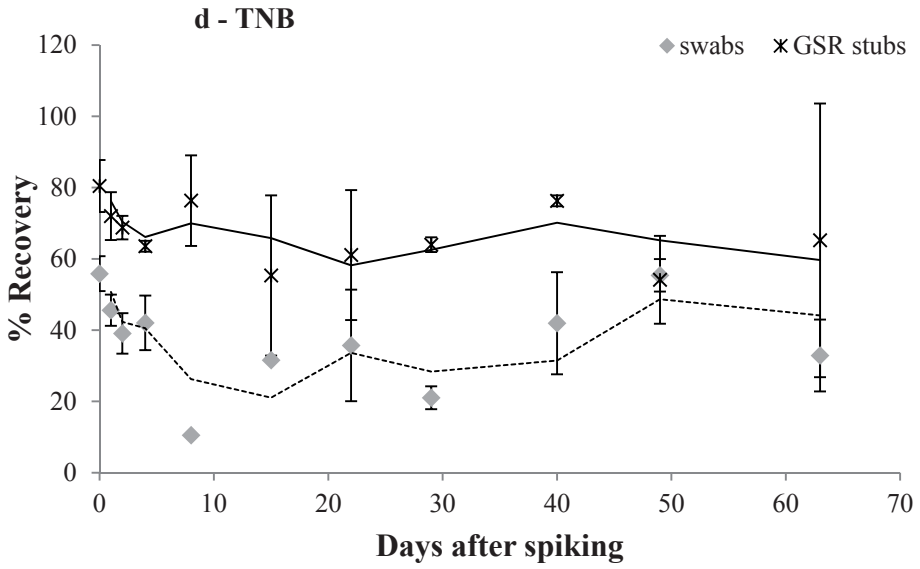

Figure 6-1 continued: Percentage recoveries of the different target compounds, namely resorcinol (a), RDX (b), HMX (c), TNB (d), m-DNB (e), NG (f), tetryl (g), TNT (h), 4-A-2,6-DNT (i), 2,4-DNT (j), N-nDPA (k), DPA (l), and EC (m) extracted using the optimised protocols (Chapter 5) from spiked swabs and stubs on several days after initial spiking. The days involved day 0, 1, 2, 4, 8, 15, 22, 29, 40, 49, 63. The spike amount of each compound was 10 ng. Error bars represent standard deviations (n = 3).

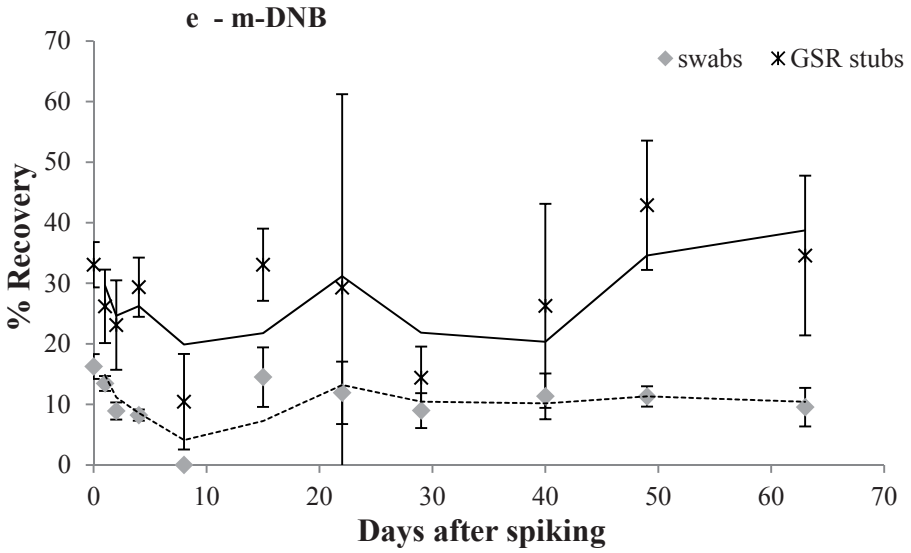

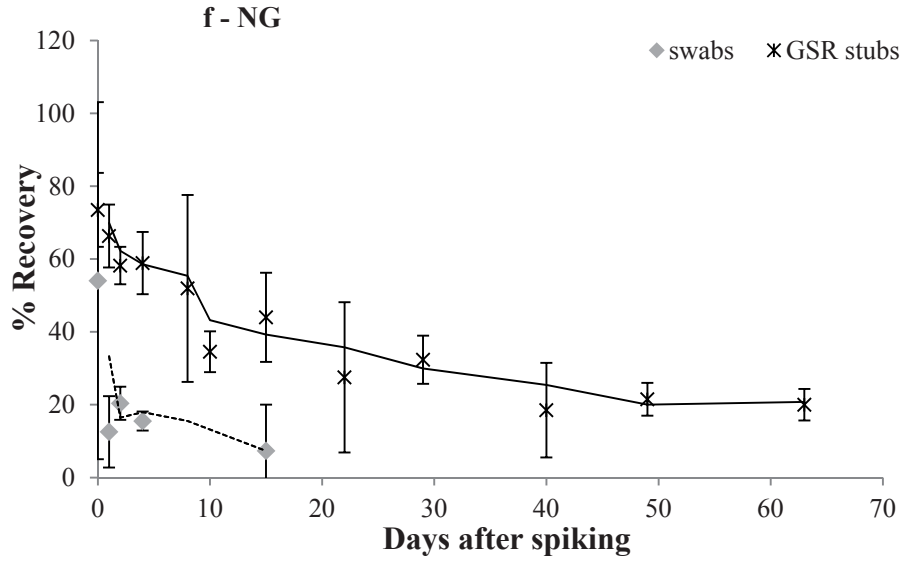

Figure 6-1 continued: Percentage recoveries of the different target compounds, namely resorcinol (a), RDX (b), HMX (c), TNB (d), m-DNB (e), NG (f), tetryl (g), TNT (h), 4-A-2,6-DNT (i), 2,4-DNT (j), N-nDPA (k), DPA (l), and EC (m) extracted using the optimised protocols (Chapter 5) from spiked swabs and stubs on several days after initial spiking. The days involved day 0, 1, 2, 4, 8, 15, 22, 29, 40, 49, 63. The spike amount of each compound was 10 ng. Error bars represent standard deviations (n = 3).

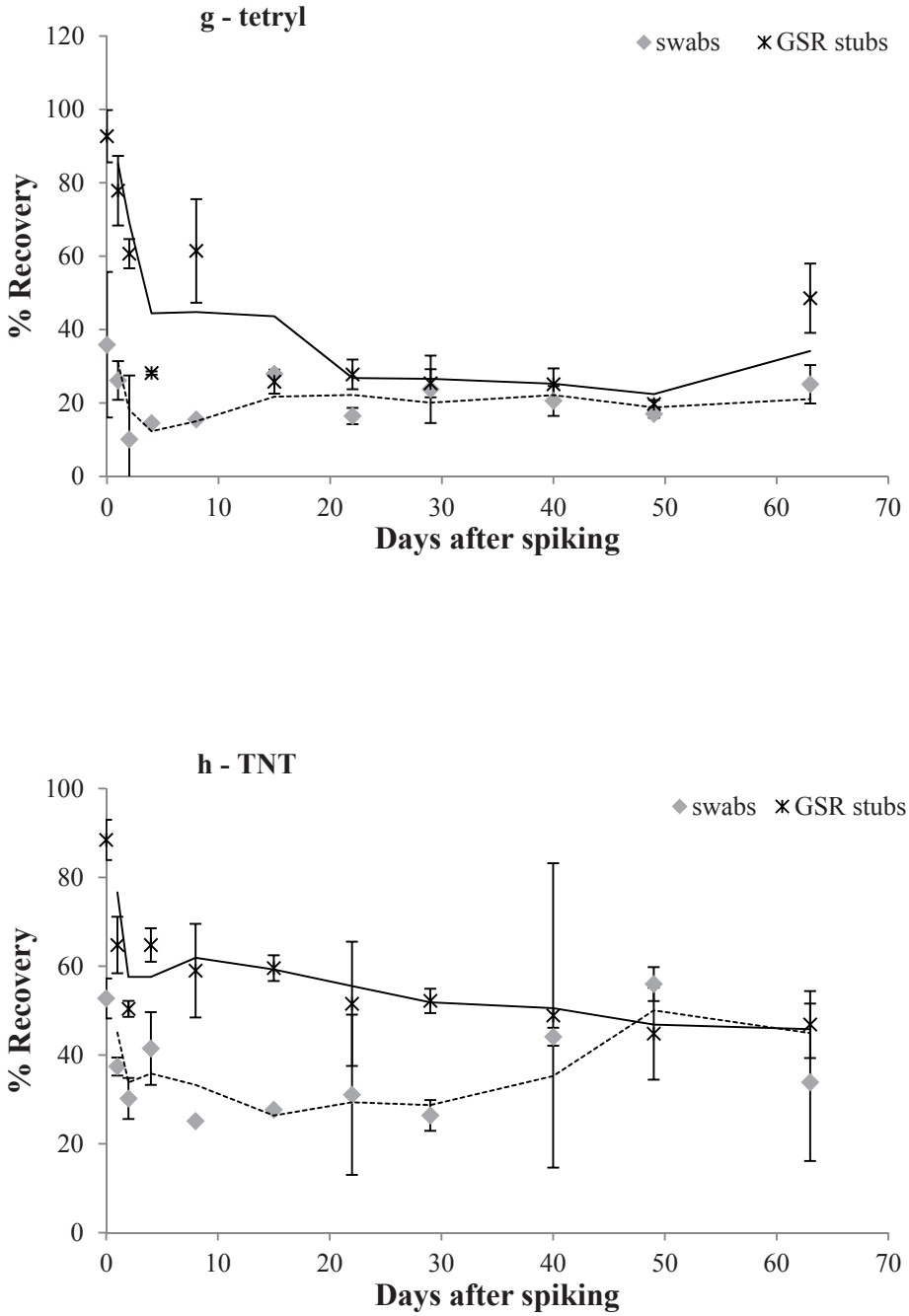

Figure 6-1 continued: Percentage recoveries of the different target compounds, namely resorcinol (a), RDX (b), HMX (c), TNB (d), m-DNB (e), NG (f), tetryl (g), TNT (h), 4-A-2,6-DNT (i), 2,4-DNT (j), N-nDPA (k), DPA (l), and EC (m) extracted using the optimised protocols (Chapter 5) from spiked swabs and stubs on several days after initial spiking. The days involved day 0, 1, 2, 4, 8, 15, 22, 29, 40, 49, 63. The spike amount of each compound was 10 ng. Error bars represent standard deviations (n = 3).

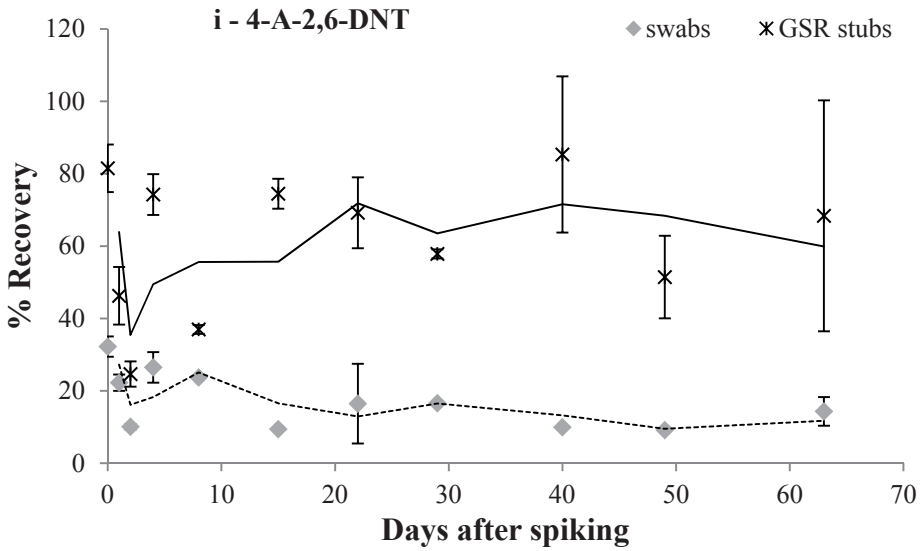

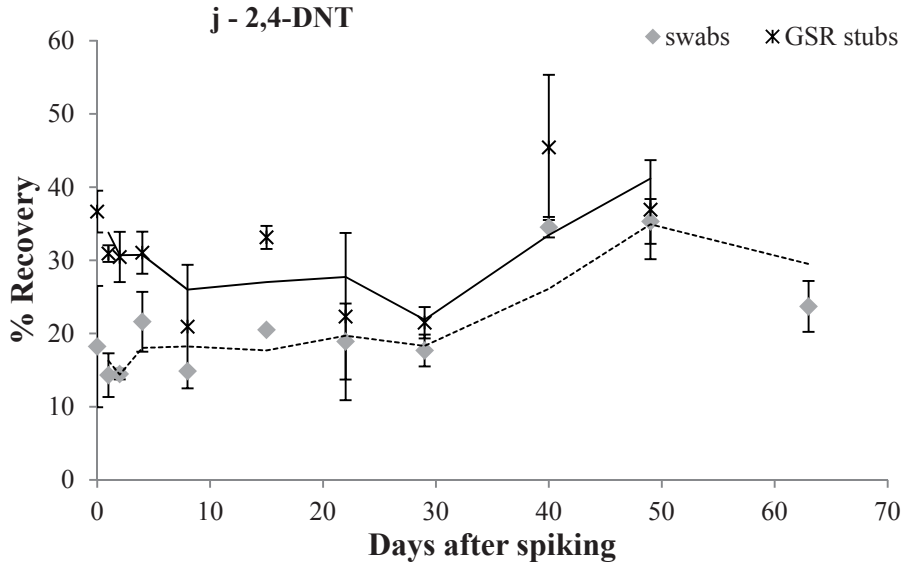

Figure 6-1 continued: Percentage recoveries of the different target compounds, namely resorcinol (a), RDX (b), HMX (c), TNB (d), m-DNB (e), NG (f), tetryl (g), TNT (h), 4-A-2,6-DNT (i), 2,4-DNT (j), N-nDPA (k), DPA (l), and EC (m) extracted using the optimised protocols (Chapter 5) from spiked swabs and stubs on several days after initial spiking. The days involved day 0, 1, 2, 4, 8, 15, 22, 29, 40, 49, 63. The spike amount of each compound was 10 ng. Error bars represent standard deviations (n = 3).

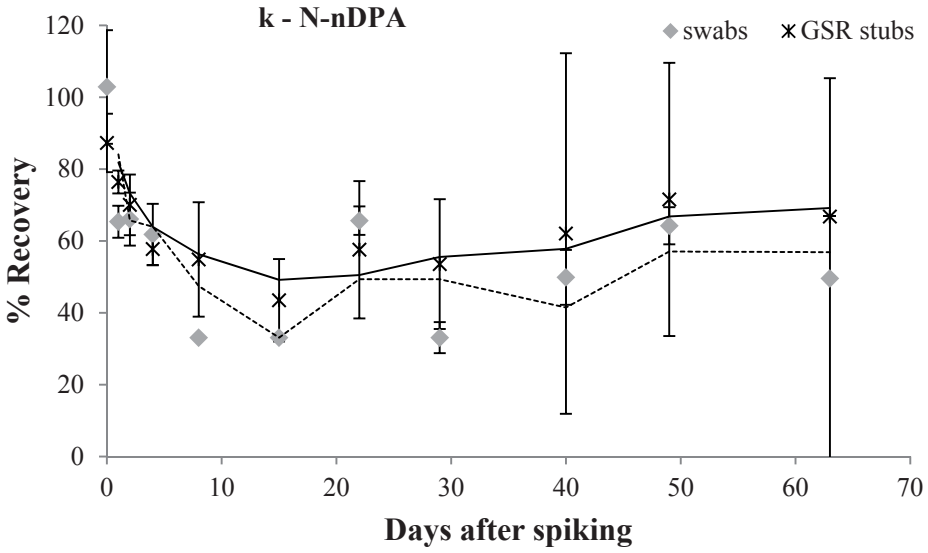

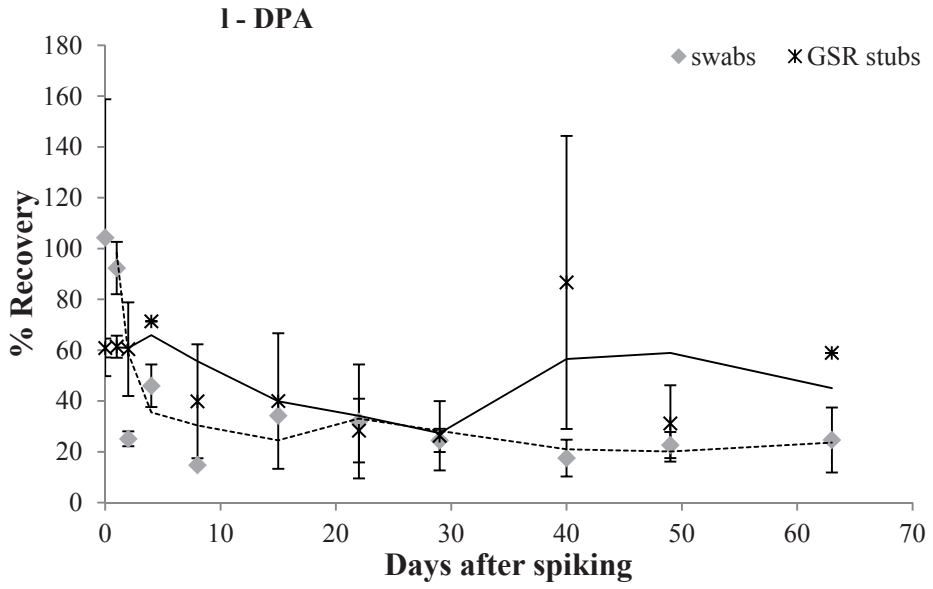

Figure 6-1 continued: Percentage recoveries of the different target compounds, namely resorcinol (a), RDX (b), HMX (c), TNB (d), m-DNB (e), NG (f), tetryl (g), TNT (h), 4-A-2,6-DNT (i), 2,4-DNT (j), N-nDPA (k), DPA (l), and EC (m) extracted using the optimised protocols (Chapter 5) from spiked swabs and stubs on several days after initial spiking. The days involved day 0, 1, 2, 4, 8, 15, 22, 29, 40, 49, 63. The spike amount of each compound was 10 ng. Error bars represent standard deviations (n = 3).

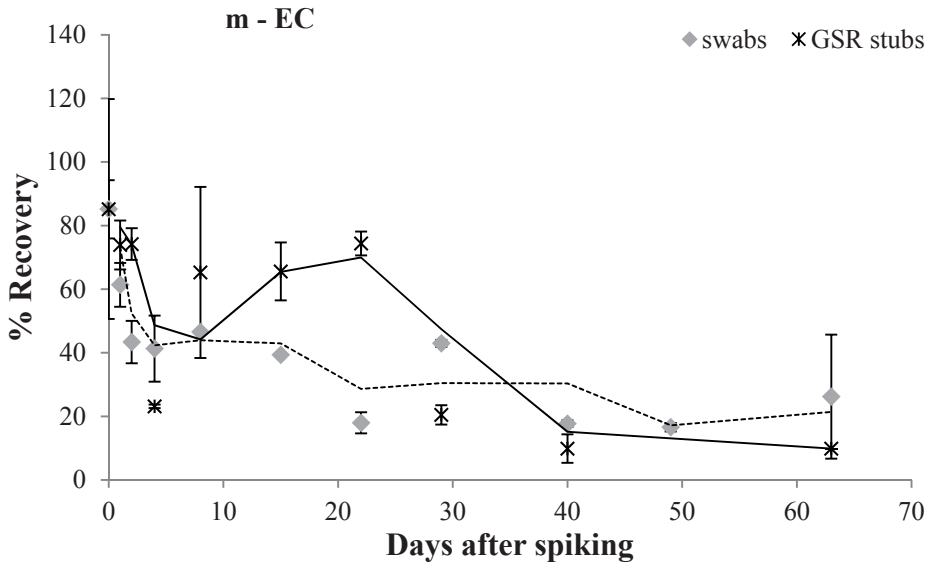

Figure 6-1 continued: continued: Percentage recoveries of the different target compounds, namely resorcinol (a), RDX (b), HMX (c), TNB (d), m-DNB (e), NG (f), tetryl (g), TNT (h), 4-A-2,6-DNT (i), 2,4-DNT (j), N-nDPA (k), DPA (l), and EC (m) extracted using the optimised protocols (Chapter 5) from spiked swabs and stubs on several days after initial spiking. The days involved day 0, 1, 2, 4, 8, 15, 22, 29, 40, 49, 63. The spike amount of each compound was 10 ng. Error bars represent standard deviations (n = 3).

6.4 Conclusion

An evaluation of storage on the stability of OGSR highlighted a number of interesting trends. It was observed that the highest degree of degradation of the target OGSR occurred during the first four days. This has significant implications on the collection protocols proposed in Chapter 5 in that OGSR collected on GSR stubs may partially degrade during initial IGSR analysis and preliminary storage. Commonly found OGSR such as NG, DPA, and EC showed relatively high overall degradation in contrast to energetic compounds more commonly found in explosive devices (RDX, HMX, TNB). It was proposed that some compounds such as TNT or DPA might form derivatives and degradation products that could potentially impede the approach to link unfired ammunition to OSGR based on their profile.

Chapter 7: Conclusions and Future Research

Chapter 7: CONCLUSIONS AND FUTURE RESEARCH

The work presented in this thesis provides a rounded approach to GSR investigations as it addresses a variety of aspects of GSR investigation including screening, collection and analysis, specimen pre-concentration, and finally the influence of storage on the stability of OGSR compounds.

There is a strong need for a sensitive, selective and portable screening technique for compounds in OGSR. Advantages for case work include the possibility to screen in-field, the rapid analysis time and reducing the number of specimens to be analysed. This should be achieved without affecting possible succeeding confirmatory analysis for OGSR and IGSR analysis using SEM-EDX. A screening technique was developed based on fluorescence quenching of pyrene on microfluidic decives, μPADs. Explosive compounds potentially present in OGSR quench the fluorescence of deposited pyrene, which is a non-destructive process and allows for subsequent confirmatory OGSR analysis. An in-house prototype instrument was constructed which produces a visual signal when the quenching process is detected. No false-negatives were observed indicating a high selectivity of the developed screening technique. Furthermore, it showed LODs in the ng range suggesting its applicability to OGSR screening on people who either shot a weapon or handled explosives.

Although the developed screening technique provided promising results for explosive screening, specimens collected at a shooting range failed to produce an alarm. In Chapter 4 and 5 no energetic compounds were found in any of the hand specimens taken from a shooter analysed using UHPLC-UV/MS. Therefore, it is reasonable to assume that the negative results were due to the absence of any of the

target explosives in the simulated case specimens. These results are in agreement with previous studies [6, 175] and confirm the need to focus on the additives in smokeless powders when targeting OGSR, namely DPA and its derivatives, EC and MC. Although this might conclude that the value of the developed screening technique is limited for OGSR, it provided promising results for explosive screening in an environmental and forensic perspective and could find application in a wide range of fields.

Future research into screening techniques should focus on the additives in smokeless powders, particularly the stabilisers. Important factors to be considered when developing such a screening technique are to ensure it is non-destructive and – if specimens have to be collected - collected using a collection device that allows for subsequent confirmatory OGSR analysis and IGSR analysis using SEM-EDX as achieved here. The non-destructive nature is important to preserve the deposition pattern which can provide useful information for event reconstruction and differentiation of GSR and GSR-like material. Performing such an in-field test could not only immediately determine whether it makes sense to proceed with time and labour consuming sample preparation and laboratory based analysis, but also whether the GSR trace is worth considering in the investigation of a firearm related event. IMS has recently been proposed as screening method and appears promising as it can target stabilisers present in OGSR [206]. However, it is a destructive technique and it still needs to be defined how IMS could be incorporated in current GSR SOPs without influencing subsequent OGSR and IGSR analysis.

The amounts of detected OGSR in specimens collected directly after discharge and under relatively controlled conditions are commonly relatively low. It is therefore reasonable to assume that the anticipated amounts in case specimens

would be even lower. Thus, a pre-concentration technique may be required for real case specimens. Commonly, SPE is applied for pre-concentration of samples/specimens containing trace amounts of the compounds of interest.

A proof-of-concept study using a robotic on-line SPE instrument robot, RapidFire®, coupled to a QQQ-MS was conducted. The detection of various compounds present in OGSR was achieved in 8 sec using the optimised method. Further optimisations in regards to cartridge type and sample preparation are expected to lower the current ng LODs and LOQs to achieve the necessary sensitivities required for real case application. Additionally, the possibility to pre-concentrate specimens by loading multiple injections on one cartridge before elution should also be further explored. The extremely short analysis time makes this an attractive approach for specimen screening to reduce the specimen number undergoing more timely UHPLC-UV/MS analysis.

Following a positive screening result, an analytical method for the detection of a wide range of compounds potentially present in OGSR that can be sequenced with IGSR analysis is required. Operation laboratories often lack access to MS instrumentation and it was recommended that a UHPLC method with UV detection would be more useful. The method developed was the first involving an application of ANNs in the field of GSR analysis. The final gradient program is able to separate 32 potential OGSR compounds in less than 27 min. The method was fully validated and tested using unfired smokeless powders and specimens collected at a firing range. The sensitivity and selectivity of the developed method proved sufficient for case work application and allowed for the characterisation of all smokeless powders based on their composition. Additionally, a MS/MS method using QQQ-MS was

developed to confirm the presence of OGSR detected in specimens previously analysed using the UHPLC-UV method.

During the first 10 min of the developed method, mostly energetic compounds potentially present in OGSR are targeted. Considering that in none of the tested simulated case specimens taken at a shooting explosive compounds were detected, future research could focus on further optimising the method by reducing the run time. This could be achieved by employing a higher initial MeOH concentration, shortening the isocratic step at the beginning of the method, or increasing the gradient.

To facilitate the analysis of both OGSR and IGSR during GSR investigations, careful integration of the developed UHPLC method was investigated by developing and optimising a combined collection protocol for IGSR and OGSR. While organic traces are often collected using cotton swabs, it is common procedure to collect IGSR using double sided adhesive on GSR stubs.

Three protocols for the combined collection and specimen preparation of OGSR and IGSR using alcohol swabs and GSR stubs were developed and the two superior protocols in regards to extraction efficiencies optimised. The two optimised protocols were compared and further evaluated using specimens collected from the hands of a shooter at a firing range. 14 different firearm-ammunition combinations were chosen and specimens collected after a single discharge and following three discharges using both swabs and GSR stubs. The specimens were processed using the developed protocols, with IGSR and OGSR results compared. GSR stubs showed a superior collection efficiency for OGSR in that the amount of OGSR compounds and IGSR particles detected on the stub specimens was generally higher.

Interestingly, the amount of OGSR did not correlate with the number of shots fired whereas the number of IGSR particles detected generally did.

Overall, OGSR compounds were detected in the low ng range. Even though the conditions at the firing range were relatively controlled, i.e. no wind, ambient temperature, the variations between shootings using the same firearm and ammunition were relatively large indicating that each shooting event can generate different amounts of OGSR. The variations were so large that in some triplicate shootings, no OGSR were detected for one discharge, while for the next one OGSR were detected. These observed variations could potentially complicate the attempt to link OGSR to the associated unfired smokeless powders based on the comparison of unfired and fired powder composition. The fact that in some specimens no OGSR were detected could be either a result of no OGSR being present on the hands of the shooter, human errors during the specimen preparation, or instrument limitations.

It is important to acknowledge, that although the developed collection protocol and analytical technique were able to detect OGSR in some of the simulated case specimens, still much work needs to be done from a forensic perspective. This should for example include large background studies to evaluate the baseline levels of GSR in the general populations. Furthermore, persistence studies should be conducted estimating the time frame in which OGSR might still be detectable on the hands of a shooter. An overall view of the presence and persistence of OGSR can evaluate the evidential value of OGSR for forensic purposes and thus the value of the developed SOP for casework involving the actual or suspected use of firearms.

Finally, the influence of storage durations up to two months was investigated. This is important considering that demands on operational laboratories

will typically dictate a storage period prior to analysis by UHPLC-UV/MS and SEM-EDX. The bulk of the degradation process was found to occur during the first four days of storage. Stabilisers appeared to degrade more rapidly over time, while explosive compounds were found to be relatively stable. This is a disadvantageous trend for the detection of OGSR considering that the most commonly detected compounds are stabilisers. Interestingly, it was found that some compounds including 2,4-DNT, 4-A-2,4-DNT, DNB, and N-nDPA stabilised or even increased in their concentration after the initial decrease. It was hypothesised that the degradation of DPA, TNT and TNB could contribute to the increased concentration of the selected compounds. This is highly relevant in a forensic perspective as it might not only complicate any attempts to link OGSR to associated unfired smokeless powders based on their profile, but also identify new compounds that could be targeted for OGSR detection formed during the storage of specimens.

Further research should investigate the influence on various storage conditions such as temperature, light exposure on the degradation of OGSR. Furthermore, the proposed theory of DPA, TNT, and TNB forming degradation products should be tested, degradation products identified and their use as target compounds evaluated.

Overall, the research presented in this thesis targeted multiple gaps present in current SOPs for GSR investigations. A full SOP covering specimen collection and analysis has been proposed which integrates OGSR analysis into current GSR protocols. This addresses limitations originating from the increasing use of LF and HMF ammunitions and can potentially strengthen the evidential value of current GSR investigations in that more information can be retrieved from the combined OGSR and IGSR analysis. However, an opportunity remains to fully evaluate the

impact of GSR traces through extensive studies into transfer, persistence and background.

REFERENCES

1. N. Ralston and G. Kwek, *100 shootings and counting: Merrylands tops drive-by list*. The Sydney Morning Herald, **issued 11.09.2012**; Available from: http://www.smh.com.au/nsw/100-shootings-and-counting-merrylands-tops-driveby-list-20120911-25psc.html; [*cited 20.10.2012*].

2. *Is australia starring down the barrel of a gun crisis*. news.com.au, **issued 02.08.2015**; Available from: http://www.news.com.au/national/is-australia-staring-down-the-barrel-of-a-gun-crisis/story-fncynjr2-1226690018325; [*cited 04.12.2015*].

3. G. Lekakis, *Spike in handgun crimes reveals nation's secret problem*. The Newdaily, **issued 10.11.2015**; Available from: http://thenewdaily.com.au/news/2015/11/10/australias-secret-gun-problem-exposed/; [*cited 04.12.2015*].

4. H.-h. Meng and B. Caddy, *Gunshot residue analysis - a review.* Journal of Forensic Sciences, **1997**. ***42***(4): p. 553-570.

5. V. J. M. Di Maio,in *Gunshot wounds - practical aspects of firearms, ballistics, and forensic techniques*. **1999**, Boca Raton: CRC Press: Florida.

6. D. Laza, B. Nys, J. D. Kinder, A. Kirsch-De Mesmaeker and C. Moucheron, *Development of a quantitative lc-ms/ms method for the analysis of common propellant powder stabilizers in gunshot residue*.* Journal of Forensic Sciences, **2007**. ***52***(4): p. 842-850. DOI: 10.1111/j.1556-4029.2007.00490.x.

7. L. Fojtášek, J. Vacínová, P. Kolář and M. Kotrlý, *Distribution of gsr particles in the surroundings of shooting pistol.* Forensic Science International, **2003**. ***132***(2): p. 99-105. DOI: 10.1016/s0379-0738(03)00018-5.

8. J. Bueno and I. K. Lednev, *Raman microspectroscopy chemical mapping and chemometric classification for the identification of gunshot residue on adhesive tape.* Anal. Bioanal. Chem., **2014**. ***406***: p. 4595-4599.

9. O. Dalby, D. Butler and J. W. Birkett, *Analysis of gunshot residue and associated materials—a review.* Journal of Forensic Sciences, **2010**. ***55***(4): p. 924-943. DOI: 10.1111/j.1556-4029.2010.01370.x.

10. H. Meng and B. Caddy, *Fluorescence detection of ethyl centralite in gunshot residues.* Journal of Forensic Sciences, **1994**. ***39***(5): p. 1215-1226.

11. W. A. MacCrehan, K. D. Smith and W. F. Rowe, *Sampling protocols for the detection of smokeless powder residues using capillary electrophoresis.* Journal of Forensic Sciences, **1998**. ***43***(1): p. 119-124.

12. M. H. Mach, A. Pallos and P. F. Jones, *Feasibility of gunshot residue detection via its organic constituents. Part i: Analysis of smokeless powders by combined gas chromatography-chemical ionization mass spectrometry.* Journal of Forensic Sciences, **1978**. ***23***(3): p. 433-445.

13. M. H. Mach, A. Pallos and P. F. Jones, *Feasibility of gunshot residue detection via its organic constituents. Part ii: A gas-chromatography-mass spectrometry method.* Journal of Forensic Sciences, **1978**. ***23***(3): p. 446-455.

14. J. Andrasko, *Characterization of smokeless powder flakes from fired cartridge cases and from discharge patterns on clothing.* Journal of Forensic Sciences, **1992**. ***37***(4): p. 1030-1047.

15. Z. Wu, Y. Tong, J. Yu, X. Zhang, C. Yang, C. Pan, X. Deng, Y. Wen and Y. Xu, *The utilization of ms-ms method in detection of gsrs.* Journal of Forensic Sciences, **2001**. ***46***(3): p. 495-501.

16. E. O. N. Espinoza and J. I. Thornton, *Characterization of smokeless gunpowder by means of diphenylamine stabilizer and its nitrated derivatives.* Analytica Chimica Acta, **1994**. ***288***(1–2): p. 57-69. DOI: 10.1016/0003-2670(94)85116-6.

17. D. B. Dahl and P. F. Lott, *Gunshot residue determination by means of gunpowder stabilizers using high-performance liquid chromatography with electrochemical detection and analysis of metallic residues by graphite furnace atomic absorption spectrophotometry.* Microchemical Journal, **1987**. ***35***(3): p. 347-359.

18. R. A. D. Kumarawickrama, *The characterization and identification of organic gunshot residue.* Master of Science Thesis, University of Strathclyde, UK, **1985.**

19. J. Pichtel, *Distribution and fate of military explosives and propellants in soil: A review.* Applied and Environmental Soil Science, **2012**. ***2012***: p. 33. DOI: 10.1155/2012/617236.

20. D. M. Northrop and W. A. MacCrehan, *Smokeless powder residue analysis by capillary electrophoresis.* Department of Justice, National Institute of Justice, **1997**. Washinton DC: US, Report Number: 600–91.

21. D. M. Northrop, *Gunshot residue analysis by micellar electrokinetic capillary electrophoresis: Assessment for application to casework. Part i.* Journal of Forensic Sciences, **2001**. ***46***(3): p. 549-559.

22. B. Paull, C. Roux, M. Dawson and P. Doble, *Rapid screening of selected organic explosives by high-performance liquid chromatography using reversed-phase monolithic columns`.* Journal of Forensic Sciences, **2004**. ***49***(6): p. 1-6.

23. B. Heard,in *Handbook of firearms and ballistics: Examining and interpreting forensic evidence*. **2008**, John Wiley & Sons Ltd: Sussex, UK.

24. R. S. Maloney and J. I. Thornton, *Color tests for diphenylamine stabilizer and related compounds in smokeless gunpowder.* Journal of Forensic Sciences, **1982**. ***27***(2): p. 318-329.

25. Z. Brożek-Mucha, *Comparison of cartridge case and airborne gsr—a study of the elemental composition and morphology by means of sem-edx.* X-Ray Spectrometry, **2007**. ***36***(6): p. 398-407. DOI: 10.1002/xrs.990.

26. S. Basu, *Formation of gunshot residues.* Journal of Forensic Sciences, **1982**. ***27***(1): p. 72-91.

27. S. F. Romolo and P. Margot, *Identification of gunshot residue: A critical review.* Forensic Science International, **2001**. ***119***(2): p. 195-211. DOI: 10.1016/s0379-0738(00)00428-x.

28. G. M. Wolten, R. S. Nesbitt, A. R. Calloway, G. L. loper and P. F. Jones, *Final report on particle analysis for gunshot residue detection.* The Ivan A. Getting Laboratories, The Aerospace Corporation C. a. P. Laboratory, **1977**. T. A. Corporation: El Segundo, CA, ***September 1977***. Report Number: ATR-77(7915)-3.

29. L. Guindon and D. Allard, *Low toxicity primer composition*, **issued 26.07.1993**. S. I. T. Inc., Patent Number:US5388519 A, Available from: https://www.google.com.au/patents/US5388519; [*cited 17.09.2015*].

30. L. Niewoehner, *Guide for gunshot residue analysis by scanning electron microscopy/energy-dispersive x-ray spectrometry*, in *ENFSI*. **2008**: Prague.

31. L. Niewoehner, J. Andrasko, J. Biegstraaten, L. Gunaratnam, S. Steffen, S. Uhlig and S. Antoni, *Gsr2005—continuity of the enfsi proficiency test on identification of gsr by sem/edx.* Journal of Forensic Sciences, **2008**. ***53***(1): p. 162-167. DOI: 10.1111/j.1556-4029.2008.00594.x.

32. L. Gunaratnam and K. Himberg, *The identification fo gunshot residue particles from lead-free sintox ammunition.* Journal of Forensic Sciences, **1994**. ***39***(2): p. 532-536.

33. Z. Oommen and S. M. Pierce, *Lead-free primer residues: A qualitative characterization of winchester winclean™, remington/umc leadless™, federal ballisticlean™, and speer lawman cleanfire™ handgun ammunition*.* Journal of Forensic Sciences, **2006**. ***51***(3): p. 509-519. DOI: 10.1111/j.1556-4029.2006.00107.x.

34. A. Harris, *Analysis of primer residue from cci blazer lead free ammunition by scanning electron microscopy?Energy dispersive x-ray.* Journal of Forensic Sciences, **1995**. ***40***(1): p. 27-30.

35. A. Martiny, A. P. C. Campos, M. S. Sader and M. A. L. Pinto, *Sem/eds analysis and characterization of gunshot residues from brazilian lead-free ammunition.* Forensic Science International, **2008**. ***177***(1): p. e9-e17. DOI: http://dx.doi.org/10.1016/j.forsciint.2007.07.005.

36. S. Hales, *Improving forensic casework analysis and interpretation of gunshot residue (gsr) evidence.* doctoral thesis, University of Technology, Sydney, Center of Forensic Science, **2011.**

37. Z. Abrego, N. Grijalba, N. Unceta, M. Maguregui, A. Sanchez, A. Fernandez-Isla, M. A. Goicolea and R. J. Barrio, *A novel method for the identification of inorganic and organic gunshot residue particles of lead-free ammunitions from the hands of shooters using scanning laser ablation-icpms and raman micro-spectroscopy.* Analyst, **2014**. ***139***(23): p. 6232-6241. DOI: 10.1039/C4AN01051E.

38. M. D. Cole, N. Ross and J. W. Thorpe, *Gunshot residue and bullet wipe detection using a single lift technique.* AFTE Journal, **1992**. ***24***(254).

39. S. Ståhling and T. Karlsson, *A method for the collection of gunshot residues from skin and other surfaces.* Journal of Forensic Sciences, **2000**. ***45***(6): p. 1299-1302.

40. M. Steinberg, Y. Leist and M. Tassa, *A new field kit for bullet hole identification.* Journal of Forensic Sciences, **1984**. ***29***(1): p. 169-176.

41. A. Santos, P. Ramos, L. Fernandes, T. Magalhães, A. Almeida and A. Sousa, *Firing distance estimation based on the analysis of gsr distribution on the target surface using icp-ms—an experimental study with a 7.65 mm × 17 mm browning pistol (.32 acp).* Forensic Science International, **2015**. ***247***(0): p. 62-68. DOI: http://dx.doi.org/10.1016/j.forsciint.2014.12.006.

42. F. S. Romolo, *Organic gunshot residue from lead-free ammunition.* PhD Thesis, Université de Lausanne, Ecole de Sciences Criminelles Institut de Police Scientifique, **2004.**

43. J. A. Goleb and J. R. Midkiff, *Firearms discharge residue sample collection techniques.* Journal of Forensic Sciences, **1975**. ***20***: p. 701-707.

44. A. Zeichner, B. Eldar, B. K. Glattstein, A. , T. Tamiri and D. Muller, *Vacuum collection of gunpowder residues from clothing worn by shooting suspects, and their analysis by gc/tea, ims and gc/ms.* Journal of Forensic Sciences, **2003**. ***48***(5): p. 961-972.

45. J. M. F. Douse and R. N. Smith, *Trace analysis of explosives and firearm discharge residues in the metropolitan police forensic science laboratory.* Journal of Energetic Materials, **1986**. ***4***(1-4): p. 169-186. DOI: 10.1080/07370658608011340.

46. J. M. F. Douse, *Dynamic headspace method for the improved clean-up of gunshot residues prior to the detection of nitroglycerine by capillary column gas chromatography with thermal energy analysis detection.* Journal of Chromatography A, **1991**. ***464***(0): p. 178-185. DOI: 10.1016/s0021-9673(00)94234-1.

47. J. B. F. Lloyd, *Glyceryl dinitrates in the detection of skin contact with explosives and related materials of forensic science interest.* Journal of the Forensic Science Society, **1986**. ***26***: p. 341-348.

48. J. M. F. Douse, *Improved method for the trace analysis of explosives by silica capillary column gas chromatography with thermal energy analysis detection.* Journal of Chromatography A, **1987**. ***410***(0): p. 181-189. DOI: 10.1016/s0021-9673(00)90046-3.

49. S. S. Krishnan, *Detection of gunshot residues on the hands by trace element analysis.* Journal of Forensic Sciences, **1977**. ***22***(2): p. 304-324.

50. J. B. F. Lloyd, *Liquid chromatography of firearms propellants traces.* Journal of Energetic Materials, **1986**. ***4***(1-4): p. 239-271. DOI: 10.1080/07370658608011344.

51. J. S. Wallace and W. J. McKeown, *Sampling procedures for firearms and/or explosives residues.* Journal of the Forensic Science Society, **1993**. ***33***: p. 107-116.

52. J. D. Twibell, T. Wright, D. G. Sanger, R. K. Bramley, J. B. F. Lloyd and N. S. Downs, *The efficient extraction of some common organic explosives from hand swabs for analysis by gas liquid and thin-layer chromatography.* Journal of Forensic Sciences, **1984**. ***29***(1): p. 277-283.

53. Y. Tong, Z. Wu, C. Yang, J. Yu, X. Zhang, S. Yang, X. Deng, Y. Xu and Y. Wen, *Determination of diphenylamine stabilizer and its nitrated derivatives in smokeless gunpowder using a tandem ms method.* Analyst, **2001**. ***126***(4): p. 480-484.

54. J. D. Twibell, J. M. Home, K. W. Smalldon, D. G. Higgs and T. S. Hayes, *Assessment of solvents for the recovery of nitroglycerine from hands using cotton swabs.* Journal of Forensic Sciences, **1982**. ***27***(4): p. 792-800.

55. I. Jane, P. G. Brooks, J. M. F. Douse and K. A. O'Callaghan, *Detection of gsr via analysis of their organic constituents*. in *International Symposium on the Analysis and Detection of Explosives*. **1983**. Washington, DC: US: Government Printing Office.

56. S. Benito, Z. Abrego, A. Sánchez, N. Unceta, M. A. Goicolea and R. J. Barrio, *Characterization of organic gunshot residues in lead-free ammunition using a new sample collection device for liquid chromatography–quadrupole time-of-flight mass spectrometry.* Forensic Science International, **2015**. ***246***(0): p. 79-85. DOI: http://dx.doi.org/10.1016/j.forsciint.2014.11.002.

57. A. Zeichner and B. Eldar, *A novel method for extraction and analysis of gunpowder residues on double-side adhesive coated stubs.* Journal of Forensic Sciences, **2004**. ***49***(6): p. 1194-1206.

58. A. Zeichner, S. Abramovich-Bar, T. Tamiri and J. Almog, *A feasibility study on the use of double-sided adhesive coated stubs for sampling of explosive traces from hands.* Forensic Science International, **2009**. ***184***(1): p. 42-46.

59. M. Morelato, A. Beavis, A. Ogle, P. Doble, P. Kirkbride and C. Roux, *Screening of gunshot residues using desorption electrospray ionisation–mass spectrometry (desi–ms).* Forensic Science International, **2012**. ***217***(1–3): p. 101-106. DOI: 10.1016/j.forsciint.2011.10.030.

60. E. Rudzitis, M. Kopina and M. Wahlgren, *Optimization of firearm residue detection by neutron activation analysis.* Journal of Forensic Sciences, **1973**. ***18***(2): p. 93-100.

61. S. S. Krishnan, *Detection of gunshot residue on the hands by neutron activation and atomic absorption analysis.* Journal of Forensic Sciences, **1974**. ***19***(4): p. 789-797.

62. J. W. Kilty, *Activity after shooting and its effect on the retention of primer residue.* Journal of Forensic Sciences, **1975**. ***20***(2): p. 219-230.

63. R. D. Koons, D. G. Havekost and C. A. Peters, *Analysis of gunshot primer residue collection swabs using flameless atomic absorption spectrophotometry: A reexamination of extraction and instrument procedures.* Journal of Forensic Sciences, **1987**. ***32***(4): p. 846-865.

64. R. Cooper, J. M. Guileyardo, I. C. Stone, V. Hall and L. Fletcher, *Primer residue deposited by handguns.* American Journal of Forensic Medicine and Pathology, **1994**. ***15***(4): p. 325-327.

65. M. Ravreby, *Analysis of long-range bullet entrance holes by atomic absorption spectrophotometry and scanning electron microscopy.* Journal of Forensic Sciences, **1982**. ***27***(1): p. 92-112.

66. G. E. Reed, P. J. McGuire and A. Boehm, *Analysis of gunshot residue test results in 112 suicides.* Journal of Forensic Sciences, **1990**. ***35***(1): p. 62-68.

67. Z. Brożek-Mucha, *Variation of the chemical contents and morphology of gunshot residue in the surroundings of the shooting pistol as a potential contribution to a shooting incidence reconstruction.* Forensic Science International, **2011**. ***210***(1-3): p. 31-41.

68. Z. Brożek-Mucha, *Distribution and properties of gunshot residue originating from a luger 9 mm ammunition in the vicinity of the shooting gun.* Forensic Science International, **2009**. ***183***(1-3): p. 33-44.

69. R. S. White and A. D. Owens, *Automation of gunshot residue detection and analysis by scanning electron microscopy/ energy dispersive x-ray analysis (sem/ edx).* Journal of Forensic Sciences, **1987**. ***32***(6): p. 1595-1603.

70. A. Zeichner and N. Levin, *Casework experience of gsr detection in israel, on samples from hands, hair, and clothing using an autosearch sem/edx system.* Journal of Forensic Sciences, **1995**. ***40***(6): p. 1082-1085.

71. M. J. Bailey, K. J. Kirkby and C. Jeynes, *Trace element profiling of gunshot residues by pixe and sem-eds: A feasibility study.* X-Ray Spectrometry, **2009**. ***38***(3): p. 190-194. DOI: 10.1002/xrs.1142.

72. R. D. Voyksner and J. Yinon, *Trace analysis of explosives by thermospray high-performance liquid chromatography-mass spectrometry.* Journal of Chromatography A, **1986**. ***354***: p. 393-405.

73. D. B. Dahl, S. C. Slahck and P. F. Lott, *Gunshot residue determination by high-performance liquid chromatography with electrochemical detection.* Microchemical Journal, **1985**. ***31***(2): p. 145-160. DOI: 10.1016/0026-265x(85)90024-4.

74. T. L. Davis,in *The chemistry of powder and explosives*. **1941**, Wiley: New York.

75. J. M. F. Douse, *Trace analysis of explosives at the low picogram level using silica capillary column gas chromatography with thermal energy analyser detection.* Journal of Chromatography, **1983**. ***256***: p. 359-362.

76. J. Andrasko, T. Norberg and S. Ståhling, *Time since discharge of shotguns.* Journal of Forensic Sciences, **1998**. ***43***(5): p. 1005-1015.

77. G. L. Burleson, B. Gonzalez, K. Simons and J. C. C. Yu, *Forensic analysis of a single particle of partially burnt gunpowder by solid phase micro-extraction–gas chromatography-nitrogen phosphorus detector.* Journal of Chromatography A, **2009**. ***1216***(22): p. 4679-4683. DOI: 10.1016/j.chroma.2009.03.074.

78. C. Weyermann, V. Belaud, F. Riva and F. S. Romolo, *Analysis of organic volatile residues in 9 mm spent cartridges.* Forensic Science International, **2009**. ***186***(1–3): p. 29-35. DOI: 10.1016/j.forsciint.2009.01.005.

79. D. H. Fine, *Picogram analysis of explosive residues using the thermal energy analyzer (tea).* Journal of Forensic Sciences, **1984**. ***29***(3): p. 732-746.

80. C. E. Wissinger and B. R. McCord, *A gradient reversed phase hplc procedure for smokeless powder compoarison.* Journal of Forensic Sciences, **2002**. ***47***(1): p. 168-174.

81. J. B. F. Lloyd, *High-performance liquid chromatography of organic explosives components with electrochemical detection at a pendant mercury drop electrode.* Journal of Chromatography A, **1983**. ***257***(0): p. 227-236. DOI: 10.1016/s0021-9673(01)88178-4.

82. O. Cascio, M. Trettene, F. Bortolotti, G. Milana and F. Tagliaro, *Analysis of organic components of smokeless gunpowders: High-performance liquid chromatogaphy vs. Micellar electrokinetic capillary chromatography.* Electrophoresis, **2004**. ***25***(10-11): p. 1543-1547. DOI: 10.1002/elps.200305883.

83. C. M. Mahoney, G. Gillen and A. J. Fahey, *Characterization of gunpowder samples using time-of-flight secondary ion mass spectrometry (tof-sims).* Forensic Science International, **2006**. ***158***(1): p. 39-51. DOI: 10.1016/j.forsciint.2005.02.036.

84. M. Zhao, S. Zhang, C. Yang, Y. Xu, Y. Wen, L. Sun and X. Zhang, *Desorption electrospray tandem ms (desi-msms) analysis of methyl centralite and ethyl centralite as gunshot residues on skin and other surfaces.* Journal of Forensic Sciences, **2008**. ***53***(4): p. 807-811. DOI: 10.1111/j.1556-4029.2008.00752.x.

85. R. V. Taudte, A. Beavis, L. Blanes, N. Cole, P. Doble and C. Roux, *Detection of gunshot residues using mass spectrometry.* BioMed Research International, **2014**. ***2014***. DOI: 10.1155/2014/965403.

86. S. Willis, *Enfsi guideline for evaluative reporting in forenisc science.* European Network of Forenisc Science Institutes (ENFSI), **2015**. ENFSI: Report Number:

87. A. Biedermann, S. Bozza and F. Taroni, *Probabilistic evidential assessment of gunshot residue particle evidence (part ii): Bayesian parameter estimation for experimental count data.* Forensic Science International, **2011**. ***206***(1–3): p. 103-110. DOI: 10.1016/j.forsciint.2010.07.009.

88. A. Biedermann, S. Bozza and F. Taroni, *Probabilistic evidential assessment of gunshot residue particle evidence (part i): Likelihood ratio calculation and case pre-assessment using bayesian networks.* Forensic Science International, **2009**. ***191***(1): p. 24-35.

89. A. Biedermann and F. Taroni, *A probabilistic approach to the joint evaluation of firearm evidence and gunshot residues.* Forensic Science International, **2006**. ***163***(1): p. 18-33.

90. E. Lindsay, M. J. McVicar, R. V. Gerard, E. D. Randall and J. Pearson, *Passive exposure and persistence of gunshot residue (gsr) on bystanders to a shooting: Comparison of shooter and bystander exposure to gsr.* Can. Soc. Forensic Sci. J., **2011**. ***44***(3): p. 89-96.

91. J. Andrasko and S. Ståhling, *Time since discharge of rifles.* Journal of Forensic Sciences, **2000**. ***45***(6): p. 1250-1255.

92. J. Andrasko and S. Ståhling, *Time since discharge of pistols and revolvers.* Journal of Forensic Sciences, **2003**. ***48***(2): p. 307-311.

93. J. Andrasko and S. Ståhling, *Time since discharge of spent cartridges.* Journal of Forensic Sciences, **1999**. ***44***(3): p. 487-495.

94. M. Gallidabino, C. Weyermann, F. S. Romolo and F. Taroni, *Estimating the time since discharge of spent cartridges: A logical approach for interpreting the evidence.* Science & Justice, **2013**. ***53***(1): p. 41-48. DOI: 10.1016/j.scijus.2011.12.004.

95. S. Charles, M. Lannoy and N. Geusens, *Influence of the type of fabric on the collection efficiency of gunshot residues.* Forensic Science International, **2013**. ***228***(1–3): p. 42-46. DOI: http://dx.doi.org/10.1016/j.forsciint.2013.02.022.

96. V. Mastruko, *Detection of gsr particles on clothing of suspects.* Forensic Journal International, **2003**. ***136***(SUPPL. 1): p. 153-154.

97. A. Zeichner, N. Levin and E. Springer, *Gunshot residue particles formed by using different types of ammunition in the same firearm.* Journal of Forensic Sciences, **1991**. ***36***(4): p. 1020-1026.

98. S. Charles, B. Nys and N. Geusens, *Primer composition and memory effect of weapons—some trends from a systematic approach in casework.* Forensic Science International, **2011**. ***212***(1–3): p. 22-26. DOI: http://dx.doi.org/10.1016/j.forsciint.2011.05.001.

99. A. J. Schwoeble and D. L. Exline,in *Current methods in forensic gunshot residue analysis*. **2000**, Boca Raton: CRC Press: Florida, US.

100. H. Ditrich, *Distribution of gunshot residues--the influence of weapon type.* Forensic Science International, **2012**. ***220***(1-3): p. 85-90. DOI: 10.1016/j.forsciint.2012.01.034.

101. M. Grassberger and H. Schmid,in *Todesermittlung. Befundaufnahme & spurensicherung: Ein praktischer leitfaden für polizei, juristen und ärzte*. **2010**, Springer DE.

102. J. A. Mathis and B. R. McCord, *Gradient reversed-phase liquid chromatographic-electrospray ionization mass spectrometric method for the comparison of smokeless powders.* Journal of Chromatography A, **2003**. ***988***(1): p. 107-116. DOI: 10.1016/s0021-9673(02)02055-1.

103. M. R. Reardon, W. A. MacCrehan and W. F. Rowe, *Comparing the additive composition of smokeless gunpowder and its handgun-fired residues.* Journal of Forensic Sciences, **2000**. ***45***(6): p. 1232-1238.

104. W. A. MacCrehan, M. R. Reardon and D. L. Duewer, *Associating gunpowder and residues from commercial ammunition using compositional analysis.* Journal of Forensic Sciences, **2002**. ***47***(2): p. 260-266.

105. M. López-López, J. J. Delgado and C. García-Ruiz, *Analysis of macroscopic gunshot residues by raman spectroscopy to assess the weapon memory effect.* Forensic Science International, **2013**. ***231***(1–3): p. 1-5. DOI: http://dx.doi.org/10.1016/j.forsciint.2013.03.049.

106. M. Lopez-Lopez, J. L. Ferrando and C. Garcia-Ruiz, *Ammunition identification by means of the organic analysis of gunshot residues using raman spectroscopy.* Anal. Chem., **2012**. ***84***: p. 3581-3585.

107. W. A. MacCrehan, E. R. Patierno, D. L. Duewer and M. R. Reardon, *Investigating the effect of changing ammunition on the composition of organic additives in gunshot residue (ogsr).* Journal of Forensic Sciences, **2001**. ***46***(1): p. 57-62.

108. Z. Brożek-Mucha and A. Jankowicz, *Evaluation of the possibility of differentiation between various types of ammunition by means of gsr examination with sem–edx method.* Forensic Science International, **2001**. ***123***(1): p. 39-47. DOI: 10.1016/s0379-0738(01)00518-7.

109. C. Torre, G. Mattutino, V. Vasino and C. Robino, *Brake linings: A source of non-gsr particles containing lead, barium, and antimony.* Journal of Forensic Sciences, **2002**. ***47***(3): p. 494-504.

110. B. Cardinetti, C. Ciampini, C. D'Onofrio, G. Orlando, L. Gravina, F. Ferrari, D. Di Tullio and L. Torresi, *X-ray mapping technique: A preliminary study in discriminating gunshot residue particles from aggregates of environmental occupational origin.* Forensic Science International, **2004**. ***143***(1): p. 1-19. DOI: 10.1016/j.forsciint.2004.01.019.

111. P. V. Mosher, M. J. McVicar, E. D. Randall and E. H. Slid, *Gunshot residue-similar particles produced by fireworks.* Canadian Society of Forensic Science Journal, **1998**. ***31***: p. 157-168.

112. M. Grima, M. Butler, R. Hanson and A. Mohameden, *Firework displays as sources of particles similar to gunshot residue.* Science & Justice, **2012**. ***52***(1): p. 49-57. DOI: 10.1016/j.scijus.2011.04.005.

113. M. A. Trimpe, *Analysis of fireworks for particles of the type found in primer residue (gsr).* International Association for MicroAnalysis **2003**. ***4***(1): p. 1-19.

114. L. Garofano, M. Capra, F. Ferrari, G. P. Bizzaro, D. Di Tullio, M. Dellâ€™Olio and A. Ghitti, *Gunshot residue: Further studies on particles of environmental and occupational origin.* Forensic Science International, **1999**. ***103***(1): p. 1-21.

115. J. S. Wallace and J. McQuillan, *Discharge residues from cartridge-operated industrial tools.* Journal of the Forensic Science Society, **1984**. ***24***(5): p. 495-508. DOI: 10.1016/s0015-7368(84)72329-2.

116. W. A. MacCrehan, M. J. Layman and J. D. Secl, *Hair combing to collect organic gunshot residues (ogsr).* Forensic Science International, **2003**. ***135***(2): p. 167-173.

117. L. S. Leggett and P. F. Lott, *Gunshot residue analysis via organic stabilizers and nitrocellulose.* Microchemical Journal, **1989**. ***39***(1): p. 76-85.

118. P. Margot, *Traçologie: La trace, vecteur fondamental de la police scientifique.* Revue Internationale de Criminologie et de Police Technique et Scientifique 01/2014, **2014**. ***67***: p. 72-97.

119. R. E. Berk, S. A. Rochowicz, M. Wong and M. A. Kopina, *Gunshot residue in chicago police vehicles and facilities: An empirical study.* Journal of Forensic Sciences, **2007**. ***52***(4): p. 838-841. DOI: 10.1111/j.1556-4029.2007.00457.x.

120. J. French, R. Morgan and J. Davy, *The secondary transfer of gunshot residue: An experimental investigation carried out with sem-edx analysis.* X-Ray Spectrometry, **2014**. ***43***(1): p. 56-61. DOI: 10.1002/xrs.2498.

121. S. Charles and N. Geusens, *A study of the potential risk of gunshot residue transfer from special units of the police to arrested suspects.* Forensic Science International, **2012**. ***216***(1–3): p. 78-81. DOI: http://dx.doi.org/10.1016/j.forsciint.2011.08.022.

122. D. M. Gialamas, E. F. Rhodes and L. A. Sugarman, *Officers, their weapons and their hands: An empirical study of gsr on the hands of non-shooting police officers.* Journal of Forensic Science, **1995**. ***40***(6): p. 1086-1089.

123. S. Pettersson, *What conclusions can be drawn from the presence of gunshot residues?* Forensic Science International, **2003**. ***136***: p. 158-158.

124. J. French and R. Morgan, *An experimental investigation of the indirect transfer and deposition of gunshot residue: Further studies carried out with sem–edx analysis.* Forensic Science International, **2015**. ***247***(0): p. 14-17. DOI: http://dx.doi.org/10.1016/j.forsciint.2014.10.023.

125. L. Ali, K. Brown, H. Castellano and S. J. Wetzel, *A study of the presence of gunshot residue in pittsburgh police stations using sem/eds and lc-ms/ms.* Journal of Forensic Sciences, **2016**.

126. J. Arndt, S. Bell, L. Crookshanks, M. Lovejoy, C. Oleska, T. Tulley and D. Wolfe, *Preliminary evaluation of the persistence of organic gunshot residue.* Forensic Science International, **2012**. ***222***(1-3): p. 137-145.

127. J. W. Moran and S. Bell, *Skin permeation of organic gunshot residue: Implications for sampling and analysis.* Analytical Chemistry, **2014**. ***86***(12): p. 6071-6079. DOI: 10.1021/ac501227e.

128. J. D. Twibell, J. M. Home, K. W. Smalldon and D. G. Higgs, *Transfer of nitroglycerine to hands during contact with commercial explosives.* Journal of Forensic Sciences, **1982**. ***27***(4): p. 783-791.

129. A. Zeichner, B. Eldar, B. Glattstein, A. Koffman, T. Tamiri and D. Muller, *Vacuum collection of gunpowder residues from clothing worn by shooting suspects, and their analysis by gc/tea, ims, and gc/ms.* Journal of Forensic Sciences, **2003**. ***48***(5): p. 961-972.

130. L. Reid, K. Chana, J. W. Bond and M. J. B. Almond, S., *Stubs vs swabs? A comparison of gunshot residue collection techniques.* Journal of Forensic Sciences, **2010**. ***55***(3): p. 753-756.

131. S. J. Speers, K. Doolan, J. McQuillan and J. S. Wallace, *Evaluation of improved methods for the recovery and detection of organic and inorganic cartridge discharge residues.* Journal of Chromatography A, **1994**. ***674***(1â€“2): p. 319-327.

132. B. Glattstein, A. Vinokurov, N. Levin and A. Zeichner, *Improved method for shooting distance estimation. Part1. Bullet holes in clothing items.* Journal of Forensic Sciences, **2000**. ***45***(4): p. 801-806.

133. B. Glattstein, A. Zeichner, A. Vinokurov and E. Shoshani, *Improved method for shooting distance determination. Part 2-bullet holes in objects that cannot be processed on the laboratory.* Journal of Forensic Sciences, **2000**. ***45***(5): p. 1000-1008.

134. B. Glattstein, A. Vinokurov, L. Nadav, C. Kugel and J. Hiss, *Improved method for shooting distance estimation. Part iii. Bullet holes in cadavers.* Journal of Forensic Sciences, **2000**. ***45***(6): p. 1243-1249.

135. D. Muller, A. Levy, A. Vinokurov, M. Ravreby, R. Shelef, E. Wolf, B. Eldar and B. Glattstein, *A novel method for the analysis of discharged smokeless powder residues.* Journal of Forensic Sciences, **2007**. ***52***(1): p. 75-78.

136. A. J. Bandodkar, A. M. O'Mahony, J. Ramirez, I. A. Samek, S. M. Anderson, J. R. Windmiller and J. Wang, *Solid-state forensic finger sensor for integrated sampling and detection of gunshot residue and explosives: Towards 'lab-on-a-finger'.* Analyst, **2013**. ***138***(18): p. 5288-5295. DOI: 10.1039/C3AN01179H.

137. D. A. DeTata, P. A. Collins and A. J. McKinley, *A comparison of solvent extract cleanup procedures in the analysis of organic explosives.* Journal of Forensic Sciences, **2013**. ***58***(2): p. 500-507. DOI: 10.1111/1556-4029.12035.

138. I. Aleksandar, *Is there a way to precisely identify that the suspect fired from the firearm?* Forensic Science International, **2003**. ***136 (Supplement 1)***: p. 158-159.

139. M. Steinberg, Y. Leist, P. Goldschmidt and M. Tassa, *Spectrophotometric determination of nitrites in gunpowder residue on shooter's hands.* Journal of Forensic Sciences, **1983**. ***29***(2): p. 464-470.

140. H. Engelhardt, J. Meister and P. Kolla, *Optimisation of post-column reaction detector for hplc of explosives.* Chromatographia, **1993**. ***35***(1-2): p. 5-12. DOI: 10.1007/BF02278550.

141. S. Stahling, *Modified sheet printing method (mspm) for the detection of lead in determination of shooting distance.* Journal of Forensic Sciences, **1999**. ***44***(1): p. 179-181.

142. J. A. Lekstrom and R. D. Koons, *Copper and nickel detection on gunshot targets by dithiooxamide test.* Journal of Forensic Sciences, **1986**. ***31***(4): p. 1283-1291.

143. M. A. M. Lucena, G. F. de Sa, M. O. Rodrigues, S. Alves, M. Talhavini and I. T. Weber, *$Znal_2o_4$-based luminescent marker for gunshot residue identification and ammunition traceability.* Analytical Methods, **2013**. ***5***(3): p. 705-709. DOI: 10.1039/C2AY25535A.

144. I. T. Weber, A. J. G. Melo, M. A. M. Lucena, E. F. Consoli, M. O. Rodrigues, G. F. de Sá, A. O. Maldaner, M. Talhavini and S. Alves Jr, *Use of luminescent gunshot residues markers in forensic context.* Forensic Science International, **2014**. ***244***(0): p. 276-284. DOI: http://dx.doi.org/10.1016/j.forsciint.2014.09.001.

145. I. T. Weber, A. J. G. de Melo, M. A. d. M. Lucena, M. O. Rodrigues and S. Alves Junior, *High photoluminescent metal–organic frameworks as optical markers for the identification of gunshot residues.* Analytical Chemistry, **2011**. ***83***(12): p. 4720-4723. DOI: 10.1021/ac200680a.

146. J.-S. Yang and T. M. Swager, *Fluorescent porous polymer films as tnt chemosensors: Electronic and structural effects.* Journal of the American Chemical Society, **1998**. ***120***(46): p. 11864-11873. DOI: 10.1021/ja982293q.

147. S. W. Thomas, G. D. Joly and T. M. Swager, *Chemical sensors based on amplifying fluorescent conjugated polymers.* Chemical Reviews, **2007**. ***107***(4): p. 1339-1386. DOI: 10.1021/cr0501339.

148. P. Anzenbacher, L. Mosca, M. A. Palacios, G. V. Zyryanov and P. Koutnik, *Iptycene-based fluorescent sensors for nitroaromatics and tnt.* Chemistry – A European Journal, **2012**. ***18***(40): p. 12712-12718. DOI: 10.1002/chem.201200469.

149. Y. Xin, Q. Wang, T. Liu, L. Wang, J. Li and Y. Fang, *A portable and autonomous multichannel fluorescence detector for on-line and in situ explosive detection in aqueous phase.* Lab on a Chip, **2012**. ***12***(22): p. 4821-4828.

150. S. Zhang, L. Ding, F. Lu, T. Liu and Y. Fang, *Fluorescent film sensors based on sams of pyrene derivatives for detecting nitroaromatics in aqueous solutions.* Spectrochimica acta. Part A, Molecular and biomolecular spectroscopy, **2012**. ***97***: p. 31-7. DOI: 10.1016/j.saa.2012.04.041.

151. J. Wang, M. Pumera, M. P. Chatrathi, A. Escarpa, M. Musameh, G. Collins, A. Mulchandani, Y. Lin and K. Olsen, *Single-channel microchip for fast screening and detailed identification of nitroaromatic explosives or organophosphate nerve agents.* Analytical Chemistry, **2002**. ***74***(5): p. 1187-1191. DOI: 10.1021/ac0111356.

152. A. W. Martinez, S. T. Phillips, B. J. Wiley, M. Gupta and G. M. Whitesides, *Flash: A rapid method for prototyping paper-based microfluidic devices.* Lab on a Chip, **2008**. ***8***(12): p. 2146-2150.

153. J. Nie, Y. Zhang, L. Lin, C. Zhou, S. Li, L. Zhang and J. Li, *Low-cost fabrication of paper-based microfluidic devices by one-step plotting.* Analytical Chemistry, **2012**. ***84***(15): p. 6331-6335. DOI: 10.1021/ac203496c.

154. E. M. Fenton, M. R. Mascarenas, G. P. López and S. S. Sibbett, *Multiplex lateral-flow test strips fabricated by two-dimensional shaping.* ACS Applied Materials & Interfaces, **2008**. ***1***(1): p. 124-129. DOI: 10.1021/am800043z.

155. X. Li, J. Tian, T. Nguyen and W. Shen, *Paper-based microfluidic devices by plasma treatment.* Analytical Chemistry, **2008**. ***80***(23): p. 9131-9134. DOI: 10.1021/ac801729t.

156. X. Li, J. Tian, G. Garnier and W. Shen, *Fabrication of paper-based microfluidic sensors by printing.* Colloids and Surfaces B: Biointerfaces, **2010**. ***76***(2): p. 564-570. DOI: 10.1016/j.colsurfb.2009.12.023.

157. K. Abe, K. Suzuki and D. Citterio, *Inkjet-printed microfluidic multianalyte chemical sensing paper.* Analytical Chemistry, **2008**. ***80***(18): p. 6928-6934. DOI: 10.1021/ac800604v.

158. K. Abe, K. Kotera, K. Suzuki and D. Citterio, *Inkjet-printed paperfluidic immuno-chemical sensing device.* Analytical & Bioanalytical Chemistry, **2010**. ***398***(2): p. 885-893. DOI: 10.1007/s00216-010-4011-2.

159. E. Carrilho, A. W. Martinez and G. M. Whitesides, *Understanding wax printing: A simple micropatterning process for paper-based microfluidics.* Analytical Chemistry, **2009**. ***81***(16): p. 7091-7095. DOI: 10.1021/ac901071p.

160. Y. Lu, W. Shi, L. Jiang, J. Qin and B. Lin, *Rapid prototyping of paper-based microfluidics with wax for low-cost, portable bioassay.* Electrophoresis, **2009**. ***30***(9): p. 1497-1500. DOI: 10.1002/elps.200800563.

161. Y. Lu, W. Shi, J. Qin and B. Lin, *Fabrication and charaterization of paper-based microfluidics prepared in nitrocellulose membrane by wax printing.* Analytical Chemistry, **2010**. ***82***(1): p. 329-335.

162. A. W. Martinez, S. T. Phillips, G. M. Whitesides and E. Carrilho, *Diagnostics for the developing world: Microfluidic paper-based analytical devices.* Analytical Chemistry, **2010**. ***82***(1): p. 3-10. DOI: 10.1021/ac9013989.

163. M. S. Meaney and V. L. McGuffin, *Investigation of common fluorophores for the detection of nitrated explosives by fluorescence quenching.* Analytica Chimica Acta, **2008**. ***610***(1): p. 57-67. DOI: 10.1016/j.aca.2008.01.016.

164. K.-S. Focsaneanu and J. C. Scaiano, *Potential analytical applications of differential fluorescence quenching: Pyrene monomer and excimer emissions as sensors for electron deficient molecules.* Photochemical & Photobiological Sciences, **2005**. ***4***(10): p. 817-821.

165. Y. Salinas, R. Martinez-Manez, M. D. Marcos, F. Sancenon, A. M. Costero, M. Parra and S. Gil, *Optical chemosensors and reagents to detect explosives.* Chemical Society Reviews, **2012**. ***41***(3): p. 1261-1296. DOI: 10.1039/C1CS15173H.

166. J. V. Goodpaster and V. L. McGuffin, *Fluorescence quenching as an indirect detection method for nitrated explosives.* Analytical Chemistry, **2001**. ***73***(9): p. 2004-2011. DOI: 10.1021/ac001347n.

167. P. Beyazkilic, A. Yildirim and M. Bayindir, *Formation of pyrene excimers in mesoporous ormosil thin films for visual detection of nitro-explosives.* ACS Applied Materials & Interfaces, **2014**. ***6***(7): p. 4997-5004. DOI: 10.1021/am406035v.

168. R. D. Wauchope and F. W. Getzen, *Temperature dependence of solubilities in water and heats of fusion of solid aromatic hydrocarbons.* Journal of Chemical & Engineering Data, **1972**. ***17***(1): p. 38-41. DOI: 10.1021/je60052a020.

169. L. Z. Zhu and C. T. Chiou, *Water solubility enhancements of pyrene by single and mixed surfactant solutions.* J. Environ. Sci. (China), **2001**. ***13***(4): p. 491-496.

170. R. Q. Thompson, D. D. Fetterolf, M. L. Miller and R. F. Mothershead II, *Aqueous recovery from cotton swabs of organic explosives residues followed by solid phase extraction.* Journal of Forensic Sciences, **1999**. ***44***(4): p. 795-804.

171. E. Korman, L. J. Langman and P. J. Jannetto, *High-throughput method for the quantification of lacosamide in serum using ultrafast spe-ms/ms.* Therapeutic Drug Monitoring, **2015**. ***37***(1): p. 126-131. DOI: 10.1097/ftd.0000000000000115.

172. M. Razavi, L. E. Frick, W. A. LaMarr, M. E. Pope, C. A. Miller, N. L. Anderson and T. W. Pearson, *High-throughput siscapa quantitation of peptides from human plasma digests by ultrafast, liquid chromatography-free mass spectrometry.* Journal of Proteome Research, **2012**. ***11***(12): p. 5642-5649. DOI: 10.1021/pr300652v.

173. D. Danso, P. J. Jannetto, R. Enger and L. J. Langman, *High-throughput validated method for the quantitation of busulfan in plasma using ultrafast spe-ms/ms.* Therapeutic Drug Monitoring, **2015**. ***37***(3): p. 319-324. DOI: 10.1097/ftd.0000000000000159.

174. R. V. Taudte, C. Roux, D. Bishop, L. Blanes, P. Doble and A. Beavis, *Development of a uhplc method for the detection of organic gunshot residues using artificial neural networks.* Analytical Methods, **2015**. DOI: 10.1039/C5AY00306G.

175. B. McCord and J. Thomas, *Rapid screening and confirmation of organic gsr using electrospray mass spectrometry.* U.S. Department of Justice, **2013**. Report Number:

176. J. B. F. Lloyd, *Adsorption characteristics of organic explosives compounds on adsorbents typically used in clean-up and related trace analysis techniques.* Journal of Chromatography A, **1985**. ***328***: p. 145-154. DOI: http://dx.doi.org/10.1016/S0021-9673(01)87386-6.

177. U. N. O. o. D. a. Crime, *Global study on homicide - trends, contexts, data.* UNODC, **2011**. Vienna, Report Number:

178. A. M. O'Mahony, J. R. Windmiller, I. A. Samek, A. J. Bandodkar and J. Wang, *"Swipe and scan": Integration of sampling and analysis of gunshot metal residues at screen-printed electrodes.* Electrochemistry Communications, **2012**. ***23***(0): p. 52-55. DOI: http://dx.doi.org/10.1016/j.elecom.2012.07.004.

179. C. D. o. F. a. Wildlife; Available from: http://www.dfg.ca.gov/wildlife/hunting/lead-free/; *[cited 22.10.*].

180. P. Chiaramonte, **2013**; Available from: http://www.foxnews.com/us/2013/12/21/end-line-for-lead-bullet-regulations-bans-force-switch-to-green-ammo/; *[cited 22.10.*].

181. J. L. Thomas, D. Lincoln and B. R. McCord, *Separation and detection of smokeless powder additives by ultra performance liquid chromatography with tandem mass spectrometry (uplc/ms/ms).* Journal of Forensic Sciences, **2013**. ***58***(3): p. 609-615. DOI: 10.1111/1556-4029.12096.

182. S. M. Chesnut and J. J. Salisbury, *The role of uhplc in pharmaceutical development.* Journal of Separation Science, **2007**. ***30***(8): p. 1183-1190. DOI: 10.1002/jssc.200600505.

183. L. V. Fausett,in *Fundamentals of neural networks*, D. Fowley, Editor. **1994**, Prentice-Hall, Inc.: New Jersey, US.

184. R. Webb, P. Doble and M. Dawson, *Optimisation of hplc gradient separations using artificial neural networks (anns): Application to benzodiazepines in post-mortem samples.* Journal of Chromatography B-Analytical Technologies in the Biomedical and Life Sciences, **2009**. ***877***(7): p. 615-620. DOI: 10.1016/j.jchromb.2009.01.012.

185. P. Doble, M. Sandercock, E. Du Pasquier, P. Petocz, C. Roux and M. Dawson, *Classification of premium and regular gasoline by gas chromatography/mass spectrometry, principal component analysis and artificial neural networks.* Forensic Science International, **2003**. ***132***(1): p. 26-39. DOI: http://dx.doi.org/10.1016/S0379-0738(03)00002-1.

186. A. T. K. Tran, R. V. Hyne, F. Pablo, W. R. Day and P. Doble, *Optimisation of the separation of herbicides by linear gradient high performance liquid chromatography utilising artificial neural networks.* Talanta, **2007**. ***71***(3): p. 1268-1275. DOI: 10.1016/j.talanta.2006.06.031.

187. E. Marengo, V. Gianotti, S. Angioi and M. C. Gennaro, *Optimization by experimental design and artificial neural networks of the ion-interaction reversed-phase liquid chromatographic separation of twenty cosmetic preservatives.* Journal of Chromatography A, **2004**. ***1029***(1–2): p. 57-65. DOI: http://dx.doi.org/10.1016/j.chroma.2003.12.044.

188. S. Casamento, B. Kwok, C. Roux, M. Dawson and P. Doble, *Optimization of the separation of organic explosives by capillary electrophoresis with artificial neural networks.* Journal of Forensic Sciences, **2003**. ***48***(5): p. 1075-1083.

189. V. K. Gupta, H. Khani, B. Ahmadi-Roudi, S. Mirakhorli, E. Fereyduni and S. Agarwal, *Prediction of capillary gas chromatographic retention times of fatty acid methyl esters in human blood using mlr, pls and back-propagation artificial neural networks.* Talanta, **2011**. ***83***(3): p. 1014-1022. DOI: http://dx.doi.org/10.1016/j.talanta.2010.11.017.

190. J. W. Dolan, *Temperature selectivity in reversed-phase high performance liquid chromatography.* Journal of Chromatography A, **2002**. ***965***(1–2): p. 195-205. DOI: http://dx.doi.org/10.1016/S0021-9673(01)01321-8.

191. P. L. Zhu, L. R. Snyder, J. W. Dolan, N. M. Djordjevic, D. W. Hill, L. C. Sander and T. J. Waeghe, *Combined use of temperature and solvent strength in reversed-phase gradient elution i. Predicting separation as a function of temperature and gradient conditions.* Journal of Chromatography A, **1996**. ***756***(1–2): p. 21-39. DOI: http://dx.doi.org/10.1016/S0021-9673(96)00721-2.

192. P. L. Zhu, J. W. Dolan and L. R. Snyder, *Combined use of temperature and solvent strength in reversed-phase gradient elution ii. Comparing selectivity for different samples and systems.* Journal of Chromatography A, **1996**. ***756***(1–2): p. 41-50. DOI: http://dx.doi.org/10.1016/S0021-9673(96)00722-4.

193. T. Borch and R. Gerlach, *Use of reversed-phase high-performance liquid chromatography–diode array detection for complete separation of 2,4,6-trinitrotoluene metabolites and epa method 8330 explosives: Influence of temperature and an ion-pair reagent.* Journal of Chromatography A, **2004**. ***1022***(1–2): p. 83-94. DOI: http://dx.doi.org/10.1016/j.chroma.2003.09.067.

194. Z. P. Wu, Y. Tong, J. Y. Yu, X. R. Zhang, C. X. Pan, X. Y. Deng, Y. C. Xu and Y. X. Wen, *Detection of n,n'-diphenyl-n,n'-dimethylurea (methyl centralite) in gunshot residues using ms-ms method.* Analyst, **1999**. ***124***(11): p. 1563-1567.

195. J. B. F. Lloyd and R. M. King, *One-pot processing of swabs for organic explosives and firearms residue traces.* Journal of Forensic Sciences, **1990**. ***35***(4): p. 956-959.

196. O. Dalby and J. W. Birkett, *The evaluation of solid phase micro-extraction fibre types for the analysis of organic components in unburned propellant powders.* Journal of Chromatography A, **2010**. ***1217***(46): p. 7183-7188. DOI: 10.1016/j.chroma.2010.09.012.

197. J. Bueno and I. Lednev, *Advanced statistical analysis and discrimination of gunshot residue implementing combined raman and ftir data.* Analytical Methods, **2013**. DOI: 10.1039/C3AY40721G.

198. N. Song-im, S. Benson and C. Lennard, *Evaluation of different sampling media for their potential use as a combined swab for the collection of both organic and inorganic explosive residues.* Forensic Science International, **2012**. ***222***(1–3): p. 102-110. DOI: http://dx.doi.org/10.1016/j.forsciint.2012.05.006.

199. D. Perret, S. Marchsese, A. Gentili, R. Curini, A. Terracciano, E. Bafile and F. S. Romolo, *Lc-ms-ms determination of stabilizers and explosive residues in hand-swabs.* Chromatographia, **2008**. ***68***: p. 517-524.

200. C. A. Crowson, H. E. Cullum, R. W. Hiley and A. M. Lowe, *A survey of high explosives traces in public places.* Journal of Forensic Sciences, **1996**. ***41***(6): p. 980-989.

201. J. M. F. Douse, *Trace analysis of explosives at the low nanogram level in handswab extracts using columns of amberlite xad-7 porous polymmer beads and silica capillary column gas chromatography with thermal energy analysis and electron-capture detection.* Journal of Chromatography A, **1985**. ***328***(0): p. 155-165. DOI: 10.1016/s0021-9673(01)87387-8.

202. A.-L. Gassner, C. Ribeiro, J. Kobylinska, A. Zeichner and C. Weyermann, *Organic gunshot residues: Observations about sampling and transfer mechanisms.* Forensic Science International, **2016**. ***266***: p. 369-378. DOI: http://dx.doi.org/10.1016/j.forsciint.2016.06.029.

203. J. D. Twibell, J. M. Home, K. W. Smalldon and D. G. Higgs, *The quantities of nitroglycerine recovered from hands after contact with commercial explosives.* Journal of Forensic Sciences, **1982**. ***27***(4): p. 783-791.

204. T. L. Davis and A. A. Ashdown, *Transformations of diphenylamine during the aging of smokeless powder.* Industrial & Engineering Chemistry, **1925**. ***17***(7): p. 674-675. DOI: 10.1021/ie50187a007.

205. W. A. Schroeder, E. W. Malmberg, L. L. Fong, K. N. Trueblood, J. D. Landerl and E. Hoerger, *Chromatographic investigations of smokeless powder.* Industrial & Engineering Chemistry, **1949**. ***41***(12): p. 2818-2827. DOI: 10.1021/ie50480a037.

206. B. Yeager, K. Bustin, J. Stewart, R. Dross and S. Bell, *Evaluation and validation of ion mobility spectrometry for presumptive testing targeting the organic constituents of firearms discharge residue.* Analytical Methods, **2015**. *7*(22): p. 9683-9691. DOI: 10.1039/C5AY02417J.

APPENDICES

Appendix I: Front (left column) and back (right column) of printed wax pattern heated to 60 °C for 5 min (a) and 150 °C for 5 min (b). No change of the printed pattern can be observed when heated to 60 °C.

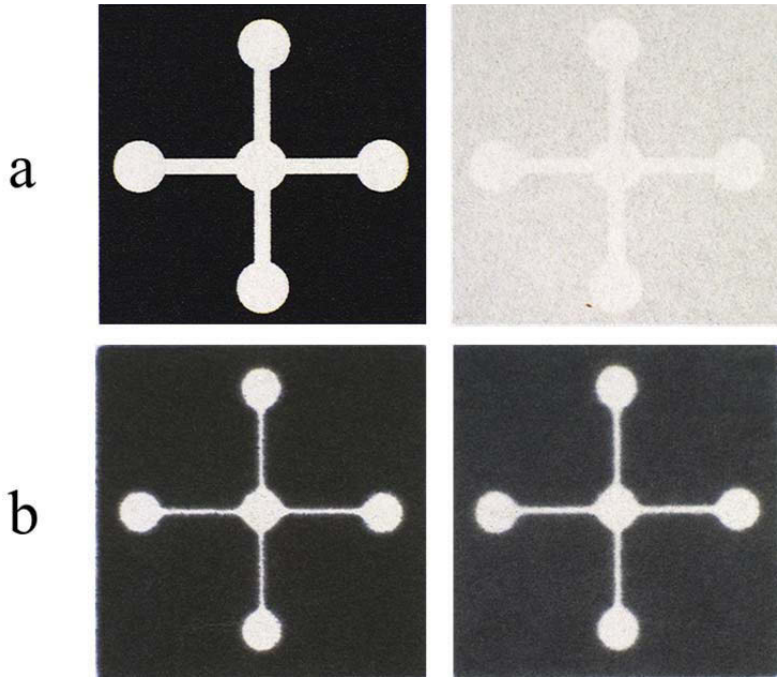

Appendix II: Non- heated (left column) and heated (right column; 150 °C at 5 min) vertical and horizontal lines with nominal widths ranging from 0.100-1.000 mm with 0.100 mm increments. The different printing colours were yellow (a), blue (b), magenta (c) and black (d).

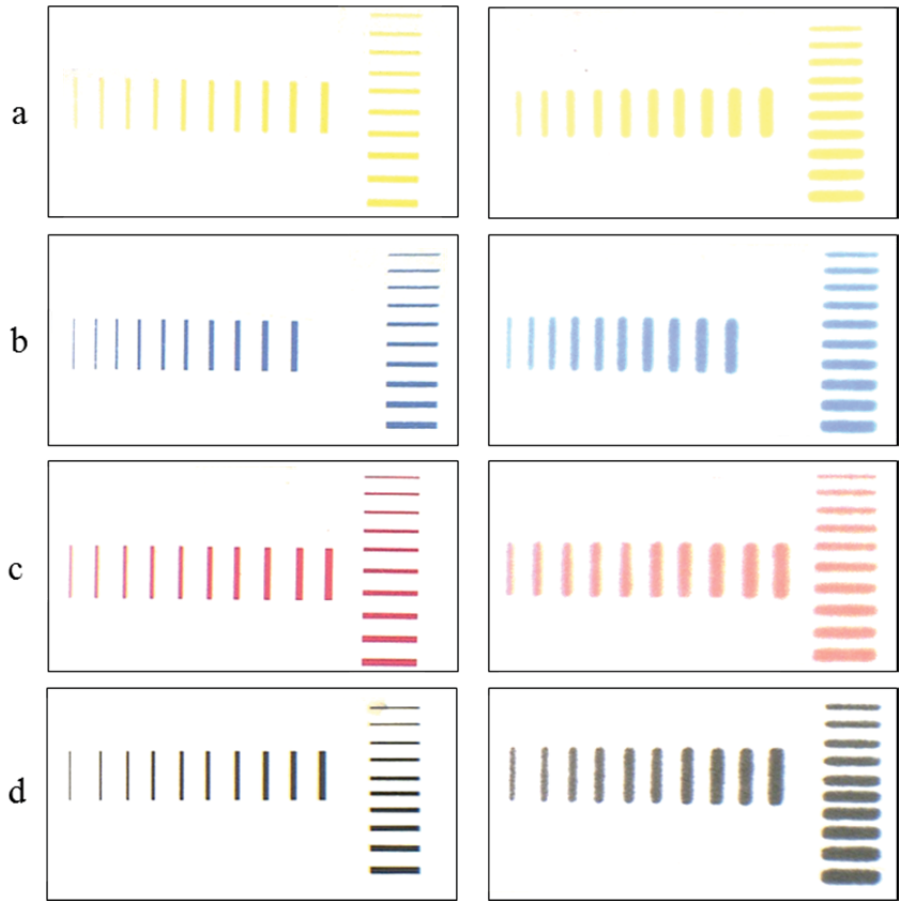

Appendix III: Data of triplicate measurements of nominal width (W_N), printed width (W_P), and heated width (W_H) of vertical and horizontal lines with W_Ns ranging from 0.100-1.000 mm with 0.100 mm increments. SD = standard deviation.

Yellow Vertical [mm]				
W_N	W_P (average)	W_P (SD)	W_H (average)	W_H (SD)
0.1	0.195	0.015	0.907	0.047
0.2	0.268	0.009	1.033	0.030
0.3	0.374	0.005	1.293	0.061
0.4	0.466	0.012	1.277	0.015
0.5	0.626	0.008	1.827	0.012
0.6	0.657	0.010	1.887	0.032
0.7	0.760	0.009	2.050	0.026
0.8	0.852	0.003	2.227	0.051
0.9	0.997	0.003	2.387	0.059
1	1.110	0.017	2.547	0.045

Yellow Horizontal [mm]				
W_N	W_P (average)	W_P (SD)	W_H (average)	W_H (SD)
0.1	0.212	0.012	0.965	0.021
0.2	0.342	0.015	1.187	0.031
0.3	0.444	0.009	1.303	0.050
0.4	0.495	0.014	1.550	0.066
0.5	0.602	0.046	1.647	0.055
0.6	0.739	0.017	1.800	0.026
0.7	0.793	0.029	1.933	0.055
0.8	0.947	0.023	2.093	0.025
0.9	1.003	0.015	2.303	0.025
1	1.133	0.006	2.197	0.006

Appendix III continued: Data of triplicate measurements of nominal width (W_N), printed width (W_P), and heated width (W_H) of vertical and horizontal lines with W_Ns ranging from 0.100-1.000 mm with 0.100 mm increments. SD = standard deviation.

Cyan Vertical [mm]				
W_N	W_P (average)	W_P (SD)	W_H (average)	W_H (SD)
0.1	0.179	0.005	1.014	0.027
0.2	0.283	0.003	1.230	0.026
0.3	0.378	0.007	1.473	0.046
0.4	0.524	0.009	1.770	0.017
0.5	0.614	0.009	1.893	0.076
0.6	0.662	0.003	1.930	0.036
0.7	0.822	0.003	2.210	0.046
0.8	0.857	0.010	2.227	0.047
0.9	0.998	0.003	2.387	0.059
1	1.067	0.006	2.463	0.070

Cyan Horizontal [mm]				
W_N	W_P (average)	W_P (SD)	W_H (average)	W_H (SD)
0.1	0.258	0.011	1.133	0.025
0.2	0.378	0.022	1.320	0.080
0.3	0.424	0.016	1.370	0.026
0.4	0.535	0.024	1.470	0.046
0.5	0.650	0.003	1.647	0.029
0.6	0.704	0.014	1.750	0.035
0.7	0.817	0.016	1.957	0.049
0.8	0.922	0.016	2.053	0.051
0.9	1.043	0.006	2.187	0.006
1	1.150	0.010	2.353	0.040

Appendix III continued: Data of triplicate measurements of nominal width (W_N), printed width (W_P), and heated width (W_H) of vertical and horizontal lines with W_Ns ranging from 0.100-1.000 mm with 0.100 mm increments. SD = standard deviation.

Magenta Vertical [mm]				
W_N	W_P (average)	W_P (SD)	W_H (average)	W_H (SD)
0.1	0.198	0.009	1.457	0.080
0.2	0.330	0.010	1.850	0.044
0.3	0.425	0.005	2.013	0.021
0.4	0.540	0.001	2.167	0.015
0.5	0.599	0.010	2.233	0.076
0.6	0.729	0.008	2.407	0.015
0.7	0.827	0.016	2.617	0.091
0.8	0.917	0.004	2.770	0.046
0.9	1.006	0.007	2.950	0.090
1	1.107	0.006	3.130	0.121

Magenta Horizontal [mm]				
W_N	W_P (average)	W_P (SD)	W_H (average)	W_H (SD)
0.1	0.246	0.022	1.310	0.053
0.2	0.340	0.004	1.550	0.017
0.3	0.426	0.011	1.790	0.095
0.4	0.522	0.003	1.930	0.026
0.5	0.571	0.012	2.000	0.046
0.6	0.681	0.009	2.190	0.050
0.7	0.804	0.006	2.423	0.065
0.8	0.920	0.011	2.493	0.146
0.9	1.053	0.012	2.520	0.062
1	1.143	0.006	2.860	0.017

Appendix III continued: Data of triplicate measurements of nominal width (W_N), printed width (W_P), and heated width (W_H) of vertical and horizontal lines with W_Ns ranging from 0.100-1.000 mm with 0.100 mm increments. SD = standard deviation.

Black Vertical [mm]				
W_N	W_P (average)	W_P (SD)	W_H (average)	W_H (SD)
0.1	0.182	0.008	1.083	0.045
0.2	0.300	0.019	1.373	0.061
0.3	0.382	0.010	1.677	0.070
0.4	0.560	0.019	1.917	0.055
0.5	0.632	0.003	2.050	0.080
0.6	0.672	0.009	2.097	0.110
0.7	0.778	0.017	2.250	0.017
0.8	0.946	0.019	2.507	0.064
0.9	0.976	0.005	2.610	0.115
1	1.133	0.006	2.700	0.078

Black Horizontal [mm]				
W_N	W_P (average)	W_P (SD)	W_H (average)	W_H (SD)
0.1	0.248	0.010	1.190	0.056
0.2	0.320	0.004	1.333	0.023
0.3	0.399	0.006	1.580	0.062
0.4	0.520	0.012	1.810	0.078
0.5	0.647	0.013	2.047	0.067
0.6	0.668	0.016	2.157	0.050
0.7	0.803	0.018	2.283	0.115
0.8	0.917	0.008	2.447	0.012
0.9	1.040	0.035	2.627	0.055
1	1.150	0.017	2.910	0.069

Appendix IV: Coloured hydrophobic circles in black (a), magenta (b), cyan (c), yellow (d) and green (e) with nominal widths of the inner circle from 0.050- 0.450 mm with increments of 0.050 mm (see left column) generated under the same conditions as in Figure 3. All circles are filled with 5 µL of a 1 mg/mL Orange G aqueous solution (1) or Acid Green (2). The marked areas highlight inner circles which are not reliable hydrophobic barriers as the solution does not stay within them. Image is taken under visible light.

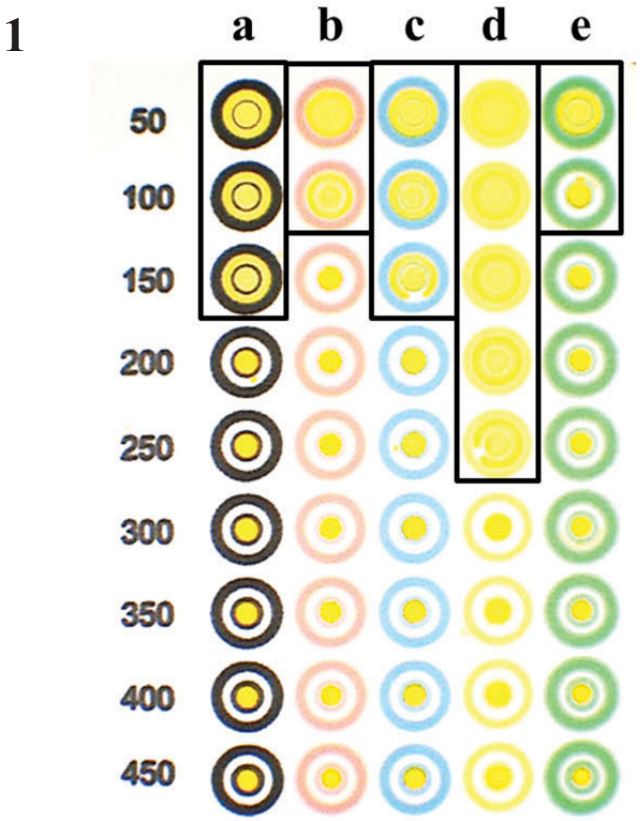

Appendix IV continued: Coloured hydrophobic circles in black (a), magenta (b), cyan (c), yellow (d) and green (e) with nominal widths of the inner circle from 0.050- 0.450 mm with increments of 0.050 mm (see left column) generated under the same conditions as in Figure 3. All circles are filled with 5 µL of a 1 mg/mL Orange G aqueous solution (1) or Acid Green (2). The marked areas highlight inner circles which are not reliable hydrophobic barriers as the solution does not stay within them. Image is taken under visible light.

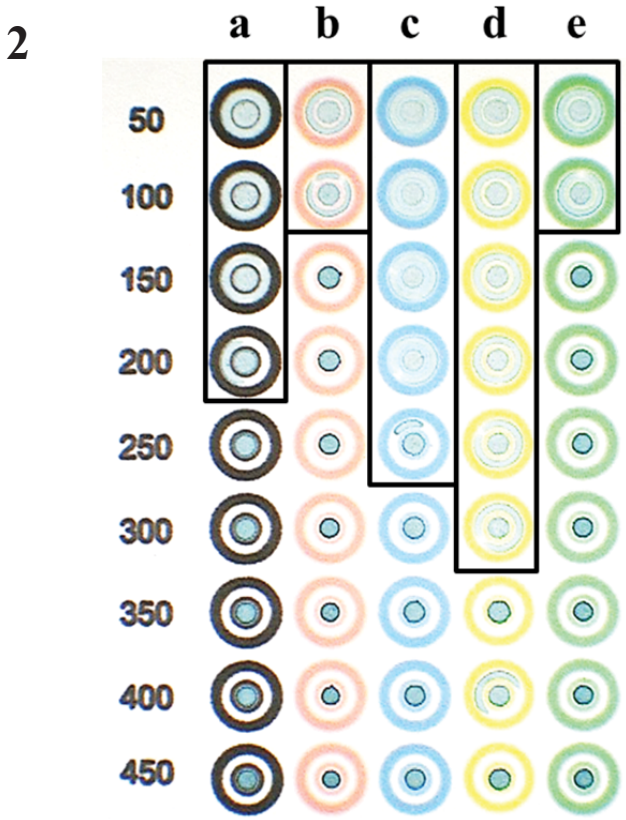

Appendix V: Hydrophobic circles of 0.050-0.300 mm nominal width with increments of 0.050 mm for five mixed colours; orange (b), dark green (c), light green (d), blue (e) and dark purple (f) and a reference standard, magenta (a) filled with 5 µL of Orange G. The marked areas highlight inner circles which are not reliable hydrophobic barriers as the solution does not stay within them. Image is taken under visible light.

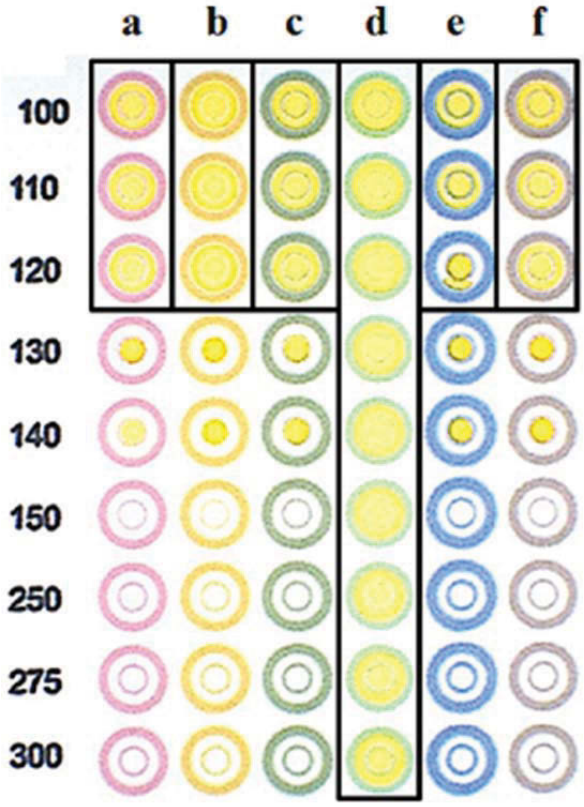

Appendix VI: Test of the hydrophobic quality of the wax circles after pretreating each of them with 5 µL hexane (a) or 5 µL methanol (b). After drying, 5 µL of various solvent mixtures were pipetted in the circles. The solvent compositions of the columns are: A-methanol:water mixture, B-ethanol:water mixture, C-propanol:water mixture and D-acetonitrile:water mixture. Ratios of organic solvents:water are given in the left column starting from 10 % organic solvent at the top to 100 % at the bottom. Picture is taken with visible light. All solutions are coloured with 1 mg/mL Terasil Blue.

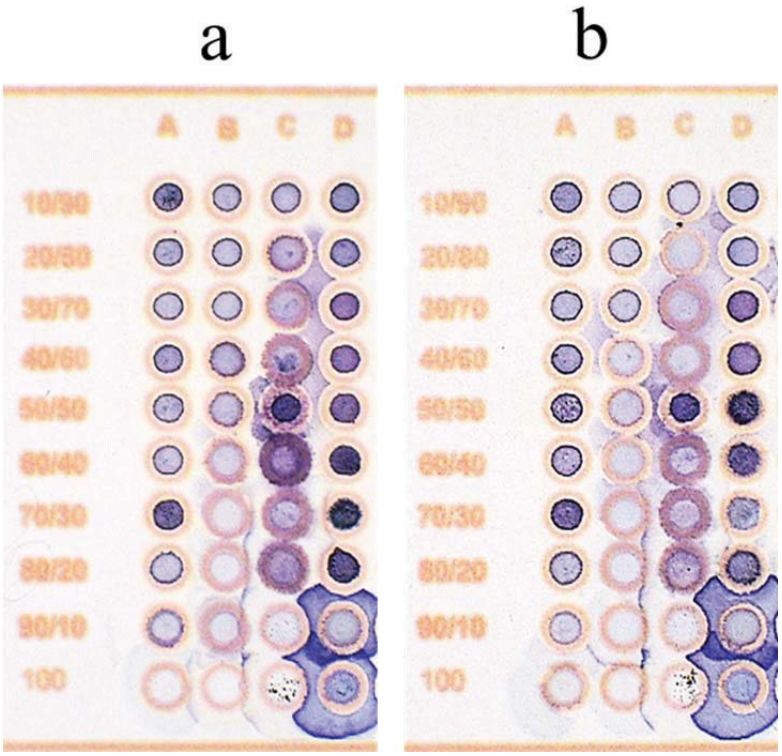

Appendix VII: List of compounds detected in unfired smokeless powders and specimens collected from the hands of a shooter after discharging various ammunition-firearm combinations. PETN was excluded as interferences for these compounds were previously found on samples taken from hands. S&W = Smith&Wesson; ND = not detected, <LOD = compounds were detected, however below the calculated LOD. More details about ammunitions and firearms can be found in Table 4-3.

Ammunition	Firearm	Collection device	No of shots	Compounds detected [ng]												
				1,3-DNG	1,2-DNG	NG	2,4-DNT	m-NT	DEP	MC	N-nDPA	DPA	2,4-DNDPA	2-NDPA	EC	DBP*
WinClean 45 Auto CP Winchester (AUS)	-	-	-	6.69	10.77	1881.66						87.27		1.39	5.78	48.05
	Pistol Colt (USA)	swab	**1**	<LOD	<LOD	3.19 [ND-5.11]						1.17 [ND-3.04]		1.46 [0.13-2.16]	ND	ND
			3	ND	ND	25.43 [4.08-54.86]						3.56 [ND-9.29]		ND	ND	6.69 [ND-12.75]
		stub	**1**	ND	0.39 [0.33-0.47]	6.48 [3.20-11.46]						ND		ND	0.79 [0.70-0.91]	5.89 [2.54-10.52]
			3#													
45 Auto CP Winchester (AUS)	-	-	-	33.46	53.85	5128.42		<LOD	44.63			30.30		10.76	5.36	38.79
	Pistol Colt (USA)	swab	**1**	<LOD	<LOD	5.90 [4.03-9.54]		<LOD	ND			3.77 [0.75-5.38]		ND	ND	7.09 [5.61-8.03]
			3	<LOD	<LOD	4.46 [ND-9.71]		ND	ND			0.03 [ND-0.08]		ND	ND	4.05 [ND-8.54]
		stub#														
44 REM Magnum PMC (USA)	-	-	-	6.10	7.33	1316.41		1.42	49.51			89.72		14.07		
	Pistol S&W (USA)	swab	**1**	<LOD	<LOD	1.73		<LOD	ND			5.73		4.94		
			3	<LOD	<LOD	<LOD		<LOD	ND			8.20		3.76		
		stub	**1**	ND	0.04	ND		0.22	ND			1,13		ND		
			3	0.03 [ND-0.05]	0.85 [0.47-1.24]	2.9 [2.35-3.47]		ND	ND			ND		ND		
44 REM Magnum, Winchester (Australia)	-	-	-	3.06	7.98	5118.6			56.19			2.19		ND	107.7	
	Pistol S&W (USA)	swab	**1**	ND	ND	1.01 [ND-2.73]			ND		ND	6.10 [ND-18.29]		2.69 [0.62-6.51]	0.81 [0.40-1.11]	
			3	ND	ND	0.95 [ND-1.66]			ND		ND	6.73 [ND-11.96]		1.99 [0.13-3.69]	1.77 [ND-4.21]	
		stub	**1**	ND	0.58 [0.19-1.18]	6.27 [3.71-11.01]			ND		2.24 [1.21-3.99]	0.10 [ND-0.30]		ND	0.62 [ND-1.35]	
			3	ND	0.90 [0.81-0.98[]	ND			**ND**		ND	ND		ND	2.92 [ND-5.61]	
9 mm Parabellum CCI (USA)	-	-	-	13.04	9.97	4904.59					ND	3.06		1.34	107.9	11.26
	Pistol Beretta (Italy)	swab	**1**	ND	ND	2.82 [ND-5.46]					ND	ND		6.00 [4.12-7.40]	2.11 [ND-4.05]	2.21 [ND-4.96]
			3	ND	ND	7.05 [ND-11.66]					ND	ND		5.38 [4.21-6.18]	2.59 [2.36-2.92]	141.75 [108.64-162.99]
		stub	**1**	ND	ND	8.87 [6.65-14.46]					1.59 [1.45-1.77]	1.91 [1.47-2.18]		4.20 [ND-5.72]	2.68 [2.19-2.66]	22.34 [ND-36.45]
			3	ND	0.34 [0.15-0.49]	ND					0.80 [ND-1.25]	1.29 [ND-2.58]		1.82 [ND-5.46]	1.39 [ND-2.20]	ND
357 Magnum Winchester (Australia)	-	-		ND	5.57	1908.95	2.32	74.67	40.76			134.30	30.96	9.77	512.56	92.35
	Revolver S&W (USA)	swab	**1**	ND	ND	ND	ND	ND	0.50 [ND-1.44]			ND	ND	1.89 [0.14-3.64]	0.74 [0.39-1.09]	23.81 [ND-47.95]
			3	ND	ND	ND	ND	ND	ND			0.10 [ND-0.31]	ND	2.24 [1.44-2.76]	0.35 [ND-0.80]	56.76 [ND-95.64]
		stub	**1**	0.04 [ND-1.01]	0.53 [0.48--.60]	ND	<LOD	ND	0.84 [0.65-1.11]			0.71 [ND-2.12]		0.29 [ND-0.61]	1.04 [0.47-1.42]	2.77 [2.13-3.74
			3	ND	0.43 [0.06-0.80]	ND	ND	ND	0.34 [ND-0.68]			ND	ND	ND	0.22 [ND-0.45]	1.34 [0.71-1.98]

* It should be noted that the quantification of DBP might not be reliable due to UV interferences collected from hands (5.3.1.6)
# Specimens could not be collected due to a malfunction of the firearm

Appendix VII continued: List of compounds detected in unfired smokeless powders and specimens collected from the hands of a shooter after discharging various ammunition-firearm combinations. PETN was excluded as interferences for these compounds were previously found on samples taken from hands. S&W = Smith&Wesson; ND = not detected, <LOD = compounds were detected, however below the calculated LOD.

Ammunition	Firearm	Collection device	No of shots	Compounds detected [ng]											
				1,3-DNG	1,2-DNG	NG	2,4-DNT	m-NT	DEP	MC	N-nDPA	DPA	2,4-DNDPA	2-NDPA	EC	DBP*
357 Magnum PMC (USA)	-	-	-	6.55	104.52	1448.67			65.12		<LOD	98.94		15.84	ND	ND
	Revolver S&W (USA)	swab	1	ND	2.76 [ND-4.14]	ND			ND		ND	ND		2.40 [ND-6.16]	ND	6.28 [ND-18.86]
			3	ND	ND	ND			ND		ND	ND		2.08 [1.04-3.48]	ND	30.04 [ND-86.61][
		stub	1	ND	0.51 [ND-1.07]	3.84 [ND-11.52]			ND		0.50 [ND-1.51]	0.14 [ND-0.43]		ND	ND	1.23 [ND-1.95]
			3	ND	0.85 [0.33-1.58]	1.43 [ND-4.30]			ND		ND	0.55 [ND-1.66]		ND	ND	0.61 [ND-1.02]
22 LR High Velocity Remington (USA)	-	-	-		18.70	2445.25		0.98			0.12	68.88	28.70	5.74	9.35	
	Pistol Sports King (USA)	swab	1		ND	13.91 [ND-43.33]		ND			ND	ND	ND	1.81 [0.74-3.05]	0.83 [0.66-1.45]	
		stub	1		0.09 [ND-0.26]	7.97 [ND-14.26]		ND			2.86 [2.05-4.03]	3.78 [1.82-7.12]	ND	2.13 [1.84-2.19]	3.07 [ND-5.14]	
22 LR High Velocity SuperSpeed Winchester (Australia)	-	-	-	1164	117.46	2027.27			86.49			66.50		10.51	6.00	39.69
	Pistol Sports King (USA)	swab	1	ND	ND	0.40 [ND-0.64]			ND			ND		0.65 [ND-1.39]	ND	37.32 [6.00-54.35]
		stub	1	ND	0.30 [ND-0.77]	ND			ND			0.82 [ND-1.26]		ND	ND	2.02 [1.61-1.81]
22 LR High Velocity Remington (USA)	-	-	-		18.70	2445.25					0.12	68.88	28.70	5.74	9.35	
	Rifle Marlin (USA)	swab	1		ND	ND					ND	ND	ND	ND	ND	
			3		ND	ND					ND	ND	ND	ND	ND	
		stub	1		ND	ND					ND	ND		ND	ND	
			3		ND	ND					ND	ND		ND	ND	
22 LR High Velocity SuperSpeed Winchester (AUS)	-	-	-	11.64	117.46	2027.27		86.49				66.50		10.51	6.00	39.69
	Rifle Marlin (USA)	swab	1	ND	ND	ND		ND				ND		0.78 [0.44-1.26]	0.41 [0.17-0.74]	62.76 [51.49-74.98]
			3	ND	ND	0.15 [ND-0.45]		ND				ND		1.18 [0.65-2.10]	1.16 [0.51-2.42]	81.00 [69.73-89.41]
		stub	1	0.24 [ND-0.48]	1.12 [0.20-2.04]	0.89 [ND-1.78]		ND				ND		ND	0.13 [ND-0.25]	3.13 [2.85-3.40]
			3	ND	0.47 [0.23-0.83]	ND		ND				0.16 [ND-0.47]		0.42 [ND-1.09]	0.18 [ND-0.40]	2.91 [2.71-3.11]
40 WinClean S&W Winchester (AUS)	-	-		53.54	137.6	4141.70	36.74		122.64	ND	18.91			6.93	1.28	5.24
	Pistol Glock (USA)	swab	1	ND	ND	3.25 [ND-9.76]	ND		0.87 [0.53-1.08]	ND	ND			3.75 [0.91-5.73]	2.54 [1.40-4.07]	73.18 [16.76-106.23]
			3	ND	ND	0.44 [ND-1.15]	ND		0.81 [0.47-1.00]	ND	1.46 [ND-4.38]			2.25 [1.25-3.38]	3.64 [2.45-5.55]	63.02 [16.76-102.87]
		stub	1	ND	0.05 [ND-0.14]	14.39 [ND-16.60]	ND		1.38 [ND-2.12]	2.35 [1.85-2.79]	1.51 [1.48-1.57]			2.16 [1.87-2.64]	2.67 [2.27-2.99]	ND
			3	ND	0.90 [0.49-1.31]	1.33 [ND-2.65]	ND		ND	ND	0.09 [ND-0.188]			ND	0.82 [0.30-1.34]	0.32 [ND-0.64]

* It should be noted that the quantification of DBP might not be reliable due to interferences collected from hands (5.3.1.6)
# Specimens could not be collected due to a malfunction of the firearm

Appendix VII continued: List of compounds detected in unfired smokeless powders and samples collected from the hands of a shooter after discharging various ammunition-firearm combinations. PETN and DBP were excluded as interferences for these compounds were previously found on samples taken from hands. S&W = Smith&Wesson; ND = not detected, <LOD = compounds were detected, however below the calculated LOD.

Ammunition	Firearm	Collection device	No of shots	Compounds detected [ng]											
				1,3-DNG	1,2-DNG	NG	2,4-DNT	m-NT	DEP	MC	N-nDPA	DPA	2,4-DNDPA	2-NDPA	EC	DBP*
40 S&W Winchester (AUS)	-	-	-	10.64	138.65	3153.90			91.291	33.126		115.45		12.50	2.61	18.32
	Pistol Glock (USA)	swab	**1**	ND	ND	5.99 [2.98-10.55]			8.08 [ND-10.10]	1.08 [0.63-1.48]		ND		1.99 [0.98-2.91]	2.97 [1.40-5.64]	81.65 [74.86-90.12]
			3	ND	0.29 [ND-0.54]	6.05 [3.94-8.86]			11.02 [0.54-12.57]	1.38 [1.10-1.61]		ND		1.80 [1.22-2.11]	2.89 [0.25-6.45]	93.11 [78.98-102.11]
		stub	**1**	ND	0.45 [ND-0.77]	1.21 [ND-3.64]			ND	0.35 [ND-1.05]		ND		1.39 [ND-4.17]	1.60 [0.26-2.63]	2.95 [2.19-4.00]
			3	ND	0.28 [ND-0.56]	2.68 [1.32-4.04]			8.89 [3.01-12.02]	0.87 [0.78-0.96]		ND		3.89 [3.74-4.04]	1.66 [1.51-1.80]	1.42 [0.81-2.03]
12 gauge SuperX Winchester (Australia)	-	-	-	8.93	ND	4003.38		1.30	93.23		0.56	61.97	0.41	14.07	6.56	40.30
	Shotgun Remington (USA)	swab	**1**	ND	ND	ND		ND	ND		ND	3.39 [ND-7.97]	ND	2.19 [2.09-2.31]	1.54 [0.59-3.10]	49.03 [0.05-113.42]
			3	ND	ND	ND		ND	ND		1.47 [ND-1.40]	2.34 [1.99-2.86]		1.97 [1.80-2.07]	1.33 [0.85-1.58]]	99.19 [84.95-111.06]
		stub	**1**	ND	0.82 [0.63-1.00]	ND		ND	ND		2.94 [2.68-3.20]	ND		1.21 [1.05-1.37]	3.06 [2.77-3.35]	1.00 [0.24-1.75]
			3	ND	0.02 [ND-0.07]	ND		ND	ND		0.76 [ND-2.28]	ND		ND	0.99 [ND-2.98]	ND

* It should be noted that the quantification of DBP might not be reliable due to interferences collected from hands (5.3.1.6)
# Specimens could not be collected due to a malfunction of the firearm

Appendix VIII: Extraction recoveries of the 15 target compounds using MTBE and different extraction techniques, i.e. sonication (15 min), centrifugation (5 min at 4 rpm), combined techniques (15 min sonication + 5 min centrifugation at 4 rpm), and combined techniques with increased temperature (15 min sonication with increased temperature (40 °C) and 5 min centrifugation at 4 rpm) at three different concentrations, i.e. 12 ng, 20 ng, and 30 ng spiked onto the alcohol wipe. Error bars represent standard deviations (n = 3).

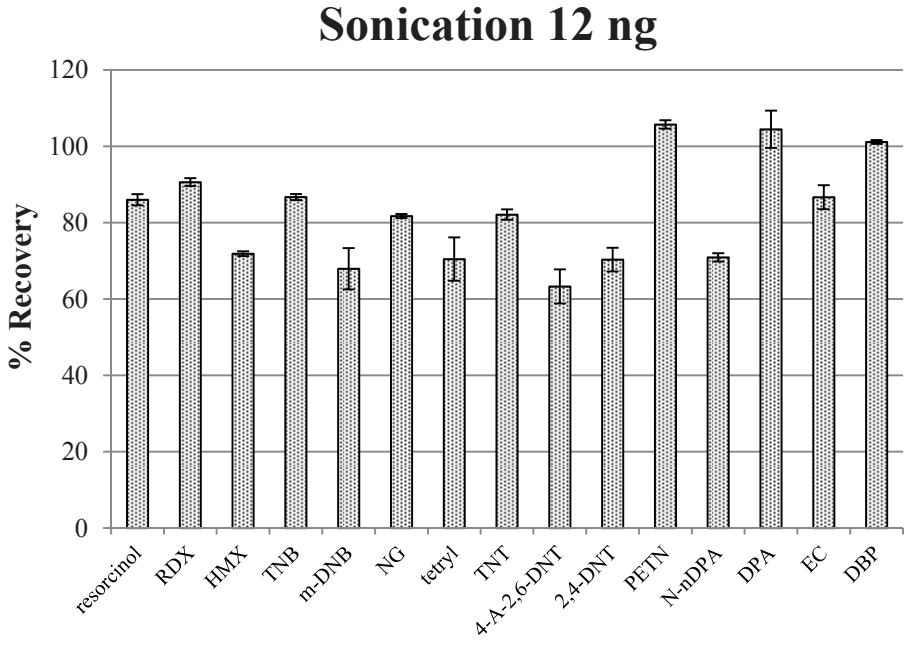

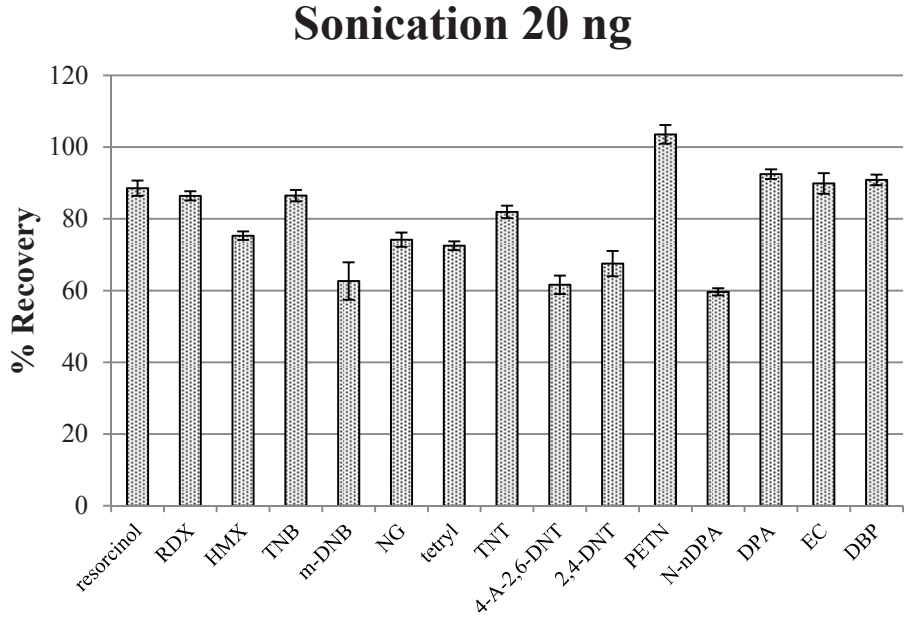

Appendix VIII continued: Extraction recoveries of the 15 target compounds using MTBE and different extraction techniques, i.e. sonication (15 min), centrifugation (5 min at 4 rpm), combined techniques (15 min sonication + 5 min centrifugation at 4 rpm), and combined techniques with increased temperature (15 min sonication with increased temperature (40 °C) and 5 min centrifugation at 4 rpm) at three different concentrations, i.e. 12 ng, 20 ng, and 30 ng spiked onto the alcohol wipe. Error bars represent standard deviations (n = 3).

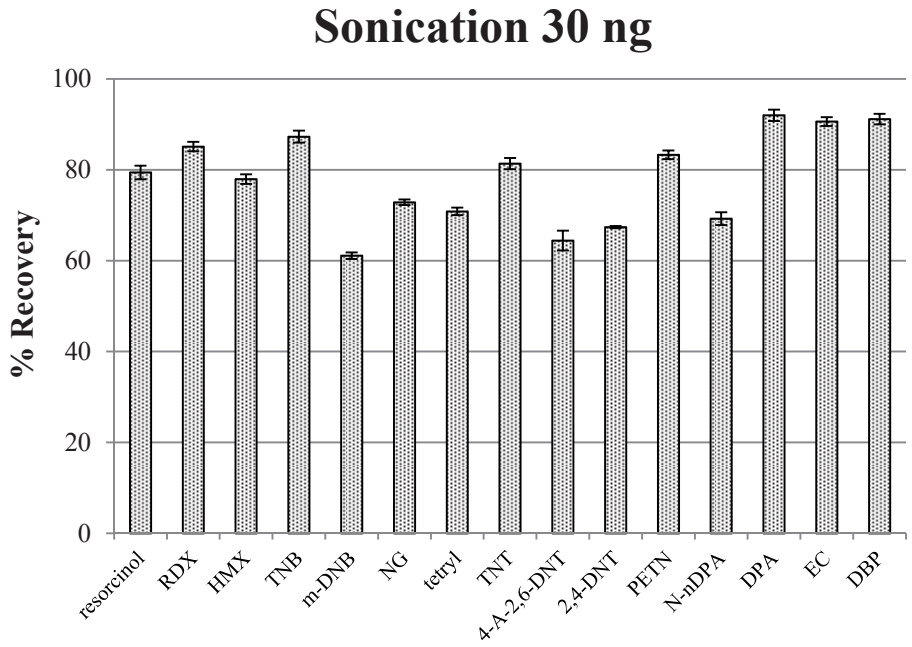

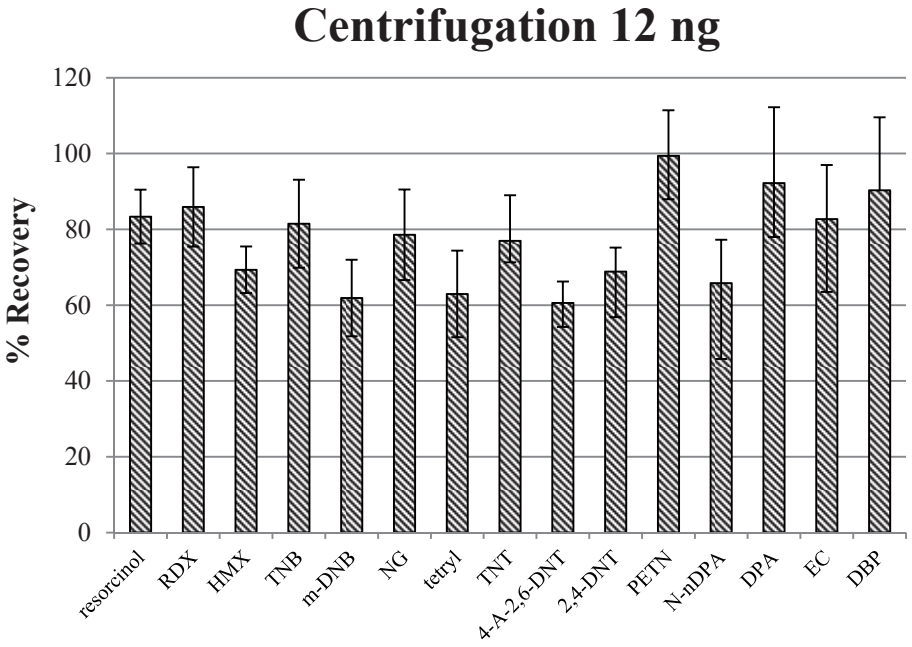

Appendix VIII continued: Extraction recoveries of the 15 target compounds using MTBE and different extraction techniques, i.e. sonication (15 min), centrifugation (5 min at 4 rpm), combined techniques (15 min sonication + 5 min centrifugation at 4 rpm), and combined techniques with increased temperature (15 min sonication with increased temperature (40 °C) and 5 min centrifugation at 4 rpm) at three different concentrations, i.e. 12 ng, 20 ng, and 30 ng spiked onto the alcohol wipe. Error bars represent standard deviations (n = 3).

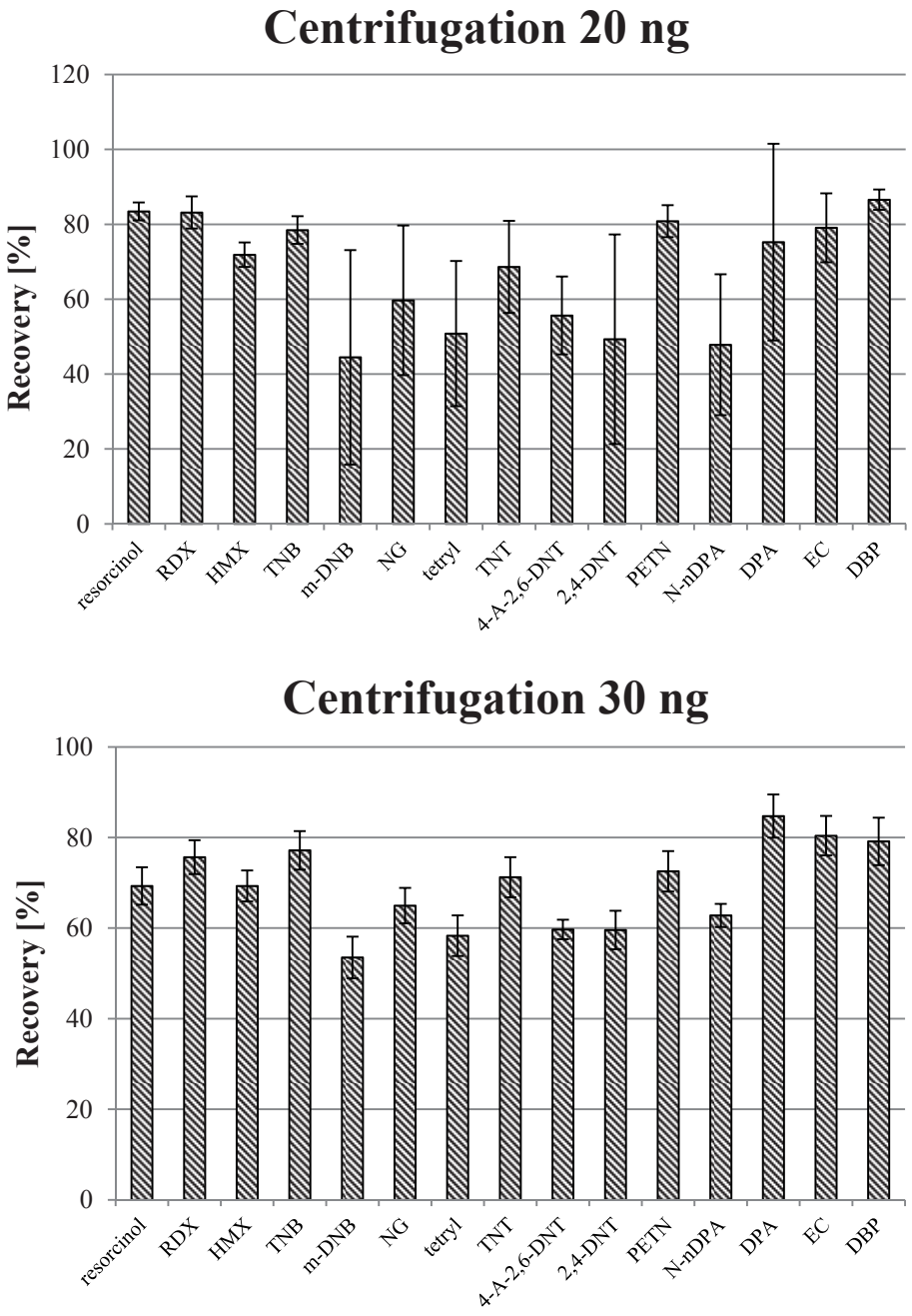

Appendix VIII continued: Extraction recoveries of the 15 target compounds using MTBE and different extraction techniques, i.e. sonication (15 min), centrifugation (5 min at 4 rpm), combined techniques (15 min sonication + 5 min centrifugation at 4 rpm), and combined techniques with increased temperature (15 min sonication with increased temperature (40 °C) and 5 min centrifugation at 4 rpm) at three different concentrations, i.e. 12 ng, 20 ng, and 30 ng spiked onto the alcohol wipe. Error bars represent standard deviations (n = 3).

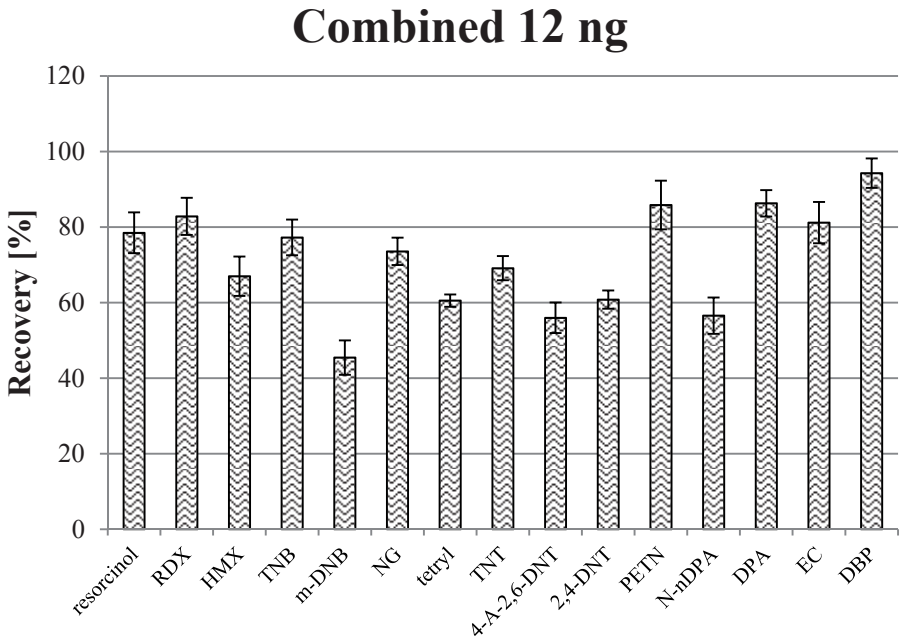

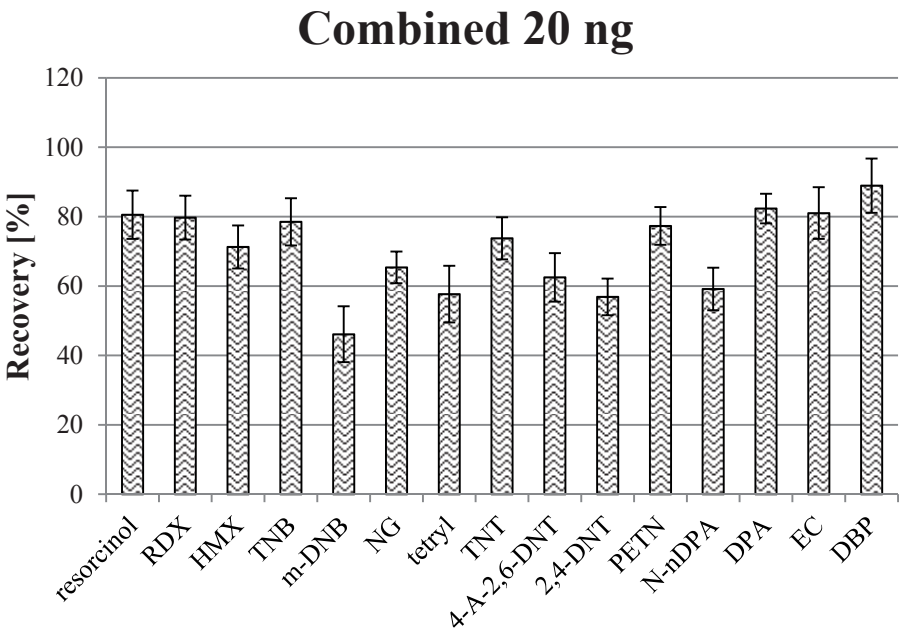

Appendix VIII continued: Extraction recoveries of the 15 target compounds using MTBE and different extraction techniques, i.e. sonication (15 min), centrifugation (5 min at 4 rpm), combined techniques (15 min sonication + 5 min centrifugation at 4 rpm), and combined techniques with increased temperature (15 min sonication with increased temperature (40 °C) and 5 min centrifugation at 4 rpm) at three different concentrations, i.e. 12 ng, 20 ng, and 30 ng spiked onto the alcohol wipe. Error bars represent standard deviations (n = 3).

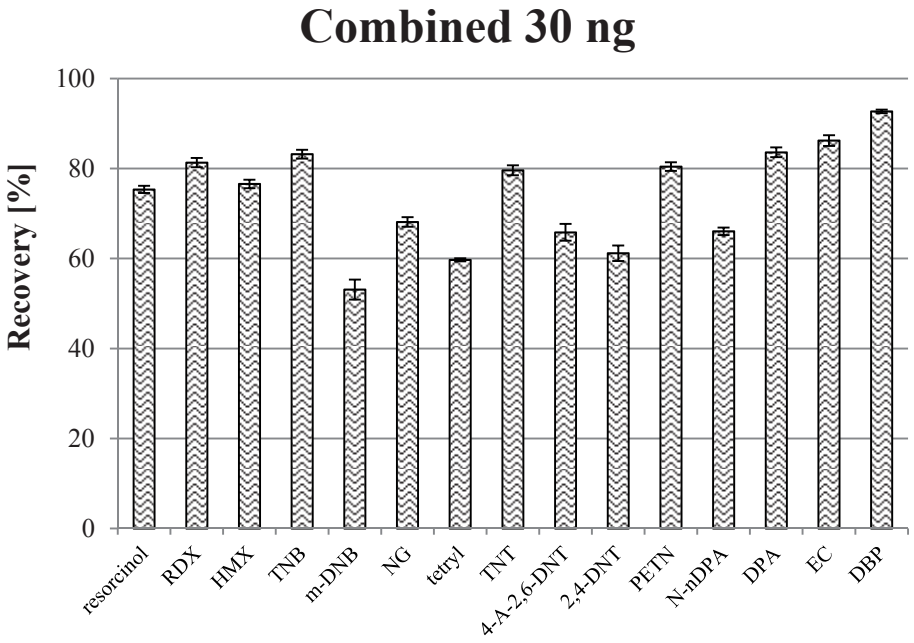

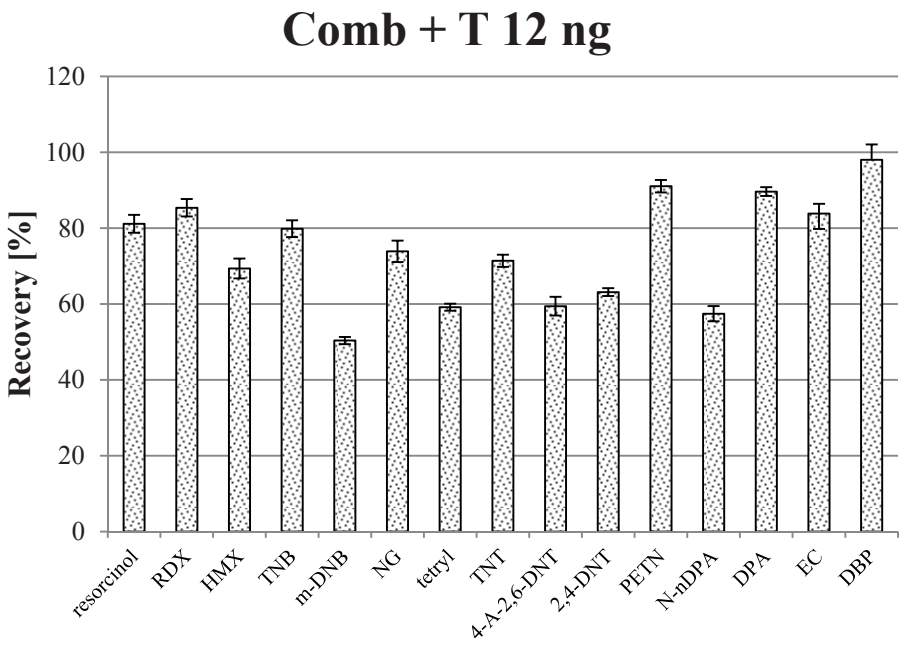

Appendix VIII continued: Extraction recoveries of the 15 target compounds using MTBE and different extraction techniques, i.e. sonication (15 min), centrifugation (5 min at 4 rpm), combined techniques (15 min sonication + 5 min centrifugation at 4 rpm), and combined techniques with increased temperature (15 min sonication with increased temperature (40 °C) and 5 min centrifugation at 4 rpm) at three different concentrations, i.e. 12 ng, 20 ng, and 30 ng spiked onto the alcohol wipe. Error bars represent standard deviations (n = 3).

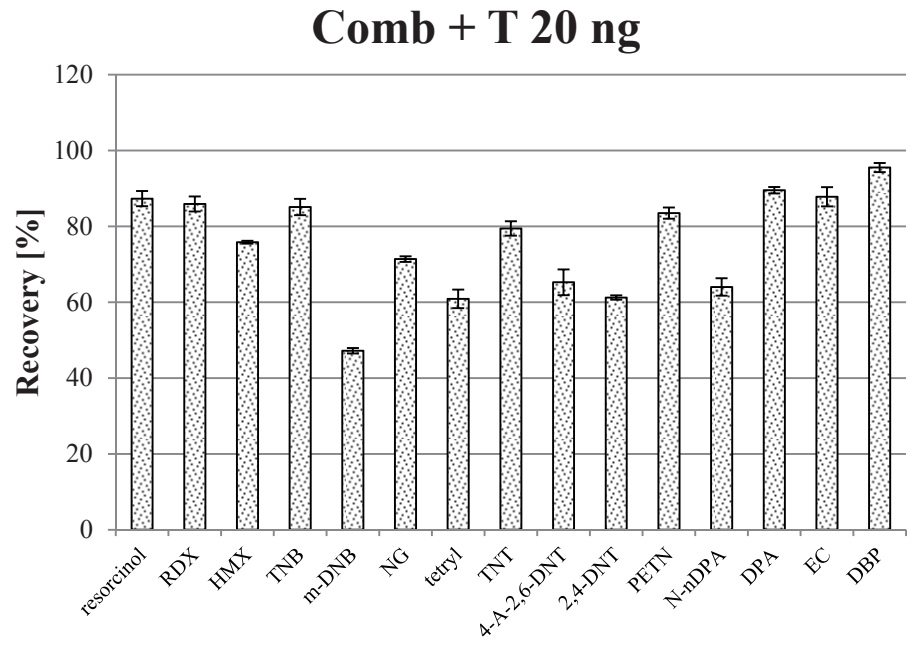

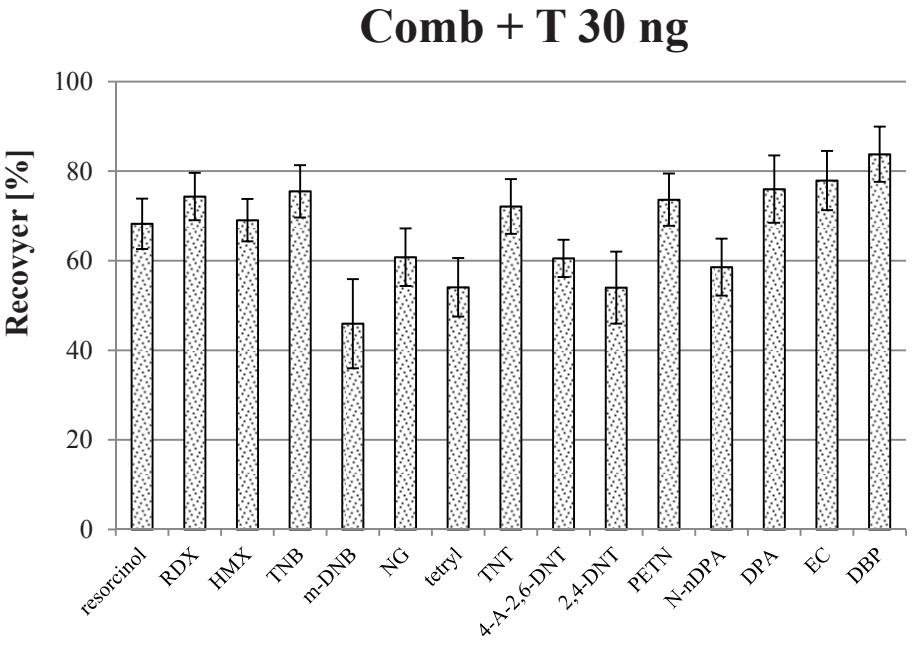

Appendix IX: Comparison of the number of characteristic GSR particles per mm^2 detected after firing different ammunition-firearm combinations when collected using medi wipes or GSR stubs. ND = not detected; LF = lead free.

Ammunition-firearm combination	No of shots	Medi wipes		GSR stubs	
		No of PbBaSb particles/mm^2	Average no of PbBaSb particles/mm^2	No of PbBaSb particles/mm^2	Average no of PbBaSb particles/mm^2
Pistol (Colt, USA) WinClean (LF) 45 Auto CP (Winchester, AUS)	**1**	ND ND ND	**ND**	0.299 0.272 0.202	**0.258**
	3	ND 0.550 0.367	**0.305**	0.299 0.408 0.316	**0.341**
Pistol (Colt, USA) 45 Auto CP (Winchester, AUS)	**1**	1.300 0.504 0.620	**0.808**	0.475 0.796 1.271	**0.847**
	3	2.846 1.493 0.576	**1.638**	0.498 1.156 1.408	**1.020**
Pistol (Smith&Wesson, USA) 44Rem Magnum (PMC, USA)	**1**	1.120 ND 0.161	**0.427**	0.215 0.422 0.315	**0.317**
	3	ND 0.403 0.864	**0.422**	0.184 0.721 0.622	**0.509**
Pistol (Smith&Wesson, USA) 44Rem Magnum (Winchester, AUS)	**1**	0.304 ND 0.149	**0.151**	0.703 0.120 0.991	**0.605**
	3	0.316 2.016 ND	**0.777**	3.467 1.762 1.254	**2.161**

Appendix IX continued: Comparison of the number of characteristic GSR particles per mm^2 detected after firing different ammunition-firearm combinations when collected using medi wipes or GSR stubs. ND = not detected; LF = lead free.

Ammunition-firearm combination	No of shots	Medi wipes		GSR stubs	
		No of PbBaSb particles/mm^2	Average no of PbBaSb particles/mm^2	No of PbBaSb particles/mm^2	Average no of PbBaSb particles/mm^2
Pistol (Beretta, Italy) 9 mm Parabellum (CCI, USA)	**1**	ND ND ND	**ND**	0.520 0.733 2.546	**1.268**
	3	ND 0.081 0.390	**0.157**	0.738 0.957 0.925	**0.873**
Revolver (Smith&Wesson, USA) 357 Magnum (Winchester, AUS)	**1**	1.961 1.222 0.336	**1.173**	0.139 0.175 0.120	**0.145**
	3	0.504 1.673 0.384	**0.854**	0.474 ND 0.172	**0.215**
Revolver (Smith&Wesson, USA) 357 Magnum (PMC, USA)	**1**	0.117 0.124 0.122	**0.121**	0.108 0.192 0.097	**0.132**
	3	0.124 ND 0.529	**0.218**	0.114 0.112 0.258	**0.161**
Pistol (High Standard, USA) 22 LR High Velocity (Remington, USA)	**1**	ND 0.331 ND	**0.110**	0.329 0.949 0.537	**0.604**

Appendix IX continued: Comparison of the number of characteristic GSR particles per mm^2 detected after firing different ammunition-firearm combinations when collected using medi wipes or GSR stubs. ND = not detected; LF = lead free.

Ammunition-firearm combination	No of shots	Medi wipes		GSR stubs	
		No of PbBaSb particles/mm^2	Average no of PbBaSb particles/mm^2	No of PbBaSb particles/mm^2	Average no of PbBaSb particles/mm^2
Pistol (High Standard, USA) 22 LR High Velocity Super Speed (Winchester, AUS)	**1**	0.336 0.114 0.461	**0.303**	0.973 0.366 0.124	**0.488**
Rifle (Marlin, USA) 22 LR High Velocity (Remington, USA)	**1**	ND 0.126 0.316	**0.147**	0.417 0.384 0.556	**0.452**
	3	0.128 1.152 ND	**0.427**	0.207 0.474 0.244	**0.308**
Rifle (Marlin, USA) 22 LR High Velocity Superspeed (Winchester, AUS)	**1**	0.117 ND 0.124	**0.080**	0.139 0.484 ND	**0.208**
	3	0.106 ND 0.397	**0.168**	0.152 0.537 0.288	**0.326**
Pistol (Glock, Austria) 40 Smith&Wesson WinClean (LF) (Winchester, USA)	**1**	ND ND 0.179	**0.060**	0.163 ND 0.556	**0.240**
	3	0.283 ND 0.139	**0.141**	0.591 0.192 0.907	**0.563**

Appendix IX continued: Comparison of the number of characteristic GSR particles per mm^2 detected after firing different ammunition-firearm combinations when collected using medi wipes or GSR stubs. ND = not detected; LF = lead free.

Ammunition-firearm combination	No of shots	Medi wipes		GSR stubs	
		No of PbBaSb particles/mm^2	Average no of PbBaSb particles/mm^2	No of PbBaSb particles/mm^2	Average no of PbBaSb particles/mm^2
Pistol (Glock, Austria) 40 Smith&Wesson (Winchester, USA)	**1**	0.091 ND 0.091	**0.060**	0.654 1.612 0.864	**1.042**
	3	ND 0.054 ND	**0.018**	0.081 0.600 0.078	**0.253**
Shotgun (Remington, USA) SuperX 12 gauge (Winchester, Australia)	1	0.027 0.027 0.027	**0.027**	0.329 2.126 1.065	**1.173**
	3	ND 0.107 0.107	**0.072**	0.154 0.122 0.090	**0.122**